

*Modular Architecture for an Adaptive,  
Personalisable Knee-Ankle-Foot-Orthosis  
Controlled by Artificial Neural Networks*

---

DISSERTATION

IN ORDER TO OBTAIN THE DOCTORAL DEGREE  
"DOCTOR RERUM NATURALIUM"  
OF THE GEORG-AUGUST-UNIVERSITÄT GÖTTINGEN

IN THE DOCTORAL PROGRAM  
THEORETICAL AND COMPUTATIONAL NEUROSCIENCE (PTCN) OF  
THE GEORG-AUGUST UNIVERSITY SCHOOL OF SCIENCE (GAUSS)

SUBMITTED BY  
JAN-MATTHIAS BRAUN  
OF GÖTTINGEN, GERMANY  
(PLACE OF BIRTH)



GEORG-AUGUST-UNIVERSITÄT GÖTTINGEN  
GÖTTINGEN, GERMANY  
OCTOBER 2015

Thesis committee

**Prof. Dr. Florentin Wörgötter,**

Biophysik - III. Physikalisches Institut, Georg-August-Universität Göttingen

**Prof. Dr. Dario Farina,**

Department of Neurorehabilitation Systems, Universitätsmedizin Göttingen

**Prof. Dr. Alexander Gail,**

Sensorimotor Group, Deutsches Primatenzentrum, Göttingen

Members of the examination board

First Reviewer: **Prof. Dr. Florentin Wörgötter,**

Biophysik - III. Physikalisches Institut, Georg-August-Universität Göttingen

Second Reviewer: **Prof. Dr. Dario Farina,**

Department of Neurorehabilitation Systems, Universitätsmedizin Göttingen

Other members of the examination board:

**Prof. Dr. Alexander Gail,**

Sensorimotor Group, Deutsches Primatenzentrum, Göttingen

**Prof. Dr. Poramate Manoonpong,**

CBR Embodied AI & Neurorobotics Lab,

The Maesk Mc-Kinney Moller Institute, University of Southern Denmark

**Prof. Dr. Jörg Enderlein,**

Biophysik - III. Physikalisches Institut, Georg-August-Universität Göttingen

**Prof. Dr. Walter Paulus,**

Klinik für Klinische Neurophysiologie, Universitätsmedizin Göttingen

Date of the oral examination:

19<sup>th</sup> of November, 2015

## ABSTRACT

Walking is so fundamental in everyday life that it is, for most people, an unconscious action. Loss or limitations in the ability to walk or stand directly impair our mobility and independence. Reasons of limitations can be stroke, paraplegia, or other damages to nerves, muscles, tendons, or limbs, encephalitis, brain abscesses, myopathies and further incidents and diseases affecting the motor control or the musculoskeletal system. In many cases, patients can be helped by, e.g., the use of orthoses for the lower limbs which assist to support the body and enable the patients to regain their movement abilities.

Important factors and problems dominate the choice and usage of the suitable device: (i) *Individualisation*: The individual patients' neurological status and remaining motor function have to be compatible with the support provided by the device. Particularly with regard to preserve—and not to interfere with—the remaining abilities, the device is selected to provide as little support as possible. As the remaining abilities largely vary with the individual expression of medical indications, the matching process is personalised and patient centred. (ii) *Specialised Design*: The movements a device supports are determined by its controller. Thereby, mobility is often limited to one or two basic movements, like walking and sitting. This specialisation imposes restrictions on the patient's mobility. (iii) *Target Group*: The matching of the individual's need for assistance with the controller's abilities substantially restrict the target group of a device. (iv) *Asymmetric Use*: Patients often favour their healthy limb, leading to asymmetric gait and other gait deviations, implying consequential damage. (v) *Device Acceptance and User Opinions*: Device acceptance by its user is affected by many factors, as, for instance, comfort, the applicability in daily activities, cosmetic factors, and the patients' impression if their opinions were considered in the process of device selection. Several studies indicate that, although a device might fit from an orthopaedic point of view, 60 % up to nearly 100 % of patients abandoned it for subjective reasons.

Here, we assume that all these five problems can be addressed by the device's controller. So far, controllers are only used to tackle some of these problems isolated. We propose a modular controller architecture, which is designed for flexible use, expandability, and adaptation, e.g., learning from individually observed gait samples and intent recognition, solving the set of problems. The development was realised on a semi-active Knee-Ankle-Foot-Orthosis with hydraulic knee-damper and tested on a healthy walker.

To address *specialised design*, we develop a controller based on a gait-independent formalism: An artificial neural network abstracts gait progress by decoding the sensory input. On top of this gait progress representation a device-specific

network provides hardware control. To facilitate *individualisation*, the gait progress representation is learned from the patient's gait samples, and a user interface allows direct user-interaction to define the control output, embedding the *user's opinions* directly in the process to provide support for the individual motions. The use of artificial neural networks provides adaptation algorithms.

The support of individual gaits leads itself to a specialisation of the controller. Here, we developed fast and reliable intent recognition with gait switching. The switching is done between per-gait modules, which consist of networks for gait progress abstraction, control output generation and internal models to predict gait dynamics. The prediction error identifies the optimal gait. This modular approach does not limit the number of movements, in contrast, it allows to extend the controller by further gaits in a formalised manner. It completes the solution to the problem of *specialised design* with a formalism which allows to extend the number of supported gaits with respect to the patient's requirements.

The proposed controller architecture focuses on the patient's gait dynamics. The used sensors describe the joint dynamics and are not bound to a specific hardware-design. Tests on two variations of the presented orthosis prototype support this hypotheses. This reduces the requirements on the patients' remaining abilities to the initiation of periodic motion with the support of the orthosis, *expanding the target group*. The support of *individual* gait allows the patients to develop their own gait, the patients do not have to force their gait into a pattern recognisable by the controller, providing a possibility for *more symmetric gait*.

In a gait laboratory study, combining motion capture and electromyography, we investigated the user-device-interaction and how it alters the subject's gait. We found that 1. the deviations imposed by the hardware dominate those by the controller, 2. we located the upper body as the place with the largest deviations, and 3. we conclude that controller optimisation can be driven by a careful analysis of additional muscular activity in electromyographic recordings. This study shows that the presented controller supports the healthy walker's gait, but shows the limitations of the controller's impact due to hardware and sensory restrictions. The localisation of gait deviations identifies potential for manual and on-line controller-adaptation.

To summarise, in this thesis we developed a controller on an orthosis prototype with a healthy walker based on a modular architecture allowing individual patient support. The system learns in a training process from observed gait samples and allows a simple and fast adaptation to gait changes and, in addition, enables easy extensions with further gaits. The evaluation of the user-device-interaction indicates deviations in the upper body and muscle work against the orthosis. This relation enables us in the next steps to infer how the devices' support can be optimised and how an automatic adaptation mechanism can quantify its impact on the patient's gait. Based on the here presented groundwork of an adaptive controller architecture, now it is possible to develop an observing, adapting controller, which is capable of basic patient surveillance, complementing medical treatment and rehabilitation.

# Contents

<b>Terms and Abbreviations</b>	<b>xi</b>
<b>List of Figures</b>	<b>xiii</b>
<b>List of Tables</b>	<b>xvii</b>
<b>1. Introduction</b>	<b>1</b>
1.1. Problem Definition . . . . .	4
1.1.1. Gait Independent Control . . . . .	5
1.1.2. Individual Gait Control . . . . .	5
1.1.3. Multi-Gait and Environment Support . . . . .	6
1.1.4. Adaptive Gait Control . . . . .	6
1.2. Outline . . . . .	7
<b>I. Orthopaedic Background</b>	<b>11</b>
<b>2. Human Gait</b>	<b>13</b>
2.1. Stability of Legged Locomotion . . . . .	13
2.2. Description of Human Gait . . . . .	15
2.2.1. A Short History of Gait Analysis . . . . .	16
2.2.2. Hierarchical Description of the Stride . . . . .	18
2.3. Important Dynamic Properties of Gait-Phase-Transitions . . . . .	22
2.4. Motion Generation and Coordination . . . . .	24
2.4.1. Neural Control of Force Generation . . . . .	24
2.4.2. Models for Mechanical Properties of Muscles . . . . .	26
2.5. Summary . . . . .	27

## Contents

<b>3. Treatment of Gait Pathologies</b>	<b>29</b>
3.1. Impaired Gait . . . . .	29
3.1.1. Changes in Statistical Properties of Human Gait . . . . .	30
3.2. Quantification of Medical Indications . . . . .	32
3.3. Treatment of Impaired Gait . . . . .	34
3.3.1. State of the Art: Joints & Actuation . . . . .	34
3.3.2. Side-Effects of Prosthesis- and Orthosis-use . . . . .	38
3.3.3. Patient's Perspective and Device Abandonment . . . . .	39
3.4. Summary: Individualisation to Increase Device Acceptance . . . . .	41
<b>4. Passive Support with the Presented Orthosis' Brace</b>	<b>43</b>
4.1. The Knee-Ankle-Foot-Orthosis . . . . .	43
4.2. Medical Indications for Semi-Active Orthosis Use . . . . .	45
4.3. Discussion: The Orthosis' Impact on Gait . . . . .	49
4.3.1. Physiological and Mechanical Constraints . . . . .	49
4.3.2. Recovery of Healthy Gait . . . . .	51
4.3.3. Expectation Management . . . . .	52
<b>II. Control-Problem and Sensors</b>	<b>55</b>
<b>5. Definition of the Control Problem</b>	<b>57</b>
5.1. Approaches to Achieve Adaptive Gait Support . . . . .	57
5.2. State of the Art for Control Approaches . . . . .	59
5.2.1. Threshold Switching . . . . .	59
5.2.2. Finite State Machine based Controllers . . . . .	61
5.2.3. Artificial Neural Networks . . . . .	62
5.2.4. Gait Recognition . . . . .	63
5.3. Control Problem Evaluation . . . . .	64
5.3.1. Determination of Control Output . . . . .	65
5.3.2. Gait Progress Representation . . . . .	65

5.4.	Conclusions . . . . .	67
5.4.1.	Requirements on the Gait Progress Representation . . . . .	67
5.4.2.	Consequences for the Choice of Sensors . . . . .	68
<b>6.</b>	<b>Orthosis Controller Experiments on RunBot</b>	<b>71</b>
6.1.	RunBot . . . . .	71
6.1.1.	RunBot Set-Up . . . . .	73
6.1.2.	Locomotion Generation in RunBot . . . . .	74
6.2.	Comparison of RunBot's Gait to Human Gait . . . . .	75
6.2.1.	Comparing against the reduced dynamics of locking orthoses . . . . .	78
6.2.2.	Consequences for Gait Modelling with RunBot . . . . .	78
6.3.	Evaluation of Possible Experiments with RunBot . . . . .	80
6.3.1.	Mimicking Patient's Conditions . . . . .	81
6.3.2.	Reduction of the Signal Amplitude . . . . .	81
6.3.3.	Hardware Manipulations . . . . .	82
6.3.4.	Complex Modelling of Patient's Conditions . . . . .	83
6.3.5.	Conclusions and Choice of Experiment . . . . .	84
6.4.	Experiment: Gait-Timing Based Control on RunBot . . . . .	84
6.4.1.	Experimental setup . . . . .	87
6.4.2.	Results . . . . .	88
6.5.	Discussion . . . . .	90
6.5.1.	Consequences for the Orthosis Controller . . . . .	90
<b>7.</b>	<b>The Orthosis' Sensors</b>	<b>93</b>
7.1.	Data Acquisition Framework . . . . .	93
7.1.1.	C-Leg-Interface . . . . .	94
7.1.2.	USB-Dux DAQ-Interface . . . . .	95
7.1.3.	Dedicated Embedded i/o-Interface . . . . .	97
7.2.	Sensory Configuration . . . . .	98
7.2.1.	Joint instrumentation . . . . .	100
7.2.2.	Foot instrumentation . . . . .	101
7.3.	Summary . . . . .	103

<b>III. Orthosis Controller</b>	<b>107</b>
<b>8. Orthosis Feedforward Control</b>	<b>109</b>
8.1. Locomotion Generation in Orthosis Control . . . . .	111
8.2. Requirements on the Controller . . . . .	111
8.2.1. Basic Considerations . . . . .	111
8.2.2. Control Flow . . . . .	112
8.2.3. Timing unit . . . . .	115
8.2.4. Shaping Unit & User Feedback . . . . .	116
8.3. Implementation . . . . .	117
8.3.1. Timing Unit . . . . .	117
8.3.2. Shaping Unit & User Interface . . . . .	119
8.3.3. Segmentation of Gait Recordings . . . . .	122
8.4. Evaluation . . . . .	123
8.4.1. Ability to track the Patient's Gait . . . . .	124
8.4.2. Influence of smoothing of the gait phase . . . . .	132
8.4.3. Gait phase models of different complexity . . . . .	132
8.4.4. Handling of Step Variations . . . . .	135
8.4.5. Ability to Tune to the Patient's Needs . . . . .	135
8.4.6. Ability to Capture Different Gaits . . . . .	138
8.5. Discussion . . . . .	139
8.5.1. Detailed Discussion . . . . .	141
8.5.2. Ability to Cope with Stumbling Situations . . . . .	145
8.5.3. Comparison to other Methods . . . . .	145
8.5.4. Advantages of the Presented Controller . . . . .	149
8.5.5. Limitations of the Presented Controller . . . . .	150
8.5.6. How to Go On . . . . .	151
8.5.7. Incorporation of Multigait-Support . . . . .	154
<b>9. Support for Multiple Gaits</b>	<b>157</b>
9.1. Introduction . . . . .	158
9.2. Overview . . . . .	160



9.3. Predicting Gait Models . . . . .	162
9.3.1. Model Prediction . . . . .	162
9.3.2. History Length defines Switching Times and Accuracy .	163
9.3.3. Selection of Prediction Input . . . . .	164
9.3.4. Scaling of Sensory Input . . . . .	166
9.4. Decision unit . . . . .	166
9.4.1. Post-processing . . . . .	166
9.4.2. Gait Selection Strategy . . . . .	168
9.5. Evaluation . . . . .	170
9.5.1. Accuracy of Gait-Detection . . . . .	170
9.6. Discussion . . . . .	177
9.6.1. Evaluation of Selection Accuracy . . . . .	178
9.6.2. Comparison to other approaches . . . . .	180
9.6.3. Improving the Performance and Behaviour . . . . .	181
9.6.4. Significance for the Controller-Architecture . . . . .	184
9.6.5. Alternative Approaches . . . . .	187

**IV. Gait Laboratory Evaluation 191**

**10. User-Device-Interaction 193**

10.1. Introduction . . . . .	194
10.1.1. Motion Capture . . . . .	195
10.1.2. Electromyography . . . . .	196
10.2. Experimental Setup . . . . .	199
10.2.1. Experimental Procedure . . . . .	200
10.2.2. Motion Capture . . . . .	203
10.2.3. Electromyography (EMG) . . . . .	203
10.3. Methods . . . . .	207
10.3.1. Analysis Pre-Processing . . . . .	207
10.3.2. Motion Capture Data Analysis . . . . .	209
10.3.3. EMG Data Analysis . . . . .	213

## Contents

10.4. General Results . . . . .	216
10.4.1. Recording Synchronisation . . . . .	217
10.4.2. Heel-Strike Approximation . . . . .	217
10.4.3. Step Filters and Recording Quality . . . . .	222
10.5. Motion Capture Data . . . . .	223
10.5.1. Results . . . . .	223
10.5.2. Discussion . . . . .	233
10.6. EMG Data . . . . .	238
10.6.1. Results . . . . .	238
10.6.2. Summary EMG . . . . .	254
10.7. Conclusions . . . . .	255
<b>V. Conclusions &amp; Outlook</b>	<b>257</b>
<b>11. Conclusions</b>	<b>259</b>
11.1. Summary of Contributions and Limitations . . . . .	260
11.1.1. Feed-Forward Controller . . . . .	260
11.1.2. Multi-Gait Support . . . . .	262
11.1.3. Interaction Between the User and the Device . . . . .	264
11.2. Contributions in the Broader Context . . . . .	266
<b>12. Outlook</b>	<b>269</b>
12.1. Adaptation . . . . .	270
12.1.1. Adaptation to Changes in Gait . . . . .	270
12.1.2. Adaptation to New Gaits . . . . .	271
12.1.3. Adaptation of Control Output . . . . .	271
12.1.4. Self-Learning Controller . . . . .	273
12.1.5. Online Gait Analysis . . . . .	273
12.1.6. Conflicting Adaptation by User and Device—Timescales of Adaptation . . . . .	275
12.1.7. Summary—Adaptation . . . . .	276
12.2. Next Steps . . . . .	276
<b>Bibliography</b>	<b>279</b>

# List of Acronyms

**AEA** anterior extreme angle.

**BCI** brain computer interface.

**BF** biceps femoris.

**COM** centre of mass.

**DAQ** data acquisition.

**EMG** electromyography.

**FES** functional electrical stimulation.

**FSM** finite state machine.

**FSR** force sensing resistor.

**GL** gastrocnemicus lateralis.

**GM** gastrocnemicus medialis.

**IMU** inertia measurement unit.

**KAFO** Knee-Ankle-Foot-Orthosis.

**LBP** low back pain.

**MoCap** motion capture.

**MUAP** motor unit action potential.

*Terms and Abbreviations*

**RBF** radial basis function.

**RF** rectus femoris.

**SCKAFO** Stance-Controlled Knee-Ankle-Foot-Orthosis.

**SO** soleus.

**TA** tibialis anterior.

**VL** vastus lateralis.

**VM** vastus medialis.

# List of Figures

## 1. Introduction

1.1.	A picture of the author testing the presented prototype on stairs.	2
1.2.	The thesis' topic lies in the cross section of several areas of research	3
1.3.	Thesis outline . . . . .	8
1.4.	Controller components and their interaction . . . . .	9

## 2. Human Gait

2.1.	Eadweard Muybridge's photographs of a galloping horse . . . . .	17
2.2.	Hierarchy of gait phases, tasks and periods . . . . .	19
2.3.	The Gait Cycle . . . . .	20
2.4.	Gait cycle partitioning . . . . .	21
2.5.	Efferent path way of motor control commands . . . . .	25
2.6.	Mechanical properties of Hill-Type muscle models . . . . .	27

## 3. Treatment of Gait Pathologies

3.1.	Example for reduced joint motion . . . . .	31
------	--	----

## 4. Passive Support with the Presented Orthosis' Brace

4.1.	Orthosis schematics . . . . .	46
4.2.	Target patient muscle status . . . . .	48
5.1.	Example for a finite state machine based controller . . . . .	60

## 5. Definition of the Control Problem

5.2.	Gait phase variable $\varphi$ . . . . .	66
------	---	----

## List of Figures

5.3.	Phase diagrams: uncontrolled, foot-switch . . . . .	69
<b>6. Orthosis Controller Experiments on RunBot</b>		
6.1.	Chapter outline: Virtual Orthosis Controller for RunBot . . . . .	72
6.2.	RunBot . . . . .	73
6.3.	Gait comparison: RunBot to Orthosis . . . . .	76
6.4.	The Anterior Extreme Angle . . . . .	77
6.5.	Gait comparison: healthy walker to locking orthosis . . . . .	79
6.6.	Friction stabilises RunBot's . . . . .	82
6.7.	RunBot inter-limb coordination . . . . .	85
6.8.	Experiment: RunBot virtual orthosis controller . . . . .	86
6.9.	Virtual knee orthosis controller . . . . .	88
6.10.	Joint trajectories for RunBot's virtual orthosis. . . . .	89
<b>7. The Orthosis' Sensors</b>		
7.1.	Chapter overview: Orthosis sensors and interfaces . . . . .	94
7.2.	Hardware interface with USB-Dux . . . . .	95
7.3.	Motor neuron transfer function . . . . .	96
7.4.	Data Acquisition Interface . . . . .	97
7.5.	Schematics for orthosis prototypes . . . . .	98
7.6.	Photos of the orthosis prototypes . . . . .	99
7.7.	Development of ground contact sensor application . . . . .	102
7.8.	Evaluation of FSR placement . . . . .	104
7.9.	Final FSR setup on heel & toe . . . . .	105
<b>8. Orthosis Feedforward Control</b>		
8.1.	Chapter overview: Orthosis Feedforward Control . . . . .	110
8.2.	Core controller control flow . . . . .	113
8.3.	Sketch: Radial-Basis-Function representation of damping function	121
8.4.	User interface for damping tuning . . . . .	122
8.5.	Smoothness of gait phase representation . . . . .	127
8.6.	Histogram of gait phase increments $\Delta\varphi$ . . . . .	129
8.7.	Influence of the smoothing on gait tracking accuracy . . . . .	133

8.8.	Errors when training different ann architectures . . . . .	136
8.9.	Step duration and stride length adaptation . . . . .	137
8.10.	Typical results for damping tuning . . . . .	139
8.11.	Reproducibility of gait tuning . . . . .	154
<b>9. Support for Multiple Gaits</b>		
9.1.	Control flow of extended controller . . . . .	161
9.2.	Structure of the predicting models . . . . .	163
9.3.	Predicting gait model on stair case landing . . . . .	165
9.4.	Flow diagram of the decision unit . . . . .	167
9.5.	Gait transition with predicting gait model . . . . .	169
9.6.	Staircase landing of the testing environment . . . . .	171
9.7.	Evaluation of Accuracy and Timing . . . . .	173
9.8.	Confusion matrix for predicting gait models . . . . .	175
9.9.	Transition Step: A False Positive in Detail . . . . .	176
<b>10. User-Device-Interaction</b>		
10.1.	Calculation of joint angles form marker trajectories . . . . .	196
10.2.	Function of surface EMG . . . . .	197
10.3.	Gait-lab setup . . . . .	200
10.4.	One Step of motion capture (MoCAP) recording . . . . .	204
10.5.	EMG electrode placement . . . . .	206
10.6.	Hip-tilt angle . . . . .	210
10.7.	Body axes . . . . .	212
10.8.	EMG: Raw Data, Envelope, and Standard deviation. . . . .	215
10.9.	Flat ground comparison of MoCAP approximations to heel-force sensing resistor (FSR) . . . . .	218
10.10.	Heel-FSR approximation on a recording without orthosis . . . . .	219
10.11.	Performance of MoCAP features to approximate heel-FSR . . . . .	222
10.12.	Changes of the mean hip and knee angle for different conditions . . . . .	225
10.13.	Tilting of Hip in the Frontal Plane . . . . .	227
10.14.	Leaning of the vertical axis . . . . .	228
10.15.	Orientation and Amplitude of Transversal Trunk Rotation . . . . .	229

*List of Figures*

10.16. Variability in Trunk Rotation . . . . . 230  
10.16. Variability in Trunk Rotation (Continued) . . . . . 231  
10.17. Determining thresholds for normalised steps . . . . . 240  
10.18. Problems with threshold definition on noisy recordings . . . . . 241  
10.19. Problems with threshold definition with low standard deviation . 242  
10.20. Distribution of standard deviations . . . . . 244  
10.21. Distribution of area below the envelope . . . . . 245  
10.22. Changes in activities of biceps femoris and vastus lateralis . . . 246  
10.22. Changes in activities of gastrocnemicus lateralis and tibialis an-  
terior . . . . . 247  
10.23. Details for ipsilateral biceps femoris . . . . . 249  
10.24. Details for ipsilateral vastus lateralis . . . . . 250  
10.25. Details for ipsilateral gastrocnemicus lateralis . . . . . 251  
10.26. Details for ipsilateral tibialis anterior . . . . . 252  
10.27. Phases of activity for EMG channels which show no huge changes. 253

**12. Outlook**

12.1. Asymmetric Gait in Stance Phase Proportions . . . . . 275



# List of Tables

3.1. Muscle status values after Janda . . . . .	33
8.1. Calibration procedure . . . . .	119
8.2. Phase shifts of the timing unit . . . . .	128
10.1. List of Recording Trials in the Gait-Lab . . . . .	202
10.2. Marker-positions for MoCAP recording. Donning of the orthosis required the replacement of the markers on the right leg. . . . .	203
10.3. Muscles recorded in the EMG-Experiments . . . . .	207
10.4. Sampling Frequency Errors . . . . .	217
10.5. Coefficients for heel-strike approximation . . . . .	221
10.6. Channels with High Fraction of Saturated Steps . . . . .	223



*Our freedom can be measured by the number of things  
we can walk away from.*

Source unknown (attributed to Vernon Howard)

# 1

## Introduction

When we move in our environment every day, for most of us walking is an unconscious, an unnoticed act.

Nonetheless, bipedal gait is inherently unstable [66, 104], as the centre of mass (COM) is high above the ground; with only two legs, we can achieve no static stability. Therefore, we need additional effort to balance the body, using additional sensory cues, like the sense of balance and vision.

This increases the complexity of bipedal locomotion in comparison to other kinds of locomotion based on a higher number of legs which provide static stability without balancing. As a consequence, while many animals can walk within hours of their birth, the formation of a mature gait takes years in humans. Although a step reflex exists from birth on, we observe that learning to walk is far from easy, when children in western cultures start their first steps with help around the age of one [96]. The process of gait maturation then goes to around three to seven years [22, 96], depending on the associated characteristics.

## *Introduction*

The importance of locomotion surfaces, when pain, or bandages hinder our movements, or we are constrained to a wheelchair or a bed. While reasons are manifold, a reduction of our mobility directly confines the number of things we can do independently. Crossing gaps, navigating stairs, obstacles and uneven ground become hurdles, which to overcome we need assistance.

To provide this assistance many supporting technologies have been developed. From simple splints, crutches, wheelchairs, prostheses, orthoses as a more general form of splints, to modern exoskeletons. All these devices can be used to assist movement with the aim to restore stability, mobility and in the end independence.

From a medical point of view, the choice of assistive technology depends on the patient's conditions and if these are compatible with given support and the load the device puts onto its user. For orthoses, it is important that the device is not giving too much support, lest the user's abilities might degrade due to missing training. The opposite effect should be achieved with a carefully chosen device [35, 36]: An increase in the range of kinematic parameters and walking speed.

After all, these devices change their subjects' gaits. To the better, for they regain mobility, but at the same time the design of the splint and especially its joints limit movements [61]. Thus, the devices requi-



**Figure 1.1.:** A picture of the author testing the presented prototype on stairs.

re the user to adapt their gait; this fact and the underlying medical reason often results in asymmetric gait with secondary conditions [21]. The comfort a patient experiences with a specific device is naturally a very subjective impression.

From a patient’s perspective, many factors define if the device really is used or abandoned in the end. It depends on the comfort provided in every day life, for example the ability to easily don/doff the device as well as on cosmetic properties, i.e., how the device alters users in their perception of their own, or those of others [3, 61, 83]. [44] cites several studies whose subjects abandoned their orthoses with rates in a range “from 60 % to nearly 100 %”: in the case of [76] 35 of 60 users of lower extremity braces abandoned their devices. In another survey targeting 250 veterans at 22 months after rehabilitation programmes, only 16 of 73 reached patients were still actively using their braces, the other 78 % had abandoned their devices [32]. In [64], of 35 replies 31 % indicated to not use their brace anymore and “60 % continued to use their wheelchair as their main means of displacement”. These abandonment rates give a huge weight to the patient’s perspective of the prescribed brace.

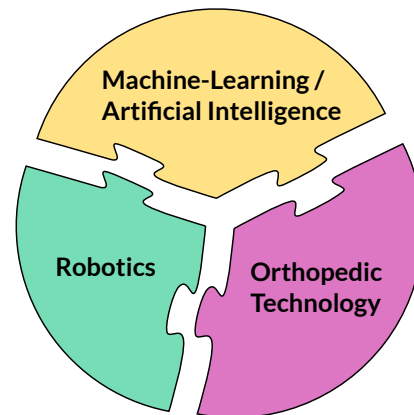


**Figure 1.2.:** This thesis’ topic lies in the cross section of machine-learning, robotics and orthopaedic technology. Our focus lies on the technical aspects of the orthotic device’s controller, but the introduction will include a mixed background from all fields.

This thesis evolved around a BFNT-Göttingen project in collaboration with the company Otto Bock HealthCare GmbH to design and implement an adaptive controller for a semi-active Knee-Ankle-Foot-Orthosis (KAFO), which spans from the upper thigh down to, including, the foot (see Figure 1.1). The knee joint

## *Introduction*

is equipped with an C-Leg™hydraulic damper, which allows applying resisting moments to support the wearer's body weight and help him or her to stabilise their gait.

Our focus lies on the development of a controller architecture with extensive patient fitting and behaviour adaptation. To achieve this, the presented work mixes techniques from the fields of machine-learning/artificial intelligence, robotics and orthopaedic technology, as in Figure 1.2.

### **1.1. Problem Definition**

The mechanical structure of the KAFO is intended to support their users' body weight while walking. It is equipped with a computer controlled hydraulic damper, which allows stance- and swing-phase control. Therefore, it constitutes a semi-active device, which allows fine grained control over passive properties of the knee joint.

Reasons to use such a device are manifold, but generally, a loss of control or muscle force leads to the need of assistance for standing and walking.

Given specific patient conditions and a suitable hardware frame and supportive technology, in our case the hydraulic damper, the control strategy plays an important role for the mobility the patient gains and the final adaptation of the device by the user, for which comfort and aesthetics also play an important role, as has been discussed above.

In the following, we want to take a look at several aspects of the device's lifetime and role for the patient, which will be discussed in more detail in the following chapters:

- **Initial contact:** can the device and patient work together, i.e., does the patient fulfil the requirements of the control paradigm? Training to use the orthosis in an appropriate manner, tuning & customising the controller to the patient including considerations (weight, comfort).

- **Every day use:** how well does the control paradigm fit the individual gait? How well are different gaits and environments supported? Stairs, slopes, etc..
- **Long-term issues:** Amount of avoidance movements, reduction of gait deviations. Can the amount of support the device gives be adjusted to changes in gait? Does the device track these changes? Is an expert required to change parameters?

We propose an adaptive control paradigm, which focuses on the ability to change the function of the device; leveraging the flexibility of the used methods, to extend the individualisation and customisation of the controller, to achieve a better fit with the patient's gait. This fitting should be complemented by learning from patient observations and direct patient feedback in the process. Due to this fitting and tuning process, we strive to broaden the target audience, by removal of dynamic requirements on the patient's gait.

### **1.1.1. Gait Independent Control**

To allow the application of the controller to specific gaits and environments, we propose a model based abstraction of gait progress. Based on local sensors, the model implements a simple kind of online gait analysis. The locality of sensors is important to ensure easy application, especially donning/doffing of the orthosis. Thus, a suitable set of sensors has to be identified.

### **1.1.2. Individual Gait Control**

From controller side a few things can be done to increase device acceptance. The controller can make it easy to use different gaits and the individual gait the patients use to achieve as much mobility as they can. The device should not force a movement or gait activation onto the patient, but should transparently support what the patient does.

## *Introduction*

Therefore, to support individual gaits, we propose the use of machine learning approaches, which allow the device to learn from walking samples. At the end of this learning phase stands a transformation from individual gait to an abstract and general representation of gait progress, which allows the patient to influence the device's behaviour in a predictable manner.

### **1.1.3. Multi-Gait and Environment Support**

As different gaits and environments require different patient-support, the controller has to actively support changes in gait. Problems to achieve this aim are the balance between reliable gait recognition without fatal false positives and fast reaction times, which seamlessly integrate into regular walking.

To achieve this, we again propose model based approaches to identify the ongoing motion as part of an online gait analysis process.

### **1.1.4. Adaptive Gait Control**

To gain flexible control, all steps of the proposed controller have to be designed to facilitate this aim and enable change at runtime or in controlled phases. An important aspect for our design are guiding and screening applications.

Patients adapt their gait to orthosis use from initial fitting [35] over a timescale of months [36]. The authors in [36] show changes in kinematic variables like velocity, stride length, peak knee flexion and others. But some kinematic variables *reached significant change levels only at the six-month mark*. To keep gait support optimal over long time scales, changes might be necessary. This suggests including continuous gait screening which uses methods of online gait analysis to evaluate changes in the patient's gait to suggest device maintenance or orthopaedic intervention.

An advanced project would be to try to guide this adaptation in a way similar to rehabilitation training. For this to work, it is important to understand the changes



the device induces in the patient's gait. This allows developing cost functions whose optimisation can help to improve the patient's gait by gradual extension of the patient's mobility.

Although the final implementation of these two aspects is beyond the scope of this thesis, we will consider implications for controller design and discuss the opportunities the proposed controller opens to tackle these advanced problems.

## 1.2. Outline

The thesis is structured as follows (cmp. Figures 1.3 and 1.4): in chapter 2, we will establish the necessary background and nomenclature to deal with human gait. A short description of the dynamics will produce the general task of body support for the lower-limbs orthosis.

With a description of walking dynamics, we will lay the foundation to take look at gait pathologies and their treatment in chapter 3. The evaluation of existing joint technologies and important factors in patient acceptance will provide a set properties, an orthosis should possess. Here we carve out why the ability to focus on the individual patient will not only provide advantages in comfort, but why this is practical and of utmost importance for the acceptance and use of the device. After these general considerations, we present our orthosis frame (the brace) in chapter 4. Together with the medical indication and the general demands formulated in the previous chapters, we can identify the possible influence on the user's gait and we will formulate aims for the orthopaedic influence of a modern lower-limb orthosis.

In the following, we will take a look at the control problem in chapter 5. We will discuss the general control task and the state of the art for the controller side. We go on with the formulation of possibilities to gain an individualised and adaptive orthosis controller and produce a first abstract description of the fundamental feed-forward controller which lies at the centre of this thesis and which maps sensory input to a gait progress measure  $\varphi$ .

## Introduction

Based on this abstract controller, we will validate the applicability with an experiment on the bipedal walking robot RunBot in chapter 6. In this chapter, we will test the training approach and gain requirements on the sensory input necessary for the feed-forward controller. The RunBot experiments directly converge onto the orthosis hardware-equipment with sensors and the corresponding interfaces in chapter 7.

Based on the hardware design, we can then go on implementing the feed-forward orthosis controller in chapter 8, which learns the users' individual gait from observed samples and allows the users to directly control the amount of support the controller applies based on the current gait progress  $\varphi$ .

In chapter 9 we will extend the feed-forward controller to support multiple gaits. This is necessary, as the training of the feed-forward controller not only allows supporting individual gait, but will produce specialised gait support. Therefore, we will extend the controller-structure with another layer, which will coordinate a set of known gaits.

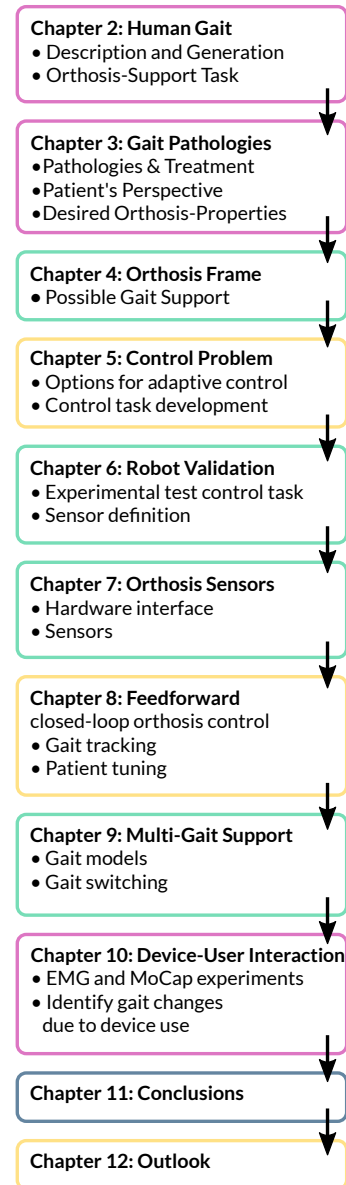


**Figure 1.3.:** Thesis outline

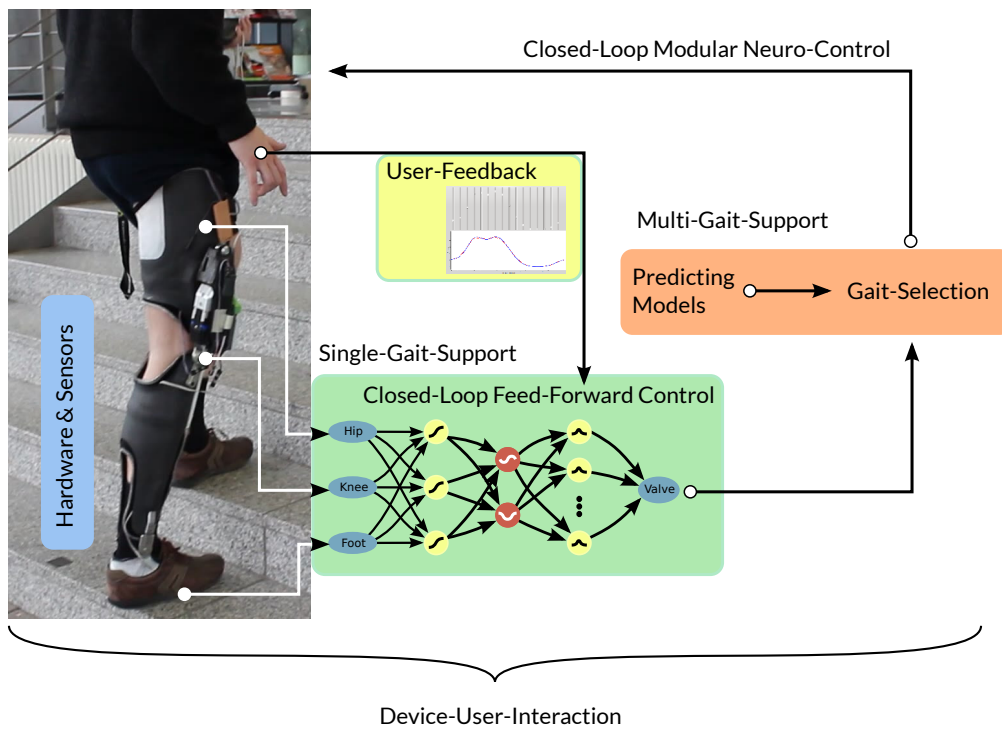


**Figure 1.4.:** Interaction of controller components: In the first chapters, human gait, its pathologies and human-device-interaction define the support the brace should provide. This results in the formulation of the control problem in chapter 5 and the definition of the sensory equipment in chapters 6 and 7. Chapter 8 provides the basic feedforward controller, which is extended with multi-gait switching in chapter 9. The device-user interaction will be evaluated in chapter 10.

To evaluate the effect of the orthosis onto its bearer, we will conduct present gait lab experiments in chapter 10. Here, we will measure and discuss the effect of the orthosis on its subject by means of MoCAP and EMG analysis.

The thesis is concluded in chapter 11 with a general discussion of the controller and its results and take an extended outlook into the possibilities this controller provides to implement adaptive, learning and still traceable orthosis control. In chapter 12, we take an outlook at advanced opportunities for controller development and will discuss higher level control tasks, as patient surveillance, online learning and adaptation.



**Part I.**

**Orthopaedic Background**



# 2

## Human Gait

Although the primary focus of this thesis lies on robotics and machine learning, with the application to a lower-limb orthosis we need to take aspects from orthopaedy, physiology, and bipedal walking into consideration, too. The orthosis, the combination of the brace and the controller will be attached to the patient's leg and has the main purpose to provide support to its users when standing and walking.

Thus, we start the work at hand with a description of human gait and the physiological components involved in its generation to gain an understanding of what and when the presented controller is supporting. To this end we approach bipedal gait from the perspective of classical gait analysis, which was developed as a diagnostic tool for orthopaedists. The nomenclature and dynamics will serve us as a description of how gait progresses.

Based on this general description of human gait, we will consider gait pathologies and discuss their treatment and open problems in the next chapter to develop a detailed description of what the presented orthosis can and should support.

### 2.1. Stability of Legged Locomotion

Locomotion is the act of spatial transport, moving a being—be it an animal, human, or robot—from one place to the other. In our environment, constraining

## *Human Gait*

ourselves to land based locomotion, we see several realisations: The most common ones are legged. One can find millipedes with several hundred legs, insects with six legs, lots of bigger animals are quadrupeds, and last but not least humans, employing bipedal locomotion.

Here, we start the description of gait with a general discussion of stability, as inherent instability is a fundamental property of bipedal gait, which makes balancing control and the prevention of falls so crucial and human gait so special when compared to other forms of legged locomotion.

Depending on the number of legs, the organism makes use of different gaits for locomotion. Here, a gait describes a cyclic sequence of leg movements which will be referenced as *gait cycle*. Every gait has specific dynamic properties; gaits may be selected for speed [15], or gaits may be selected for environmental conditions, for example when climbing stairs.

### **Stability of Six-Legged Gaits**

Six-legged locomotion has the great advantage, that stability can be achieved at any time. The fastest, always stable gait with six legs is the tetrapod gait, which is moving three legs at a time in alternating pairs of triangles, so that the centre of mass is always supported. Other possible gaits include quadruped, giving body support with four legs and a crawl, or wave gait, which only lifts one leg at a time. Compared to the tetrapod gait, these gaits are slower but more stable and allow robust locomotion even in inaccessible environments.

### **Stability of Quadrupedal Gait**

Quadrupeds employ locomotion on four legs, which allows full stability in standing and slow gaits, with just one leg in the air, but also allows for faster movements with two, three or partially even all four legs off the ground as shown in figure 2.1 for a galloping horse. For horses, for example, one distinguishes at least *walk*, *trot*, *canter*, and *gallop*. These can be distinguished by properties



like beat and symmetry. The beat is the rhythm, the number of audible foot contacts per cycle; symmetry denotes alternating motion of leg pairs. The symmetry of a gait is defined by the pattern of limbs moving together.

### **Stability of Bipedal Gait**

In contrast to locomotion with four or more legs, bipedal gait is never statically stable, as is suggested by the model of the inverted pendulum [66]: the bipedal walker always balances against gravity. Bipedal gait can be described as controlled falling-forward under influence of gravity.

Therefore it is argued, that bipedal walking is a task of higher complexity; that it involves more control, especially from higher levels of the nervous system. This would be needed to incorporate additional sensory cues, for example the sense of balance, and visual cues. In general, bipedal stability needs more sensory input than for example a gait like the tetrapod, where in theory there is always time to correct the foot placement to external disturbances. Due to this complexity, it takes a human child around 7 years ([22]) to achieve stable, adult walking patterns.

## **2.2. Description of Human Gait**

In the previous section we stated, that there are many different gaits, which are cyclic movements with the aim to reliably propel the body forward. There are many gaits available, like running, walking, and stair climbing. And of course there are many other forms, like walking sideways or backwards.

In this section we are presenting the nomenclature for talking about bipedal gait, which is typically used in the analysis of gait. The characteristics depend on the gait involved; gaits might be changed as a consequence of the individual physiology, changes in the environment, like slopes or stairs, or speed. For gait

changes with velocity, the exact velocity of change is commonly assumed to be determined by energetic optimality [15, 85].

For humans *walking* and *running* are the most important gaits, whereas we are restraining ourselves to walking in this work, especially due to the higher impact forces related to the flight phase involved in running gait, for which the foot frames of many orthoses, including the presented orthoses, are not optimal.

### **2.2.1. A Short History of Gait Analysis**

Reference [1] gives a nice summary over early gait analysis, starting with recorded statements dating back as far as to Aristotle (384-322 BCE). With time, theoretical considerations and observation of gait were extended with a physiological, anatomical, and mechanical understanding of the human body. Later on, observational methods were refined with instrumentation. Here, instrumentation means subject- as well as environmental-instrumentation, like instrumented joint angle-sensors, shoes or force measuring plates in the ground, which were in use already in the late 19th century.

Photography based gait observation developed in the 19th century, too. First installations ranged from a set of cameras to the development of high-speed cameras, showing the gait as a sequence of pictures which could be animated or superimposed on the same photo plate. Figure 2.1 shows an early application of this technique, which settled the discussion over the existence of a flight phase in horse's gallop.

Already at around 1890 the first 3D-reconstruction of human gait has been performed in the labs of Braune and Fischer, long before modern high-speed, multi-camera installations allow the computer-aided, model based 3d-reconstruction of motion. For more information, please take a look at section 10.1.1.

In the 1960s and 1970s electromyographic recordings were introduced to record muscle activation in the living object. This technique is presented in more detail in section 10.1.2.

## 2.2. Description of Human Gait

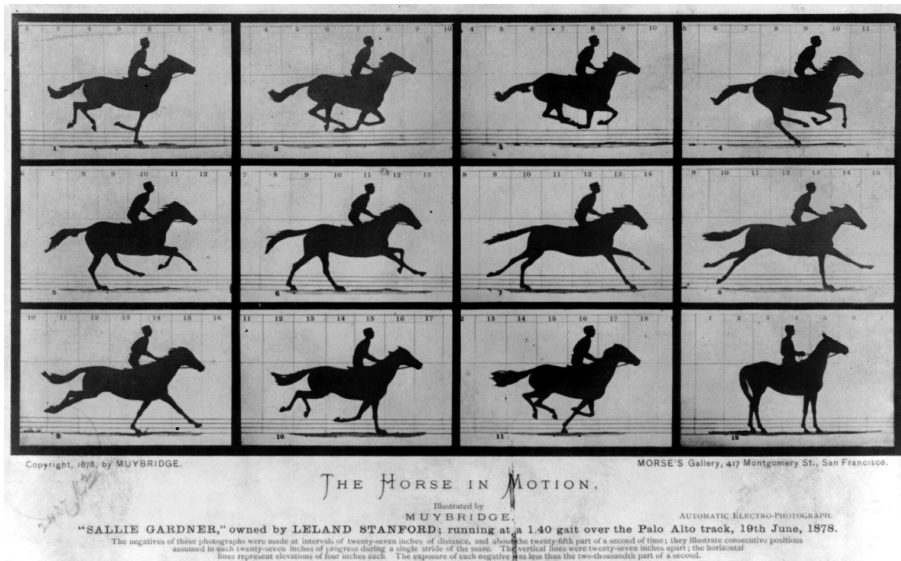


**Figure 2.1.:** Eadward Muybridge's photographs of a galloping horse, as taken for Leland Stanford in 1877. With these photographs, Stanford settled an ongoing argument in the USA, if the horse's gallop included a flight phase and are a famous example of photography based gait analysis. In 1872 the same argument was settled in Europe using force-measurement-shoes for a horse.

All these tools have been applied to observe human gait, understand human gait dynamics and mechanics, and describe pathological gait deviations for humans, as well as for animals.

## **2.2.2. Hierarchical Description of the Stride**

With the methods for gait-analysis over time a set of formalised descriptions of bipedal gait emerged. These form a hierarchy of partitions and events, a common example from [84] has been reproduced in Figure 2.2, which differentiates the *gait cycle* from the *stride* into *gait phases*, which are subdivided into *tasks* and *periods*. We will now go through the for us important parts of this hierarchy.

### **The Stride**

Individual gait is a cyclic movement, which can be described with schemes as in figures 2.3 or 2.2. It is measured from heel strike to heel strike of the same foot. This measure defines the *stride* and thus covering two alternating steps.

### **Gait Phases**

The stride is divided into two phases, the *swing-* and *stance-phase* respectively, see Figure 2.3. For this differentiation to be unique, we have to choose the perspective of one leg, as the phases of gait are phase shifted for both legs. This is more important later on, when we will describe the gait and controller from the perspective of the impaired leg wearing the orthosis. We call this the ipsilateral leg, naming the other leg the contralateral leg. In this nomenclature, the stance phase is defined by the ground contact of the ipsilateral leg.

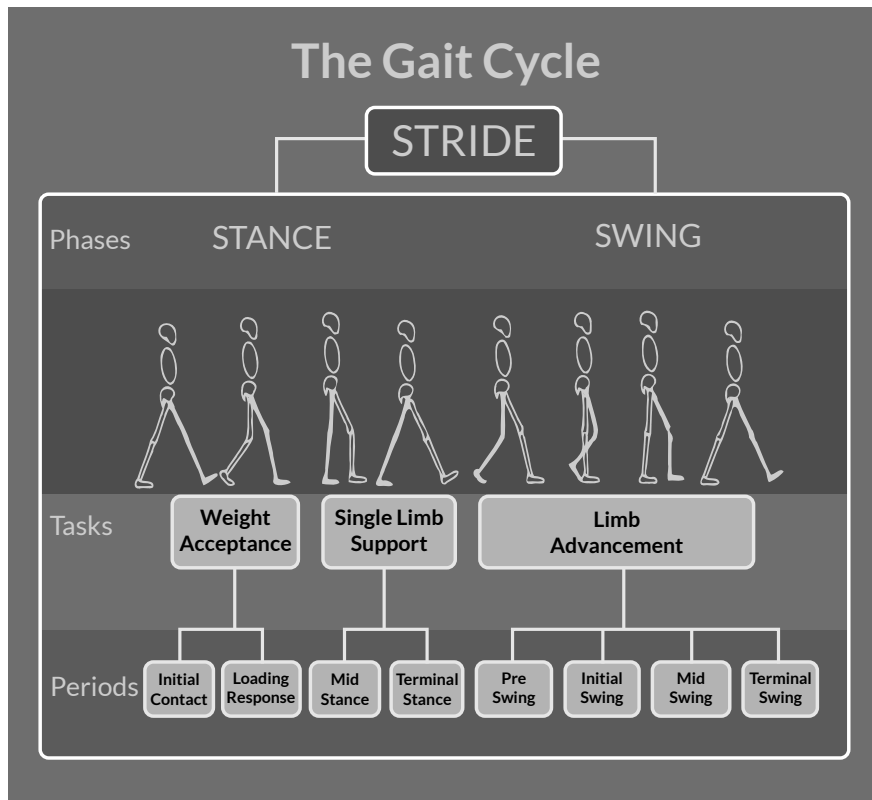


**Figure 2.2.:** In [84], Gamble and Rose describe the gait cycle as stance-phase and swing-phase, which they further differentiated into 3 tasks and 8 periods. This partitioning of the stride is from the perspective of the solid white leg. (Diagram adapted from [84].)

## Human Gait

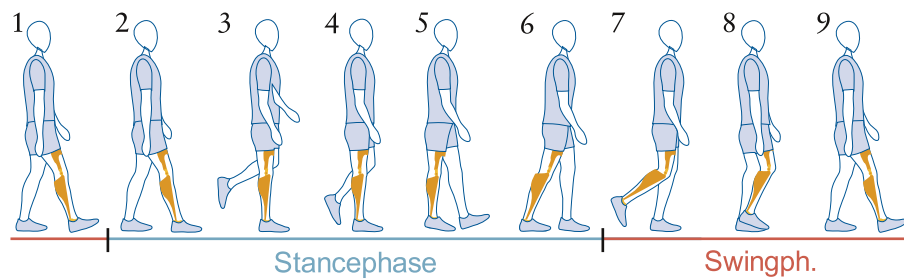


**Figure 2.3.:** Simple sequence showing the gait cycle, limited to the two gait phases: stance- and swing-phase. This diagram shows an important relation: the stance-phase constitutes around 62 % compared to around 38 % swing-phase during walking gait. This sketch will be used throughout the thesis for illustrations and is a modification of a figure © Otto Bock HealthCare GmbH [72].

### Phase Transitions

A consequence of the phase shift between the two legs is, as sketched in Figure 2.4, that while one leg swings, the body is in *single limb support*. These single limb support phases are mixed with intermittent phases of *double limb support*, in which the supporting leg is changed. The previously supporting leg then initiates swing phase and thereby the next step, which ends with the heel-strike, which starts the next *double limb support* phase and so on. While symmetrical, one single limb support/swing-phase makes up for around 38 % of the gait cycle, and one double limb support phase accounts for  $\approx 12\%$ . Taking these numbers together for one leg, the resulting stance-phase to swing-phase-relation for one leg is about 62 : 38 [43]; in other words, the leg swings only one third of the gait cycle.

These transitions between the stance- and swing-phases occur at events defined by foot contact: the heel-strike, or, more generally, the foot-strike, and foot-off of both feet, which happen in the sequence foot-strike at 0 % of the gait cycle, opposite foot-off at  $\approx 12\%$ , opposite foot strike at  $\approx 50\%$ , and foot-off at  $\approx 62\%$ . [43] further differentiates the gait cycle with ipsilateral *foot clearance* and ipsilateraltibia vertical events.

## 2.2. Description of Human Gait

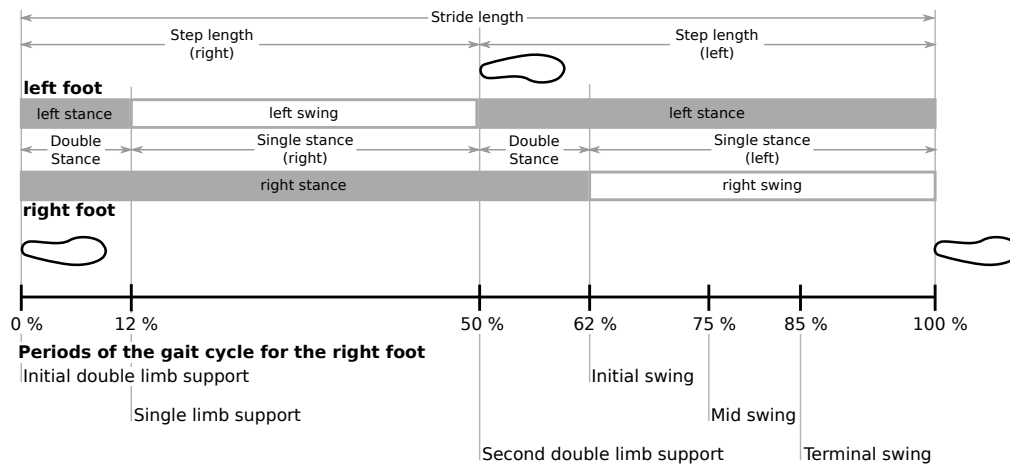


**Figure 2.4.:** Partitions the of gait cycle, as detailed in [43]. Shown are important geometric measures, body support- and gait phases. In the lower part of the figure, the *periods* of the right leg are aligned to the gait cycle (compare to Figure 2.2).

### Tasks

Connected to the alternation between standing and swinging is the description of tasks in Figure 2.2: Weight acceptance describes the transition of body support from one leg to the other during double limb support. This transition is finished for the following single support, when the contralateral leg is in swing phase. And limb advancement describes the step of the ipsilateral leg in swing.

### Periods

Advancing, whole hierarchies of refinements have been defined, the common ones include around 8 periods (like in Figure 2.2, but depending on the level of detail or focus of the investigation this varies), which the authors denote as periods and which we will describe now.

Commonly included are the *heel-strike*, or more general, the *initial (ground) contact*, and *toe-off*, [74, 84]. These phases are determined either observable events,

and sometimes by their role in gait dynamics. For stance phase, [84] defines the periods *initial contact*, *loading response*, *mid stance*, *terminal stance*, and *pre swing*.

The *initial (ground) contact* names the transition from swing to stance phase. During the *loading response* the body weight is transferred (sometimes called *initial double limb support*); it ends with the contralateral foot-clearance. The loading response is followed by a *single limb support* phase in *mid stance*, when the leg directly supports the body weight. In terminal stance, the heel starts to rise and the opposite foot touches ground. *Pre swing* is the end of the *second double limb support* phase, directly before ipsilateral foot-clearance.

In swing [84] differentiate between the *initial swing* which initiates with *toe-off* (or *push-off*). *Midswing* begins with maximum knee flexion and end with the leg perpendicular to the ground, which marks the start of *terminal swing* [43, 84]. In *terminal swing* the swing leg decelerates and goes to swing retraction before touch down and foot contact at the foot strike, as detailed in Figure 2.4.

## 2.3. Important Dynamic Properties of Gait-Phase-Transitions

Whereas empirical descriptions of observable events and the walker's geometry are quite common, the detailed understanding of gait dynamics are subject of on-going research and debate. Progress in the research of gait dynamics is propelled by modern developments for prostheses, measuring units and computer simulations, like the investigation of swing-leg retraction [77] or the interpretation of push-off [54, 81], which we will discuss now.

These events are important for us, as they are the transitions between stance and swing phases. When controlling an Stance-Controlled Knee-Ankle-Foot-Orthosis (SCKAFO), an assisting technology to support the body weight, these



### 2.3. *Important Dynamic Properties of Gait-Phase-Transitions*

transitions mark critical points where the device should change its state according to the period descriptions: from body support, which is generally marked by higher torques in the knee joint, the device has to go to a mode where the free leg swing is supported and vice versa. Working harmonised to the user's motion is of utmost importance.

For this reason we pick the transitions between swing- and stance-phases—the swing leg retraction and the push-off. An understanding of their role in gait dynamics allows us to estimate what a controller for a passive lower limbs orthosis may achieve; and they give a good idea of current developments on the understanding and interpretation of bipedal gait.

**The swing leg retraction** The retraction of the swing leg after maximal extension of the leg, but before heel strike, is called swing leg retraction. For humans, this can be seen for all walking speeds: the higher the velocity, the higher the retraction speed [77]. This effect is argued to reduce the impact shock and to stabilise gait dynamics.

**The push-off** During push-off, the ankle has a peak power output. This dynamic event was originally thought to reduce the contralateral impact forces and propel human walking. But recent model based studies [54, 81] suggest, that both reasons are unlikely, because the mass of the body is much too high and the timing of the main power output is after the stance leg's knee release [48], which would prevent the impulse to reach the body, but would support the acceleration of the swing leg, suggesting, that the energy stored in the ankle joints muscles and tendons while loading in the stance phase is used to initiate swing phase.

A set of studies [56, 67] analysing lower limb exoskeletons show strong agreement with these results. They found that a positive energy contribution to the patients gait could be achieved, when the ankle joint was powered at  $\approx 43\%$  of

the gait cycle. The actuation could be applied in the range from  $37 \pm 1 - 45 \pm 2$  % of the gait cycle to gain net energy reduction.

## **2.4. Motion Generation and Coordination**

After the description of human walking, we will now shortly summarise physiological components involved in motion generation. This will be important to understand the effects of gait impairment and their treatment with orthoses in the next chapter. And it will also be needed for the later introduction to EMG in chapter 10.

To get the necessary overview, we first briefly describe the nerve pathway driving the muscle activity, which us provides with a list of contributors. And then we shortly describe the role of muscles as force generating components with the help of Hill-type muscle models, which allows us to identify active and passive, elastic and dissipating properties of the musculoskeletal apparatus which produces human gait.

### **2.4.1. Nerval Control of Force Generation**

Active muscles generate force and thus actuate the body, and these muscles activity is controlled via motoneurons in the spinal cord. These motoneurons get feedback from nerve fibres in the limb and muscles, as well es motor commands from the motor cortex. We do not want to go into much detail as to where motion is controlled. Evidence has been found, that the human exhibit pattern generator-like behaviour after spinal cord damages, when stimulated: the stimulation leads to a cyclic stepping motion. But to which degree local pattern generation, modulated by afferent sensor signals, and higher layers in the cortical structure contribute to motion generation is the topic of an ongoing scientific debate.

It seems save to assume, that motion is initiated by means of abstract motor commands from the cortex, whereas the muscle activation is handled at the spinal

## 2.4. Motion Generation and Coordination

cord. Balancing is a process, which is driven by sensory input from the balancing sense in the ear lobe and optical information from the eyes and which influences, e.g., foot placement and ankle joint torques.

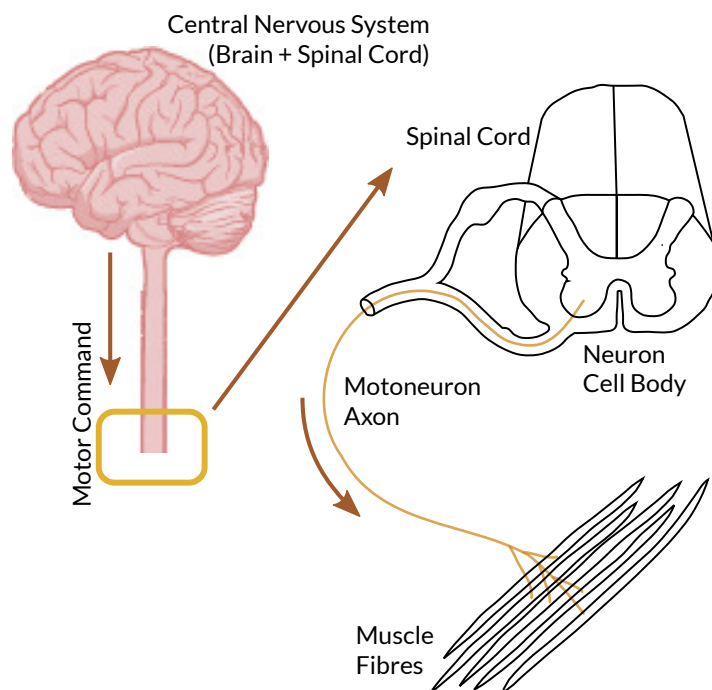


**Figure 2.5.:** Efferent path way of motor control commands from the central nervous system to the muscle fibres. License for the original brain image: CC BY Attribution 3.0 [11], original author: OpenStax College [71]. Spine & muscle fibre adapted according to [2].

At the end of this process is a set of action potentials which each enervate a set of muscle fibres and causes contraction of these fibres. In presence of an action potential, a relaxed muscle fibre will contract to around 57% of its rest length [2].

The conglomerate of motoneuron and innervated muscle fibres is called a *motor unit*. The action potential from the motoneuron is called motor unit action potential (MUAP). Each muscle consists of many muscle fibres, which are grouped to different motor units. These motor units have different number of fibres, and

fibres with different contraction speeds and forces. When motion is generated, the nervous system *recruits* sets of motor units to generate the desired forces. The number of motor units and their varying properties allow the control of short pulses as well as long-lasting contractions of different forces.

As muscle fibres can only contract, the human skeleton is packed with antagonistic muscle pairs. Only in combination of antagonistic muscles, the human body can generate flexion and extension of joints.

## 2.4.2. Models for Mechanical Properties of Muscles

Muscles are the actuators of gait: They produce the forces necessary to support the body, propel it and keep it stable. While we do not need to know the details of how muscle fibres contract, it will help us to see how muscle forces can be modelled to understand the consequences of pathologies as well as the mechanical support a specific orthopaedic joint can give.

In this section we will present simple models of muscles. We will limit this overview to *Hill-Type models* of mechanical properties—to the extent necessary to understand parallels between the orthosis as external body support system and native human muscles [105, 108]. We choose Hill-Type muscle models, as they define damping and spring-like mechanical properties in a very accessible way.

From the 1920ies on, experiments characterised mechanical properties of muscle fibres. 1938, Hill published his work [31] on heat output of muscles contraction and lengthening, including isometric tetanisation, load on the fibres and muscle contraction speed, which gave these muscle models their name. He showed on frog muscle fibres, that stimulated muscles can be described as visco-elastic bodies [31, 108].

In common Hill-Type models, such as in Figure 2.6, the muscle is a mechanical object which can exert a force on its surrounding. A muscle is composed of a

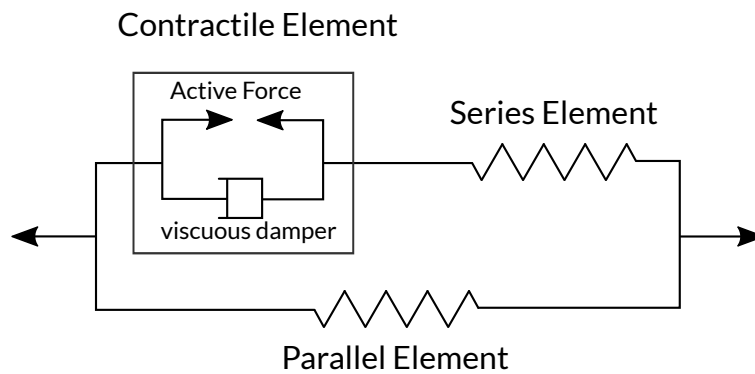


**Figure 2.6.:** Diagram of a general Hill-Type muscle model: The contractile element provides active features, e.g., to create force or behave like a viscous damper. The series and parallel elastic elements model passive properties of muscle-tendon apparatus and the surrounding tissue.

*contractile element*, which can actively shorten a muscle and dampen the movement. This contractile element is complemented by connective tissue, which is considered passive and is modelled as *series elastic element* or *parallel elastic element* and may include further visco-elastic dampers [105]. These types of models can have arbitrary levels complexity, depending the modelled dynamics and desired degree of detail.

Here, we want to focus only on a few properties: A muscle generates force depending on mechanic properties, for example load, contraction speed, length, and stimulation by the motor neurons [105]. It can store and release energy, in a nonlinear-spring-like way, and it can dissipate energy. These properties result from a combination of passive tissue (the muscle-tendon apparatus and connective tissue) as well as actuation due to excitation of motor units.

## 2.5. Summary

We now possess a nomenclature to describe walking gait in humans, which the presented orthosis is ought to support. With the detailed description of the gait cycle and the transition between the phases we already got an impression of what

## *Human Gait*

the controller for the presented orthosis has to do to harmonise with its user's motion, e.g., coordination of forces at knee-joint level to allow body support in stance and free movement in swing phase. Taking swing-leg retraction and push-off into account, we can pin the moments of knee-release and support to these phenomena.

Muscle forces can be modelled from damping and elastic contributions by muscle fibres and surrounding tissue. This facilitates dissipation of energy in the damping component as well as the energy storage and release in the elastic components. The activation of muscle fibres is initiated by nerve pathways which come from the motor cortex over the motoneurons in the spinal cord, and which incorporate sensory information about limb configuration, muscle stretch, load and balancing.

The description of components which take part in motion generation allows us to now go on to pathologies of human gait in the next chapter. There, we will formulate a more detailed description of what passive, assisting technology for the lower limbs can and should achieve.

# 3

## Treatment of Gait Pathologies

In the previous chapter, we have developed a description of human gait and briefly listed components contributing to the generation of human gait. This enables us to take a look at pathologies and reasons for impaired gait. Again, we won't go into the details: we want to know how the need for assistive devices in human gait arises.

We will complement this excursion with an overview of available assistive technologies and their interaction with the patient. We will summarise studies on how the patient benefits from supportive devices and is able to regain mobility, but we will also take a look at problems and gait deviations in orthosis users. We will shortly pick up the important question of device acceptance, which determines if a patient will really use an orthosis, or if it will be abandoned shortly after prescription.

This collection of medical indications, together with the compilation of assistive technologies and their acceptance by patients will allow us to define what we can expect from a passive KAFO.

### 3.1. Impaired Gait

In general, for the devices discussed in this thesis we will be facing a lack of control by the user. The reasons lie along the whole pathway we described in section 2.4.1, for example

- damages in the cortex after stroke, encephalitis or brain abscesses
- paraplegia, multiple sclerosis, or other damages of the efferent nerves, at the spine level after accident or operation, or below spine level towards muscle groups or single muscles
- damages of the muscle-tendon apparatus, for example myopathy

The result is the inability to create specific forces which are needed to complete the gait cycle. This may be due to too little strength to hold the body weight, or to immobilise a joint in support or due to a reduction of the mobility in the joints.

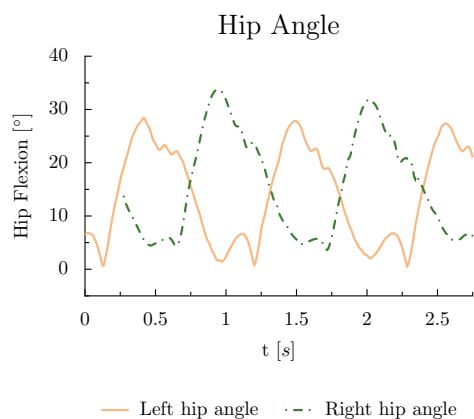
The effects on the patient's gait can range from such reduced joint motion, see Figure 3.1, to the inability to walk. In between lies the full range of asymmetric gait due to preference of a healthier side, limping and other features which often result from a combination of impairment and technical support, which we will visit in more details in section 3.3.2 with a review on side effects of orthosis-use.

### **3.1.1. Changes in Statistical Properties of Human Gait**

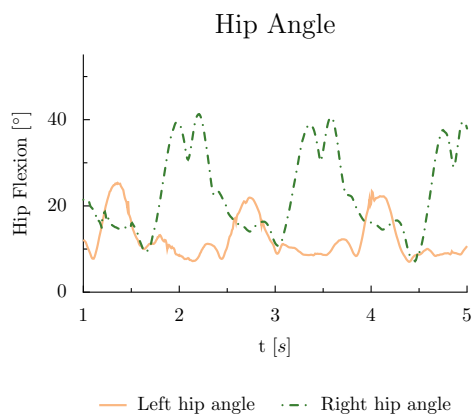
It is interesting to note, that there are fundamental consequences for statistical properties of human gait, which have been analysed for specific cases like Parkinson's disease [28]. The argument has already been made in the previous chapter, that because inherently unstable, human gait is often referred to as "falling forward in a controlled way", which is a free reformulation of the inverted pendulum model. [49, 66] Statistical properties reveal an insight into the walkers ability to control disturbances. From the perspective of the controller they might provide an easy way to integrate measures of gait stability.

Step frequency is quite stable in healthy walkers, the stride time variability is low. For other statistical measures, like the fractal index of stride times or the stride width variability, it seems to be an indication of impaired walking if the

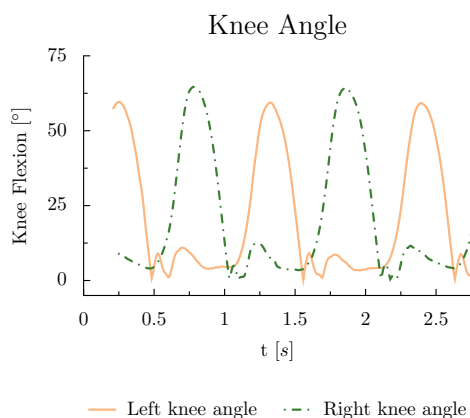




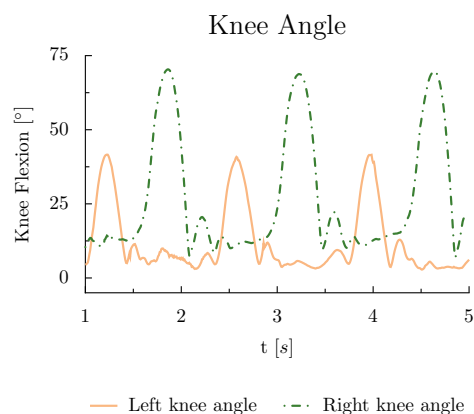
(a) Hip motion of healthy walker



(b) Hip motion of orthosis patient



(c) Knee motion of healthy walker



(d) Knee motion of orthosis patient

**Figure 3.1:** Reduced joint motion. Left: healthy walker with mostly symmetric knee and hip joint range. Right: orthosis patient with reduced knee joint range and in consequence completely asymmetric hip motion.

variability is very low or high [27]. Such measures seem to show the walker's ability to adapt to external influences: the walker's trace of gait stabilisation can be tracked in the statistics. [27] could associate increased stride-to-stride fluctuations in the stride time with a higher falling risk. In [28], the influence of Parkinson's disease on gait statistics showed an increase in variability, too.

[103] investigated the variability of *kinematic and kinetic patterns in human gait*, concluding that the within-subject variability in terms of kinematics are quite low, but that the *moment of force patterns at hip and knee were highly variable* with the latter variability leading to *identical joint angle patterns during stance phase of walking*.

In consequence, variability in gait statistic can be used to measure the ability to stabilise gait. The ability to produce a highly variable moment of force pattern at hip and knee seem to be a requirement for regular walking. This creates a direct connection between reduced muscle forces and muscle control and the regularity of statistical gait properties.

## **3.2. Quantification of Medical Indications**

Considering the loss in control and muscle force, and the resulting changes in the patient's gait, the question is how the deviation of gait or loss in control and muscle strength can be assessed for the treatment with an orthosis. This is the task of clinical gait analysis [101]. Again, we will only scratch this topic to the degree necessary to understand the medical indications for the presented orthosis.

In general, it is possible to analyse how the possible motion compares to regular gait. To this end there exist gait deviation indexes, which take the information gathered in a gait laboratory and reduce the multi-dimensional data to a simple index. [87] for example uses principal component analysis to reduce the dimensionality of gait laboratory data and to extract a single number which indicates the distance of a specific gait to the averages of walkers without abnormalities.

### 3.2. Quantification of Medical Indications

Level	Short	Description
5	normal	full, regular strength (This says nothing endurance and other properties).
4	good	Around 75 % of regular strength; a resistance of medium strength can be overcome.
3	fair	Around 50 % of regular strength; a full movement against gravity is possible.
2	poor	Around 25 % of regular strength; a full movement is possible, but not against gravity.
1	trace	Around 10 % of regular strength; a trace of tension.
0	zero	No muscle contraction possible when movement is tried.

**Table 3.1.:** Muscle status after Janda: after test the muscle ability is classified from 5, full strength, to 0, no strength. In this way, the remaining abilities of a patient can be mapped to a simple scheme.

While gait normality indexes can assess the form of a patient's gait, the orthopaedist needs a different tool to measure the remaining abilities of a patient and compare this against the support a supportive device provides. One such tool is the definition of the muscle-status after Janda [38]. The patient's remaining abilities can be tested with muscle-specific movements: can the patients induce muscle contraction, are they able to generate motion and against which resisting forces can they generate movement? The answer to these questions provides a simple number according to table 3.1 for every muscle group, which describe the patient's remaining abilities. For an example, please check section 4.2, which includes the counter piece for the presented orthosis.

### **3.3. Treatment of Impaired Gait**

Depending on the strength of the gait abnormality, the amount of affected muscles, and the confinement of the patient's mobility, different approaches are suitable. We will first compile state of the art joint-technology, before we will review the literature on the effect and use of current braces by patients.

The literature covered will include orthoses and prostheses. It is important to keep in mind, that a loss of control or muscle force is in contrast to limb loss, where prostheses are applied. For the application of orthoses, additional factors have to be considered, which impose additional limits on the device in question: in comparison to prostheses, volume and weight are important factors, as the patient's original leg is still there; the orthosis as a splint has to have a low weight to reduce the stress of load on the patient; and it should exhibit a low volume, to keep a low aesthetic and dynamic footprint, as we will see later.

We will not cover other procedures, for example functional electrical stimulation (FES), which is able to excite muscle fibres. FES can be used to short-circuit defective nerve pathways to reestablish a functional muscle as actuator. As we are interested in mechanical assistance, this is not covered, although it would be possible to use the presented controller in combination with FES.

#### **3.3.1. State of the Art: Joints & Actuation**

Nowadays, specialised prostheses produce incredible feats, for example as in the dance presentation in Hugh Herr's TED-talk "The new bionics that let us run, climb and dance". For specialised prostheses it is an ongoing debate, if they can perform better in their domain of specialisation than the corresponding human limb, like in the case of Oscar Pistorius at the World Championships in Athletics. Nonetheless, in terms of flexibility and general comfort of wear, assistive technologies still have a long way to go—and besides those exceptional examples, in everyday life they aren't used because of their superiority, but because they are needed to do things their users otherwise couldn't achieve.

### 3.3. Treatment of Impaired Gait

The development of assistive devices is long. The oldest known device which could be described as a prosthesis was found in an Egyptian mummy of ca. 3000 years age [68], the big toe has been replaced with a wooden toe model, finely carved and painted. Even evidence of splints is even older and reaches back to the Old Kingdom (ca. 2400 BC) [70]. A more than 4500 year old depiction of a crutch can be found in Hirkouf's tomb, which was built around 2830 BC [33].

Today, there exist many technical devices and control strategies for assistive devices. These range from stiff splints, over computer controlled joints to active devices, some of which are even to be controlled via brain computer interfaces (BCIs).

We shortly discuss joint mechanisms and actuation methods to prepare for a more detailed discussion of control approaches, which we will relate to the design aims of this work. We will restrict our overview to established mechanical assistive technologies. For a list of further readings, please see in the next section.

The actuation can be sorted according to different categories. As this thesis is mostly concerned with the controller, we will take an according perspective on possible actuation, differentiating between passive, i.e., no actuation; semi-active actuation, which means actuators which are not powering movement; and active actuation including exoskeletons, which can sustain the whole motion of the limb or body. The reason for this sorting is, that devices and controllers of interest for the presented work fall into the category of semi-active and active devices.

For this reason, we will use the term semi-active for all devices, which include a controlled actuator, even if it only is a two-state joint lock.

From a technical perspective, it is tempting to separate the devices into mechanical, hydraulic, pneumatic, electric, etc., according to their technology. If you are interested in a structured and more elaborate overview, please consult [5, 39]. [106] puts a focus on mechanical control mechanisms for Stance-Controlled

Knee-Ankle-Foot-Orthosis (SCKAFOs), but includes one electromagnetic control mechanism. The book [33] provides a comprehensive overview, which includes contemporary devices. Many of these sources name the combination of hardware control system and control software the control system.

## **Passive Devices**

Passive devices are devices without actuation and no active control logic. They range from inlays for shoes, and crutches to leg splints which can be mechanically locked by user intervention. We include non-controlled locking mechanisms too.

All these devices have in common, that their behaviour is defined in the mechanics of the joint lock. Many of these devices are lightweight because of simple and small joints and the lack of batteries and actuators. They often are suited for patients with need for little or specific support.

The simplest splints allow to lock the knee joint for standing and walking and unlocking for sitting. Walking with an continuously extended knee joint naturally leads to problems in the swing phase. Joints with automatic locking mechanisms often apply a kind of threshold switching [52, 106], which we describe in the control approach section.

## **Semi-Active Devices**

As for passive devices, semi-active devices have quite a variety in their complexity. From electromagnetically released mechanical locks in [106], to complex pneumatic or hydraulic systems as in [92, 109] or the present work. Semi-active devices cover every kind of lock, brake, damper or even spring mechanisms [90].

Actuators in these devices influence joint properties; as no big masses are actuated, these devices are more energy efficient than active devices and therefore the most advanced devices in the field.

#### **Active Devices**

Active devices and exoskeletons provide actuation; these devices can not only be used to assist impaired walkers, but also to boost the abilities of healthy walkers [17].

As these devices can initiate locomotion, they can target many patients which do not possess the mobility to use passive or semi-active devices. Especially for prostheses on the upper limbs, active devices are needed to introduce voluntary motion. By contrast, lower limb orthoses can react to motion induced by the mechanical coupling through the patient's body.

Current technical problems include the battery duration [17, 93], as active motion of masses consumes energy, and the additional weight of the battery and actuators which either the patient has to bear, or a voluminous frame could handle. The size of powerful actuators and the holding frame is a cosmetic concern, which is a more pressing issue for orthoses than for prostheses, were the amputated or missing limbs leave room for technical apparatus.

Therefore, active devices are most common in technical facilities, like factories. In rehabilitation, were the short battery life is not a concern or the device can be connected to the power grid. Finally, for upper body prosthesis, where the patient's body is strong enough to bear the weight and actuation is needed to initiate, for example, a grasping action.

Active devices provide a wide variety of actuation mechanisms including contractile polymer gels, shape memory alloys. It is outside the scope of this thesis to cover all existing actuation mechanisms and the interested reader is suggested

to read further literature like [5, 17]. We will restrict ourselves mostly to mechanisms and works, which have been used with applications and control mechanisms which are interesting in the scope of this work.

In current devices we often find pneumatic actuators in [94, 99]. In [93], a DC-motor driven ball-screw is presented which is applied in [50, 51, 95, 100]. [29] presents a device actuated by a magnetorheological fluid, and [6] work with a Series Elastic Actuator (SEA), a combination of a spring element and a DC-motor.

Whether for prostheses or orthoses, all these devices allow actuation and therefore possess elaborate control mechanisms which are of interest. Still, for everyday use, these devices are too power consuming or heavy [17, 93]. Nonetheless, many of these devices can be used for shorter periods of time, in rehabilitation at home or in clinics. Examples include [82] for the upper, or the gait trainer LOPES for robotic treadmill training [18].

### **3.3.2. Side-Effects of Prosthesis- and Orthosis-use**

Another aspect of the human-orthosis interaction are deviations which are a consequence of the device or missing trust into it.

The review [21] collects possible deviations in combination with prosthesis use. This includes a general favouring of the impact limb. This leads to additional stress on the healthy body side which in consequence can lead to secondary conditions. Possible consequences are (1) degenerative changes like trunk asymmetry, osteoarthritis, and scoliosis; (2) pain (in the lower back or the hip and knee joints), or (3) general deconditioning. Visible symptoms include an asymmetric and slower gait. Examples for this asymmetry in gait include the step initiation with weight on intact limb, or pelvic tilt to compensate missing hip extension (hip hiking).

Specially for orthoses with fully extended knees, [107] lists compensatory gait patterns, like “increased upper-body lateral sway , ankle plantar flexion of the



contralateral foot (valving) hip elevation during swing phase (hip hike) or leg circumduction”.

[83] advises that “the physiotherapist should teach efficient control of the prosthesis through postural control, weight transference and use of proprioception”. This stresses the fact, that a device often imposes specific compensatory movements.

The literature review [65] comes to the conclusion, that “there is a large amount of variability with regard to how patients respond to orthosis”, after considering factors like orthosis build and effects on load, ground reaction forces and changes in joint motion.

All these studies suggest, that the individual fitting of the orthosis can have a significant impact on the outcome, concerning the gait as well as the orthosis’ perception by its users. Furthermore, the changes induced in a patient’s gait surface on long timescales ([35, 36]); [83] speaks from a “lifetime of adjustments”. Thus, the ability to influence the devices behaviour and fitting onto the patient are important features. For the best medical outcome as well as patient acceptance, the specialist as well as the user’s comfort have to be considered.

#### 3.3.3. Patient’s Perspective and Device Abandonment

The last aspect of comfort and patient acceptance of the device is of utmost importance for the brace to make a difference, as many studies suggest that patients will silently abandon devices which do not comply with their expectations and life-style: It depends on the comfort provided in every day life, for example the ability to easily don/doff the device as well as on cosmetic properties, i.e., how the device alters users in their perception of their own, or those of others [3, 61, 83].

The authors of [44] cite several studies whose subjects abandoned their orthoses with rates in a range “from 60 % to nearly 100 %”. In the case of [76] 35 of 60

## *Treatment of Gait Pathologies*

users of lower extremity braces abandoned their devices. The authors identified as top reasons for device abandonment

1. “change in the need of the user”, i.e., changes in priorities or medical indications.
2. “ease of obtaining the device from the supplier”, i.e., the effort to get access to the same device again.
3. “device performance”, i.e., if the “device met the user’s expectations for effectiveness, reliability, durability, comfort, safety and ease of use”.
4. “whether the user’s opinion was considered in the selection process”, although it was not important, if there were “alternatives to choose from”.

In [64], of 35 replies 31 % indicated to not use their brace anymore and “60 % continued to use their wheelchair as their main means of displacement”. As reasons the authors cite the opinions on the device as being “too difficult and time consuming”, or a “lack of suitable space in the home environment for proper use”, besides other reasons. These opinions focus on the practicality of the device, like the ease to don and doff, and the volume requirements.

In a survey targeting 250 veterans by [32] at 22 months after rehabilitation programmes, only 16 of 73 reached patients were still actively using their braces, the other 78 % had abandoned their devices. Analysing the answers their survey, the authors could rule out marital status, educational level, employment status, living arrangements, social activities and sports participation. However, they found significant relation “to the level of injury, severity of injury, medical complications and the level of dependence on their status in activities of daily living”. Where the first group of reasons is connected to the patients remaining abilities and the last refers the the ability to easily don and doff the device.

These abandonment rates give a huge weight to the patient’s perspective of the prescribed brace. In a survey on consumer opinions regarding a SCKAFO [3] the authors observe, that the patient’s impressions mainly stayed the same from 1 to 3 to 6 months after orthosis fitting and training and that “all participants mainly

### 3.4. Summary: Individualisation to Increase Device Acceptance

commented on size, weight, and appearance of the knee joint”. Especially in comparison to simpler mechanics, that the orthosis was “more difficult to don and doff”, cosmesis was “slightly less than acceptable” up to the point that the selection of clothing was difficult due to the volume of the apparatus.

## 3.4. Summary: Individualisation to Increase Device Acceptance

We have determined defects, which lead to a loss of control or muscle force and made a brief review on assistive devices (for a review of control strategies see section 5.2). These devices help their users to regain control over walking, to increase their walking speed and range of joint motion. But we found extensive discussions of problems in the literature, which pertain *patient behaviour*, as the favouring of the healthy limb, and consequential changes to the musculoskeletal system with secondary conditions up to sclerosis.

Finally, we found literature on what is important from the patient’s perspective. Presented studies show high rates of abandonment, which are related to the comfort and ease of use, but also to cosmetic considerations and the inclusion of the patient into the process, which suggest the individualisation of the patient centring of the orthotic intervention [61].

For these reasons, we deem it important to demand the ability to tune the device’s behaviour to the maximum extend to the patients individual gait and allow the patient to influence the devices level of support. The sensory equipment has to be included in the orthosis frame to keep the ease of use as high as possible, although the controller can not influence the needed volume and ease of don and doff of the frame.



# 4

## Passive Support with the Presented Orthosis' Brace

Up to now we considered human gait and impaired gait. We discussed problems arising from the treatment with orthoses and started to formulate requirements regarding the individualisation of the brace and its behaviour in the previous chapter. We will now relate these observations with the hardware features of our orthosis frame, the so called brace.

Then, considering the shortcomings and problems of prolonged orthosis-use, the presented orthosis frame and its medical indication, we will discuss the support the presented prototype can give in general and formulate requirements and aims for the controller, before we will go on to the control problem in the next chapter.

### 4.1. The Knee-Ankle-Foot-Orthosis

Our experiments has been conducted with a Knee-Ankle-Foot-Orthosis by Otto Bock, which have been developed in the course of project 3a of the Bernstein Focus Neurotechnology Göttingen. The devices are spanning from the upper thigh down to and including the foot. At the knee joint, a C-Leg<sup>TM</sup>-element controls the joint's damping properties for knee flexion with a hydraulic system. Control over knee extension is intended but was deactivated for security reasons by Otto Bock's engineers. The C-Leg<sup>TM</sup>-element includes motors, which can

open and close valves in the hydraulics as to dampen or prevent movement in the knee joint. These motors can be controlled via software.

By design, the presented device is classified as a *Stance Control*-type (SCO) of *Knee-Ankle-Foot-Orthosis* (KAFO) or combined as SCKAFO. Stance control refers to orthoses which allow for knee flexion during swing phase and body support in stance phase. Thereby allowing a more natural swing. On their homepage, Otto Bock describes that a free swing phase in comparison to an extended leg in swing decreases *Vaulting*, *Hip hiking*, and *Circumduction*. These are common problems for orthoses with static knee extension [107]—it can easily be seen, that the patient has to take special measures in swing phase, when the swing leg is fully extended.

A Knee-Ankle-Foot-Orthosis spans the lower limbs from upper thigh down to and including the foot. Amongst other uses, Knee-Ankle-Foot-Orthoses may be applied to support or stabilise from the hip downwards. The mechanical structure can be used to limit or correct and control the joint movement. As the focus of this study does not lie on these orthopaedic applications of the mechanical structure, but on the knee damping control with the aim to optimally support bipedal gait, we will focus on the latter. Possible conditions for optimality were discussed in section 4.3.

**Mechanics:** During the course of this project, collaborators from Otto Bock devised two prototypes with differing ankle joints, as shown in Figure 4.1. The controller was initially developed on a model with a compliant shank bar, as in Figure 4.1(a), which presents a fixed ankle joint for patients with insufficient muscle status in the lower leg, like in the case of drop-foot.

Later on, a prototype with schematics as in Figure 4.1(b) with a flexible ankle joint was developed. The ankle joint is a standard orthosis joint by Otto Bock, with tunable stiffness and movement limitation. The preliminary controller was transferred without changes and used for the experiments presented in this study. Thus together, both prototypes allow more differentiated support of the patient.

Development and tests on both devices allow broader application of the presented controller, which is built without an explicit model of the hardware. The sensors capture the positional configuration of the device and thereby the walking dynamics. The device is therefore only modelled implicitly via the patients gait dynamics.

**The Sensors** are detailed in chapter 7. The sensor selection is based on the experiments presented in chapter 6. The first prototype, sketched in Figure 4.1(a) had a knee joint which allowed to instrumented. The experiments preceding the construction of the current C-Leg™-knee-joint in Figure 4.1(b) led to the inclusion of an angle sensor based on the hall-effect by Otto Bock. At the end of the BFNT-Project, Otto Bock quipped an additional strain gauge on the right side of the ankle joint. Angle sensors based on inertia measuring units (IMUs) were provided by Otto Bock in course of the cooperation. These angle sensors allow to determine the orientation in a plane relative to the centre of gravitation.

## 4.2. Medical Indications for Semi-Active Orthosis Use

After the introduction of the here used orthosis prototype, we will take a look at its medical indication to get the orthopaedic and orthopaedic technology background for controller development in the next chapters. Throughout the thesis and the accompanying project, two orthosis-prototypes were developed which are shown in Figure 4.1. The first in Figure 4.1(a) has a compliant shank bar and was developed by Otto Bock together with the medical in indications in this section. The later prototype in Figure 4.1(b) has an ankle joint and therefore is better suited for patients with better muscle status at the ankle.

This section about the medical indications is a result of orthopaedic patient analysis by Otto Bock and had first been published in the Bernstein Focus Neur-

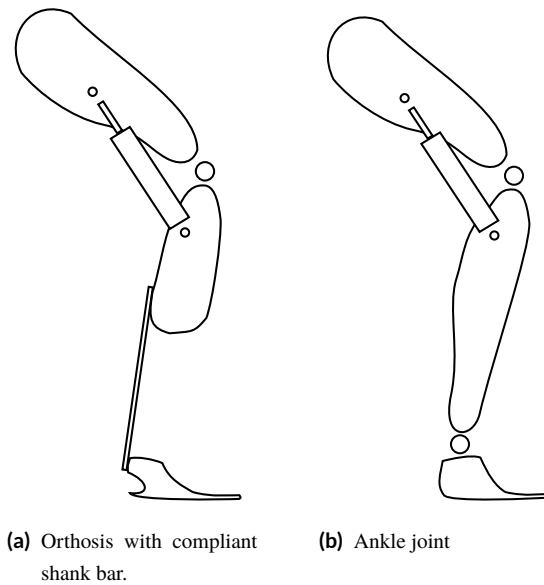


**Figure 4.1.:** Schematics for the available orthosis setups. In 4.1(a) the ankle joint is realised with a compliant shank bar, which can store energy during roll over and release it push-off. The otherwise fixed ankle may support drop foot. 4.1(b) is equipped with an ankle joint, which can be rotated freely or can be fixed to limit joint motion. While the sole is still flexible, the device is intended for patients with higher muscle status at the ankle. The medical indications presented in this chapter refer to the first prototype (with the compliant shank bar).



#### *4.2. Medical Indications for Semi-Active Orthosis Use*

otechnology Göttingen technical report of 2011 in German language [4]. The cited work was done by employees of Otto Bock for the Project 3a and has been translated for this thesis.

The orthosis is a knee-ankle-foot-stabilising-orthosis (KAFO = Knee-Ankle-Foot-Orthosis) with monocentric orthosis knee joint and a hydraulic damping element. The damping element allows active control over the knee joint's damping over a wide range with an electronic interface. Carbon components allow high stress and a dynamic carbon spring at ankle level limits the ankle joint movement to ca 2°.

Extensive gait analysis, as conducted by the Otto Bock Health-Care GmbH, suggest a very broad area of application. This includes patients with reduced motor function of the lower extremities based on a partial paraplegia or on a apoplexy, as well as myopathy, multiple sclerosis, encephalitis and brain abscesses. Provision is conceivable for patients with a muscle status after Janda according to Figure 4.2.

On the strength of past insight, exclusion criteria are: remaining mobility of  $< 2^\circ$  in the ankle joint; ankle arthrodesis; body mass  $> 120$  kg; knee bending contracture  $> 5^\circ$ ; deviation of the leg axis of the frontal plane  $> 10^\circ$  valgus or  $> 0^\circ$  varus; uncontrollable spasticity; bad trunk- or arm-control.

It has to be noted, that this original report about the medical indications has been pursued for a prototype with a compliant bar at the shin, which stiffens the ankle and is able to support problems like drop-foot. Please compare Figure 4.1(a) in section 4.1, The Knee-Ankle-Foot-Orthosis.

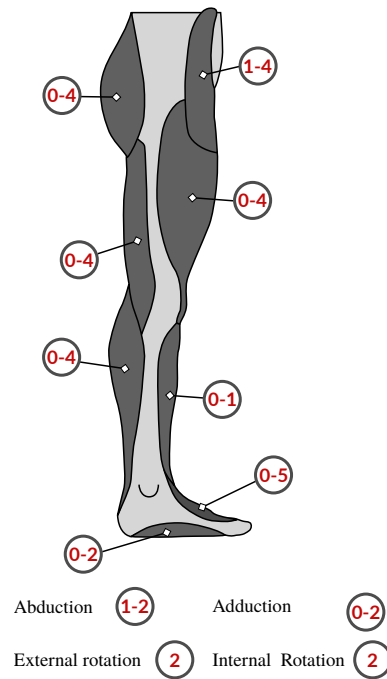


**Figure 4.2.:** Muscle status after Janda (compare Table 3.1), for which the presented orthosis prototype is suitable [4]. Required are remaining abilities for hip flexion, abduction, external and internal rotation, i.e., the leg as a whole can be reoriented and swung below the body. Figure adapted from material provided by Otto Bock for [4].

## 4.3. Discussion: The Orthosis' Impact on Gait

Taking everything together, we will formulate aims for an adaptive orthosis controller, based on the presented facts on human gait, human-orthosis-interaction, and the identified opportunities for an adaptive controller. We will go through these parts one at a time.

### 4.3.1. Physiological and Mechanical Constraints

First, we will take a look at the constraints coming from a human with limited walking abilities in combination with the probable device category.

#### Passivity of the Device

The presented orthosis is a *semi-active* orthosis, which means that its active properties are no actuators for motion, but acting on passive properties in the gait dynamics. The motivations for this restriction are simple: such a device will never actively harm the user, while it uses much less energy than a device, which will move body parts. Its lower energy consumption is also important, as the total load on the patient is a critical parameter for patients with reduced muscle capabilities.

As a consequence, the patient has to provide all the energy to induce locomotion. The controller can only try to activate its components as energy-efficient as possible. This includes the energy-efficiency of the user as well as the efficiency of the device. Further constraints are discussed in the next section Hydraulic Damping.

The damper passively provides body support, which is a stance-phase task. Our main contributions to energy efficiency may be achieved at the transitions, during foot-lift-off and heel-strike. According to the effects described in section 2.3, we should allow (1) swing leg retraction and be able to optimise the lift-off. For

### *Passive Support with the Presented Orthosis' Brace*

swing leg retraction, this might include knee flexion immediately before heel strike. For the lift-off, we might have to allow a release the knee-locking immediately before contralateral heel-strike. Both of these effects may conflict with traditional safety measures in orthosis control, e.g., maximum stability due to long knee stiffness at initiation of swing, and early locking of the knee joint.

In general, experience and above arguments make clear, that a higher energy consumption through use of the device is likely, but subject to optimisation.

### **Hydraulic Damping**

The implications of the hydraulic damper at the knee-joint concern what we can do, and what we can't in terms of extending the available muscle activity. Hill-Type muscle models (compare section 2.4.2) provide a combination of damping and stiff components. The damping provides energy dissipation, whereas the different stiff components provide passive tissue properties as well as active muscle contraction, in other words energy storage and use.

With a hydraulic damper, we can only extend the abilities to dissipate energy, from a minimal break up to an effective joint lock.

Again we conclude, that the device will impose higher energy demands of the patient, in this case due to active dissipation.

### **Interaction with the Patient's Abilities**

The presented device aims to support patients, where their abilities do not enable stable walking, with the desired abilities in the range defined in section 4.2.

But in the discussion so far it became clear, that the device will lead to higher energy costs when comparing a healthy walker with and without orthosis.

On one hand this means, that the patient has to provide force and momentum with other muscle groups, complementing the stability provided by the orthosis

### 4.3. Discussion: The Orthosis' Impact on Gait

with actuation. As sketched in section 3.3.2, the patients tend to favour the contralateral leg and may use almost any body part to induce moment, including turns in the upper body (see chapter 10).

Patients will show very individual, yet systematic deviations, as reaction to their muscle status. We have to assume, that the introduction of the orthosis as disturbance will lead to a change in these systematic deviations [35], which will most likely settle while the patient gets used to the device, although this might be on timescales beyond 6 months [36].

As a consequence, firstly for optimal gait support the device should be able learn the patient's gait. And secondly, the ideal device should be able to adjust its memory of gait to gradual changes in the patients motion.

On the other hand, the muscle status of the whole body constitutes the range of motion the patient can access. So if a patient will be able to walk stairs will depend on other muscle groups than his ability to walk on flat ground. The device can only support abilities for which its users provide the necessary actuation. Depending on the muscle status, other orthosis skeletons might be indicated (compare section 7).

Whereas we have been discussing the ways, in which the device can support the patient, it has to be noted, that the device should not support above the necessary measure. Otherwise, training effects will be reduced and the patients might lose abilities, they could preserve with additional training through reduced support. To optimally support individual abilities, it is therefore helpful to allow detailed tuning of amount of support the device provides.

#### 4.3.2. Recovery of Healthy Gait

A simple approach to define the aim for an orthosis controller would be to recover the patient's gait to a gait comparable to those of healthy walkers. In theory, there are many indexes available which *quantify deviations from normal gait* [87, 88]. While these indexes often include gait laboratory equipment, one could assume

that an aim for orthosis and controller development could be the reduction of this gait deviation.

But given the device's passivity and accounting for systematic deviations in a patient's gait, including avoidance movements with preference of the contralateral leg; and asymmetric propulsion through asymmetric muscle status in many patients, it is unlikely that it is possible to reduce the deviation to 0. At least a certain amount of asymmetry will stay.

It might be possible to design a system, which will distribute avoidance movements on more or different muscle groups, thereby reducing the stress on singular muscles, effectively influencing the arousal of secondary orthopaedic problems.

Another approach could be to try to restore symmetry of gait. But although this seems to be a viable direction of change, there is no reason to assume, that this will actually help the orthosis' users.

Therefore, we want to focus on the impression of the user of the orthosis. Although quantification is difficult, the patient's impression with the help of orthopaedic seems a reasonable approach.

### **4.3.3. Expectation Management**

To reach all aims discussed in this section is out of the scope of this thesis. Therefore we want to pick a set of aims we can actively pursue.

We will not focus on energetic optimisation of the controller, nor do we strive to restore the gait of an unimpaired walker.

We want to create controller, which

1. is able to capture the individual features of patient's gait; and
2. supports adaptation to changes in the patient's gait.

### *4.3. Discussion: The Orthosis' Impact on Gait*

3. allows to reduce the amount of support given according to the patient's needs, and
4. can be tuned in a way, which leads to comfortable and secure gait.
5. The controller should support the patients in as many environments as needed in their daily life, enhancing their mobility, whereas current controllers often support only a number of gaits fixed at design time (compare section 5.2.2).
6. We want to implement this controller such, that one can influence the control-output in the activity of specific muscle groups.





## **Part II.**

# **Control-Problem and Sensors**



# 5

## Definition of the Control Problem

In the previous chapters, we defined aims based on the hardware's abilities and affordances and influenced by the patient's perspective. Namely, we want to design the controller in a way which is highly customisable with regard to individual gait and needed support, with easy integration of patients feedback. To this end, we will now develop the principal controller components based on the idea to include the user as an external pattern generator, driving the motion as well as the controller directly.

We will start with observations on how adaptive gait support can be achieved. In the state of the art, we will discuss existing solutions to this regard and develop the idea of gait progress driven control. Based on these considerations on human gait sample data, we will develop prerequisites for the sensory equipment.

### 5.1. Approaches to Achieve Adaptive Gait Support

As a consequence of the previous sections, the aim for adaptive gait support with passive or semi-active orthoses cannot be healthy gait (compare section 4.3.2), as most patients will be unable to preserve and restore, or generate power in the same way a healthy patient can do.

Thus, we define possible aims for adaptive gait support, some of which will be implemented and/or discussed in the present work:

### *Definition of the Control Problem*

- **Passive support:** The device allows sparing the patients' energy reserves. This enables them to longer maintain the ability to overcome distractions and obstacles. Through regular use and training, the patients should be able to extend their range of motion over time, as the device is not powering motion, but just supporting where the patients are unable to do so themselves. This is a property of the brace and the hardware parts of the control system, namely the hydraulic damper.
- **Individual Support:** By *Observation* (in a secure environment), the device learns the patient's individual gait, allowing a detailed level of control which is optimised for the patient's movements. The device is designed to let the patient (and orthopaedic personnel) *tune*, the controllers output to provide the desired level of support.
- **Flexible control:** The device should handle changing environments, gaits and use cases in a manner, which is unobtrusive yet reliable for the patient. The device should be able to handle static actions like standing, classical gaits like walking on flat and uneven grounds, slopes, and stairs and optimally support the patient while sitting down and standing up.
- **Adaptation:** The device should be able to change its behaviour on different time scales in response to variations in the patients performance. In the short term, over one period of use, like one day, the device should be able to recognise changes in the patients behaviour, like growing muscle fatigue or inattentiveness. On longer time scales, the device could track the patients training success or worsening of indications and adjust its control parameters for more optimal support. Connected to this part of adaptation is *surveillance*: over these longer periods, the device should be able to report a need for maintenance or professional tuning to the patient.

**Security considerations** imply, that the controller has to guarantee patient support. This means, that it should always be able to support the user even in critical situations like falling or stumbling. This demand limits the extend, to which the

design aims can be pursued. For example a completely self-learning device, which relies on the possibility to learn from errors it made, is out of question.

The demands for adaptation and flexibility require means to detect changes in the condition, or to evaluate the condition of the patient or his/her environment. These will be subject of the later chapters 9, 10 and the discussion in the outlook in chapter 12.

## 5.2. State of the Art for Control Approaches

With advances in materials and technology come more sophisticated joint mechanisms and actuators. To unleash their full potential, the control approaches have to advance likewise. The development of new control approaches is supported by advances in sensing technologies and mobile computing power [17].

All control approaches rely on sensory input to create control output which steers the device. Typically, an estimation of the ground reaction is used, for example in [6], as this dynamic variable can be used to determine the current state in the gait cycle (the gait cycle is detailed in section 2.2.2). Further common sensors include ground contact sensors and angles, angular velocities and moments.

### 5.2.1. Threshold Switching

Threshold switching mechanisms effectively are state machines with only two states: locked and unlocked. We justify a separate look at these techniques due to the ability to implement these as mechanic switches, and because of their simplicity and resulting problems for their users.

For joints with mechanical locking mechanisms and simple sensor driven controlled devices, the review [106] describes, that many of these mechanisms have threshold control. The users need to reach, for example, specific hip-extension

## Definition of the Control Problem

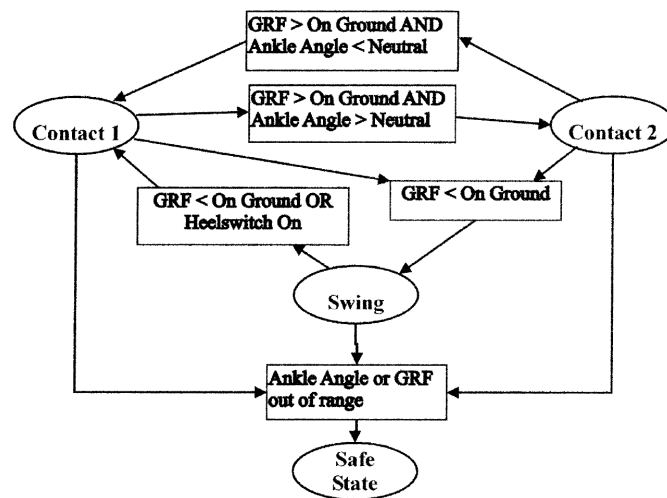


**Figure 5.1.:** Finite state machine (FSM) controller for an ankle-foot orthosis from [6]: The circles denote states, whereas the rectangles denote transitions. GRF stands for ground reaction force. Further inputs are ankle angle and a heel switch.

angles, step lengths or walking speeds. As another example, the hydraulic locking mechanism presented in [52] relies on specific angular velocities to trigger joint reaction.

While these mechanisms allow support in stance phase with an unlocked knee joint in swing, they all have in common, that it is the patient who has to ensure threshold fulfilment. This often requires constant concentration when walking causing higher risks of falling when the patient is exhausted or distracted. Furthermore, not every patient has the conditions reliably reach the required locking and unlocking conditions, thereby being not eligible for the corresponding device.

Adaptive processes are typically not included in these controllers.

## 5.2.2. Finite State Machine based Controllers

FSM based controllers contribute to a huge fraction of current control approaches. For a FSM, the gait is represented by a number of states with a defined set of transitions in between those states. These transitions occur on specific conditions, expressed in terms of sensory input or internal state and led to defined control output. Figure 5.1 is an example taken from [6], where it is used in an ankle-foot orthosis to assist drop-foot gait. They estimated the walking speed from the foot contact time to optimise the orthotic controlled plantar flexion stiffness, i.e., the stiffness and damping parameters were adjusted according to this estimation.

Generally, a FSM is a graph, which consists of a fixed number of states. A FSM which is working on a rule database is described in [109], effectively leading to a runtime definable state graph. Still, the design of states and transitions has to be careful as to make sure, that the controller never gets stuck in a single state and transitions produce a desired behaviour sequence.

The complexity of the graph mirrors the complexity of possible behaviour sequences and the more different behaviours the controller allows, the more states and transitions the graph has to provide.

In [100], a combined controller is a composite from three FSMs, with additional state transitions in between, to cover changes between walking, standing, and sitting movements. A similar approach is presented in [95] to handle slopes of varying degrees. The authors use three slope-optimised FSMs for level ground, as well as  $5^\circ$  and  $10^\circ$  slopes with a slope estimator. These approaches tackle the complexity of the overall controller via specialised modules for specific tasks with defined transitions on a higher level.

Parameter adaptation, e.g., the runtime change of state or transition parameters allows introducing flexibility and situation awareness into this approach, for example for parameter in [29] with speed estimation and [51] with for slope estimation during in standing.

### *Definition of the Control Problem*

[99] presents a Gaussian mixture model based gait switcher. This gait switcher selects from a set of FSMs. Thereby, they break the problem to create ever more states and transitions to include more behaviour. Their gait switcher uses a voting approach to allow standing and walking behaviour. The classification works on a history of means and standard deviations in the sensory input, with additional dimension reduction. At 1000 Hz sampling frequency, they optimised the history length for best outcome, achieving a 430 ms delay for gait selection.

Some of these controllers are able adapt to changes in the environment or walking speed. Still, all these approaches depend on a predefined, per-gait FSM controller. Adaptation to the patient is possible by means of state-transition-parameters, e.g., defining the level of the output signal depending on the walking speed and weight. As these controllers are more complex than the previous ones, the available amount of tuning is larger, but still limited by the design. The FSM controllers do not capture individual gait, but work on a general, parameterised rule-set.

The complexity of FSM based controllers grows directly with the number of supported actions, which make the design itself a complex task. Approaches to handle more actions exist, but still show the described limitations for each per-gait FSM and were not extended to a complete set of gaits including stairs and slopes.

### **5.2.3. Artificial Neural Networks**

Artificial neural networks are typically applied as black-box approaches. [41] uses feedback error learning to let a neural network structure learn the inverse dynamics of the controlled prosthesis to track desired gait trajectories. [62] uses a multi-layer perceptron network to determine the torque to generate a desired position and velocity profile. Both require active devices for the feedback loop to work.



In general, artificial neural networks are used as classifiers or function approximators and can be used for many tasks. These include gait classification, pathologic gait and fatigue recognition and many more. Generally criticised is the black-box nature of these approaches, which makes it difficult to verify function, and the need for trial-and-error learning phases [89].

#### **5.2.4. Gait Recognition**

Our main focus on gait recognition lies in the possibility to explicitly support different gaits. In addition to methods described with the control approaches, there are gait recognition efforts in different fields. Many of these use external information, like stationary camera systems, but still implement algorithms which might be used with local sensors on an orthosis.

##### **Image based approaches**

We briefly present approaches which work with visual data. [63] describes Hidden-Markov-Models trained to recreate sequences of features derived from visual input. The used features are body part trajectories and optical flow. The classification is performed with model-invalidation, i.e., for each gait and each sequence of image frames the model which provides the maximum probability to generate this sequence determines the classification result. [60] uses joint angles of shoulder, elbow, hip, and knee derived from image sequences, which are modelled as a second order stationary stochastic process. This study then too applies model invalidation to identify the gait. [16] extracts silhouettes from image sequences, using a so called Autoregressive–moving-average model with exogenous inputs (ARMAX model) to model the time development of the features. Again, model invalidation is used to identify the gait.

None of these approaches are designed for fast gait recognition within less than one step of input data available, nor are they intended for use when only sensors

### *Definition of the Control Problem*

attached to the orthosis, i.e., one leg, are used. Nonetheless, the model-invalidation approach based on models of feature dynamics is applicable to orthosis control.

### **Intention recognition with BCIs and EMG-systems**

For completeness, we will only mention BCIs and EMG systems here. Intention recognition with BCIs and EMG-systems provide a good approach for early detection of patient activity. Nonetheless, they are not suitable for all patients, especially where the muscle or nerve tissue is damaged or with risks of epileptic seizure.

## **5.3. Control Problem Evaluation**

The presented prototype is equipped with a hydraulic damper at the knee joint which generates supportive damping at knee flexion up to a completely locked joint. In a very general sense this makes the orthosis a robot, although the actuator is not generation motion, but changing passive properties of the knee joint.

Therefore, the orthosis controller has to:

- *Determine the necessary damping* at the knee joint to support its user. It may only dissipate energy, as we control a hydraulic damper. Compare to section 4.1 on page 43.
- Cope with huge variances in space and time. Although the steps in human gait are periodic movements, stride length and frequency show fluctuations. These variables cannot be predicted accurately. Especially in the case of stumbling or stepping on uneven ground the controller has to *react immediately*. Therefore, estimates of the step length or the time of the step end cannot be relied on.

- Be *flexible and adaptive* to the user's movements, the environment, and changes of the user's conditions and gait over different time scales. These considerations and the necessary boundary conditions have been detailed in sections 5.1 and 4.3.

### 5.3.1. Determination of Control Output

In this chapter, we will simplify the underlying control problem for the orthosis. Formally, this will solve the question which knee damping  $d_{t+1}$  should the controller apply for a situation, we will denote by the sensory input vector as  $\vec{s}_t$ . We thus want to find a control function  $d(\vec{s}_t)$  which will achieve fast reaction times by a simple mapping

$$d_{t+1} \leftarrow d(\vec{s}_t) \tag{5.1}$$

This control function  $d(\vec{s}_t)$  will work on a minimal context. This means that it will not take into account complex analysis of the patient's gait history or clues on the environment. The focus lies on the controller's ability to react immediately, which is determined by the choice of *state representation*.

The most important consequence of this mapping is, that the control output  $d$  only changes iff the sensory input vector  $\vec{s}_t$  changes.

### 5.3.2. Gait Progress Representation

Taking into account everyday experience and the extensive descriptions of human gait in section 2, we know that all walking movements are generally of cyclic nature. This cycle is the step—thus we can expect the average sensory input  $\vec{s}$  to be periodic in space and time and therefore expect that the applied damping  $d$  will have the same periodicity.

## Definition of the Control Problem

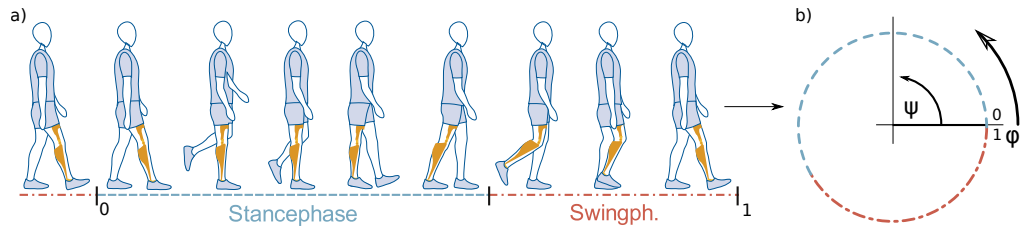


**Figure 5.2.:** The periodic gait cycle mirrors the fact that a periodic movement **a)** can be mapped to the circumference of a circle **b)**. Therefore, the position in a step can be denoted as the angle  $\psi$  on this circle, or expressed via the angle  $\psi$  as  $\varphi = \psi/2\pi$ ,  $\varphi \in [0, 1)$ . We call  $\varphi$  the *gait phase*.

We will stick to standard descriptions introduced in section 2 and express the gait progress during a step as a fraction (in time domain) of the whole step, i.e., from heel strike to heel strike of the same leg. For the controller, we choose the leg wearing the orthosis, in this context denoted as the *ipsilateral leg*.

To explicitly illustrate the periodicity of human gait, we change to a circular description of gait as shown in figure 5.2. Mapping the step onto the circle, we define the *gait phase*  $\varphi \in [0, 1)$  using the angle  $\psi \in [0, 2\pi)$  of the current step progress as

$$\varphi := \frac{\psi}{2\pi} . \quad (5.2)$$

Alternatively, we could describe the current step progress as a position  $(x_\varphi, y_\varphi)$  on a circle as

$$\begin{pmatrix} x_\varphi \\ y_\varphi \end{pmatrix} = \begin{pmatrix} \cos(2\pi\varphi) \\ \sin(2\pi\varphi) \end{pmatrix} . \quad (5.3)$$

## 5.4. Conclusions

The presented approach puts the human in the role of an external pattern generator, immediately driving the controller synchronised to its users gait. In theory, this approach provides a very high resolution; thus enabling support at any time—independent of step timing and stride length.

In conclusion, we formulate requirements on good gait progress representation and the consequences for the choice of sensors.

### 5.4.1. Requirements on the Gait Progress Representation

If we rewrite the damping function  $d$  in terms of the gait phase  $\varphi$  as  $d_{t+1} = d(\varphi)$ , we immediately see that the presented controller is not event based, but based on the gait progress: *Changes in the controller's output reflect gait progress. The quality of gait progress tracking therefore determines the detail of applicable damping control.* In other words: As the controller architecture applies damping based on the gait phase, only changes in gait phase can result in changes of the applied damping. Thus, we need the gait phase  $\varphi$  to change whenever the control output needs to be changed.

#### Ideal Linear Gait Progress Mapping

For the design of this controller, we make no assumptions about when the patient needs support. We therefore want the gait phase  $\varphi$  to change continuously and evenly over the step, to be able to exert control over the whole step. Ideally, the gait progress tracking produces a linear mapping from 0 to 1 over the gait cycle.

## 5.4.2. Consequences for the Choice of Sensors

As our periodic sensory input will in no way resemble the cyclic gait phase variable  $\varphi$ , we will need at least two sensors with periodic readings and a phase difference to accurately derive the gait phase. These could be an angle and its derivative, for example the knee angle  $\Psi_{knee}$  and the knee angle velocity  $\omega_{knee} = \dot{\Psi}_{knee}$ , or two independent angular variables with phase difference, like the knee angle  $\Psi_{knee}$  and the thigh angle  $\Psi_{thigh}$  as in Figure 5.3. But as the underlying motion is periodic, almost every set of two sensors on the device will satisfy this condition, as long as they represent the gait progress in enough detail. That means a switch, like a ground contact sensor, might not give enough detail to gain a high time resolution of the gait phase.

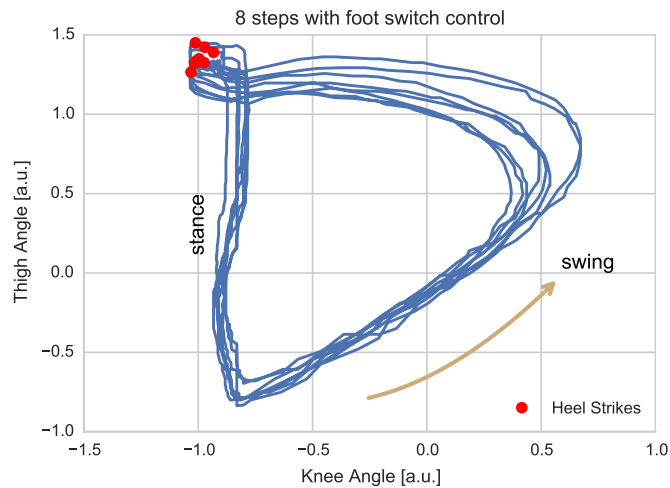
This holds true even if we do not want to estimate the gait phase. To gain an injective control function  $d(\vec{s})$ , we still need at least two sensors with the elaborated properties.

Postprocessing will be necessary for the knee  $\Psi_{knee}$  and thigh angle  $\Psi_{thigh}$  sensors, as the motion has several periodic components, as can again be seen in Figure 5.3. Using switch like ground contact sensors, which activate on heel strike, will allow us to solve the ambiguity of the loop.

But based on two such sensory readings, we can deduce the current gait progress in terms of the gait phase  $\varphi$  or otherwise identify the exact state of the user's gait. For our first experiments, we test the ability of RunBot to recover from a condition with uncontrollable knee motor using the thigh and knee angle information for a separate controller.



(a) Healthy patients walks with uncontrolled orthosis.



(b) Healthy patients walks with foot-switch controller.

**Figure 5.3.:** Thigh angle over knee angle for 8 steps; heel strikes are marked with red dots. The data for 5.3(a) has been recorded using the uncontrolled orthosis prototype. You can clearly see the knee bending in stance phase during thigh extension on the left side, which is typical for healthy walkers. For a simple stance control orthosis preventing knee flexion, this bending cannot be observed; for example see the minimalist foot-switch controller in 5.3(b), which blocks the knee bending at ground contact. Still, the loop around ground contact exists.





# 6

## Orthosis Controller Experiments on RunBot

Based on the general considerations in the previous chapter, we validate our design for a feed-forward controller and the suitability of the chosen sensors (hip and knee joint angle) in a robot experiment, before we proceed on to a more complex implementation on the orthosis in the next chapter.

We will start in section 6.1.1 with an outline of RunBot's [24] setup (Figure 6.1 (a)) and in section 6.1.2 with the controller (Figure 6.1 (b)). The suitability of this setup will be discussed in a comparison to human gait samples in section 6.2. These considerations will help to devise an experiment (Figure 6.1 (c)) in sections 6.3 - 6.4, which allows us to test the applicability of internal representation of gait progress, which corresponds to the gait phase as detailed in section 5. Based on this test we discuss the fitness of the sensory setup for the implementation on the orthosis in chapters 7ff.

### 6.1. RunBot

At project start, the orthosis prototype was still to be developed. Therefore, preliminary concepts and the sensory configuration were devised and tested on RunBot. The initial Idea was to simulate different walking disorders with Run-

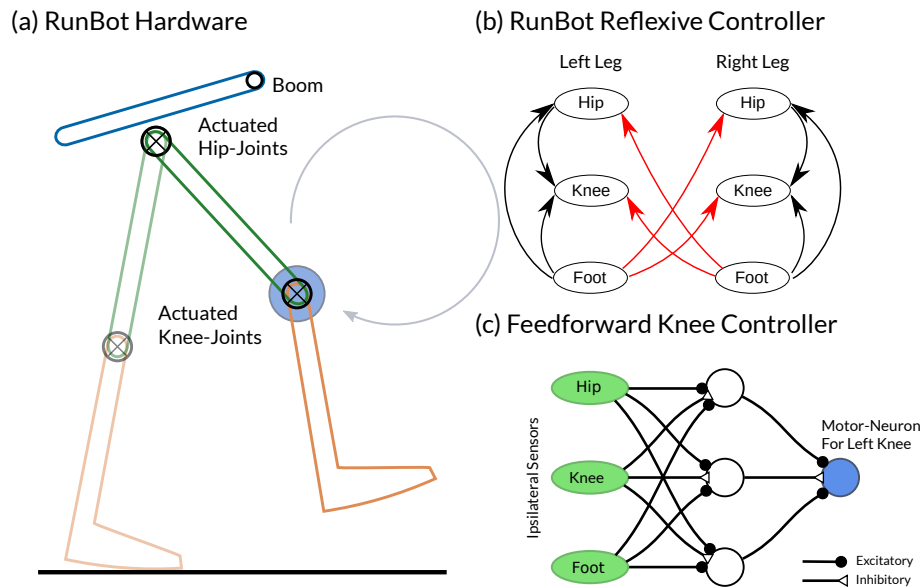


**Figure 6.1.:** Chapter outline: We start with an introduction to Runbot (a), a bipedal, 2D dynamic walking robot. Its controller produces inter-limb coordination and motion generation via reflexes, indicated by arrows in (b). For validation, we implement a virtual knee-orthosis controller (c) which learns to reproduce RunBot’s original knee motor commands.

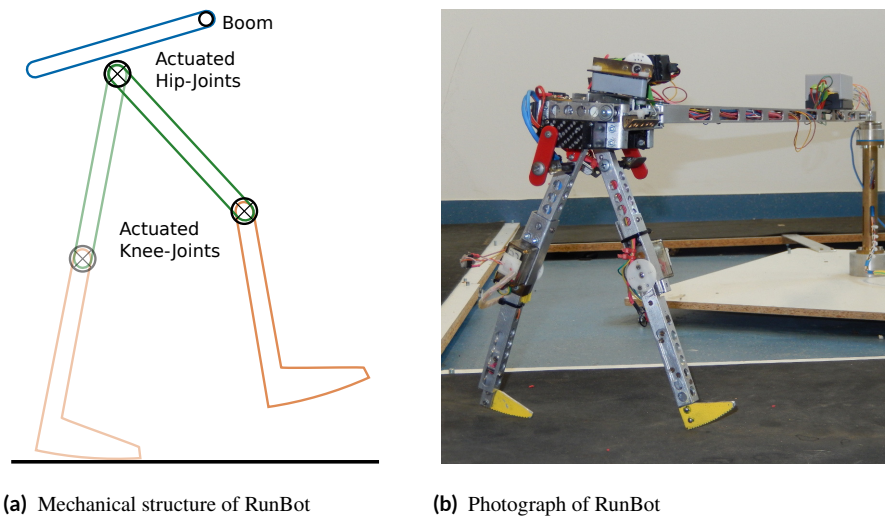


**Figure 6.2.:** The RunBot model equipped with curved feet. Motion comes from four actuated joints at the two hip and knee joints each. Sensory input comes from angle sensors at all joints and ground contact sensors in each foot.

Bot, but this proved difficult because of the inherent stability of RunBot's joints, which is caused by gear-friction in the servo motors.

We will start with a short description of RunBot and its gait, but will leave the details to the extensive existing literature (e.g. [23, 25, 59]). Then we will discuss RunBot's use as a model system for human gait and conclude with a summary of early controller experiments on RunBot.

### 6.1.1. RunBot Set-Up

RunBot's set-up is in general unchanged to the original literature [23, 25, 59]. Over the course of the thesis and an accompanying bachelor's thesis [45] mechanical refinements have been done, which alter the gait dynamics only marginally. These include a slip-ring contact and later on compliant ankles. Further changes in the set-up move the boom to match the hip joint's axis of rotation.

RunBot is a 2D-Walking robot. His upper body is tightened to a boom at the hip plate. This boom prevents him from falling to the side. The original version has four joints: 2 hip- and 2 knee joints, which are all actuated with fast servo motors. At the joints angle sensors are attached. Also, all versions have ground contact switches. The original design has stiff rounded feet, whose curvature corresponds to a circle with a radius of the leg length. Later on, a design from [47] has been applied, which implements a passive ankle joint with springs. In this thesis the design with stiff ankle and rounded feet was used.

The controller is reflex-based, meaning that every actuation is triggered by a direct sensory impulse. This could be ground contact, or an indirect impulse, like the measured hip angle reaching a threshold. This closed-loop controller depends on the physical interaction of the robot with its environment to complete its gait. Every ground contact triggers the next step; as a consequence, without a physical environment the stepping motion will stop. The coupling of the two legs is realised via sensory impressions from the contralateral leg.

Parameters of the controller are threshold angles and motor gains [23], which roughly translate to posture and angular velocity in the joints. Many gait variations and speeds can be created by varying these parameters, whereas the walking gait stays fixed, as it is determined by the neuronal couplings. Due to the hardware not being designed for the higher impacts of a flight phase, running is not feasible.

In the next section, we will see how these walking gaits compare to human walking, and to which degree RunBot can act as a model for a human wearing an orthosis.

### **6.1.2. Locomotion Generation in RunBot**

Control heavily based on central pattern generators is often implemented in robots which have intrinsic mechanical stability because of their number of legs,

like for quadrupeds or hexapods. In these cases a mostly unperturbed gait can be altered in response to external stimuli to react to the environment.

Central pattern generated bipedal walking is much more challenging, because of the intrinsic instability. Balance control is the essence of bipedal walking and in contrast to the mostly unperturbed gait of a hexapod a bipedal gait has higher variations already on flat ground.

Therefore, for RunBot a reflex based controller was devised, which implements a physical computation [23], the combination of passive walker strategies with active control. This reflex structure which represents the linkage of sensory inputs with motor actuation is illustrated in Figure 6.7. RunBot's controller does not have a representation of speed, its motion is a combination of limb-movement and world-interaction. RunBot's reflexive controller provides stable gait without explicit balance control, it implements walking as controlled falling.

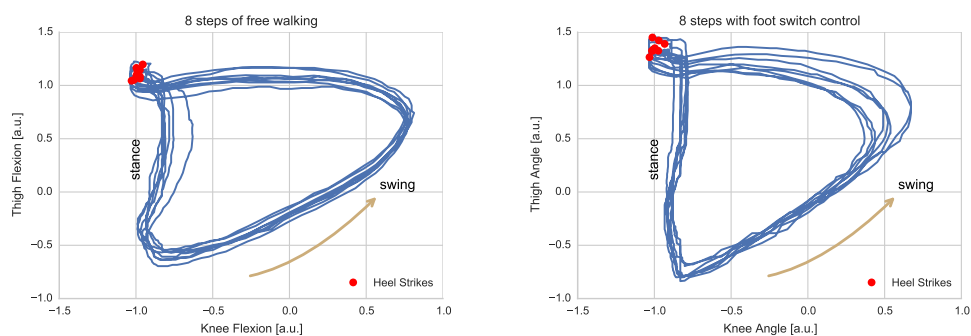
## 6.2. Comparison of RunBot's Gait to Human Gait

First, we will take a look at the walking pattern RunBot's controller generates. The literature includes investigations on many details of RunBot's controller, mostly its ability to change and control walking speeds [23, 46] and to adapt to differently sloped environments [57–59]. Its similarity to human gait has been compared via its velocity relative to the leg length [23, 59]. We will now consider the similarity of hip and knee motion and take a closer look at specific aspects of human gait.

For a direct comparison of RunBot's gait to human gait, we included the graphs from Figure 5.3 in Figure 6.3. We observe the following differences:

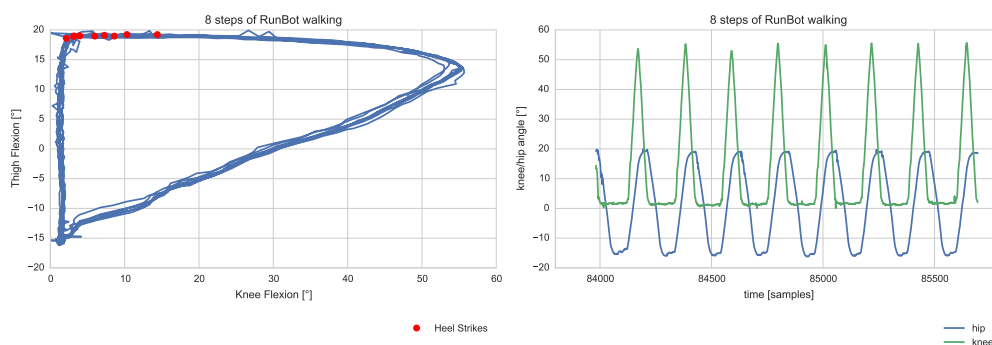
- The knee flexion is stronger pronounced, which might be due to the missing ankle actuation.

## Orthosis Controller Experiments on RunBot



(a) From Figure 5.3(a): Healthy patient with uncontrolled orthosis.

(b) From Figure 5.3(b): Healthy patients walks with foot-switch controller.



(c) RunBot with compliant ankle.

**Figure 6.3.:** RunBot's gait: On the left, thigh angle over knee angle for 8 steps, the heel strikes are marked with red dots. On the right side, the joint angle motion is shown, with the zero for the hip and knee joint in straight vertical position. This data has been recorded with compliant ankle joints. When compared to human walking, many features are missing. RunBot's walking resembles an approximation using only the ground frequencies of the corresponding channels.

## 6.2. Comparison of RunBot's Gait to Human Gait

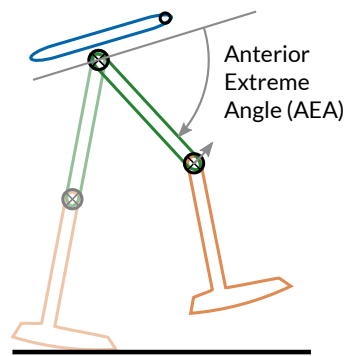


**Figure 6.4.:** The Anterior Extreme Angle (AEA) names the maximum hip flexion which determines the end of the swing phase in RunBot's reflexive controller.

- The knee flexion is less symmetric in comparison to thigh flexion, as the knee extension is triggered by reaching the Anterior extreme angle (AEA) [25] (see Figure 6.4).
- Features of higher order are missing in knee and hip motion of RunBot. There is no knee flexion at heel strike or during stance phase. Complementary features in hip motion are missing, too.
- RunBot exhibits no swing leg retraction and the impact shock is forwarded through the extended knee. This and the missing features from the previous point greatly optimise energy consumption and reduce high forces on the musculoskeletal system above the knee in human bipedal walking.
- Furthermore, based on recent findings on human push-off [48, 54, 81] we can argue, that even with compliant ankle joints, the rigid gears at knee and hip level prevent human like uptake of energy stored in the ankle joint, which is now argued to power the swing leg. Especially, as knee flexion in RunBot only starts with contralateral ground contact.

Therefore, RunBot is not reproducing many important and advanced features of human gait during the whole gait cycle (and especially at heel strike and push-off).

Still, RunBot reproduces rudimentary features of human walking, like the general order of phases as shown in section 2, including double stance phases. This allows us to employ RunBot as a model for early technical studies.

### **6.2.1. Comparing against the reduced dynamics of locking orthoses**

In comparison to the gait of patients using locking orthoses in Figure 6.5, the knee joint's trajectory is more similar. This can be seen in the dashed line of Figure 6.5(d). Patients tend to compensate their movements with other parts of the body: The hip joint's trajectories in Figure 6.5(c) give a good indication of how strong these changes may turn out. In comparison to a healthy walker in Figures 6.5(a) and 6.5(b), you can see additional or overemphasised features, e.g., a significant increase of asymmetry between the two legs. The contralateral knee joint in Figure 6.5(d) shows an additional bending at the end of the stance phase, too. Both features are likely needed to overcome the disturbance introduced by the locked knee joint.

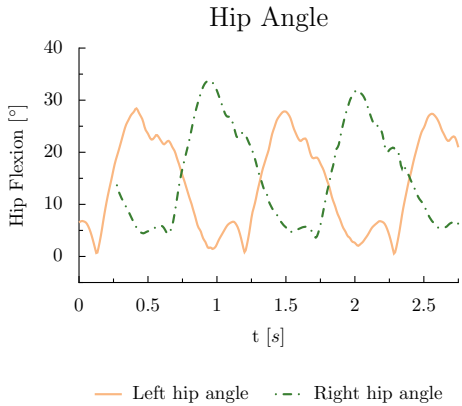
Although RunBot's knee bending does resemble the locked knee trajectory of the patient, RunBot's gait does not show any of the other features. This is due to the relative simplicity of body mechanics and gait model of RunBot. Patients are able to compensate with their whole body, which includes not only the contralateral leg, but also the torso and arms.

### **6.2.2. Consequences for Gait Modelling with RunBot**

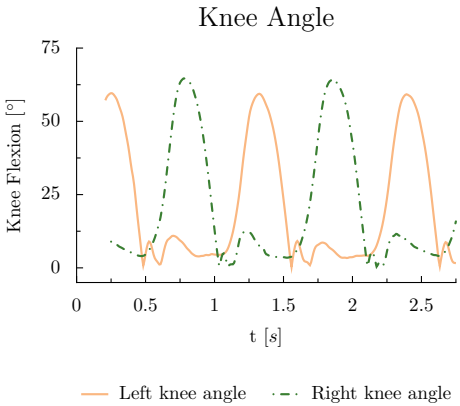
While RunBot's dynamics compare better to the orthosis' knee component than to regular human walking, the rest of the patient's body is doing additional avoidance movements, which are captured much less, as RunBot is missing a dynamic upper body, which plays a significant role in patient gaits. We conclude, that



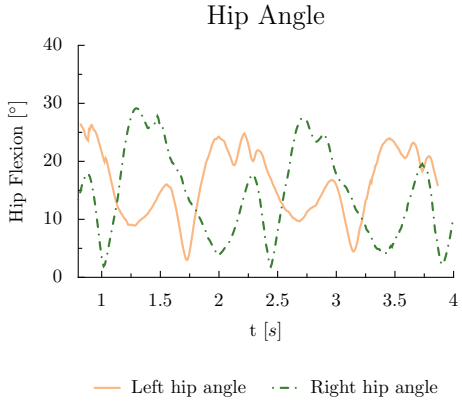
6.2. Comparison of RunBot's Gait to Human Gait



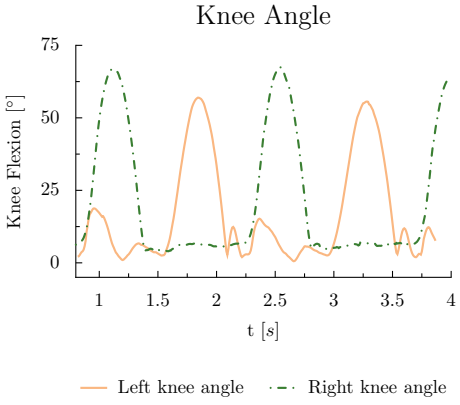
(a) Hip angle of healthy walker



(b) Knee angle of healthy walker



(c) Hip angle with locking orthosis



(d) Knee angle of patient with locking orthosis

**Figure 6.5.:** Hip and knee angle in a gait lab recording of a healthy walker and a patient with locking orthosis: In comparison, we observe the flat knee movement in stance phase for the ipsilateral knee (green slash-dotted line) in 6.5(d) and the asymmetric hip movement in 6.5(c) as response to the stiff knee.

with RunBot we face a system, which can be used to model the orthosis' mechanics and controller on a simple scale, whereas the details of general human or a patient's gait are not captured.

In consequence, we can not assume RunBot to be a realistic environment to imitate an actual patient wearing an orthosis. Nor can we try to estimate changes in performance or energy balance of the patient's gait, since RunBot's controller does not support features due to mechanical limitations.

Summing this section up, RunBot is not a detailed model for human gait, as it has many shortcomings. Nonetheless, it allows us to study basic features of bipedal locomotion. Especially in preparation of the sensory limited environment the orthosis controller will be. Therefore, we will use RunBot to implement a rudimentary controller to test the hypothesis from section 5.3. We can use the ground contact, hip and knee angle sensors to reconstruct basic gait progress.

### **6.3. Evaluation of Possible Experiments with RunBot**

After the comparison of RunBot's gait to human gait in the previous chapter, we will evaluate possibilities to experimentally imitate gait-impairments on RunBot with the aim to develop additional controllers which can compensate or lessen the introduced deviations.

Therefore, we will try to generally describe possible patient's conditions, before we compare different means of gait-impairments on RunBot. Based on this evaluation, we will design an experiment to test a first approach for the orthosis controller.

### 6.3.1. Mimicking Patient's Conditions

Walking disorders of interest to us are connected to missing or reduced muscle functionality, caused—for example— muscle atrophy, muscular dystrophy, myopathy, or injuries of muscles, and tendons. Another problem field arises from the nervous system, like stroke, spinal cord, or nerve fibre damage.

All of these disorders have a (localised) lack of control over muscle force in a muscle or muscular region in common, which in general results in instability and gait deviations like premature ground contact.

There are generally two possibilities to mimic these disorders on RunBot in a simple way. Number one would be to *model a lack of control by means of the control signal*, like a reduced signal amplitude. Alternatively the simulation could be done by *means of hardware changes*, which might be a cut signal line or additional mass attached to a leg. A more complex approach would include a simulation of the disorders symptoms, which for example would limit joint range the motor torque on the joint.

For all these cases, a virtual orthosis (controller) as supportive solution could be implemented in parallel to the existing controller. Thereby, controller architectures could be evaluated. In the following, we will evaluate these options for their feasibility on RunBot.

### 6.3.2. Reduction of the Signal Amplitude

Reducing the amplitude of RunBot's virtual motor neurons has several effects. The servo motors will move the limb slower leading to asynchronous limb motion, early ground contact and therefore hobbling. But on the other hand, we found the internal friction of the used servo's gears to be so high, that RunBot is still able to support it's own body weight. Even with disabled knee motor signal, RunBot is able to do  $\approx 5$  steps before stumbling, as shown in Figure 6.6. With higher signal amplitudes, RunBot is even able to prevent the slow decrease

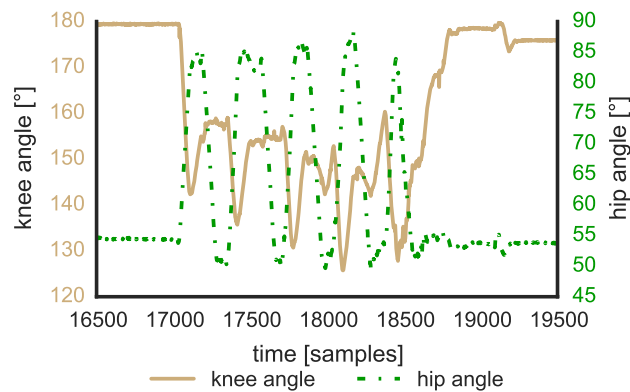


**Figure 6.6.:** With disabled motor for the right knee, the friction generated by the gears supports RunBot’s body weight for approximately 5 steps before falling. This high friction complicates the modelling of patient’s conditions.

as a combination of slow joint movement and torques resulting from the end of the swing phase. This internal friction of the servo’s gears makes it impossible to achieve a realistic patient situation with reduced muscle forces in an ad-hoc manner by only manipulating the driving signal.

### 6.3.3. Hardware Manipulations

The attachment of an additional load on a leg provides no problem for the used servos. For reasons of weight efficiency, the equipped servos are high-speed, high-torque models. The problems for RunBot’s dynamics, resulting from additional load, stem from the limb’s additional inertia, which is comparable to patients who swing their legs with too much muscle force: when stopping the swing, the robot will most likely fall. This is the opposite problem the patients are experiencing. To reduce this excess inertia, the motor-driving gain can be reduced, which leads us back to the first approach of reduced signal amplitude. As the additional weight is not impairing the servos’ capabilities, it can even be detached.

### 6.3. Evaluation of Possible Experiments with RunBot

On a side note, the changes in motor-driving gain on a leg with or without additional load will result in asymmetric gait, which can be further increased by asymmetric gait parameters for the desired hip- and knee-angles. Thus, it is possible to generate simple forms of asymmetric gait (cmp. Figure 6.5(c)), but it is still generated by a fully functional controller. The asymmetry stems from asymmetric gait parameters and is not a symptom, like in the patient's case, but would merely be a forced control condition, which could not be easily overcome by an additional controller. Therefore, direct introduction of symptoms in RunBot's controller seems to be unsuitable.

#### 6.3.4. Complex Modelling of Patient's Conditions

With these observations in mind, for a useful model of the patient's gait, we would need to reproduce the reduced muscle forces or rather joint torques using for example compliant control, which would be the consequence of the patient's conditions. This would create a realistic and proportional effect for the robot, which could be countered by an appropriate virtual orthosis.

Employing musculoskeletal simulations would allow building realistic models of human motion, from which the effects of changed muscle functionality could be deduced.

As the orthosis has an hydraulic damper, one could try to apply a musculoskeletal simulation like in [86] to derive the forces the orthosis has to provide. As the damping is one of the two passive muscle-properties Hill-Type muscle models apply [105, 108], one could try to directly control the damper, although the stiffness of the joint could not be modelled that way. This means, that not all force components would be implemented and the applied damping might needed to be modelled solely after the required supporting force.

But given the current setup of RunBot without load sensing and with high-torque servo motors which produce high internal friction, these effects (see Figure 6.6)

make the conclusive application of muscle models on RunBot a complex undertaking, which is outside of the scope of this thesis.

### **6.3.5. Conclusions and Choice of Experiment**

In summary: To be able to simulate insufficient muscle control or force, the affected joint motors would need active control to achieve passive instability. This could be done via muscle models or similar means which actively counter the gear friction or by changes in RunBot hardware setup.

Therefore, in addition to the arguments presented in the previous section, the complexity to model the patient's behaviour restrains us from use of RunBot as a detailed model of patient behaviour.

Instead, we will reduce the control signal amplitude of RunBot's controller to mimic the general control problem, which will be unstable gait due to missing body support. Although RunBot is—in contrast to a patient with completely uncontrolled knee joint—still able to walk for about a hand full of steps, we can restrain an additional controller to the sensory environment of the orthosis and thus gain insight into this dynamic system.

In the next section, we will implement and test gait progress based control on RunBot, limiting sensory input to one leg, as formulated in section 5.3.

## **6.4. Experiment: Gait-Timing Based Control on RunBot**

An orthosis equipped to one leg has to possess a control mechanism, which is able to fit into the user's gait without knowledge of the whole patient's state, as a complete instrumentation of the patient's body with sensors is unfeasible. The aim is sensory integration which allows the controller to synchronise with the motion of its user, avoiding instrumentation outside the orthosis if possible.

#### 6.4. Experiment: Gait-Timing Based Control on RunBot

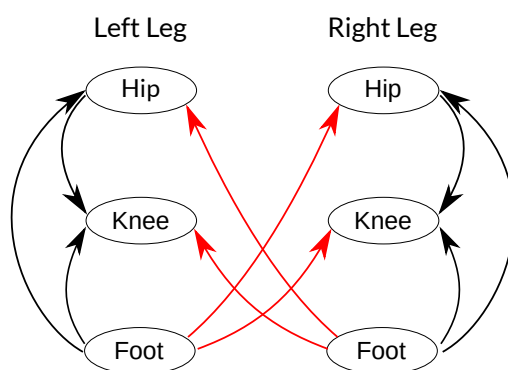


**Figure 6.7.:** RunBot’s reflexive controller uses the ground contact signal for inter-limb coordination. Each leg’s trajectory is controlled by ipsilateral sensors, but movement initiation is triggered by contralateral ground contact. Reaching the AEA in the hip joint triggers knee extension for heel-strike.

Whereas many traditional orthoses use single or few sensors to inject control at specific moments in the gait cycle, we want to gain the ability to continuously control the device, extending the moments of control to the whole gait cycle. Thereby, (1) not coupling the control to the patient’s ability to satisfy the sensory requirements of the controller, (2) heavily reducing the demand on specific patient remaining abilities for the rest of the gait cycle, and (3) implementing a control scheme, which allows transparent and detailed gait support over the whole step. We focus on methods which allow later adaptation of the controller’s behaviour, i.e., we want to be able to apply transformations at all steps of the controllers processing.

In this experiment, we implement and test a simplified virtual orthosis controller for RunBot. This virtual orthosis will have access to the sensors of its own leg. This is in contrast to RunBot’s regular walking control, which implements inter-limb-coordination by coupling the motion control of one leg with the sensors of the opposite leg, as shown in Figure 6.7. This mixed-limb sensory processing allows the system to facilitate “physical computation”, i.e., to use physical properties and the interaction with the environment to complete the gait dynamics [25].

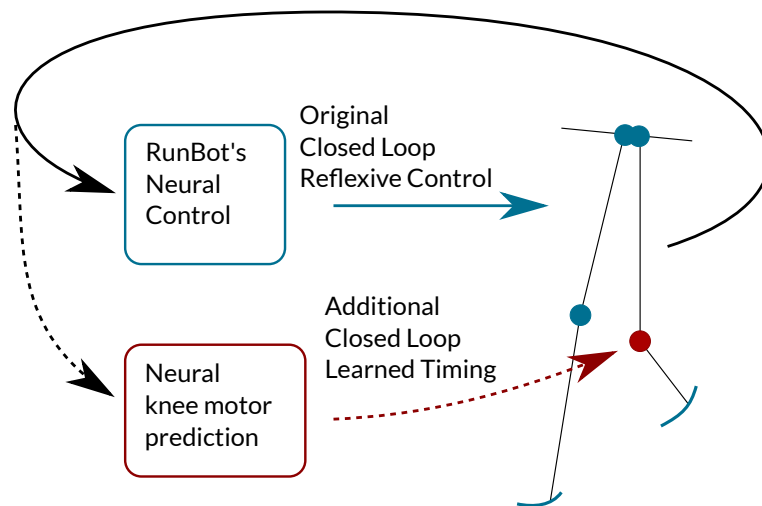


**Figure 6.8.:** Setup of the RunBot virtual orthosis controller experiment: RunBot’s regular neural control loses control of the left knee joint (compare Figure 6.7). A second controller is installed in parallel. It uses only ipsilateral sensors and original gait data for training to restore RunBot’s original gait.

Here, we want to test if we can control the knee joint only with ipsilateral sensors as proposed in section 5.3. As a test condition we reduce or remove the original controller’s signal to the affected knee motor, as sketched in Figure 6.8, producing the condition in Figure 6.6 of the previous section.

**Hypothesis:** Using ipsilateral sensors only—i.e. ground contact, hip and knee angle sensors—we can completely control one of RunBot’s knee joints sufficiently to allow continuous walking from an impaired state.

**Materials:** Used is the reflex based RunBot controller without any adaptive or learning elements, whose internal reflex connectivity is sketched in Figure 6.7. RunBot is equipped with curved feet and walks on a flat circular path. See the literature in section 6.1.1 for details.



### 6.4.1. Experimental setup

We removed control of the left knee from RunBot's controller, thus simulating impaired knee joint control. As stated above in section 6.3.1, RunBot is still able to walk for several steps because of gear friction, but after around 5 steps, RunBot's knee will eventually have bent too much and the robot falls. At the same time, the extended, "stiff" leg will make RunBot stumble due to early ground contact until the knee is bent far enough. These properties do not mimic a real patient, but the task is similar:

*Relying on ipsilateral sensors only, implement a control strategy that fits in perfectly with the original controller. Together, achieve a gait pattern that resembles the original.*

Instead of the orthosis controller to know the full state of the whole walker, it only needs to have enough information to blend in. The coupling is achieved over the ipsilateral leg, to whose sensory impression both controllers have access to, as formulated in section 5.3.

The virtual orthosis controller sketched in Figures 6.8 and 6.9 is much simpler than the real orthosis controller detailed in later sections. Here, we implement the simple feed forward controller from equation (5.1) as a perceptron using the FANN library [69].

This approach allows easy training with previously sampled data, as well as re-training during operation and therefore keeps the option for behaviour adaptation and online learning. It simplifies the implementation through an existing and tested framework.

The number of hidden neurons and layers was varied to find the optimal number; the best training results were achieved with one hidden layer of three neurons. Still, because of the desired rectangular output with smooth transfer-functions, the performance differences were small. The thus generated and trained controller is sketched in Figure 6.9 and is strictly-feed forward. Nonetheless it is a

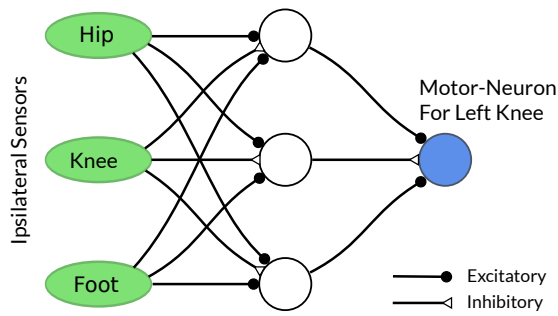


**Figure 6.9.:** The virtual controller to take over operation of RunBot’s virtually impaired knee. We use the current ground pressure, hip- and knee-angle sensors as input. After rescaling to the neurons input domain, they are processed by three hidden neurons to reproduce the unimpaired RunBot’s motor output in combination with the impaired controller and the environment in closed loop setup, as shown in Figure 6.10.

closed loop system, as the interaction with the impaired controller and the environment is necessary to produce output. It therefore creates an undelayed output for each sensory input like the original reflexive RunBot controller.

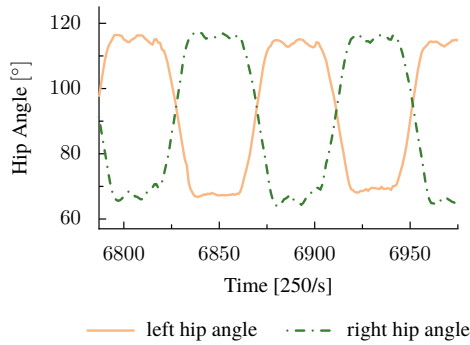
## 6.4.2. Results

The comparison of the virtual controller’s output to the original training data from a separate run can be seen in Figure 6.10(d). Whereas the achieved knee angle is compared to the original controller in Figure 6.10(c).

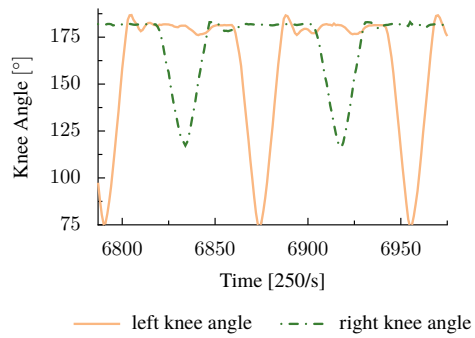
We observe that the perceptron creates artefacts around the sharp edges, which can be explained by the smooth joint angle input and the smooth transfer functions used. These smooth transfer functions have difficulties to reproduce the steep rises of the binary motor control of the original controller. The over- and undershooting of the motor neuron creates additional features in the knee angle. Still, the generated dynamics are quite similar to the original controller’s and allows stable walking<sup>1</sup>.

<sup>1</sup>Whereas a proper definition of gait stability is subject to the use case, for bipedal gait often

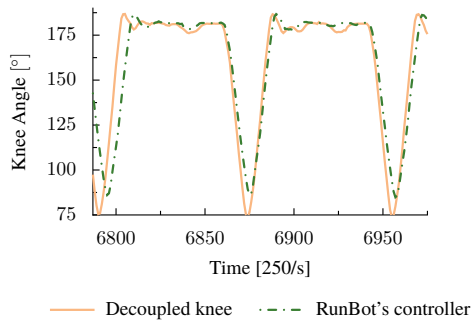
### 6.4. Experiment: Gait-Timing Based Control on RunBot



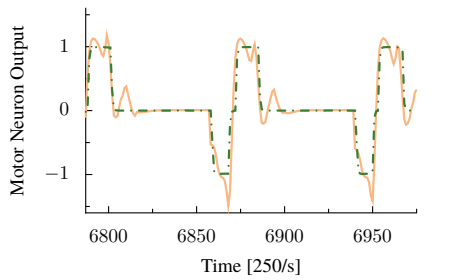
(a) Restored hip dynamics.



(b) Restored knee dynamics.



(c) Comparison of original to restored knee dynamics.



(d) Comparison of original to restored motor output.

**Figure 6.10.:** Decoupled knee controller output. In the top row, the restored hip- and knee dynamics show the cooperation of the two controllers. In the bottom row, the knee angle and knee motor neuron output are compared to the training data, e.g., to a different and dynamically independent run.

## **6.5. Discussion**

It has to be noted, that for the comparisons in Figure 6.10(c) and 6.10(d) we had to choose from two separate walking recordings with the original controller. Therefore, we compared two independent statistics with the consequence, that the step lengths are not matching well; this is generally to be expected, as for 37 steps of RunBot walking with the additional knee controller, the distribution of step times showed a standard deviation of  $0.8 \times$  the mean step duration. This huge width in the distribution of step durations might be a symptom of the inherent instability, which is not countered by active balance and stabilisation in the controller (compare to section 3.1.1).

The presented approach possesses the captivating feature of simplicity. Furthermore it can be trained with at all times, including offline with previously recorded data and run time, and therefore allows adaptation during all stages of the controller's life time.

Still, it is exercising feed forward control, which allows minimal reaction times of one controller cycle to external stimuli and therefore shows the same time characteristics as the original reflex based controller. No additional filters needed to be applied, although simple filters would have been able to restore the original binary switching behaviour of the motor neuron.

### **6.5.1. Consequences for the Orthosis Controller**

We take this as an indication, that the presented approach is able to continuously control bipedal gait over the whole gait cycle, integrating into the host controller's bipedal dynamics. A claim, which we will revisit in the following sections with extensions to the controller for this specific purpose.

---

a falling condition is used. In this case, we have achieved a restoration of fluent walking from  $\approx 5$  steps to 37 steps, which was good enough a count to stop the experiment. For a detailed considerations on bipedal stability see [79].

Summing up, this minimalist controller implemented with a perceptron allows RunBot to again achieve stable gait based on two joint angles and the ground contact sensors. Still, we can easily distinguish the motor output from the original controller's, which is due to the fact, that RunBot's original motor output is mostly a combination of unit steps. We can expect the desired control output for the orthosis controller to be of a smoother nature, which we should be able to create with a similar perceptron.

Based on this proof of concept, we are now prepared to proceed with the sensory equipment of the orthosis in chapter 7 and the design of the components of the actual orthosis controller in section 8, which will be modelled according to the RunBot model.



# 7

## The Orthosis' Sensors

In Chapter 4 we introduced the frame of the orthosis. In this chapter, we will look at the sensory equipment of the presented prototype, which is strongly inspired by RunBot as described in the previous chapter.

In this—rather short chapter—we will go all the way from the sensor readings to the controller software (compare Figure 7.1), which we split in two parts. First, we will take a look at the data exchange with the orthosis hardware, then we will consider the sensory configuration, which we developed during the course of the BFNT project and this thesis. The two parts are independent of each other; the data acquisition was abstracted and separated in form of a library. That way the backend can be switched at any time.

The general description of the Hardware as designed by Otto Bock was part of the BFNT project 3a; please see section 4.1 on page 43 for further reference. In this section, we will focus on the interfaces with the hardware and the sensory setup, as devised based on the preceding experiments with RunBot. Figure 7.5 is an extended version of Figure 4.1, in which the sensors are marked.

### 7.1. Data Acquisition Framework

Data exchange with the hardware is bidirectional. We read sensors placed on the orthosis and control the valves in the C-Leg-element. For easier development, we decided to use a standard PC for interfacing, instead of more energy efficient

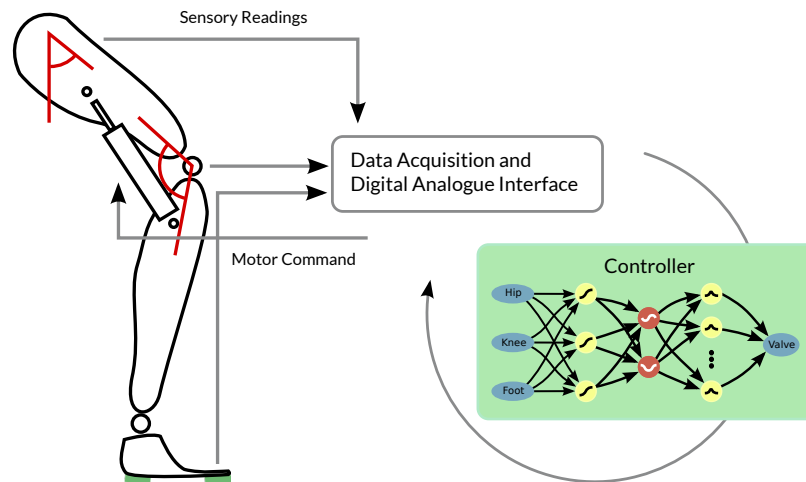


**Figure 7.1.:** Chapter overview: After introduction of the brace in Chapter 4, we examine the sensory configuration and the information flow in this. This includes the sampling- and analogue-output features as well as the placement of sensors.

embedded hardware, which might be too slow for demanding calculations<sup>1</sup> and which is more difficult to debug.

During the course of the thesis, two interfaces have been used. We will sketch the first approaches for completeness.

### 7.1.1. C-Leg-Interface

The C-Leg-element comes with an I<sup>2</sup>C-Port, which allows reading and writing access to the valve motors. Direct interfacing using an IO-Warrior USB-I<sup>2</sup>C-Adapter proved to be highly unstable. Even hardware initialisation procedures were not reproducible. Furthermore, an additional Data Acquisition (DAQ) device would have been necessary to read out the attached sensors. Therefore we went for a unified approach for valve motor control and data acquisition.

<sup>1</sup>Note that with the advent of modern embedded devices, like smart phones and a multitude of Internet of Things devices, the computational power is of no concern anymore.



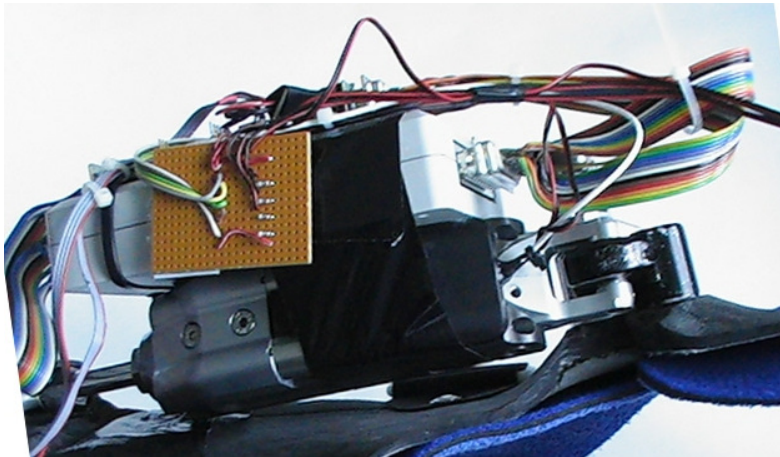


**Figure 7.2.:** The USB-Dux with additional wiring for the sensors is attached to the hydraulic damper.

### 7.1.2. USB-Dux DAQ-Interface

The USB-Dux DAQ [78] provides 8 analogue input, 4 analogue output, and 4 digital input/output channels via the comedi software stack [30]. It is part of the RunBot setup and therefore fully integrated into the neural RunBot controller, which is the foundation for the presented orthosis controller. That made it the perfect tool to bootstrap data acquisition for the initial orthosis controller.

The first generation of orthosis controllers drove the valve motors directly via USB-Dux, short circuiting the original controller chip and going directly to the amplification circuits of the original C-Leg controller board. The motor position and all other sensors were connected directly to USB-Dux and thus a control loop with up to 1 kHz update rate was possible. In reality, the orthosis control loop was never operated with more than 200 Hz.

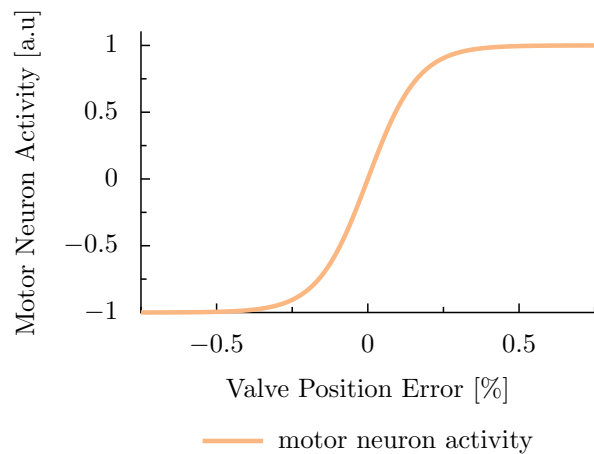


**Figure 7.3.:** Motor neuron transfer function from equation (7.1).

Motor driving was implemented via a single motor neuron, whose activity is defined as

$$a(u) = \frac{2}{\exp[s(u - \text{position})]} - 1 \quad , \quad (7.1)$$

with  $u$  being the set point, position being the current position of the driven valve motor and  $s$  defining the slope around the set point. For  $s$  the empirically chosen value of  $s = 12$  has been used.

This setup worked generally flawlessly for the development of the core controller in this chapter. But we suspected the brute force connection of the motor drivers to USB-Dux by short-circuiting the original controller chip to be responsible for dying hardware in the long run. At the same time, the 8 analogue input channels were completely in use with 2 motor valve position sensors, 3 angle sensors and 3 force sensing resistors for ground contact, and left no easy way to extend the sensory set up. This led to the development of a special solution by our cooperation partner Otto Bock.

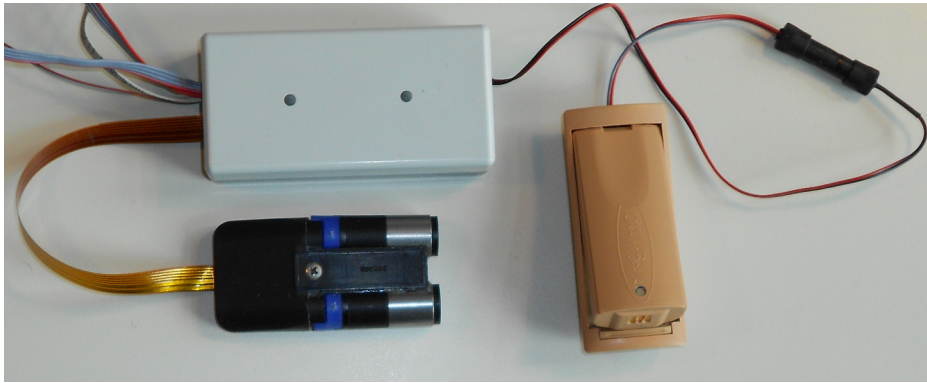


**Figure 7.4.:** Otto Bock motor control and daq: in the lower left corner the motor unit for the hydraulic damper, in the top left the cased interface for motor control and data acquisition.

### 7.1.3. Dedicated Embedded i/o-Interface

During the course of the project, Otto Bock developed a special purpose embedded board for Data Acquisition. The design was based on their internally used boards with modifications to fit our requirements. The interfacing with the C-Leg-element uses the original I<sup>2</sup>C interface. Additional analogue input lines for additional sensors complete the setup, resulting in a max of 8 analogue input channels in addition to the 2 motor valve positions sensors. The sampling rate for the additional analogue inputs is 100 Hz.

In consequence, the motor control loop to ensure set point positioning is no longer part of the presented controller and the motor neuron from the USB-Dux interface has been removed.

This interface has been used in the 2<sup>nd</sup> half of the project. And although the maximum sampling rate is an order of magnitude lower, than for the previous interface based on USB-Dux, it proved fast enough for the presented controller.

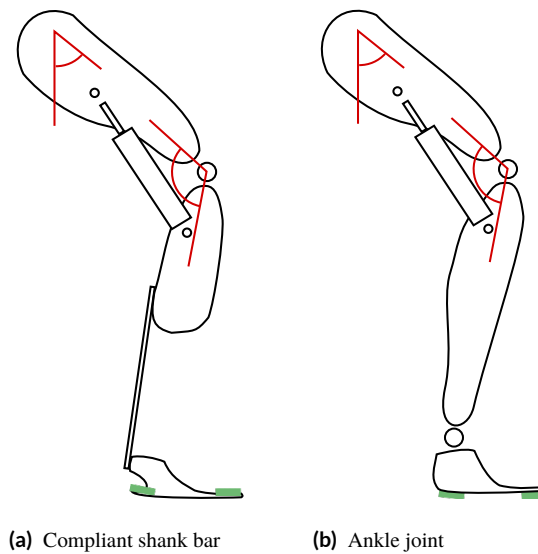
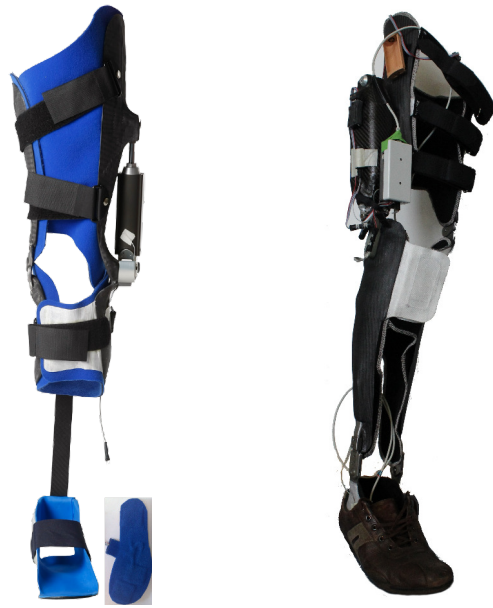


**Figure 7.5.:** Schematics for the available orthosis setups. Indicated are angle-sensors in red with reference and foot-contact-sensors in green at the sole, as well as additional acceleration sensors for impact and moment analysis.

## 7.2. Sensory Configuration

We want to implement detailed gait tracking as opposed to making assumptions on specific readings and derived measures, for example shank load or the ground reaction force. In section 5.3, *Control Problem Evaluation*, we have described the minimal control function in equation (5.1), which includes an abstract mapping of the gait progress to the control output via the sensory input.

In a simple RunBot experiment (see section 6.4), we tested the ability to continuously exert control over the whole gait cycle with a minimalist controller. We took a short look at the walking patterns of humans and RunBot and made the argument, that for RunBot two periodic sensory impressions with phase difference should be enough to exert control over the gait phase, whereas for humans additional features in the dynamics need at least another sensory input to disambiguate gait progress around the heel strike.



(a) Model with compliant shank bar

(b) Model with Ankle joint

**Figure 7.6.:** Photographs of the two prototypes described in Figure 7.5. Photograph 7.6 has been provided by Otto Bock; the inlay with force sensing resistors is beside the foot. For 7.6(b), the force sensing resistors are below between the foot-structure and the shoe. The boxing from Figure 7.7(c) minimises sensor changes through sole-shoe interaction.

With this foundation, we started to implement a sensory configuration for the orthosis, which provided features similar to RunBot. But for all that mechanical similarity, we have to keep the difference in the control problem in mind: RunBot needs active control, driving the servo motors.

In contrast, the orthosis has a hydraulic damper which can dissipate energy but lacks actuation. The orthosis controller therefore will implement some sort of stance control, which makes the ground contact an important phase of control. Still, at this point we assume RunBot as a minimal sensory setup to achieve detailed control depending on gait progress. For the choice of sensors on the orthosis, many decisions were influenced by the experience from our collaborators from Otto Bock.

### **7.2.1. Joint instrumentation**

For knee joint instrumentation, we embedded a potentiometer into a sink of the knee joint. Whereas functional, the mechanical stress on the exposed contacts lead to broken wires. Later on Otto Bock provided a hall effect based sensor fitting into the joint mechanics, which lead to a stable knee joint instrumentation.

For thigh ankle measurement we included an IMU based sensor by Otto Bock, which was developed for the E-Mag active project. Thus, we did not need to instrument the patients body on hip level, but could place the sensor on the orthosis. This sensor measures in a plane and delivers the angle relative to the vector of gravitational force. The IMU derive thigh angle in the saggital plane relative to the vertical axis and therefore does not deliver the same information as the hip joint sensors of RunBot, which represent a real joint angle as the relation between the trunk and the thigh.

The ankle joint could have been used for the prototype with a real joint in Figures 7.5(b), 7.6(b), but depending on the patient's status and their need for ankle joint support or even the need for a model with stiff ankle joint as in Figures 7.5(a),

7.6(a), we decided to not go for the ankle and leave it open for other sensors, like strain gauges.

## 7.2.2. Foot instrumentation

For ground contact detection, we settled for a set of force sensing resistors (FSRs) from Interlink Electronics (part. no 406 with  $1452 \text{ mm}^2$  active area) our collaborator suggested, and later the part. no 402 with  $39.9 \text{ mm}^2$  active area. These devices are easy to handle and access, providing one resistance per element which is reduced under pressure. The different stages of our FSR integration into the orthosis setup can be seen in Figure 7.7.

Another approach would strain gauge based sensors, which could be included in the stiff shank bar or as additional instrumentation on the ankle joints mounting. But they would not indicate the pressure distribution below the sole.

Our first approach was based on a simple testing setup to mount the FSRs to an inlay. This inlay was placed in the hard foot bed of the first orthosis prototype, as seen in Figure 7.6(a). But the sensors between the foot and the hard frame of orthosis were generating spurious sensory input independent of ground contact.

For the second orthosis prototype in Figures 7.5(b), 7.6(b), the FSRs were placed below the orthosis foot bed and the comparatively soft inner sole of the shoe. Still, the contact between the components would cause spurious sensory input.

The applied FSR models are highly sensitive with a range of  $\approx 0.1 - 100 \text{ N}$ . The resistance  $R$  changes from  $> 1 \text{ M}$  down to around  $100 \text{ k}$  with the resistance  $R \approx \propto 1/F$  [19]. Therefore, for an adult human, the FSRs are acting as ground contact switch, similar to the case of RunBot, but with smaller active area. Due to this high sensitivity, even small pressures in stance and swing phase produce quite high sensory readings with unknown fluctuations do to sensor deformation, as can be seen in the curves for FSRs 1 and 2 in Figure 7.8.

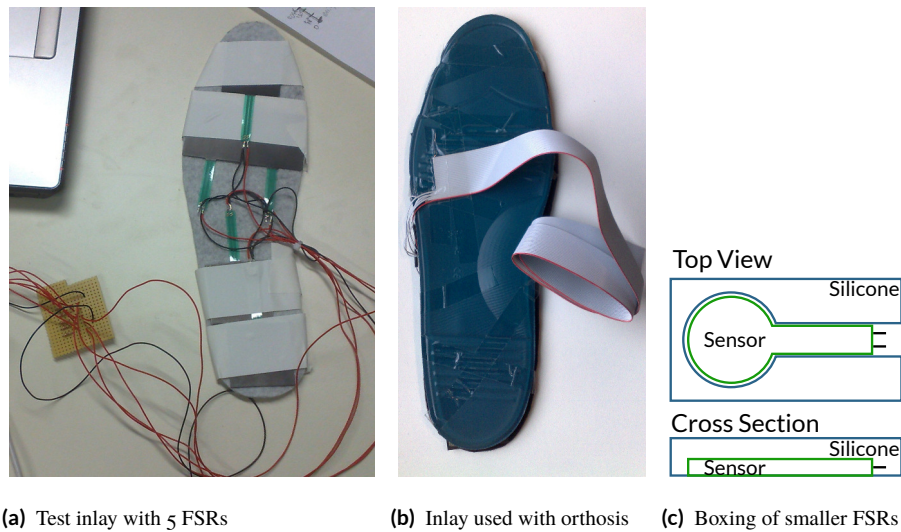


**Figure 7.7.:** Ground contact sensors: Integration of model 406 into inlay for shoes to test setup 7.7(a). The mounting on the inlay enables reproducible FSR positioning. In the middle 7.7(b): inlay for orthosis use. On the right side 7.7(c): embedding FSR model 402 in silicone to reduce signal through gauge on shoe or sole.

To overcome these spurious contacts, respectively the reduction of the sensory input range depending on shoe position and the unknown quantity of currently applied amount of torque between the leg and the orthosis frame, we changed to smaller FSRs (part. no 402) and surrounded them with an additional rubber enclosure as in Figure 7.7(c).

An additional positive effect is, that the rubber enclosure guards the soldering contacts, which were prone to mechanical stress. The reduced area of the FSR has to be taken into account when placing the sensors, but as the shoe and the orthosis frame mechanically spread pressure, every ground contact can be detected on an area which is huge compared to the area of one FSR. Because of this effect, large area FSRs have an even larger area of excitation. Smaller FSRs with additional enclosure can be used to measure the pressure distribution below the sole.



### FSR sensor placement

To determine the sensor placement, we recorded walking on flat ground with the inlay from Figure 7.7(a). Three consecutive steps are plotted in Figure 7.8: FSRs 1 & 2 always have pressure applied due to their placement, and FSR 3 has spurious activity at the start and end of the swing phase.

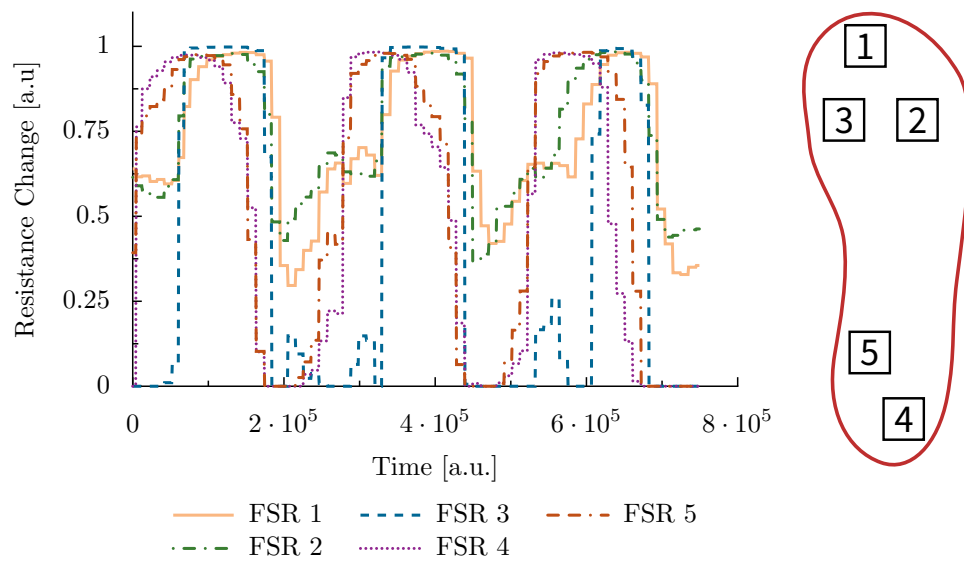
As all FSR have overlapping activity, we settled for two FSRs at positions 4, “heel”, and 1, “toes”, according to placement in Figure 7.8(b). An additional FSRs at position 2 would be advantageous, as it would complement the overlap of positions 1 and 4, but as only a limited number of analogue input channels are available we went for reduced coverage. Figure 7.9 shows the resulting signal for fluent steps of flat walking. The dashed blue line shows the envelope where at least one of both normalised sensory readings is  $\geq 0.4$ . Thus, this FSR-setup allows detection of heel-strike and foot-off. But due to mechanical instability, most experiments were conducted with the heel FSR only.

## 7.3. Summary

This setup provides the two periodic, angular sensors with additional ground contact sensors in the sole. Although the thigh and ground contact sensors are semantically different from those on RunBot, the sensory impression is comparable, as can be seen in Figures like 5.3 and 6.3.

The increased dimensions of the foot plate and the flexible orthosis structure allow more detailed ground contact detection than RunBot’s mechanical switches (Figures 7.8 and 7.9).

Thus, RunBot’s sensor-set can be seen as a subset of the orthosis’ sensors, allowing a similar flow of information processing. Naturally, we have fewer joints and as explained in section 4.1, only passive control over joint motion: the Otto Bock™-C-Leg-Element allows damping of the knee joints motion but no active actuation.



(a) Ground contact for 5 FSR positions

(b) Placement

**Figure 7.8.:** Sensory readings for 3 steps with the 5 FSRs in Figure 7.7(a) worn in a shoe with flexible sole. Because of the high excitation areas resulting from the FSR's size and the interaction with the sole, the activity is extended and FSRs 1 & 2 never relax.

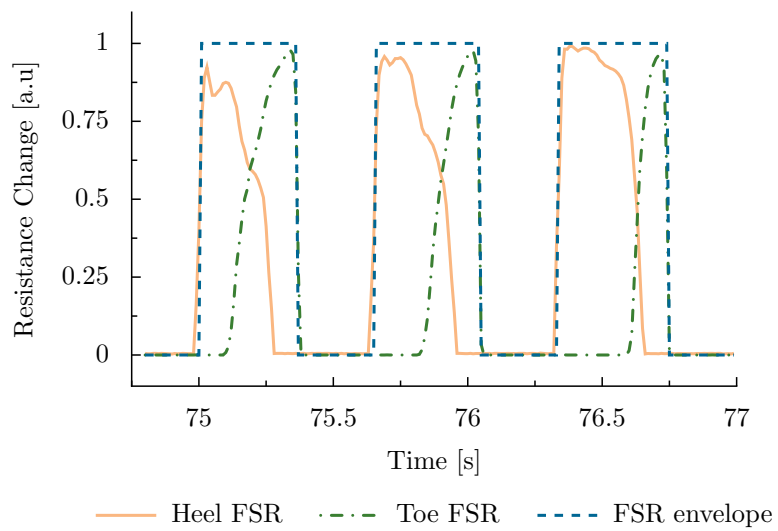


**Figure 7.9.:** Final FSR setup with a heel detection unit on position 4 and a toe unit on position 1, as compared to Figure 7.8(b). The envelope of the two sensors span the stance phase from heel strike to toe off.



**Part III.**

**Orthosis Controller**



*Small steps are better than great words.*

Willi Brand as cited by Egon Bahr

# 8

## Orthosis Feedforward Control

In this chapter, we transfer the simplified control problem from equation (5.1) in section 5.3 and its implementation for RunBot in section 6.4 to the orthosis. In the process, we extend the controller with regard to the passive operation conditions of the orthosis, while we still limit the controller to support only one gait.

For this, we will first consider design goals and requirements on the orthosis controller. Based on these, we will consider the design and implement of the actual controller. This controller will provide tunable and adaptive knee damping control. This will be implemented by means of a super-imposed modelling with a user interface.

This chapter is concluded with an evaluation of the controller regarding the presented design goals and the discussion of the implications for the further development of the presented controller, especially concerning the support of multiple gaits.

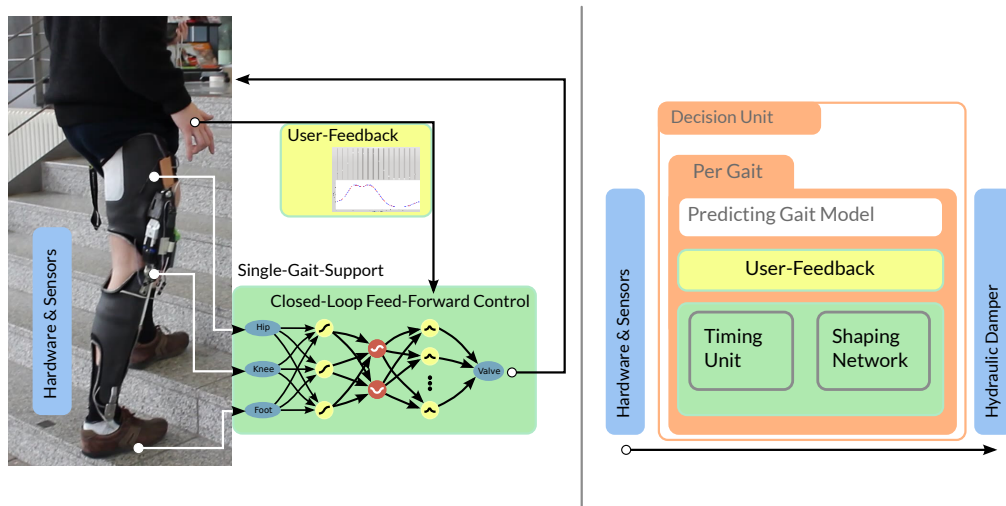


**Figure 8.1.:** Contents of this chapter: In this chapter, the feedforward-part of the controller will be presented together with the interface for user-feedback. We will start with the timing unit, which determines the gait phase and go on to the shaping network, which defines the damping applied at the knee joint. Then we will see how the user-feedback-mechanism allows to tune the behaviour and hides device-specifics from the controller. Higher-level components for multi-gait support will be handled in the next chapter.



We will discuss how to integrate online learning and adaptation. Then, a short glimpse on questions concerning the support of multiple gaits and the shortcomings of the current setup is done. This will prepare us for introduction of internal models to differentiate multiple gaits in the next chapter.

## 8.1. Locomotion Generation in Orthosis Control

For orthosis control a similar approach was devised, which has the response speed of a reflexive controller. The human can be seen as an *external pattern generator* with highly varying frequency. Because of the high variability in the human walking frequency it is unrealistic to have a central pattern generator adapt to the walking frequency. Adaptation could only work on the presented frequency, therefore an adaptive pattern generator would necessarily often lag behind.

To accommodate for this frequency adaptation problem, the orthosis controller bases its control signals around a mechanism to extract gait phase information from its sensory input. The difficulty in this is lying in limitation of sensory input to the ipsilateral leg.

Initial tests have been done with RunBot. Other groups recently started doing experiments with gait phase extraction from the contralateral side, see discussion.

## 8.2. Requirements on the Controller

### 8.2.1. Basic Considerations

As already detailed, the C-Leg-Element applies damping for knee flexion. This makes the orthosis a passive device and we can only dissipate energy. The two

important consequences are, that (1) the patients have to power the walking themselves, and (2) that we will implement a kind of stance-control, i.e., we will free the knee joint for leg swing and stabilise the stance-phase by damping the knee-joint.

Furthermore, we want to be able to apply the damping at all times of gait cycle, for example we want to enable pre-damping ahead of the heel strike. The patients will be enabled to tune the controller's behaviour, such that they increase their comfort while walking.

But neither do we know possible patients' exact muscle status in advance, nor do we know the contribution of other muscle groups to the patient's gait, i.e., to which extent they power their gait with muscle groups not used by healthy walkers and what part avoidance movements, that means systematic deviations from average healthy gait, play in the individual gait patterns.

Control of the damping in knee flexion is a control problem for one degree of freedom, which is cyclic in time. To be able to support arbitrary gaits, and to gain full support to tune the controller's output, we split the controller into two steps:

1. **Timing:** The controller determines the current position in the gait cycle for the individual patient as abstract gait phase  $\varphi$ .
2. **Output:** The output is applied as a function of the gait phase  $\varphi$ .

### **8.2.2. Control Flow**

We will not cover the complete design of the final orthosis controller, which can be found in Chapter 9. Instead, we will focus on the central part of the bulbous system, which is designed to produce a control signal in the manner of a fast feed forward system. Therefore, with the exception of user feedback, the control flow is completely linear as depicted in Figure 8.2, and it forms the innermost layer of the final controller.

## 8.2. Requirements on the Controller

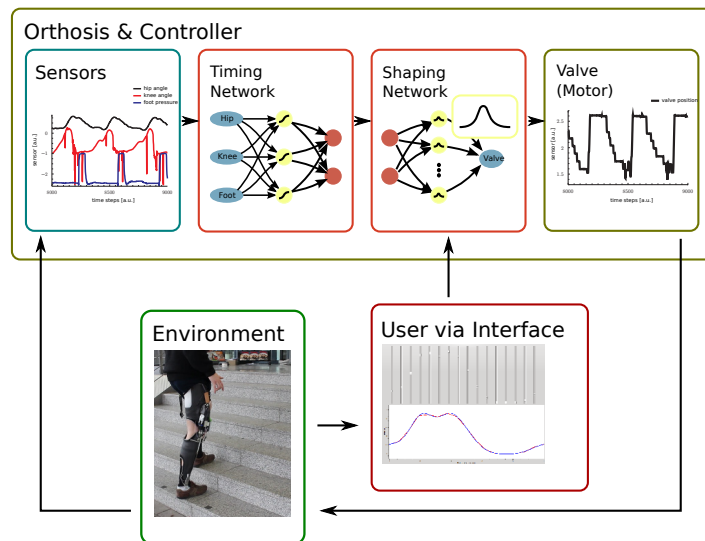


**Figure 8.2.:** Sketch of core controller: The central structure of the proposed controller is defined by a closed-loop, feed-forward signal flow, which determines the current gait phase  $\varphi$  in the timing network. The shaping network determines the desired damping as function of the gait phase, which is applied via the hydraulic damper. An user interface allows the user to tune output of the shaping network.

## *Orthosis Feedforward Control*

The most important aspect of this section is the optimal tuning of the device to fit the patient, as the core controller is concerned with this modelling of the device's behaviour to the patients needs. As we will see in later chapters, other layers of control can handle behaviour changes and adaptation. They can run in parallel to and interact with the structure presented in this section.

First, we will describe the *timing unit* which handles design goal 2.: the ability to capture the individual gait. On top of this timing unit we apply the design goal 1: the desired damping. The third design goal is transient in the presented controller by ways of the representation of gait timing and damping.

Figure 8.2 shows the control flow: To generate an arbitrary damping control signal on top of the timing unit, the timing unit has to generate a patient and gait independent intermediate representation of gait progress, which approximates the gait phase  $\varphi$  from equation (5.2). Given the sensory input  $\vec{s}$ , the timing unit performs the mapping

$$\text{timing unit} : \vec{s} \mapsto \varphi \quad . \quad (8.1)$$

The desired damping will then become a periodic function  $d(\varphi)$  of the gait phase

$$\text{shaping unit} : \varphi \mapsto d(\varphi) \quad , \text{ with } d(0) \equiv d(1) \quad . \quad (8.2)$$

Finally, the desired damping has to be mapped to the valve position in the hydraulic damper.

Then we assume, that the valve position control is handled by one of the data acquisition systems from section 7.1.

At the end of this chapter we will see that the immediate result of this tunable controller will be the over-fitting of the supported gait. In the next chapter we will address this problem with gait models to recognise and differentiate these specific movements.

In this way, additional layers address different requirements on the orthosis controller, which have been detailed in chapter 4.3.

### 8.2.3. Timing unit

The timing unit is necessary to resolve the step into an internal representation of gait progress (compare figure 5.2).

In other words, the timing unit tracks gait progress tracking and therefore has to be able to support **(a)** specific gaits of **(b)** individual patients. We formulate a set of requirements on the timing unit, which will guide the implementation and will allow us to evaluate the performance of the timing unit.

**Necessary requirements** on the timing unit are

1. *Generality*: The design makes no assumptions about patient abilities.
2. *Individualisation*: It is able to adapt to individual features of gait and hides the details from downstream processes.
3. *Abstraction*: It generates an abstract representation of gait progress from the sensory data.
4. *Time-Independence*: It scales with walking speed and stride length.
5. *Reaction*: To allow fast reactions, for example to perturbations, it should exhibit short delays.
6. *Detailed Control*: It provides a smooth and continuous representation of gait progress
7. *Adaptable*: The implementation allows to adapt changes in the users gaits.

With requirement 1 we want to keep the patient target groups as big as possible, whereas requirement 2 extends the level of support for individual patients, aiming to increase comfort and the impression of seamless integration.

Requirements 3 allows downstream processes to be independent of how the timing unit works. Requirement 4 enforces the abstraction to include variations in the gait. To be able to handle disturbances, requirement 5 includes safety concerns.

Requirement 6 warrants control for the whole gait cycle with the same accuracy: As the shaping unit is a state-less function of the gait phase, changes in control output can only happen when the gait phase changes. As we make no assumption about when the patient needs support, we need to ensure that the device is able to react over the whole gait cycle.

The ability to change the behaviour of the device later on, in an online or assisted manner, forms requirement 7, compare section 5.1 and chapter 12.

#### **8.2.4. Shaping Unit & User Feedback**

The shaping unit is responsible to determine the required damping for a specific time determined by the gait phase  $\varphi$  and request the positioning of the valve accordingly. According to equation (8.2), the shaping unit defines the desired damping  $d$  directly as a function of the gait phase  $\varphi$ .

The shaping unit is state-less. The only requirements on the shaping unit are, **(1)** that it allows defining the desired damping in sufficient detail and **(2)** that is implemented in a way, which allows later adaptation. All other properties are determined by the timing unit.

Because the user is part of the damping definition via user feedback, it seems advised include another requirement **(3)**: that the representation should be understandable and easy to visualise, so that the users can develop an intuition on how their feedback changes the devices behaviour.

## 8.3. Implementation

### 8.3.1. Timing Unit

#### Approach

The timing unit maps the sensory input directly to the gait phase  $\varphi \in [0, 1)$ , as formulated in equation (8.1) from section 5.3:

$$\text{timing unit} : \vec{s}_t \mapsto \varphi_t \quad .$$

For the implementation we chose a perceptron similar to the one in the RunBot experiment of section 6.4. To improve the smoothness and quality of the output, as compared to the bad fit of the motor voltages in Figure 6.10(d), we choose the output to be of similar form as the input and use equation (5.3) to split the timing unit into the mapping onto a circular motion in the plane

$$\hat{d} : \vec{s}_t \mapsto \begin{pmatrix} x_\varphi^t \\ y_\varphi^t \end{pmatrix} = \begin{pmatrix} \cos(2\pi\varphi_t) \\ \sin(2\pi\varphi_t) \end{pmatrix} \quad .$$

For the first sensor set, especially the potentiometer on the knee joint, a low-pass filter was included to smooth rapid changes because of noisy sensor input:

$$\begin{pmatrix} \tilde{x}_\varphi^t \\ \tilde{y}_\varphi^t \end{pmatrix} = f \cdot \begin{pmatrix} x_\varphi^t \\ y_\varphi^t \end{pmatrix} + (1 - f) \cdot \begin{pmatrix} \tilde{x}_\varphi^{t-1} \\ \tilde{y}_\varphi^{t-1} \end{pmatrix} \quad , f = 0.8 \quad ; \quad (8.3)$$

this kind of low-pass filter is the equivalent of a recurrent artificial neuron with weights  $f$  and  $(1 - f)$ .

## Orthosis Feedforward Control

Which is followed by the transformation to the gait phase  $\varphi$ :

$$\varphi = \begin{cases} \frac{1}{4} & \text{for } \tilde{x}_\varphi^t = 0 \wedge \tilde{y}_\varphi^t \geq 0 \\ \frac{1}{2\pi} \tan^{-1}(\tilde{y}_\varphi^t / \tilde{x}_\varphi^t) & \text{for } \tilde{x}_\varphi^t \neq 0 \\ \frac{3}{4} & \text{for } \tilde{x}_\varphi^t = 0 \wedge \tilde{y}_\varphi^t < 0 \end{cases}, \varphi \in [0, 1) .$$

Simply speaking, the perceptron in the timing unit is trained to map the 8 in the thigh-knee-angle graph of Figure 5.3(a) to a circle, from which the gait phase  $\varphi$  is determined.

Although all processing steps could operate on the 2D-representation  $(x_\varphi, y_\varphi)$ , compare to Figure 8.3, the 1D-representation  $\varphi$  is independent of the distance of  $(x_\varphi, y_\varphi)$  to the origin, and therefore more robust. From a practical point of view, it is easier to visualise in this thesis or the user interface. Therefore, we will stick to  $\varphi$ .

## The Network

The network is implemented using the FANN library [69] as a multilayer artificial neural network with one hidden layer of four neurons and two output neurons. The hidden layer and output neurons use a symmetric sigmoid transfer function.

## Training

Training data was recorded and then segmented according to section 8.3.3. For each step  $j$ , the stride length  $l_j$  was determined in samples. For each sample  $i$  in each segmented step  $j$ ,  $i \in [0, l_j)$ , the training dataset was generated using the



Sensor	Calibration condition	Mapped value
Thigh Angle	Straight	0
	90 ° flexed	1
Knee Angle	Straight	-1
	90 ° flexed	1
FSRs	Full weight	0
	Free	1

**Table 8.1.:** Angles used in calibration procedure. The mapping ensures values in the range  $[-1, 1]$  for the artificial neural network.

sensory values  $\vec{s}_i$  as input-vector and the output-vector  $\vec{o}_i$  determined as

$$\varphi_i = \frac{i}{l_j} \quad (8.4)$$

$$\vec{o}_i = \begin{pmatrix} o_1 \\ o_2 \end{pmatrix} = \begin{pmatrix} -\sin(2\pi\varphi_i) \\ -\cos(2\pi\varphi_i) \end{pmatrix} \quad (8.5)$$

The FANN learning function was called with a learning rate  $\mu = 0.05$ , using the quickprop backpropagation algorithm [69].

**Input calibration & scaling** was performed such that the typical range of motion produces values in the range  $[-1, 1]$ . The angles used in the calibration procedure of the orthosis controller are detailed in table 8.1. These conditions were averaged over 1000 samples, to determine controller calibration.

### 8.3.2. Shaping Unit & User Interface

Because the user is part of the damping definition via user feedback, the representation should be understandable and easily visualised. Therefore, it seems

most suitable to define the damping in terms of the actual damping, i.e., in terms of valve positions in the hydraulic unit. This simplifies our mapping, as we do not need further calibrations or transformations of the control output.

As the feedback loop for the user covers the whole mapping, including properties of the hydraulic unit and the patient's contribution to body support, these unknown contributions can be ignored on the controller side, greatly simplifying the controller design in general.

### **Internal Representation of Damping Function**

We chose to use a Radial-Basis-Function network [10, 73] on an equidistant 1d-grid to map the gait phase to the desired damping strength in the knee joint. This is a straight forward approach, which allows the user to define the one dimensional output function on a coarse grid, approximating in between the supporting points with Gaussian kernels. Similar to the perceptrons chosen for the timing unit, the Radial-Basis-Function networks allow retraining at run-time as soon as a new set of supporting points is defined; thus leading to a gradual adaptation of the internal representation with each iteration of the learning algorithm [102].

Of course, other parametrisations of the damping function would allow for the same, but the Radial-Basis-Function networks give few restraints to the function approximated. This introduces no assumptions about the role of the parameters, as these the weights of the Gaussian kernels. Only the number of kernels has to be chosen in a way which provides high enough a resolution.

The periodic boundary conditions were included by an periodic extension of the Gaussian kernels during output calculation. Thus, the training was transparently handled as well.

To allow the tuning of the device to individual needs, this mapping can be done at run time with the user interface (compare Figures 8.4, 8.10 in the next section.

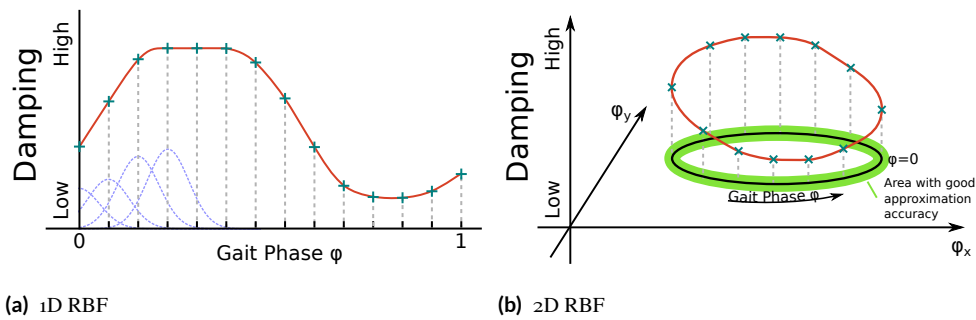


**Figure 8.3.:** Radial-Basis-Function approximation of the desired damping function. On the left side the 1D representation, which directly uses the gait phase  $\varphi$ . On the right side the 2D representation, which will loose accuracy with distance to the circle.

A 2d Radial-Basis-Function network could have been chosen for the representation in the plane, as in equation (5.3), making the handling of the periodic boundary conditions superfluous. But we had to deal with another degree of freedom, in which radial deviations from the circle on which the damping function is defined by the user, would lead to errors in the approximation. One could try to handle this by extension of the training in the radial direction, but the use of the one-dimensional representation with  $\varphi$  solves this in an elegant manner.

### User Interface for Damping Definition

The user interface in Figure 8.4 shows a set of sliders, each representing the output function's value on one point of a grid of supporting points. These can be chosen to coincide with the supporting points of the Radial-Basis-Function network, or not. Depending on the chosen width of the Gaussian kernels, the result will faithfully represent the dataset, or will show overshooting or smoothing of the user's input.

As the Radial-Basis-Function network provides universal approximation [10, 73] there is no need for the user interface to mirror the internal representation. Where-

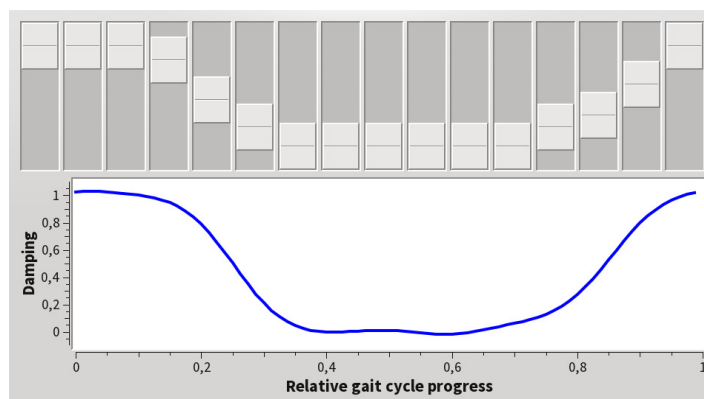


**Figure 8.4.:** User interface for damping tuning. This window allows the user to directly manipulate the damping which is applied by the valve driver. The horizontal axis shows the progress within the step from heel-strike to heel-strike. The vertical axis is manipulated through the sliders and defines the desired damping at all times. Adjustments will update the system's behaviour immediately. This enables the user to tune the device's behaviour to his expectations and needs. A set of possible damping patterns is shown in Figure 8.10.

as for patients an interface to directly manipulate the locking and release times of the knee joint with the corresponding values for the desired damping might be easier, the interface from Figure 8.4 is still sufficient to find suitable damping patterns in experiments with the healthy staff of the associated project.

### **8.3.3. Segmentation of Gait Recordings**

A problem during training data construction and the analysis of walking experiments is the segmentation of gait recordings into steps. For example, this segmentation is needed to derive the gait phase for the samples of the step or to perform analysis step-wise. In accordance with the definition of the gait cycle in chapter 2, we will cut the recordings into steps at heel-strike. Based on the heel-FSR, the pressure onset is determined by flanks in the heel-pressure. Due to the high sensibility of the FSR (section 7.2), only the onset is clearly defined and will be used. Due to interactions of ground reaction forces, the orthosis frame,

and the foot, the sensibility makes filtering necessary to ignore small changes in the pressure. Furthermore, the variability in the the heel-pressure amplitude is high due to these interactions.

For the description of this algorithm, we assume the heel-FSR readings in the range of  $[-1, 1]$  (without units), with  $-1$  meaning maximum pressure, and  $1$  no pressure. The implementation uses a hysteresis to be immune to small deviations. The threshold to detect ground contact defaults to  $0$  the threshold to detect a free heel  $0.8$ . The algorithm is implemented as a finite state machine and performs the following steps:

1. Initialise the state to ground contact or free heel depending on the first sample in comparison to the threshold for ground contact.
2. For each sample
  - a) When in ground contact state and the current sample is greater then the threshold for free heel, then change the state to free heel.
  - b) When in free heel state and the current sample is smaller then the threshold for ground contact, then change the state to ground contact.
3. Collect the sample numbers of all touch down events (state changes to ground contact) in a list.
4. Correct the sample numbers it the list to the number of the preceding sample which is closest to  $0.8$  to determine the onset.

This list of events now describes the heel-strikes in the given recording.

## 8.4. Evaluation

In this section, we will experimentally evaluate the properties of the presented controller against the requirements from section 8.2.3 as well as the interplay with the shaping unit (section 8.2.4).

### *Orthosis Feedforward Control*

As the timing unit is, by design, working on arbitrary trajectories in the joint-angle space, we will not test for requirement 1, the *Generality*. In the same way, the artificial neural network allows re-adaptation of the transformation with another training run on modified training data, satisfying to be *adaptable* (requirement 7).

A detailed analysis of timing unit's transformation properties will allow us to gain insight into its ability to map individual gait onto an abstract gait representation. The evaluation of the linearity of the gait progress tracking via the gait phase  $\varphi$  will thereby capture requirements 2 *Individualisation*, 3 *Abstraction* & 6 *Detailed Control*.

Although the *Time-Independence* and *Reaction-Speed* properties (requirements 4 & 6) are implicitly guaranteed by the mapping properties of the timing unit, we will take a look at the run-time behaviour for leaps in the gait phase and the influence of the low-pass filter.

The evaluations will be complemented by investigations on the performance of different artificial neural network and input configurations for the timing unit, as well as experiments on the effect of the selection of training data to the variability of applicable environments.

#### **8.4.1. Ability to track the Patient's Gait**

To investigate the ability to capture the patient's gait, we will consider the quality of the gait phase representation produced by the timing unit. As detailed above, the quality depends on the controller's ability to exert control. Therefore, we will check for the linearity & smoothness of the gait phase representation, to investigate the detail and the continuity of the support the controller can provide. This study has been published in [9], the results have been adopted for this section.

As the control output is determined as a mapping of sensory input  $\vec{s} \mapsto \varphi \mapsto d(\varphi)$  to the joint damping by means of the gait phase  $\varphi$ , the controller only changes its output, when the sensory input induces in change in  $\varphi$ .

As we make no assumptions about the patients abilities, the controller should be able to exert control at all phases of the gait cycle. For the user interface to give a intuitive representation of the device's behaviour, the mapping should be linear, so that a similar distance in the user interface maps to a similar phase (or timing) difference in the step.

This accounts for the demand, that a good abstraction of individual gait provides a linear and smooth mapping of the sensory input to the gait phase  $\varphi$ . The more linear the mapping, the better the level of detailed control.

Or the other way around: fast, step-like changes in the gait phase produce drastic changes in control output. Plateaus in the gait phase  $\varphi$  on the other hand are regions of reduced differentiation and bear no change in control output.

Therefore, we will investigate the increments in gait phase  $\Delta\varphi$  for timing units trained on flat ground and stairs under these two conditions.

**Hypothesis:** Training of a timing unit allows almost linear mapping of the sensory input  $\vec{s}$  to the gait phase  $\varphi$  on the terrain used for training. On unknown terrain the progress of gait phase tracking will loose its linearity and shown non-smooth behaviour, like bumps and plateaus.

**Method:** To check the linearity & smoothness of the gait phase mapping, we will compare the gait phase determined by the timing units with the ideal mapping. The latter can only be derived post heel-strike and is therefore unavailable for on-line purposes.

To compare the on-line gait phase  $\varphi$  to the ideal gait phase  $\varphi'$ , we apply a similar procedure as used for the generation of the training data, determining the ideal gait phase  $\varphi'$  according to equation (8.4).

The actual comparison is done by investigation of the slope of the gait phase representation in form of discrete increments  $\Delta\varphi$ . To be able to compare the slope for steps of different speed and length, we will interpolate all steps to 200

samples after segmentation as described in section 8.3.3. Thus, in this evaluation, for all steps the ideal slope is  $\Delta\varphi' = \frac{1}{200}$ .

## **Experimental Setup**

Used is the orthosis with thigh angle, knee angle and one heel-FSR. We use the presented controller with two timing units and disabled motor output, to investigate the gait tracking only.

In a first run, training data is gathered for walking on flat ground and stair climbing. This data is used to train the two timing units for flat ground and stairs climbing. Walking is done indoors.

## **Results**

For experimental evaluation of gait progress accuracy, the gait phases from models for flat walking and stair climbing were evaluated on the corresponding and opposite terrains. We analysed 30 steps along a floor with 38 steps of stair climbing of a healthy subject wearing the orthosis. None of these steps covered transitions between the models to circumvent problems in the interpretation due to ambiguities, compare Chapter 9.

The gait phases  $\varphi$  in Figure 8.5 were evaluated online and plotted against the off-line computed gait phase  $\varphi'$ . In Figures. 8.5(a) and 8.5(d), no model reproduces the ideal gait progress representation, but the representation is mostly monotonous with  $\varphi \approx \varphi'$ , except at heel-off, where fast heel pressure changes induce fast increases in  $\varphi$ .

For the mixed cases in Figures 8.5(b) and 8.5(c), we observe a phase shift of the heel strike of the model representation to the real heel strike event ( $\varphi' = 0$ ). Furthermore, the model for flat ground on stairs in Figure 8.5(b) shows 4 steep increases with almost constant values in between, while the model for stair



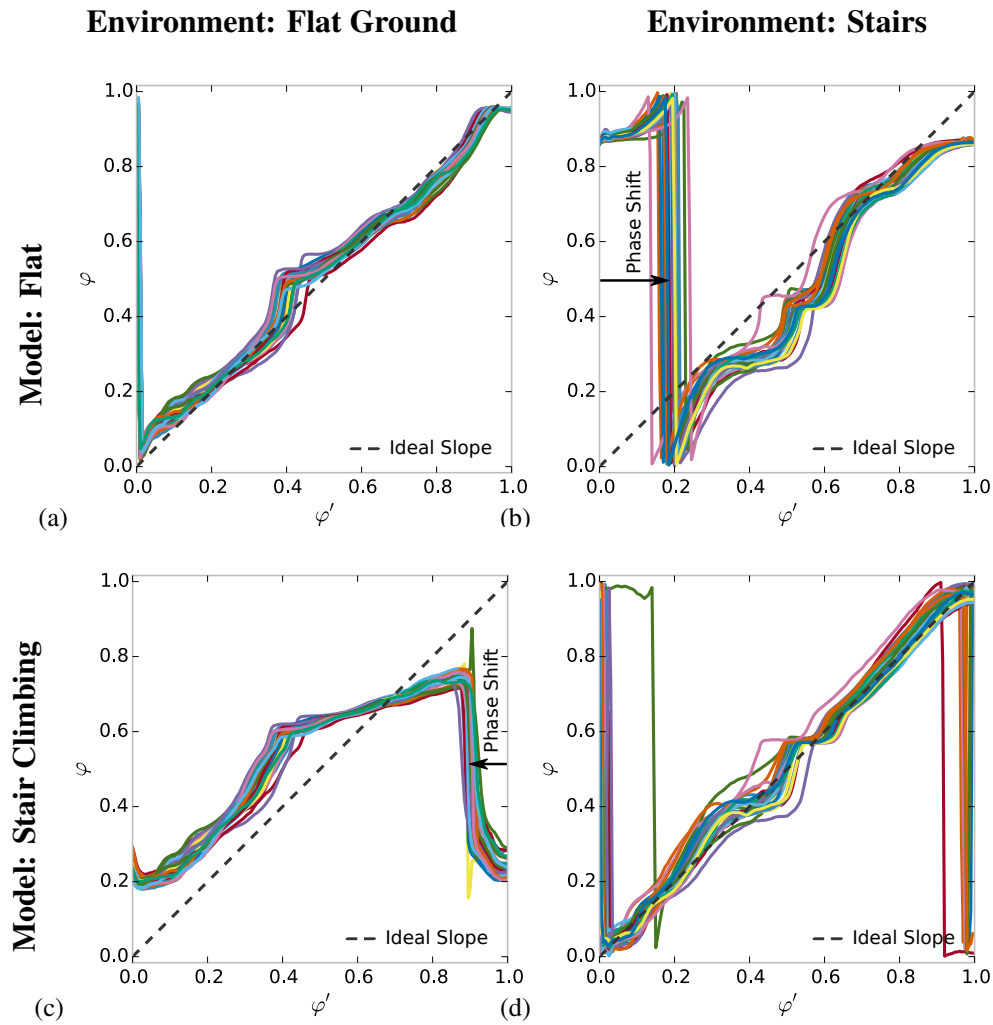


**Figure 8.5.:** Coloured lines indicate gait phases for 25 steps on flat ground and 8 on stairs. They are smoother for the native model in Figures 8.5(a) and 8.5(d), while the unfitting models in Figures 8.5(b) and 8.5(c) show phase shifts and strong deviations from the desired smooth, linear behaviour of the ideal gait phase  $\varphi'$  indicated by the dashed line.

		Environment	
		Flat Ground [°]	Stairs [°]
Model	Flat	1.8	34.2 ± 3.7
	Stair Climbing	-18.0 ± 1.2	2.5 ± 5.5

**Table 8.2.:** Phase shifts of the models for 30 steps on flat ground and while stair climbing (38 steps for flat model and 31 steps for stair climbing model).

climbing on flat ground shows a decrease in gait progress for almost 20 % of the gait cycle.

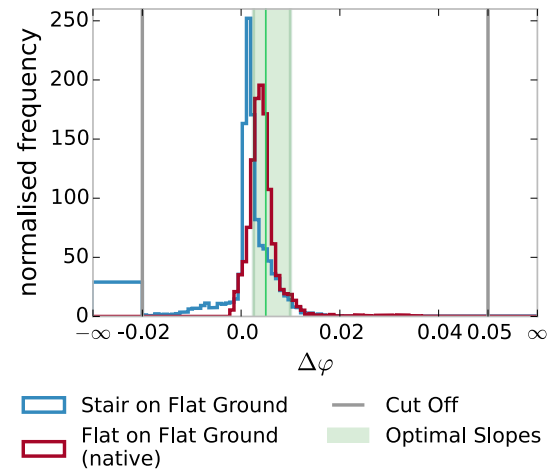
The increments  $\Delta\varphi$  of the gait phases are shown in Figures 8.6, where the native gait model is plotted in red and the unfitting model is plotted in blue.

The histogram of increments on flat ground in Figure 8.6(a) shows a tendency to smaller and more negative changes for the unfitting stair climbing model, for which increments  $\Delta\varphi < 0$  are more frequent. For the fitting model it is reversed, the distribution has a smaller deviation from the ideal increase of  $\nu_{opt} = \frac{1}{200} = 0.005$ , which means fewer negative changes and fewer increments of large value. For the flat walking model, 69 % of all increments were in the interval  $[\frac{1}{2}\nu_{opt}, 2\nu_{opt}]$ , whereas for the stair climbing model, only 31 % were inside this interval.

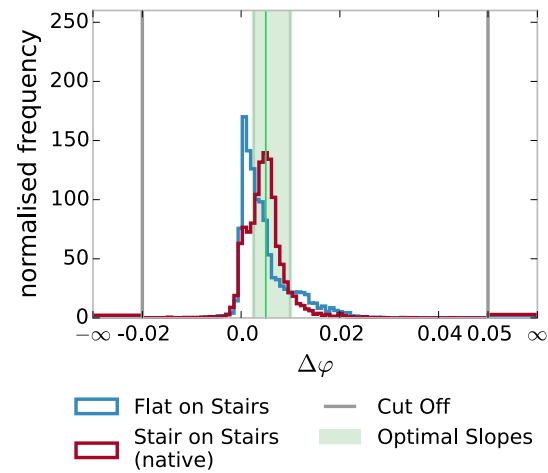
The distributions for stair climbing (in Figure 8.6(b)) have a pronounced peak around the ideal increment  $\nu_{opt}$  for the native model. Conversely, the model for flat walking has a peak for increments  $|\Delta\varphi| \ll \nu_{opt}$  and more increments of large value. For the stair climbing model, 65 % of all increments were in the interval  $[\frac{1}{2}\nu_{opt}, 2\nu_{opt}]$ , whereas for the flat walking model 40 % were inside this interval.

The evaluated phase shifts of Figure 8.5 are shown in Table 8.2.

In case of the missing steps in the statistics of the stair climbing model on stairs, the phase reset to 0 was immediately at the end of the preceding transition steps



(a) Increments on Flat Ground



(b) Increments while Stair Climbing

**Figure 8.6.:** Comparison of increments  $\Delta\varphi$  for data from Figure 8.5: the fitting model (in red) shows fewer negative or almost zero increments. For a constant function, all increments would be 0.005. The opposing model has more increments of higher magnitude (collected in one bin) while it is shifted to the left at the same time. All increments  $|\Delta\varphi|$  outside the cut off were counted in the bins to the sides; the height is according to the normalisation of a bin with identical width to all other bins.

and therefore excluded, although  $\varphi$  was at the same order of magnitude as for other steps after heel-off, i.e., close to 0.

## Conclusions

In general, it can be seen, that the fitting model not only offers a more linear increase in the gait phase representation, but the unfitting model is suffering a huge phase shift. This means, that the trained model is able to approximate the ideal gait phase far better than a model which is trained for another terrain. We can describe the error by the area of the histogram outside the area of optimal slopes. This error determines the percentage of the gait phase, which is not recognised with almost ideal slopes.

Another important figure is the phase shift, which can be interpreted as the accuracy of heel strike detection. To interpret this precision, we have to compare the absolute phase shift to the recording frequency of the device.

At 100 Hz sampling frequency, average steps have 150 – 200 samples, resulting in  $\frac{360^\circ}{200} - \frac{360^\circ}{150} = 1.8^\circ - 2.4^\circ$  per sample, which is comparable to the average precision shown in Table 8.2.

The matching of the average precision to the sampling frequency of the device is not the strongest possible statement. It would be better, if the maximum phase shift were in the order of magnitude of the sampling frequency, which is the case for the model on flat ground. But we see in Figure 8.5(d), that the majority of the high error and standard deviation is contributed by one respectively two of the 31 steps.

We conclude, that the presented gait models are able to resolve the learned gait with a distribution of slopes, which is centred around the slope of the ideal model (cmp. Fig. 8.6) and a phase reset which is matching the heel-strike (cmp. the diagonal cells in Table 8.2). This means, they offer smooth and continuous gait progress tracking, on which model-free, individualised control can be founded.

Models trained for different gaits, on the other hand, show worse performance. We observe sub-optimal increments in Fig. 8.6 and significant phase shifts of the heel-strike event as in the off-diagonal cells of Table 8.2.

As changes in the control output are bound to changes of the gait phase  $\varphi$ , an even resolution of  $\varphi$ , or in other words a narrow distribution of increments  $\Delta\varphi$ , is crucial for detailed and continuous control. Fig. 8.5(b) shows a controller, that would only have 4 events with drastic changes of its output, whereas a good phase resolution allows fine grained control which is theoretically only limited by the sampling frequency of the underlying hardware.

The phase shift is a consequence of the sensory input's inherent phase relation, which changes with gaits, like on flat ground or stairs. An example for the phase difference in different gaits is shown in Figure 9.9. This phase difference between, e.g., thigh and knee angle, makes one model for all possible gaits difficult. Nonetheless, the combination of a well chosen set of specialised gait models with appropriate gait switching (see chapter 9) implements good gait progress resolution for all gaits.

This raises the important question, how many independent motions have to be supported to gain good results for a specific use case. Furthermore, the application of a fall-back controller to provide simple control in unknown environments is a necessary precaution.

The on-off-switching characteristic of the FSR ground contact sensors lead to steps in the gait phase representation, which might be solved with additional sensors or pre-processing. But they provide a safety measure by enabling immediate reactions to stumbling. The restriction to ipsilateral sensors makes the approach suitable for real world prosthetic applications.

Although a thorough analysis with more subjects, especially subjects with need for the orthosis, would be necessary to allow a final statement, the presented data indicates the ability to map individual gait onto an abstract representation of gait progress, which allows detailed control during all phases of the gait cycle.

### **8.4.2. Influence of smoothing of the gait phase**

The introduction of smoothing in the timing unit leads to a recurrent contribution in the gait phase determination. Still, the smoothing is quite small and therefore introduces no noticeable delay, as shown in Figure 8.7.

This low-pass filter has been introduced to cope with the noise in the first generation of equipped sensors and might as well be disabled for the current sensory setup.

### **8.4.3. Gait phase models of different complexity**

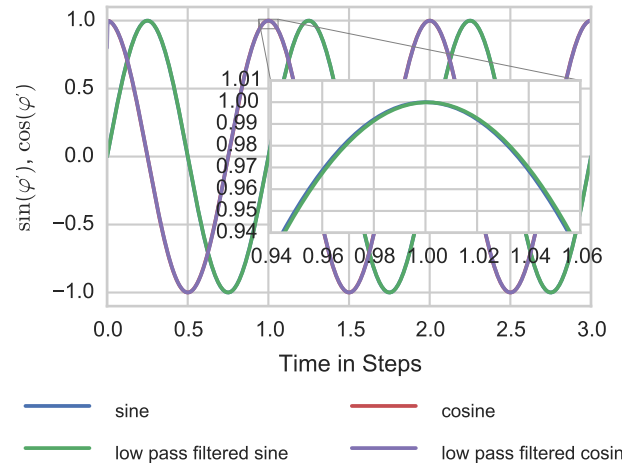
In this section, we will compare gait phase tracking with and without the toe FSR. As mentioned in chapter 7, the toe FSR is subject to higher stress, and therefore unused in most of the experiments.

Nonetheless, we will gain insight into ways to optimise the gait phase tracking.

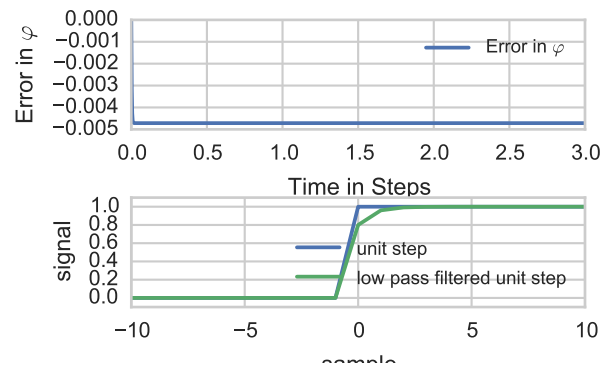
While section 8.4.1 provides a more extensive approach to evaluate the quality of gait phase tracking, in this section, we will limit the evaluation to the training performance as expressed by the training error. As long as the training sample is representative, we can assume that a thorough evaluation as in section 8.4.1 would yield similar results.

As the artificial neural networks are implemented with the FANN library [69], we will evaluate the training output of its training function. This function evaluates the learning error, which is the mean absolute error per sample, and a value called “bit fails”, which counts the number of training samples, which have an error above a limit, which has a default value of 0.35.

For an output in  $[-1, 1]$ , this error of 0.35 is about 17.5 % and therefore quite high. If we assume this to be around the highest slope of the trigonometric



(a) Delay in  $x_\varphi, y_\varphi$



(b) Top: Resulting error gait phase; bottom: low pass filtered unit step

**Figure 8.7.:** Influence of the smoothing on the timing unit. The smoothing is only minor, as can be seen in the bottom plot of 8.7(b). The actual error in  $\varphi$  is far below the actual sampling rate.

## *Orthosis Feedforward Control*

functions, this would be make a phase shift of

$$\begin{aligned}\Delta\varphi &= \sin^{-1}(0.175) - \sin^{-1}(-0.175) \\ &= 0.35 \quad ,\end{aligned}$$

or  $20^\circ$ , which is around 6 % of the gait cycle. As an approximation for the worst case, we will assume the error around the extremes of the trigonometric functions, splitting the error around the maximum

$$\begin{aligned}\Delta\varphi &= 2 \cdot [\sin^{-1}(1) - \sin^{-1}(1 - 0.175)] \\ &= 1.2 \quad ,\end{aligned}$$

or  $69^\circ$ , which is around 19 % of the gait cycle.

As absolute errors, these numbers would render the method useless.

Still, the way the fann library counts this “bit fails”, the actual importance can be neglected as the training sample for flat walking has 14467 entries from 102 steps, which makes the actual number of problem cases singularities in the data set. The low pass filter included in equation 8.3, will reduce the impact of such singular events with a small influence on the overall performance, as presented in section 8.3.1.

Therefore, we keep the default bit fail limit to be able to detect grave problems with the training data.

It has to noted, that a high number of bit fails in training can result from the selection of heterogeneous steps. To prevent this, the samples can be selected manually. In this study, on sequences of homogeneous steps a filter with a cutoff based on the standard deviation of the sequence has proven sufficient to filter periods of standing and other heterogeneities, if necessary<sup>1</sup>. As the initial training data is gathered from a training run, we train with all steps, which are in one standard deviation of the average step length. In our case, the filter removes

---

<sup>1</sup>This was only necessary for training sequences with many interruptions. The inclusion criterion was a step length in the range of the mean step length  $\pm 2$  times the standard deviation of step lengths in the sample.



delayed, start & stop steps, which mostly have to do with closed doors or other obstacles along the way.

In Figure 8.8 we see, that the different numbers of hidden layer neurons provide no significant difference in performance. The inclusion of the toe FSR provides a tendency to lower prediction errors with a small overlap from the 25 % to 75 % percentiles.

Based on these observations and the stability problems with the toe FSR, we choose an artificial neural network with 4 neurons in the hidden layer, deriving the gait phase  $\varphi$  based on thigh- and knee-angle and the heel FSR.

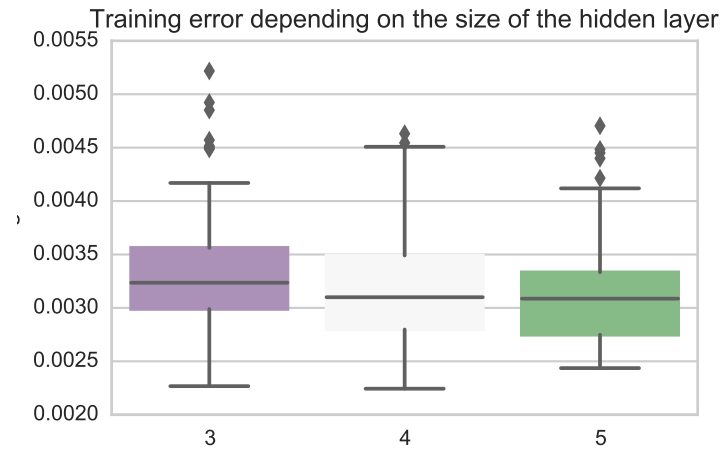
### 8.4.4. Handling of Step Variations

The training data for the timing unit includes general variations of the patient's gait. This includes deviations of the trajectories, step length, and step duration. Thus, during training, the timing unit learns an average step.

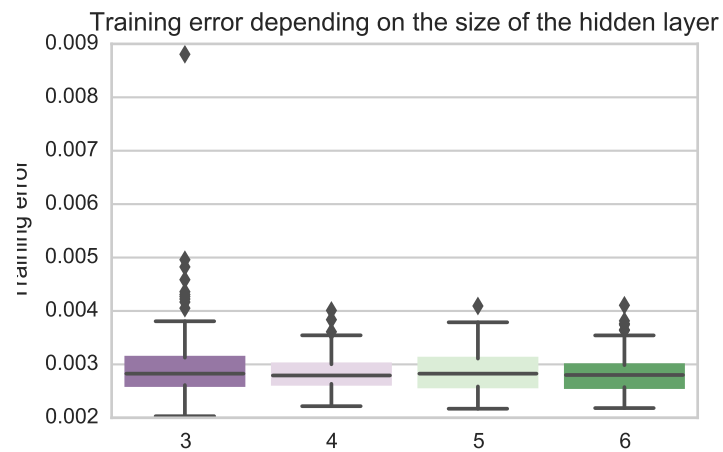
As all gait samples include this variability, the linearity investigations in section 8.4.1 cover these deviations. Here, we will take a look at specific examples of gait variability: In Figure 8.9, the control output for several steps of varying length is shown. Using the red rulers of same length below the output signal, we can see that the shown steps span a factor of two in step duration and the system handles the output quite similarly.

### 8.4.5. Ability to Tune to the Patient's Needs

The ability to tune the device's behaviour to the patient's need depends on the systems ability to generate all plausibly possible damping functions. This ability has two preconditions:



(a) heel only



(b) heel and toe

**Figure 8.8.:** Distribution of errors when training different artificial neural network architectures. The overlap of the distribution for different sizes of the hidden layer is so huge, that it can be considered insignificant.

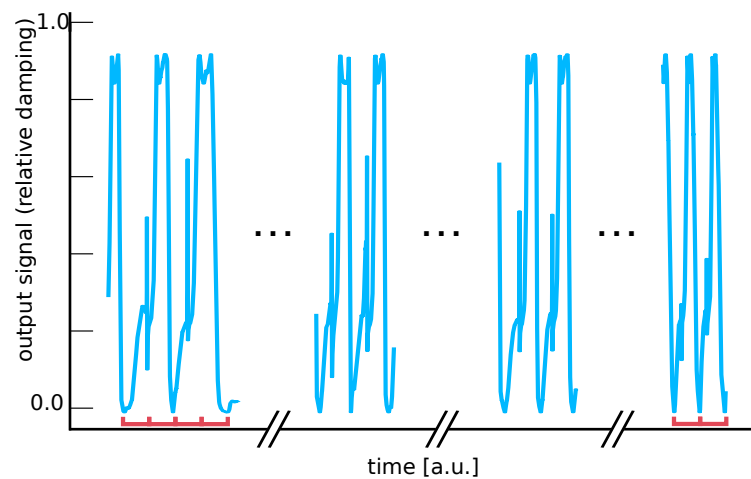


**Figure 8.9.:** The damping output of the system is independent of step duration due to the timing unit, which originally exhibits this feature. The timing unit transforms time dependent sensory input into a representation of the current position in the gait progress, which is time independent. Therefore, the timing unit can cope with different step durations. This is indicated by the red bars below the graph, which have the length of the short steps at the right side, whereas the steps on the left have double the duration.

1. The timing unit possesses a time resolution which is high enough to differentiate the gait progress. This is limited by the smoothness of the gait phase representation and the sampling rate/sensory delays of the device, as the timing unit cannot resolve the gait phase differently, as long as the input is constant.
2. A shaping unit which allows control which is fine grained enough to capture the detail of the timing unit, but it cannot exceed the time resolution of the timing unit.

As the shaping unit is merely a simple mapping from gait phase  $\varphi$  to a desired damping value  $d(\varphi)$ , we can assume, that the limiting factor in the shaping unit is in the allowed detail of the representation. In this case, it depends on the number of Gaussian kernels in Radial-Basis-Function network, but by using other means of parametrisation, e.g., gait phases values in which stance and swing phase alternate plus the intermediate damping, the detail of control over the output signal could be increased without increasing complexity of the internal representation.

For the timing unit, we have to assume, that optimal time resolution occurs, if changes in the gait phase  $\varphi$  occur monotonously and with constant increments in the frequency of the data acquisition hardware's sampling rate.

#### **8.4.6. Ability to Capture Different Gaits**

If the gait deviates strongly from the original training data, the timing unit will not represent the gait phase faithfully, as we have seen in the experiment of section 8.4.1. This leads to less smooth changes—up to steps in  $\varphi$ —over the gait cycle and therefore bears the danger of control-loss. We might end up with only a handful of control decisions.

Nonetheless, in early experiments, we tuned the damping function to work in different environments to see, if the controller could handle these situations in

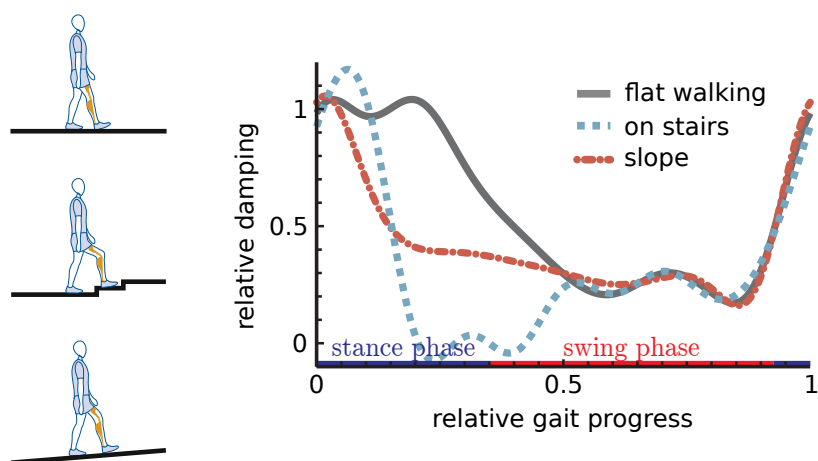


**Figure 8.10.:** Typical tuning result for the knee joints damping properties with the tool shown in figure 8.4. While in stance phase the device supports the user, whereas in swing phase, the knee is released. Presented are different damping patterns for gaits on flat ground, on stairs and on a small slope.

closed loop configuration despite the timing unit for another gait. The results can be seen in Figure 8.10.

These results are in no form a conclusive investigation, due to the small number of experiments and the fact, that the subject was a healthy walker. Nonetheless, a (sub-optimal) tuning was possible, which will be an argument in the bootstrapping problem below.

## 8.5. Discussion

The presented approach for the orthosis controller provides a generic two-step mechanism to determine the control output.

By abstraction of gait progress tracking via the timing unit, we achieve a general means to couple to individual gait, without any assumptions about the patient's abilities. This abstraction works time independent with almost immediate re-

### *Orthosis Feedforward Control*

actions in the order of magnitude of the device's sampling frequency, allowing detailed control whenever a patient may need it.

The choice of artificial neural networks as adaptive implementation allows learning the patient's gait from recorded samples and even makes later changes with new gait samples a natural procedure.

We achieve flexibility of the control output with the mapping of the gait phase to the damping function. At the same time, this mapping allows the feed-forward application of the control output. The choice of radial basis functions for the shaping unit allows easy changes at this stage in the controller, including on-line optimisation according to a set of rules, which change the weights of the Gaussian kernels.

Taking the patient into a feedback loop for damping output control simplifies the damping function as well as the definition of the damping output. At the same time, it allows the patient to change the device's behaviour according to an understandable paradigm, in this case the paradigm of applied damping on an approximately linear scale.

This interface could easily be exchanged with an arbitrary parametrisation of the damping function, allowing other paradigms or approaches for online device learning.

On the controller level, the separation of timing and shaping stages allows arbitrary combinations with other control techniques. Where suitable, the timing could be determined applying EMG or BCIs. Alternatively, the shaping unit could be replaced by physical models, or any other means, to determine the needed control variable.

### 8.5.1. Detailed Discussion

#### Enhanced Models for $\varphi$

The analysis presented in section 8.4.1 indicates that more sensors can result in a smoother and more linear resolution of gait progress. The better the coverage of the gait cycle with slowly changing signals, the better a smooth and linear gait phase representation can be built.

In the presented case, the additional FSR sensors at toe and besides the arch would increase stance phase resolution.

Still, there were problems with this extension: The soldering of the toe FSR is exposed to more stress still. Even for the smaller sensors with additional casing the contacts had to be renewed quite often, whereas the heel contacts soldering is perfectly save in the arch of foot, which is modelled into the orthosis foot piece.

In general, additional sensors with a phase shift to the presented sensors, for example angular velocities, could provide a better resolution. Adding low pass filters might lead to better resolution, too, but would introduce history-dependence into this controller and is therefore not desirable.

#### Internal Representation of $\varphi$

Several possibilities exist for the internal representation of the gait phase  $\varphi$ . For reasons of simplicity and scaling invariance we chose the 1-D representation via the  $\tan^{-1}$ . While this worked quite well in the presented work, it is possible, that small amplitudes of the underlying two cyclic variables from the timing unit produce errors and jumps in the output.

An approach working directly on the 2-D output of the timing unit with a 2-D radial basis function (RBF) network could remove the need for the  $\tan^{-1}$  in the implementation which is otherwise solely based on artificial neural networks.

But in this case, additional effort might be needed to insure invariance against changes in the radius of the timing unit's output.

### **Internal Representation of the Damping Function**

The internal RBF network representation of the damping function  $d(\varphi)$  has been chosen for reasons of simplicity.

With the user in the feedback loop, the actual damping output has been sparsely investigated. Here other parametrisations, like damping amplitude, onset, and ending come to mind, which provide fewer detail but are easier to adapt.

To be generally usable for any gait, additional studies would have to classify possible gaits and the flexibility needed in these gaits. For these studies, the chosen approach could be used to define general samples for later analysis.

In summary, the chosen solution provides accuracy which is high enough for the available hardware and is providing enough flexibility to be tuned to any gait. But for real world application, it provides too man degrees of freedom and seems unpractical for exposure to patients.

Still, the RBF representation can be used as an intermediary representation. Depending on the application, for example patient tuning or online optimisation, different additional parametrisations could be used

### **User Feedback**

The argument has been made, that by including the user's feedback, details of the mapping from the damping function to actual valve positions and resulting damping can be neglected, because they are part of the feedback loop.

Therefore, no calibration of valve behaviour and patient properties needs to be done.



On the application side, the user feedback even allows to get a working controller with a non-fitting timing unit, which inhibits phase shifts. Although not optimal, it is possible to tune the device into a working state, as for flat walking models on stairs, compare Figures 8.5(b) and 8.10.

This is not necessarily possible, when the gait phase is no longer a monotonous increasing function which explores the whole range of  $\varphi \in [0, 1]$ , as in the case of the stair climbing model on flat ground in Figure 8.5(c). For this case, two gait phases in the gait cycle, which have a phase difference of almost  $180^\circ$ , would produce the same damping.

While this behaviour underlines the flexibility of the presented approach with user feedback, the devices behaviour is more deterministic and better, if the system supports every possible gait. Then the approach allows to tune the output in an optimal fashion for each gait.

### **Bootstrapping**

A serious problem, which comes with the use of actual gait samples for training, is the bootstrapping of the device. The patients need an environment or setup which enables them to gather enough walking samples to successfully train the controller with sufficiently variable samples.

While a secured environment with crutches are a safety line from the ceiling is thinkable, it might not be the optimal solution.

Although not experimentally tested, it seems reasonable, that the device can be operated in a sufficient manner with a timing unit trained on another (or generally other) persons gait samples. As the timing unit handles variations in step length and frequency, and therefore variations in joint ranges, quite well (compare Figures 8.9, 8.5(a), and 8.5(d)), it seems reasonable to assume that the deviations are less dramatic than in the testing scenario with flat ground timing unit on stairs in Figure 8.5(b), i.e., consisting of small shifts and small deviations from the ideal slope.

## *Orthosis Feedforward Control*

While the operation of this device probably wouldn't be that comfortable, as the timing of heel-strike and toe-off are not perfectly aligned, the patients should be able to tune usable behaviour. For example by using a damping in stance phase, which provides very slow flexion but is not blocking knee flexion. This would enable the patients to walk and gain samples, which could be included into the training ensemble, gradually replacing the previous training data.

The artificial neural network could be retrained with this changing dataset, which would become gradually more specific towards the user's gait.

As the phase relation between the sensory inputs seems important for differences between the timing units, e.g., producing the heel-strike offsets, another person's model should be better suited for bootstrapping than another gait.

Although section 8.4.6 indicates that the damping function can be tuned to work with an unfitting timing unit, section 8.4.1 shows, that we could loose control in important ranges of the gait cycle. Although not evaluated, it seems reasonable to assume, that the general phase relation is similar for different people and should produce better linearity.

### **Self-learning devices**

One can base an approach for a self-learning controller on the discussion on the problem of initial bootstrapping. But in this case, the gradual replacement of the training dataset would not be limited to the initial bootstrapping. Rather, one would continually update the training dataset throughout the lifetime of the controller.

Additional care would have to be taken, that the sample steps are well selected. As we will see in the next chapter, the timing unit is specific to a motion, which we only observe for consecutive steps in the same gait. Thus a filter would be needed to make sure, that only steps of the right gait would be used, which are in the middle of a consecutive row and probably are similar in stride length and duration to the average steps in this gait.

This train of thought will be discussed in more detail at the end of the next chapter in section 9.6.4.

### Time Dependence

Especially for the first sensor set, which included a potentiometer as knee angle sensor, a low-pass filter was implemented in the timing unit on the output neurons providing  $\sin(\varphi)$  and  $\cos(\varphi)$ . This low-pass filter was able to smooth problems with the soldering of the potentiometer without adding notable delay. Therefore, the timing unit still presents a fast feed-forward controller component, which will introduce no delays which will prevent save device operation in case of drastic changes in the input.

### 8.5.2. Ability to Cope with Stumbling Situations

The controller provides feed-forward control based on the timing unit. Therefore, the controller will immediately adapt to fast changes in the sensory input as for stumbling, providing the user with body support when ground contact is established. The binary characteristic of the FSRs, together with the joint-configuration below the COM, will drive the timing unit into the corresponding domain of the gait phase  $\varphi$ .

### 8.5.3. Comparison to other Methods

State of the art methods include mostly, but are not limited to, finite state machine based controllers, like in [50, 95, 99] and devices on the market. In other research, like [53], a similar approach has been taken to derive the current dynamic state of the walker.

A thorough comparison to other Methods is difficult for three reasons.

## *Orthosis Feedforward Control*

First, the realisation of this prototypes sensory input and the controller structure are quite unlike those used in advanced state machine controllers. Whereas older devices on the market are only using single sensors, for example the thigh angle, many modern devices are working with ground reaction forces<sup>2</sup>, which our prototype is not accessing.

Second, a meaningful comparison should be done with experiments including a set of patient walkers, to which we had no access so far.

Third, a common benchmark could be used [55], but advances towards common benchmarks for bipedal walking are quite young. This is an important development for future work.

Insofar, we will not present a direct comparison of methods, but will discuss advantages and disadvantages of different approaches.

## **Finite State Based Controllers**

Concerning finite state machine based controllers, we will discuss structural differences in support for a single gait and multiple gaits.

For a given gait, the optimality of a finite state machine based controller depends on the definition of the transition condition in terms of the sensory input. If the condition can be well formulated, we can assume the switching to be in the optimal moment, Examples could be angles or loads or even the direction of ground reaction forces.

Still, three problems come to mind with this approach. First, the definition of the switching condition depends on an interpretation of the gait dynamics and depends very much on the sensors equipped. For the skills of a specific patient set, another condition might be more accurate.

Second, if the condition is achievable. For example for a critical thigh angle or specific load, the patient has to have to be able to generate this condition. For

---

<sup>2</sup>which of the above, or only c-leg

other conditions, like the direction of the ground reaction force relative to the limb, the force and pose have to be estimated accordingly.

Third, these estimations should not depend on changes in the environment. If, for example, the needed thigh angle changes with external slopes, the controller creates additional complications.

Any possible problems at this point are solved with the presented controller by means of the abstract gait phase representation. While additional sensors may increase the linearity of the gait phase tracking for specific ranges, we overcome the patient ability specificity of criteria.

For the same reason, the achievability of transition conditions is not a problem. As long as the mapping is linear enough to allow fast enough gait resolution, e.g., the precision is comparable to the sampling frequency as detailed in section 8.4.1, we can claim that almost any transition condition can be met, if it can be defined in terms of the gait phase  $\varphi$ .

For the third problem, the argument is, that as long as the environment does not lead to a different gait, the controller can handle it. The design of the timing unit allows shifts in the and amplitude changes in the input. Therefore changes in step length or angle offset through, e.g., slopes are handled transparently.

This behaviour is an advantage of using configuration space for device control. Whereas the relative direction of ground reaction forces are difficult to estimate correctly including patient-frame interaction and changes in ground orientation, or the necessary extreme angles depend on the slope, the phase relation of a gait changes only slightly.

When it comes to the coupling of several gaits, the resulting state-transition graph becomes increasingly complex, as every gait consists of a set of states and transitions between the different gaits are possible at several states. We will investigate these issues in the next chapter.

### **Similar Approaches**

In [53], the authors try to achieve a similar result by applying gait phase tracking on the healthy leg. Assuming a constant phase shift between the legs, they infer the gait phase of the controlled device.

There is a practical issue, that the contralateral leg has to be instrumented and therefore both legs are involved in donning the orthosis, which will present a hindrance to the patients.

But in my opinion more important is, that this phase relation does not hold in case of stumbling or other critical events. While such events may lead to a loss of information on the ipsilateral leg, the presented approach always faithfully reflects the device's state.

A good indication, that control based on gait phase  $\varphi$  as approach may provide benefits may be seen in [56, 67]. They presented the first approach of a prosthetic device which actually reduces the energetic costs of walking for its wearer, when the active ankle joint was powered at  $\approx 43\%$  of the gait cycle, as presented in section 2.3.

### **EMG and BCIs based control approaches**

EMG and BCIs based control approaches allow to work on patient activity, whereas the presented approach can only integrate itself in a passive manner.

While this approach is unsuitable for upper limb prostheses, where a clear intent drives the action, for lower limb orthoses this passive approach is feasible and in some cases still necessary, as the quality of EMG signals depend on muscle health, nerve tissue and the ability to exclude erroneous signals like in the case of epileptic motions.

#### 8.5.4. Advantages of the Presented Controller

The advantage of this approach lies in the simplicity of the used models with the ability to train all components with live data, i.e., to let the system learn by observation of its user. The absence of device- and motion-models allows manifold applications, even in active devices.

A part from this generality and simplicity comes from working on configuration space sensors, i.e., joint angles and ground contact. In case a specific range of the gait cycle needs a better resolution, it could be provided by the addition of additional sensors with sensitivity in this range, for example additional FSRs.

The enhanced resolution of gait cycle tracking allows not only detailed control and individual patient fitting, but also prevents the controller to rely on critical points for state transitions, like specific moments or angles, whose accessibility might reduce the target group, or worse, might be depending on the patients fatigue. It handles gaits in a generic manner.

The timing unit provides good resolution for learned gaits. With gait switching it ensures reasonable resolution for all supported gaits. As all components are adaptive, they form the basis for orthoses which adapt to the patients. Whereas up to now, the patient had to adapt.

The presented approach combines small modules, whose function can easier be understood and validated, than an approach which consists of one huge neural network. This partially addresses the black box criticism. Still, the modules represent little black boxes.

As the controller is model free, concerning the actual design of the controlled hardware and the supplied sensors, the controller can be used on varying hardware. During the course of the thesis, it has controlled devices with compliant ankle as well as with an ankle joint. Therefore, it seems plausible, that it can be used in any situation, where the requirements of section 5.3 are met.

### **8.5.5. Limitations of the Presented Controller**

In contrast to RunBot's reflex based controller or transitions in a finite state machine based controller, the presented timing unit is not event based. When exact timing based on a clearly defined external signal is needed, this approach might lead to timing errors, when the external signal would provide exact timing information. Nonetheless, the inclusion of events is thinkable. For example, a forced phase reset or the combination of smaller, timed movements which are triggered by reflexes, are possible.

For the same reason, the intentionality of transitions and reflex is lost in timing. Therefore, effects of changes in the user interface are not completely clear, but need the patient to test changes and experience the feedback.

A field study with patient experiments could help to provide insight on the comparability of time scales for different patients, so that the user interface could include hints on the time scale. While this has not been done, tests with three healthy walkers through the course of the project indicate, that a patient will adapt fast to the tuning mechanism.

On a technical side, the used models were chosen to be generic. Optimised or more efficient representations for the timing unit and damping function are possible. But the design decision was to not focus on optimality, but on the ability to easily adapt the device's behaviour at a later point or run-time.

As a side effect, the network layout might need to be optimised again, when the number or kind of sensory inputs change, although the evaluation of section 8.4.3 indicates, that the necessary changes in network layout are minimal.

Due to the user-feedback-loop, many details on the damping function are extensively investigated. This was an advantage for the presented work. Still, a more thorough evaluation and comparison, for example to human walkers, might yield interesting results. Although one has to keep in mind, that the device's damping can not be directly compared to human damping in walking experiments,



as the device is not providing the stiffness component, which is typically evaluated together with the human's damping according to typical hill type muscle models [105, 108].

The design is based on a black-box approach, as already mentioned above. While the neural modules are small enough that their behaviour might get validated, they produce non-validated behaviour at training.

Another design problem comes from the underlying orthosis of the presented control scheme to be passive. All initiative and momentum has to come from the patient. The controller is build to fit into the patient's motion and is therefore only partially applicable to active devices for patients which can not initiate movement.

Still the presented controller could be used to signal or initiate movement components, which are dependent on previous, self-generated motion, so that an approach like this could provide value for active devices.

### 8.5.6. How to Go On

There are many possibilities to go on from this point. In general, the evaluation of the device's influence with actual patients is the most pressing and interesting concern. But besides the question, how the presented approach actually operates in a patient-environment and really can deliver all on all design goals, there are many other threads to follow.

#### **Combination with EMG or skeletal muscle-models**

The timing unit can be coupled with a wide range of methods to determine the control output. A musculoskeletal model like [86] determine the forces a healthy walker would generate at knee level for body support. The presented timing unit can be used as timing input to the forces generated by such a system.

### *Orthosis Feedforward Control*

To compensate for muscle fatigue, such an approach could be extended with EMG recordings to determine the actual muscle activity. The musculoskeletal model would provide estimates of the forces this EMG-activity should create. If suitable instrumentation allows to estimate the real joint-torques, compensatory adjustments can be initiated, e.g., the damping can be increased.

In this way, the timing unit can be used as input for existing approaches, which derive the activity from EMG signals to accommodate for cases, in which the EMG signal is unreliable, for example in cases of spastic signal. Either as replacement or to complement the existing solution; for example, the timing derived from the EMG signal could be cross-checked against the current gait phase to determine critical situations.

On the other hand, the timing unit could be replaced by EMG. Allowing tuning properties of this approach be applied to other controllers.

### **Online learning**

From the authors perspective, questions concerning online learning and details on the patient's gaits are most interesting.

As outlined above in sections 8.5.1 and 8.5.1, the controller provides the foundation to explore controllers, which can learn by observing the patient in a controlled environment. The modularity of the presented approach with the gait recognition presented in the next chapter allows well defined learning tasks, as discussed in the outlook (chapter 12).

To design these learning tasks, one would need an understanding of the interaction of patient and orthosis. On one hand, as it is to be expected, that the patients will adopt their gait to the support the device provides (compare [35, 36] and the trust they have into it, i.e., if they trust to use the impaired leg more often. On the other hand, learning via an error-function or other kinds of optimisation of the device's behaviour needs a benchmark on what is to optimised. Therefore, the actual and possible effects of the device onto the patients needs to be understood,

such that learning tasks can be designed, which do not interfere with the patient adapting to the device, but which actually improve the device's behaviour. A more detailed discussion will follow in chapter 10 and the outlook.

### **General Walking & Technical Questions**

Other important questions, which can only be reliably answered in a field study, are the time or gait phase resolution the controller actually has to supply, and the number of independent movements which have to be supported by the device to allow seamless integration into the patient's everyday needs.

Additional sensory input, especially inertia measurement units (IMUs) might provide additional benefits for the controller and can possibly be used to set up learning tasks which provide optimised pre-damping.

### **Reproducibility of Damping Functions**

An aspect of general controller reliability is the reproducibility of damping functions over different walkers and situations. Due to a lack of subjects and the feedback loop, this has not been thoroughly investigated. Still, in Figure 8.11 are two damping functions for a healthy walker on flat ground. The exact shape is not identical, an evaluation with a set of patients would be nice to determine real-world fluctuations for this kind of controller definitions, especially concerning the allowed fluctuations for a self-learning and adapting controller variant.

Furthermore, it would allow to possibly optimise the parametrisation for different gaits. Such an optimised parametrisation could greatly speed up convergence of self-learning algorithms.

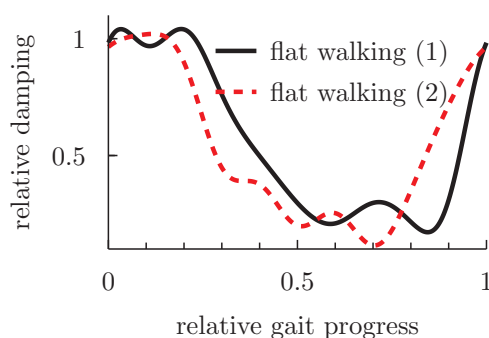


**Figure 8.11.:** Example for the variation in damping functions defined with the user interface.

## Other Applications

As the controller is model free concerning the device, it could be applied unchanged on other devices for the lower limbs. For example, our industry partner suggested the use on an ankle orthosis.

Even more interesting are changes necessary to handle active devices. For such an application, for example on RunBot, the controller has to be enhanced, as it would have to handle motion initiation, too. Instead of training complete gaits, it would be possible to train movement primitives, which in itself have a timing based on the robot's dynamics. But these movements could be triggered by reflexes or intention signals.

To allow the patient to use all limbs fully equal, step initiation would be necessary, making an application for BCIs the next step. When the user provides the intention to initiate a specific movement, the device would react timely with motion-onset for its user to reliably handle inter-limb coordination.

### 8.5.7. Incorporation of Multigait-Support

Whereas the discussion for section 8.4.1 was focused on the increase in accuracy by specialisation of the timing unit, one could argue, that this specialisation leads to worse performance for all other gaits.

In daily life we have to cope with different environments, which often need specialised gaits, for example when we encounter stairs. To support them, we have to extend the core controller in a way, which allows to use the specialisation to an advantage. Therefore we will discuss the inclusion of multiple concurrent timing units in the next chapter.



*It's hard to make predictions, especially about the future.*

Original source debated.

# 9

## Support for Multiple Gaits

In the previous chapters we established the sensory requirements for the orthosis and a core controller package, which delivers a fast, feed-forward controller response for changing sensory input. The feed-forward design ensures safety through low reaction times. The methods were selected to allow relearning of the input, i.e., individual gaits. They also make tuning of the output easy by means of a generic and simple user-interface. The modular design allows for straightforward exchange or enhancement of parts of the controller.

As could be expected, the evaluation of the core controller's behaviour revealed a high degree of specialisation due to the training process with patient gait samples. To overcome problems of the overspecialisation, we now extend the controller with an additional layer, which continuously tracks the patient's movements to determine the gait the patient currently uses. This enables the controller to select from a set of single-gait controllers to optimally support the ongoing movements.

In the introduction, we will discuss possible solutions for the problem of over-specialisation raised at the end of the previous chapter. Then we will detail the proposed solution and investigate its properties in the following sections.

## 9.1. Introduction

**The problem of Over-Specialisation** The previous chapter presented a controller, which is based on two major design elements.

1. The separation of input processing and transformation onto an internal gait phase representation (the timing unit), followed by the application of a mapping to the required damping of the knee joint (by the shaping unit).
2. The ability to train the controller with samples of the patient's gait.

The second trait introduces overspecialisation into the controller, which leads to a poor performance of the timing unit on untrained terrain respectively untrained gaits. Following, we will not distinguish between different terrains and gaits.

**Requirements** on the mechanism to support multiple gaits or environments. The mechanism

1. has to apply changes fast. To allow seamless adaptation, the change has to happen in a fraction of a step. We will discuss possible lengths later.
2. should be easily extendable for a patient specific set of gaits, as each patient's environment will impose individual demands.
3. has to resolve all supported gaits well. For use in real environments the mechanism has to have a diminishing rate of false positives or otherwise reduce the consequences of a misinterpretation to a nuisance for the patient.



4. like all parts of the presented controller, the design should support later changes of the controllers behaviour at run-time. This implies for the gait selection, that the controller's design has to support changes of individual gaits [35, 36]. The ability to recognise a frequent use of unknown gaits can further extend the safety of the gait switching mechanism.

**Possible Approaches** to this problem include:

1. The use of further generalised timing and shaping units to cover all possible gaits.
2. Gradual adaptation of the timing and shaping units during operation time. This would preserve the specificity of the units, but the affinity to specific gaits or environments would change at run-time.
3. Stick to the specialisation and provide a set of specialised controllers together with a means to distinguish the gaits and environments and associate them with the corresponding controller.

Approach 1. has the problem that with decreasing similarity of the gaits, the trainable unit will have to generalise more problems correctly. The complexity of the neuronal network scales with the complexity of possible input patterns, i.e., with the number and complexity of the supported gaits. Judging the scaling properties of this approach is quite difficult and we have not gone that path.

Approach 2. conflicts with our requirements on the reaction time to be faster than one step, as the system is unable to adapt to a gait it has not been able to record a complete step of. The fact, that the controller only uses sensory input from the ipsilateral leg further tightens the time frame; even if the contralateral leg is leading a new gait, the limited sensory input lets the controller drag behind. To gain an instantaneous reaction, the controller has to know or memorise its choices upfront.

This sets us up with approach 3.—it is generally straight forward, as we can replicate the controller from chapter 8 for each supported gait. The problem

is for the controller to decide in sufficiently short time which gait controller to apply.

In general, this approach fits nicely with our emphasis on modularity, promoting easy exchange and extension of functionality in contrast to the scaling problems of an one-design-fits-all-use-cases approach.

## 9.2. Overview

The changes introduced with the gait switching layer can be seen in a comparison from Figure 8.2 in section 8.2.2 to Figure 9.1: we duplicated Timing and Shaping Units at the top and added the Decision Unit, which uses a set of predicting gait models to orchestrate the output of the multiple controllers, in the lower right.

**Predicting Gait Models** are the basis of the gait classification system. For each supported gait, an internal gait model is trained to predict at each time step the next sensory input vector from the history of sensory input vectors  $s_t$ , as shown in figure 9.5 (a). These internal gait models are implemented with a multi-layered perceptron [69], which proved capable of handling the sensory input.

**The Decision Unit** evaluates all model's prediction errors and chooses from all models with prediction errors below a certain threshold the one with the lowest error. This process is shown in figure 9.5 (b) and (c). If no model predicts with an error below the threshold, the decision unit labels the current gait as unknown. This way a fallback controller can ensure safe orthosis operation.

In the following sections, we will detail these elements, before we take a look on the experimental evaluation of their features.

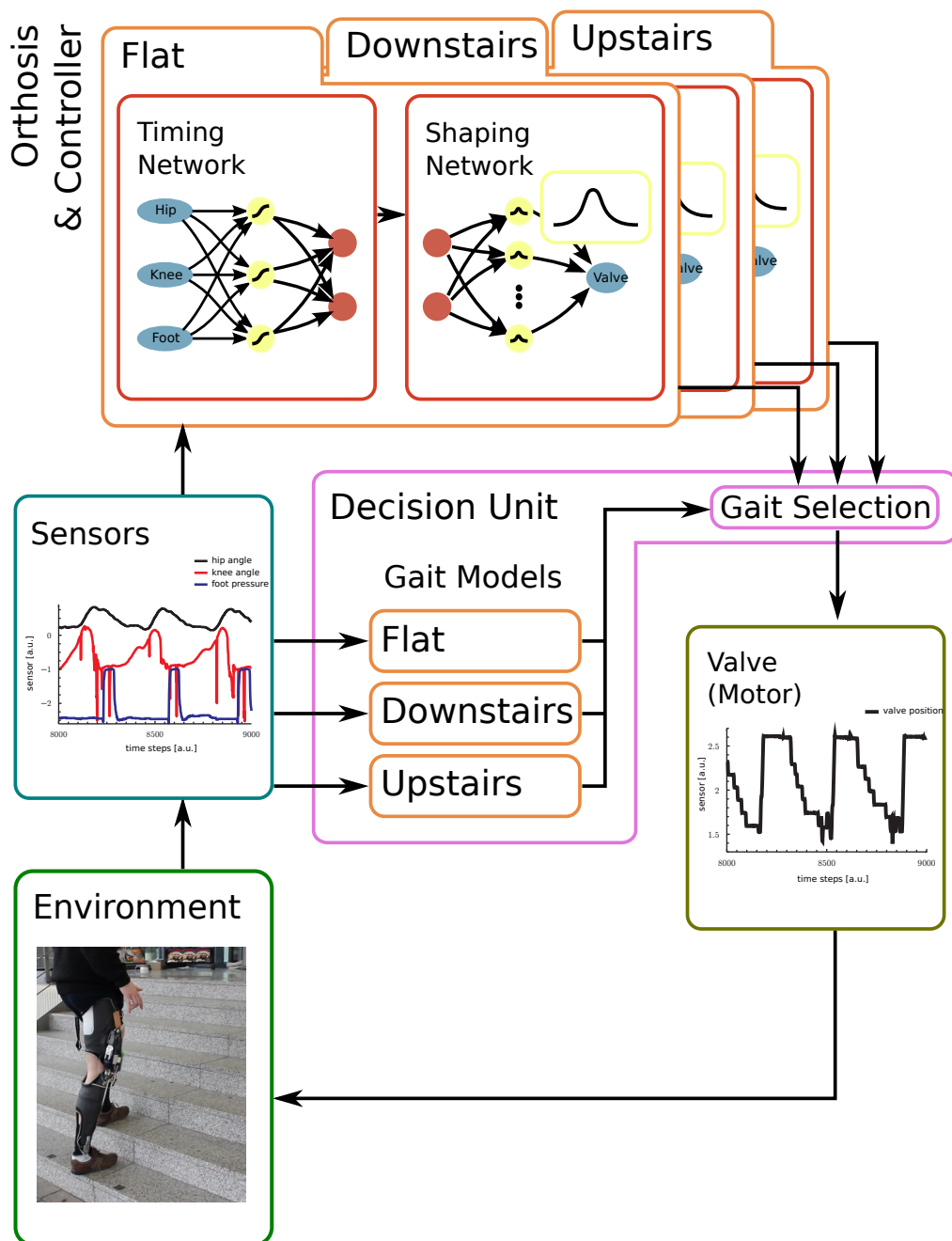


**Figure 9.1.:** Overview of the extended controller structure including support for multiple gaits and environments. For each supported gait, a controller, as defined in the previous chapter, is paired with a predicting gait model. The Decision Unit uses the gait model’s predictions to choose the appropriate controller.

## 9.3. Predicting Gait Models

Internal gait models are the basis of the gait classification system: the Decision Unit tracks the suitability of each supported gait with one specific model. Here, we consider the requirements from page 158, take a look at the actual modelling and go on to the chosen implementation.

Requirement 1 suggests a simple feed-forward solution, which works with minimal delays. Requirements 2 and 4 make a system, which learns from observation a reasonable choice.

### 9.3.1. Model Prediction

To achieve short reaction times, the system should only need few samples of a new gait, to be able to tell the difference to the previous movements. So for each supported gait, an internal gait model is trained to predict at every moment in time the next sensory input for the thigh- and knee-angle

$$\vec{p}^{t+1} = \begin{pmatrix} thigh^{t+1} \\ knee^{t+1} \end{pmatrix} = \text{prediction}(\vec{s}_t, \vec{s}_{t-1}, \dots)$$

from a history of sensory input vectors  $\vec{s}_t$ , as is shown in figure 9.3 (a). As the previous setup has proven to work quite well with gait data, and it produces a feed forward system, we again resorted to multi-layered perceptrons [69].

The output is predicted for the thigh and knee angle, not for the ground contact. As the ground contact is a binary variable, the prediction error would vary too much for useful evaluation.

If the history is filled with samples from a specific gait and the current sensory values stem from another gait, the system will immediately start to produce high prediction errors. As the history will then keep samples from at least two gaits, the prediction error will decrease for the new gait but stay high for the previous

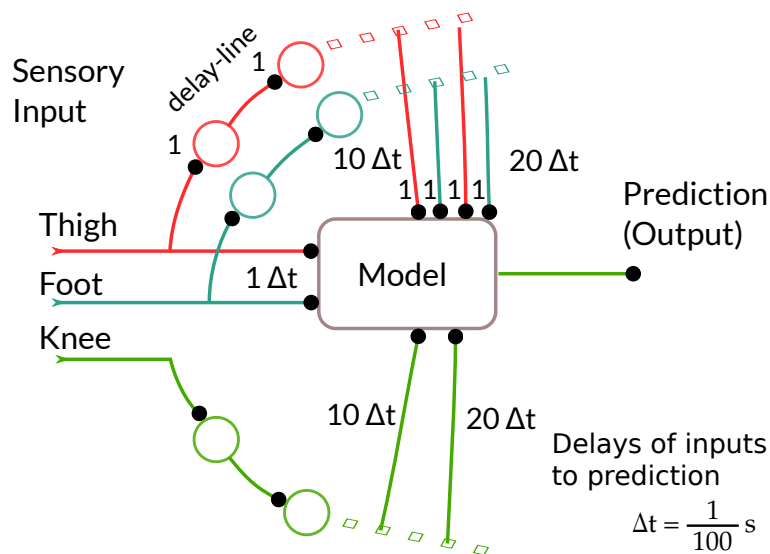


**Figure 9.2.:** Structure of the predicting models: A delay line provides a history of sensory inputs. The model uses a subset of this history to predict the output, see section 9.3.3

gait. The history length therefore defines crucial properties of the controller's behaviour and needs special consideration.

### 9.3.2. History Length defines Switching Times and Accuracy

We assume a minimal step duration  $T_{step}$  of

$$T_{step} \gtrsim 1 \text{ s}$$

for complete and intended steps, as opposed to stumbling or other unplanned changes (compare the step length comparison in section 9.5.1); and we use the stance to swing ratio of  $\approx 60 : 40$ . We further assume that gait changes can occur at any time. If we now expect half the swing or stance phase as a reasonable reaction time for the decision unit, this would account for no more than 20 % of

### *Support for Multiple Gaits*

the step length. Given the hardware-defined sampling frequency of 100 Hz, this gives us the number of samples in the history  $N_{\text{History}}$  as

$$N_{\text{History}} \lesssim 20 \text{ samples} = \frac{1}{5} \text{ s} .$$

The choice of the criterion is arbitrary: there is a trade-off between prediction accuracy and recognisable gait switching frequency. The prediction accuracy should increase for longer history lengths  $N_{\text{History}}$ , as more details about the gait may be taken into account leading to better discrimination. On the other hand, a step change will result in inaccurate predictions as long as two conflicting gaits fill the history. The time during which the history refills with samples of a singular gait can be considered the dead time of the predicting gait model and it is proportional to the history length. It thus determines the frequency, with which gait switches can be recognised in a reliable way.

The choice of  $T_{\text{History}} = \frac{1}{5} \text{ s}$  allows several gait switches per step with quite accurate results, as we will see in section 9.5 and discuss in section 9.6.3.

### **9.3.3. Selection of Prediction Input**

It has to be noted that for models which get the complete history of sensory input  $\vec{s}_t$ , the learned weights for this last input are dominating older samples. In other words, the models predict the last state they have seen, as the difference for knee and thigh angle is quite small from time step  $t$  to time step  $t + 1$  and of a similar order of magnitude as the variation in the training data provided by steps of different speed and stride length.

To solve this problem—and to force the models to use older inputs—the knee is only feed in with larger delays. The backpropagated errors in the hidden layer will prevent the same problem to occur for the thigh input. Of course, the thigh angle could have been selected, as the important difference between two gaits lies

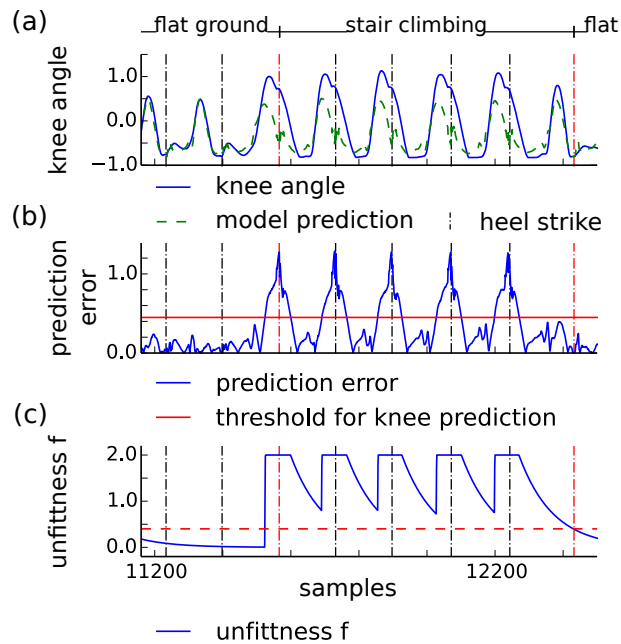


**Figure 9.3.:** Gait prediction schematics in open loop condition: a flat walking model in transitions to and from stair climbing. (a) The knee angle sensor and the model's prediction. (b) The low pass filtered prediction error and the threshold  $\theta_i$ . (c) The processed error count  $f$  on which the decision unit chooses the appropriate model. For the corresponding closed-loop experiment see Figure 9.5. The dashed red line indicates a possible threshold above which the model shows too high prediction errors.

in the phase relation of these two variables. In a process of thorough optimisation the choice of the omitted channel could be done on a per gait basis.

Therefore, the history our experiments use for prediction  $\vec{p}^{t+1}$  of the next sensory input depends on the thigh and heel pressure values for  $t$ ,  $t - 9$ , and  $t - 19$ , but only the knee readings for  $t - 9$  and  $t - 19$ , as shown in Figure fig:multi-predicting-model. The sparse selection keeps the computational complexity of the model low, although the developments for current mobile hardware does not make this necessary and allow to include more input.

### 9.3.4. Scaling of Sensory Input

To provide optimal working conditions for the artificial neural networks, the sensory inputs were scaled that gait typical signals were in the range  $(-1, 1)$  for each gait model.

## 9.4. Decision unit

The decision unit selects the appropriate controller based on the prediction errors of the gait models. Therefore, the decision unit evaluates all model's prediction errors for the thigh and knee angles (see section 9.3.3)

$$e^t = \left| p^t - \begin{pmatrix} s_t^{thigh} \\ s_t^{knee} \end{pmatrix} \right|$$

for the current time step.

### 9.4.1. Post-processing

Post-processing is necessary due to the prediction errors being localised over the gait phase, i.e., in time domain. The post-processing ensures, that singular



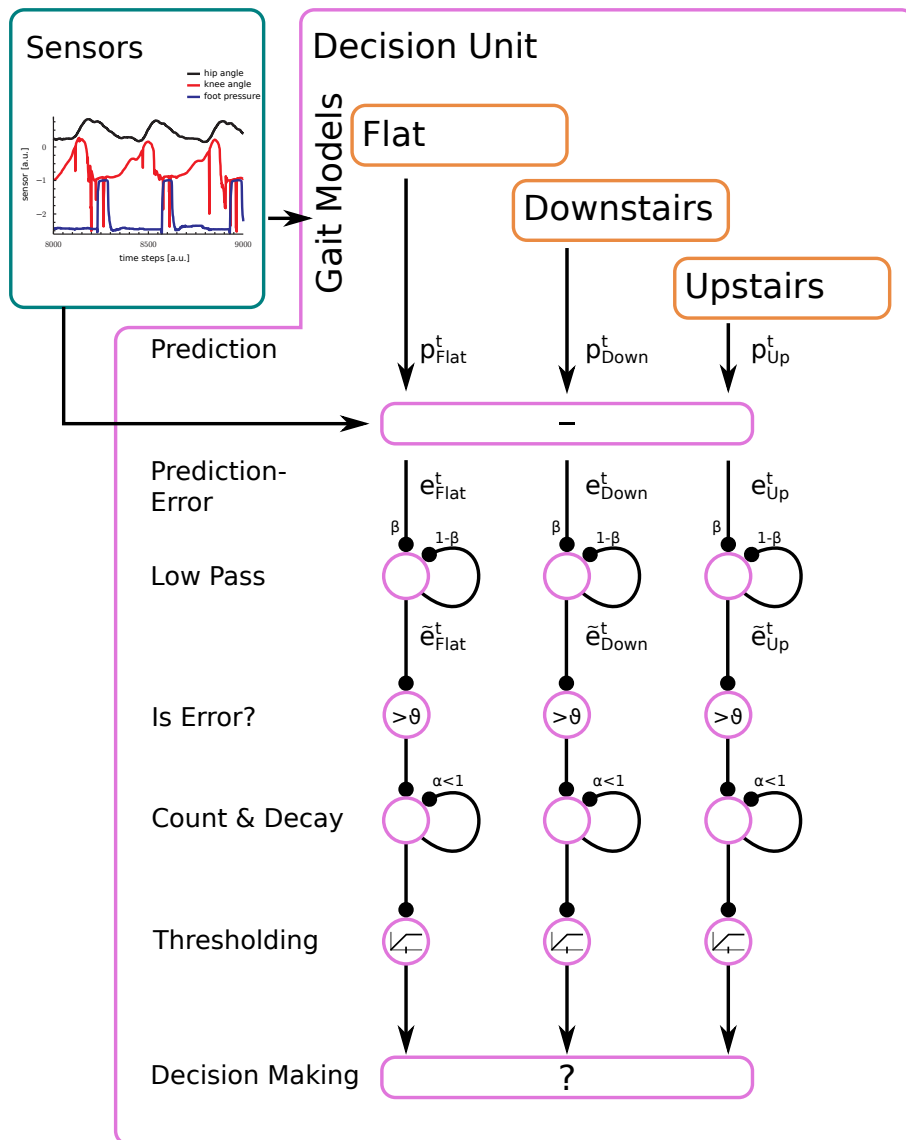


**Figure 9.4.:** Flow diagram of the decision unit: Every model predicts the sensory input, which is compared to the real input in the next time-step. After low-pass filtering and amplification, the signal decays. Finally, a threshold is applied to limit the choice to models with reasonable errors. For reasons of clarity, it is not shown, that the flow is duplicated for thigh and knee signals, and later a linear-combination is evaluated, where the coefficient is gait-dependent, as the significance of thigh and knee values are not always the same.

## Support for Multiple Gaits

noise is suppressed, whereas large errors are prolonged such that the system can react.

The first step is a low pass filter:

$$\tilde{e}_i^t = (1 - \beta)\tilde{e}_i^{t-1} + \beta e_i^t, \beta = 0.9.$$

To reduce the influence of noise, the low pass filtered errors  $\tilde{e}^t$  are checked against a model- and angle-specific threshold. They are ignored if they are below the threshold. Errors greater or equal to the threshold  $\theta_i$  are counted (see figure 9.3 (b)) for each predicted channel  $i \in \{\text{knee, hip}\}$

$$f_i^t = \alpha \times \begin{cases} f_i^t, & \text{if } \tilde{e}_i^t < \theta_i \\ \max(f_i^t + 1, 2), & \text{else} \end{cases}, \alpha \in \{\mathbb{R} | 0 < \alpha < 1\}.$$

$f$  describes how unfit the model is to capture the current sensory input. To obtain a value which can be interpreted on the time scale of a step, the capped error count  $f$  is decaying with factor  $\alpha$  (compare figure 9.3 (c)).

The predictions for knee and thigh sensory value are merged according to a gait specific weight, which reflects how specific the predictions are with respect to the gait in question.

$$f^t = \gamma f_{thigh} + (1 - \gamma) f_{knee}$$

### 9.4.2. Gait Selection Strategy

The decision unit chooses from all models with unfit values below a certain threshold the one with the best, i.e., lowest unfit value. This process is indicated with a dashed line in figure 9.3 (c). If all models produce too high unfit values  $f > 1.1$ , the decision unit labels the current gait as unknown. Then the existing default controller will ensure basic orthosis operation.

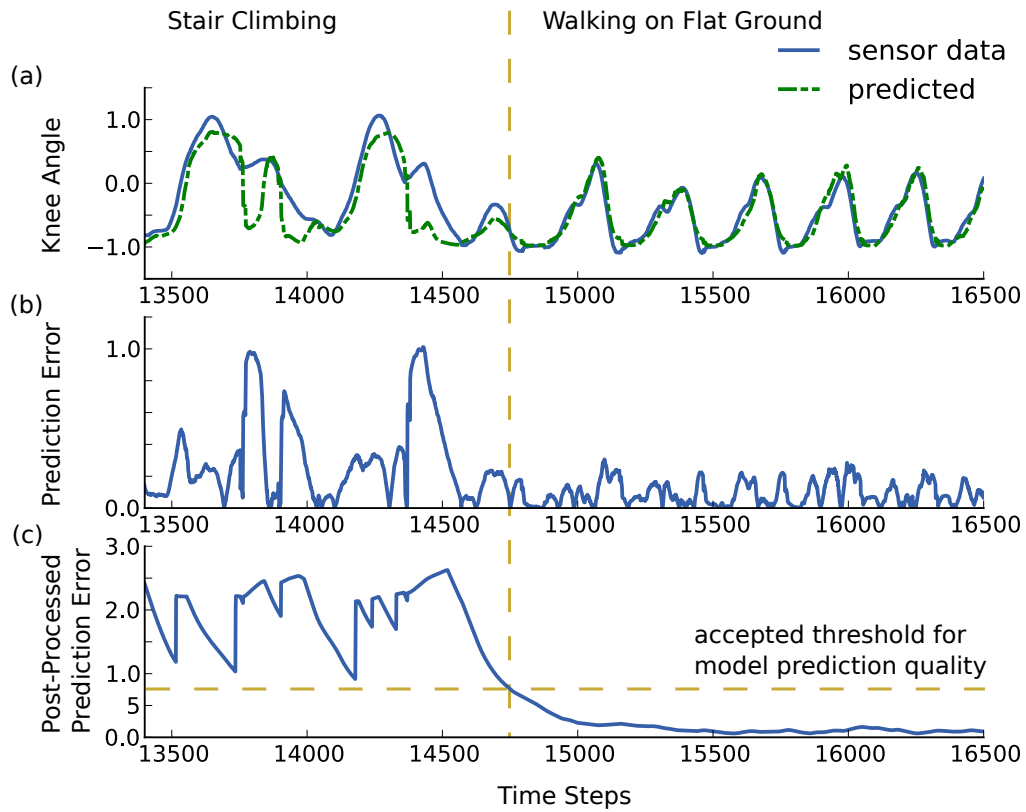


**Figure 9.5.:** Gait prediction with internal models in closed-loop condition: description for a model trained on flat walking data on the transition from stair climbing on the left to flat walking on the right side of the plot. In part (a) of the figure, the knee angle sensor data is compared to the model's prediction from the previous time step. The prediction error is plotted in part (b). The processed prediction error, on which the decision unit is choosing the appropriate model with a possible decision threshold is shown in part (c). Note that in difference to Figure 9.3, in this recording the processed prediction error includes the error count plus the prediction error. As the prediction error makes no significant difference for the decay of the error signal, the simpler notion of the error count has been used.

## **9.5. Evaluation**

To evaluate the quality of the presented approach for multi-gait support, we will have a detailed look at the classification accuracy and the classification speed, which mostly depends on the reaction of the predicting gait models.

The swing and stance-phase dynamics require similar control output for different gaits. Especially in stance phase, the possible dynamics are restrained by the orthopaedic joint and security considerations (to not release the knee joint while standing on it). Therefore, the transitions to and from stance to swing phase or most important, as the feed-forward controllers will most likely change their output there. As we have seen in section 8.4.6, the feed-forward controllers' accuracy is lost, when the gait is unknown, therefore these are the critical phases.

The transition between stance and swing phase is initiated by the patient deliberately. The ground contact switches allow good detection of foot lift-off and due to the security considerations, an initial uplifting is needed for the controller to release the joint. Faster reaction times of the decision unit will reduce the movements, but will not remove them.

The transition from swing to stance phase shows a variety of transition-dynamics. As we will see later in more detail, here the point of transition is not fixed but fluently depending on many factors, for example the distance to the new terrain, moving obstacles, etc.. Therefore, the transition from swing to stance phase is best suited for the evaluation of switching properties; we proceed with a detailed evaluation of the decision unit with a focus to the step's end.

### **9.5.1. Accuracy of Gait-Detection**

Here, we describe an experiment to assess the accuracy of gait-detection for gait switching. Excerpts of this study have been published in [7, 8] and have been adopted for this section.



**Figure 9.6.:** Picture of the staircase landing, which was used for open- and closed-loop runs for multi-gait support testing.

### Experiment Description

In order to evaluate the accuracy and timing of gait switching, the user interface is extended with the ability to log the current gait. This annotation process creates a ground truth for later comparison with the gait classification output. Both, the user's annotations and the selection units output are logged to files for offline comparison.

The controller is prepared with gait models for three gaits: walking on flat ground, stair climbing and descending stairs. Due to the high number of needed steps to gain statistics and missing security measures in the stair-cases (Figure 9.6), the evaluation of the decision unit was done with disabled damping unit (Figure 9.3, with knee bending in stance phase). The user was a healthy walker.

For comparison, Figure 9.5 shows a transition from stair-climbing to flat-walking in online-mode, as can be seen in the missing knee bending in stance phase and stems from an earlier experiment, where only stair climbing and flat walking were tested.

## Method

To quantify the quality of gait classification, we measured success rate and timing, i.e., how early the correct classification occurred. We compare to the user's annotations, which he could change at arbitrary times in the step. Therefore, for evaluation purposes, the annotation valid at heel strike was used for the whole preceding step. Figure 9.7 shows a typical recording with user annotations in black and the method's classification output in blue.

To quantify the comparison of the method's classification with the user annotation, we determine the longest range preceding the heel strike, for which both agree. This is indicated in red as the *range of certainty*. It captures the longest time span preceding the heel strike for each step, for which the classification is correct. It is normalised to the step length, to be more precise to the time between heel-FSR-off and heel-FSR-down, to get a measure which is comparable between steps of different length. A range of certainty of 100 % therefore means, that the gait is known on heel-off. A range of certainty of 0 %, in contrast, means that the gait is not classified correctly before heel strike.

To ensure, that in an on-line scenario the classification is available in time, we check against a *minimal range of certainty*. The required minimal range of certainty has to be chosen in such a way, that the controller still reacts in the same step. For our setup, which is sampling its sensors with 100 Hz, and typical step lengths between 1.3 s and 1.8 s for flat walking and stair climbing, respectively, this means that a required minimal range of certainty of  $\gtrsim 3\%$  is sufficient.

To sum this up: The range of certainty will be used as a measure for classification accuracy and the predictive quality of the proposed method. As the achieved range of certainty is depending on the individual step and the specific gait, we explore the reliability of gait recognition twofold: we investigate (a) the average success rates for all gaits, and (b) the classification accuracy if *minimal ranges of certainty* of 20 % and 3 % are demanded.

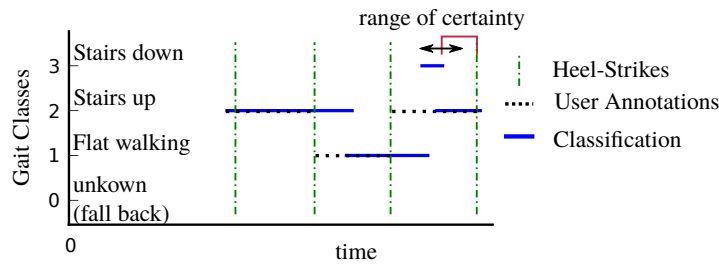


**Figure 9.7.:** User annotations over time. Gaits are denoted vertically; a sequence of three steps is shown along the horizontal axis. The user’s annotations were extended to the beginning of a step and plotted as black, dotted lines. In solid blue, the decision unit’s output is shown. We measure the interval preceding the heel strike, in which the decision unit chose the correct gait (red brace). We call this interval the *range of certainty*. It is normalised on the heel-off-to-heel-strike interval to gain a comparable measure. A sequence of such one-step-transitions is necessary for the staircase landing in Figure 9.6.

## Controller Setup

The predicting models have been created with training sets sized 146 steps for flat walking, 35 steps for stair climbing and 32 steps for descending stairs. These training sets contained selected steps from four recordings and included no gait transitions. For evaluation, three independent recordings including gait transitions have been used, totalling 215 steps (81 steps on flat ground, 64 steps mixing flat ground and stair climbing, and 70 steps mixing flat ground and stair descending).

## Results

Figure 9.8 (c) shows the dependence of the averaged classification success rate on the chosen minimal range of certainty averaging all gait models. While over 83 % of all steps are correctly classified at the beginning of the step, naturally, for all other steps the success rate increases with decreasing distance to heel-strike, i.e., when the range of certainty is reduced. In this experiment, the average

## *Support for Multiple Gaits*

success rate was slightly above 94 % within the device's reaction time before heel strike.

The distribution of the classification results can be seen in the confusion matrices for required minimal ranges of certainty of at least 20 % in figure 9.8 (a), and 3 % in figure 9.8 (b). In these matrices, the annotated gait is plotted in the vertical axis and contrasted with the model based predictions in the horizontal axes. The success rate is colour-coded according to the value of the matrix element.

In general, the classification performance is quite good for walking on flat ground with over 94 % accuracy and 100 % for stair climbing, whereas the performance for steps descending a stair is lower with at least 84 %. Noticeable are comparably low frequencies of false positives classifying flat walking as descending stairs (1 %), descending stairs as flat walking (5 %), and flat walking as stair climbing with 5 % in the case of a 20 % range of certainty. The success rates increase, when the range of certainty is reduced, as detailed in figure 9.8.

## **Conclusions**

Concerning the ability to apply knee damping in front of the heel-strike, the results for 3 % range of certainty are decisive with the presented hardware interface. For this value, the average success rate for all gaits is above 94 %.

The false positives are associated with transition steps, i.e., the gait often changes in a step. As the available stairs were crossed after four steps with the orthosis, the number of transition steps is high compared to the number of samples; the percentages account for just one error in each case. Pinning down the moment of transition to a specific point is difficult. Therefore, the ground truth created with the method of user-annotation is debatable. After inspection (compare Figure 9.9 for the transition from stairs to flat ground), the effected steps seem ambiguous and the method's output reasonable. For the same reason, a range of certainty of 100 % is not achievable for transition steps.



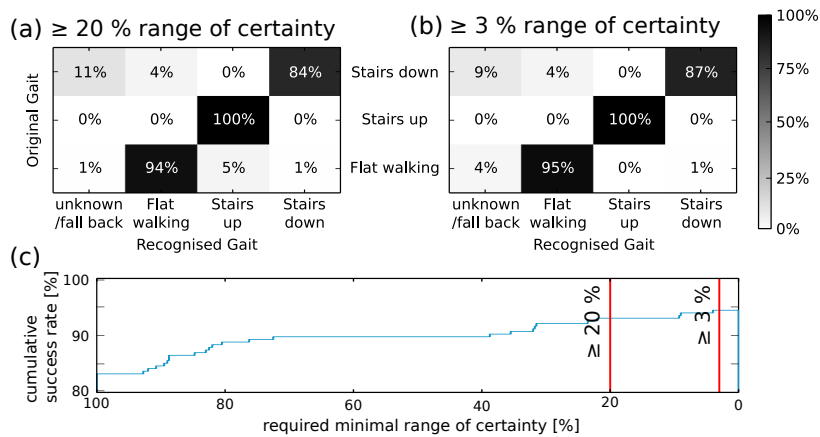
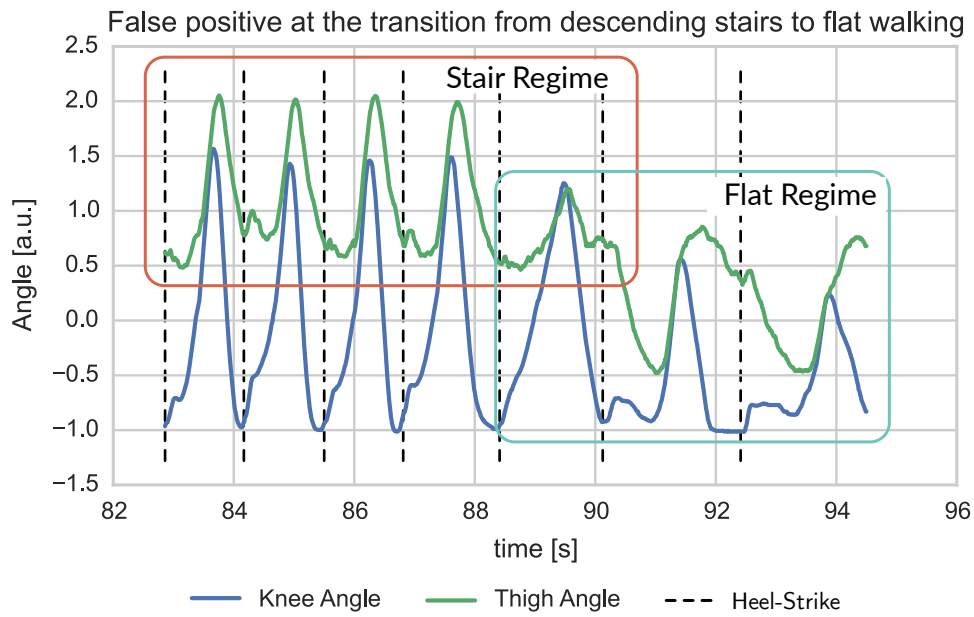
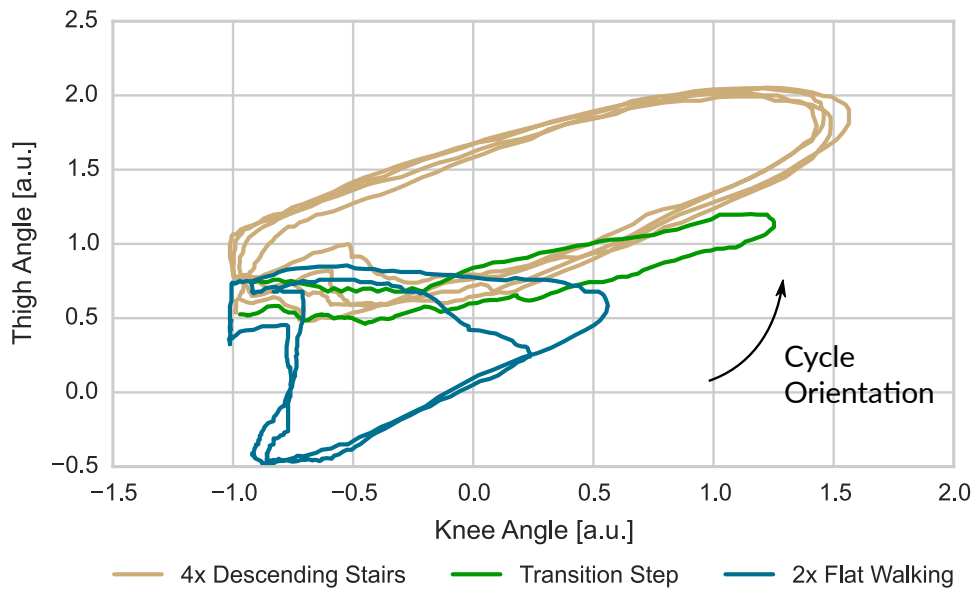


**Figure 9.8.:** For 215 steps (c) is showing the success rate depending on the required minimal range of certainty, which goes slightly above 94%. Earlier success or sequences of consecutive steps provide the high offset. For the ranges marked by the vertical red lines, at 20% and 3%, the detailed comparison is shown in (a) and (b), respectively. There the manual annotation in the rows is compared with the method’s results in the columns. The field on the intersection show the frequency of steps with a tag which end up in the corresponding class. The class ”unknown/fall back” catches all steps which no model could reliably predict, ensuring basic operation of the device. The number of false positives and unknown gaits decreases with the required minimal range of certainty.

Support for Multiple Gaits



(a) Joint Dynamics



(b) Phase Space Dynamics

**Figure 9.9.:** Transition step from stair descending to flat ground: In 9.9(a) we see, that the transition step shows thigh- and knee-joint dynamics that are in level and form similar to step on the stairs. But in 9.9(b) we see, that the transition step starts identical to steps for descending stairs and ends with the cycle similar to flat walking. The best possible fit is therefore difficult to define and uncovers ambiguities in the method.

The second important result shown in figure 9.8 is that there is a diminishing rate of false positives, even if a specific model provides lower accuracy. The proposed method classifies unrecognised steps as “unkown gait”, thus preventing the controller to treat the coming heel strike in a wrong and possibly dangerous way. This allows the system to apply a fallback control method, which always ensures the patient’s safety, although most probably sacrificing comfort.

## 9.6. Discussion

The difficulty in the design of multi-gait support in an orthosis without BCI is the missing information about its user’s intention. As the device has to synchronise with the current motion, it will always need a specific forerun on side of the user before it can follow in. This makes multi-gait support a reactive, a delayed measure.

The presented approach tries to address this problem with a focus on prediction errors: The prediction error of the employed gait models will raise immediately, when a deviation from the represented gait occurs. This error signal then decays when not reinforced through additional deviations. This introduces two time-scales: a fast reaction to an unpredicted event and a slower decay of this error-information to prolong the signal. At the same time, the correct model’s prediction error is in the state of decaying without additional reinforcements, thus enabling the transfer of control output to the desired feed-forward controller. In other words, the presented approach selects the least-unfitting-controller.

The advantages of this approach are the general applicability and flexibility of the internal models with respect to applied sensors, hardware configuration (tested on both braces in chapter 4), and classification intervals. The approach is model free concerning the hardware and only posses implicit models of the individual gait dynamics. We could demonstrate the classifier for flat walking, stair descending and ascending with comparably few (3) sensors and a low sampling frequency of 100 Hz. It makes no assumption on specific transitions between

### *Support for Multiple Gaits*

states or other dynamic properties, like a pure finite state based controller, and is able to switch at any time in the gait and as often, as the users change their intent.

The here presented method classifies gaits in an on-line scenario with reaction times fast enough for in step adaptation, high recognition rates and a diminishing rate of false positives approaching heel strike. Tests were conducted with a closed-loop controller for flat walking and stair climbing and open-loop for security reasons with stair descent.

A practical advantage is that approach is in line with the feed-forward controller from chapter 8, which allows to use the same training data. This will be important for future applications of online-adaptation.

These general statements are followed by an extended critique of the presented evaluation, a brief comparison to other methods in the literature, before we go on to measures which can be employed to further improve the performance. We finalise this discussion with a look at the overall controller-architecture and alternative to presented components.

#### **9.6.1. Evaluation of Selection Accuracy**

The presented evaluation shows a tendency to good gait recognition with a high security margin through the use of a fall-back gait controller, but there are problems with the created ground truth with ambiguous transition steps (Figure 9.9). This ambiguity prevents the final evaluation of transition steps.

A possible solution is the evasion to a more objective measure, for example Mo-CAP or EMG data as in chapter 10. Still, a suitable gait lab typically provides only a small area for walking experiments, as the camera systems mounted and the EMG equipment typically is cable bound, too. If these problems could be solved to allow free walking, the definition of a suitable measure which catches the devices ability or inability to conform to the patient's gait has to be found.

These problems aside, the controller shows a high gait recognition rate. Gait switching is fast enough to allow secure heel-strike and the dead-time between switches, defined by the history length, is short enough to allow gait switching on a sub-step time-scale.

### **Geometrical Interpretation and Transition Ambiguities**

From a geometrical perspective, the predicting models learn to predict trajectories in a space which is similar to Figure 9.9(b), except that the number of dimensions is higher according to the number of inputs used. These models can cope well with an offset in joint angles, e.g., a slow slope was still recognised as flat walking.

The accepted thresholds in the decision units create tubes of allowed trajectories in the sensory-input-history-space which are allowed for the specific models. Volumes where several predicting models overlap are ideal transition points, but transitions can happen at any point in phase space, creating trajectories which are not handled by a specific model.

Given, that the knee-locking stance phase will necessarily look similar for all gaits, these unspecific transitions are found in the swing phase, as in the case of Figure 9.9(b). This poses no risk to the patient and can be handled quite fine by any swing-phase controller.

### **Misleading Evaluation of Complete Steps**

While the training data is recorded for a series of steps without transition and the evaluation too is rated against the whole step, the user is changing its gait at any time. Therefore, the decision unit has to deal with movements of a sub-step-length. The gait models are important to distinguish the foot-off and touch-down movements of different gaits.

For this to work, the history length has been chosen to be given typical step lengths (compare sections 9.3.2 and 10.4.3).

## **9.6.2. Comparison to other approaches**

In the literature [16, 60, 63, 99, 100], many approaches apply model invalidation to different models, for example Gaussian mixture models or hidden Markov Models.

An actual performance comparison would only be possible for image sequence based approaches [60, 63], due to the selection of gaits. But image based approaches are working with a completely different data set: they provide an external view on the whole walker while the challenge for prosthetics is the limitation to the device. At the same time, the presented data set was created with a healthy walker and is too small to yield reasonable comparisons with only 215 steps. Nonetheless, average success rates over 83 % and up to 94 % is at a comparable level to other model invalidation approaches from the field of computer vision [60, 63].

For prosthetic devices, [50] present a FSM based controller for stair ascent and descent. But due to the design of FSMs the gait set is fixed and the observed overlap between swing-phase ends of flat walking and stair descent at the end of stairs is not present.

[95] present a slope estimator which couples three specialised FSM based controllers for slopes of 0°, 5°, and 10° with another FSM. Transitions are possible between neighbouring slopes based on the estimator's output. While the gait selection is not comparable, the inclusion of additional estimators would most probably have positive effects on the outcome.

[99] uses Gaussian mixture models to differentiate standing and walking and select a corresponding FSM on the fly. They sample seven signals at 1000 Hz. These samples are analysed offline to reduce the dimensionality of the input for the Gaussian mixture models. These models classify based on a fixed history

length. The performance was optimised to yield a 100 % success rate with the minimal delay working on history frames of 50, 100, 200, or 400 samples. To increase the confidence of the approach, they evaluate overlapping frames every 10 ms, storing a number of results and applying a threshold of 90 % agreement. They determined optimal conditions using a window size of 100 with an overall delay of 430 ms.

In [100], this approach was extended to sitting. The final optimal delay for 100 % success rate was 500 ms. The selection of sensors was described as task specific.

In summary, the selected gaits in literature render the approaches often incomparable. While [99, 100] show a quite similar approach with on-the-fly gait switching, the selected movements are not comparable. The use of gait phase control in the here presented feed-forward controller supersedes the need to recognise standing.

As with the feed-forward controller, our approach has the big advantage of working with configuration data of the device. The presented approach employs no explicit models or expensive feature extraction. It works with as low as 3 sensors and 100 Hz. The application of additional pose estimators and an increase in sampling frequency seems beneficial. Especially the latter action would allow detailed optimisation of the procedure, as outlined in section 9.6.3.

### 9.6.3. Improving the Performance and Behaviour

While the gait recognition is providing a working multi-gait walking experience to healthy test-subjects, the presented approach provides many parameters and opportunities for further optimisation of gait recognition. We will now discuss these parameters and the ability to extend the controller in this section.

## Degrees of Freedom and Optimisation

The presented approach has many degrees of freedom, i.e., free parameters which can be tuned to optimise the output.

As we only worked with one individually fitted prototype and one user at a time during development, extensive optimisation was not necessary, but for real world applications it is advisable to use these options.

**Free parameters per Gait Model:** Each gait model has the internal degrees of freedom of the artificial neural network, i.e., weights and level. While the topology of the network can be changed and optimised per gait, the tuning of these parameters is handled by the training procedure to minimise the prediction error on the training data.

Additional free parameters are the scaling factors for the sensory input (see below in section 9.6.3). These parameters are preparing the learning procedure by normalising the input range. Any change on these parameters should be compensated by the training procedure, at best these parameters speed up the convergence.

**Free parameters in the Decision Unit:** The decision unit provides a set of parameters, some of which are per gait, like the time constant  $\beta$  in the initial low pass filter, the time constant  $\alpha$  in decay of the unfitness measure and the coefficient  $\gamma$ , which weights the relative importance of thigh and knee unfitness, as described in section 9.4.1.

Additionally, the increase in the unfitness-value  $f$  (now an error count with  $\Delta f = 1$ ) and the maximally allowed unfitness for gait selection (now only gaits with  $f \leq 1.1$  are considered) could be changed per gait<sup>1</sup>, but the pair of them are not independent of each other.

---

<sup>1</sup>Instead of scaling the maximally allowed unfitness per gait, the use of the  $\gamma$  parameter could be changed to scale the error for a specific gait.



This makes four free parameters per gait which could be optimised over a training sample. But the training sample would have to be representative to not end up with a decision unit which fails to generalise. The necessary size of the training sample would need additional investigations.

### **History length—Trade-Off between Accuracy and Switching Frequency**

Thorough optimisation is possible and in general, a longer history provides a better basis for prediction, as investigated in more detail in [99, 100]. But the maximum possible switching frequency will decrease with longer history, as the dead-time to refill the history increases. With the considerations from section 9.3.2, only a shortening of history length seems plausible, which is undesirable as it will likely reduce the prediction performance.

### **Influence of Sensory Scaling**

It is generally advisable to make sure that the input for artificial networks is scaled in such a way, that it neither saturates too early, nor that a signal is dominant due to a huge scaling difference in the inputs. Therefore, in the course of development, the sensory input has been rescaled for each predicting gait model.

Strictly speaking, it is not necessary to do so and all gait models can work on the same input ranges. Still, the rescaling for each predicting gait model optimises the learning period for the corresponding gait, by making full use of the input range for typical gait.

We omit a detailed study at this point, but for the sake of completeness we here note that the presented approach works without a specific scaling, but that it helps to employ the distinct ranges in sensory input, seen for example in stair climbing compared to flat walking.

### **Scaling—Application of Additional Sensors and more Gaits**

It is difficult to estimate the scaling properties concerning more gaits and additional sensors of the presented controller without extensive experiments.

But generally we assume that, as long as a model is predicting the sensory input with a sufficiently small error, the controller can apply a control scheme fitting for this model. The important elements for successful application are (a) a set of suitable sensors, to resolve the different dynamics; (b) thresholds, which define if the prediction error is still acceptable and (c) a set of gaits, the controller can actually handle. As long, as these factors are well chosen, the presented method is independent of the set of sensors and the actual geometry of the device, to which it is applied.

In other words, additional sensors extend the input dimensions and therefore allow to differentiate more gaits against the same error margins. A suitable choice of sensors will therefore help to improve the performance as well as it allows extending the number of supported gaits.

Without additional sensors we have to assume, that the number of overlaps in history-space gets quite high, which could result the decision unit to constantly switch between models. But this does not necessarily imply bad patient support. Therefore, a thorough investigation of independent movements in the patient's gaits could help to settle the question how many gaits are actually needed to be supported. This could lead to the definition of an optimised sensor set.

#### **9.6.4. Significance for the Controller-Architecture**

In this section, we want to discuss the impact of the presented gait classification and selection for the overall controller. We will make the argument that not before the input is recognised, it is possible to change the behaviour of the device online and in a desired way. At the same time, this allows the system to record unknown motion.

### **Input Recognition Enables Gait Adaptation**

The applied multi-layer perceptrons can easily be retrained when new training data accumulates, as discussed in section 8.5.1. This approach can track changes in the patient's gait, when old data is discarded in time.

To implement this approach, the controller needs to know to which gait's training data the current sample belongs. The algorithm would need to select steps without transitions and small prediction errors and could modify the training data of an existing gait. As the predicting gait models of the multi-gait approach and the timing units of the underlying feed-forward controllers use the same sensory input, a common sample database could be cultivated so that the both modules stay in sync.

### **Recognition of Unkown Gaits**

The classification produces the label unknown to indicate the use of a fall-back controller. At the same time, this could be used as an indication that there is a new gait to be learned.

Of course, extreme caution has to be applied, lest the controller tries to learn every possible transition from gait specific trajectories as described in section 9.6.1. Therefore, it seems advisable to

1. Only collect unkown gaits, if the gait is applied for more than one step, to ensure that the controller can get enough training data.
2. Collected sequences of unknown gait could still include more than one gait and additional filtering with clustering methods could be applied, or—in combination with an online adaptation mechanism as described in the previous section—it could be tested if a new gait model will converge fast enough to not include several gaits.
3. A new feed-forward needs to be trained, too.

### *Support for Multiple Gaits*

These precautions can be used to make a new gait gradually better supported and comfortable. It could be tested, if the first precaution is unnecessary, but for these consideration to be sustainable, a detailed analysis of distinguishable gaits and limb motions had to be conducted.

### **Modularity of the approach**

The presented approach follows the preference of small modular units, whose functionality is self-contained. Whereas large neuronal networks are often criticised for being difficult to confirm for all possible situations, the presented circuits are reasonably small and one could try to verify their operations. Still, a more important aspect of the modularity is, that the gait switching is modifying the behaviour of the underlying feed-forward controllers from the previous chapters. The components of the controller-architecture are interacting with each other, but their functionality can be tested independent of each other. This modularity allows to extend the behaviour by the extension with additional gait modules.

### **The Decision Unit Introduces Time Dependency**

The decision unit as well as the gait models introduce time dependencies in the system, which was independent of its history. This is desired, as a gait is an ongoing movement, but the gait models are only working for velocities, which were part of their training data.

As a consequence, this works best when different gaits have an associated velocity range and larger changes in velocity lead to a change of gait. Luckily, this is typical for human walking, as for the example of walking and running (compare chapter 2, although running gait might not be a realistic test case for patients wearing a orthosis).

### 9.6.5. Alternative Approaches

The modularity of the approach allow to exchange parts or the whole gait-selection mechanism. In this section we discuss some obvious alternatives and promising approaches from the literature.

#### Replacing the delay-line based Prediction Models

Examples for alternatives to delay lines are recurrent networks. The recurrent connections provide a trace of earlier activity in the network and thus enable the network to provide memory of former input. An example for a very flexible and powerful approach to employ recurrent networks are liquid-state networks [12], where a recurrent neuronal network will provide the reservoir to extract information with additional, task related neuronal networks.

Although this approach is very promising in terms of accuracy and power. But due to the complexity of the internal workings and the increased computational power through the higher number of nodes, we stayed with presented approach.

#### Why to Not Predict Sensory Input on the Basis of the Gait Phase

The timing unit presented in the previous chapter already tracks the patient's individual gait. The predicting model could therefore be implemented on top of the gait phase, generating approximate limb configurations for each gait phase  $\varphi$ . This is for several reasons not desirable:

1. the gait models create a prediction, which needs some sort of velocity approximation,
2. the presented models scale quite nicely regarding shifts of sensory input like on small slopes,

### *Support for Multiple Gaits*

for both reasons, more information on the current status than just the current gait phase would be needed. Although the gait velocity can be estimated as  $\dot{\varphi}$ , we would still need to include additional sensory input (for example the current angular offset), which would again induce a history-like behaviour.

As we cannot get around additional sensory input, and the gait phase-estimation is not reliable for untrained gait data as elaborated in section 8.4.1), we stick to internal models of the gait dynamics which only rely on direct sensory input.

### **Alternative Gait Selection Policies**

After the determination of the unfitness of all available gaits, the question remains how to use this estimation of unfitness.

The gait selection policy in the proposed controller is a classical *winner takes all* strategy. This choice seems best as, although alternative selection policies are available, our results indicate (compare section 8.4.1), that controllers with higher prediction errors are working on a less faithful representation of the gait phase, which would lead to non-reliable results.

Take a weighted mixing policy for example, which mixes the different gaits depending on their prediction error: if the gait is not similar enough, the gait phase of unfitting gaits will most likely consist of a set of plateaus with sharp rises. Depending on the state of the other Timing Units, we might likely end up with extreme phases, like mid stance or mid swing, with full or no damping. The weighted average therefore would not be a reasonable average, but a set of gaits won't have any contribution, others contribution full damping to the output. The result would be distorted by the discrete gait phase representations of unfitting gaits. The necessary cut-off, which is already implemented in the maximum considered error, would mean, that only in areas of high similarity mixing would take place.

Lastly, the gait models approximate a trajectory in an arbitrarily high dimensional space of the history components (section 9.6.1). The areas of vicinity,

## *9.6. Discussion*

in which weighted averages would be applied, are comparatively small and the local development of gait phase and damping should by all means already be similar. The winner takes all therefore should be a good approximation to the weighted mixing in case of gait transitions and the best choice otherwise.





## **Part IV.**

# **Gait Laboratory Evaluation**



*Premature optimization is the root of all evil.*

D.E. Knuth

# 10

## User-Device-Interaction

In the first parts of this thesis, we developed a modular controller architecture for adaptive orthosis control. A prominent feature of this controller architecture is the ability to learn individual gait via models which abstract gait progress (in section 8.2.3) and general gait dynamics (in section 9.3).

While previous chapters tried to answer the question on the performance of these controller components, the question remains, how the orthosis-controller-system interacts with its users and how it alters their gaits. To answer this question is more difficult, as it cannot be answered by sensors on the device, but we have to take into account the whole walker.

This is important for several reasons:

1. For get a realistic impression of the controller's performance, the effect on the user and the user's acceptance matter most.

2. To develop an adaptive or even self-learning device, we have to understand in which way the user benefit, how this constitutes their changed gait, and how we can measure this in a way, that the device can work towards such an improvement. This covers the driving measure behind adaptation as well as patient condition monitoring.
3. To understand time-scales, on which the users adapt their gaits. This is important to define the time-scales on which the device alters its behaviour to allow for homoeostasis in the patient-device-adaptation.

Here, we cannot answer all of these questions. Instead, we will focus on a small study with a healthy walker to compare the influence of the device with and without a set of controllers. We consider the orthosis' hardware-controller combination as a disturbance to a healthy walker. Thus, we can infer how the presented controller will interfere with its user and identify measures which are able to quantify the controller's impact. The presented analysis can be thought of as a pre-study to evaluate possible experiments for a later, comprehensive patient study.

## **10.1. Introduction**

To investigate how the interaction of the orthosis with its users changes the gait of the latter, we conduct a set of treadmill runs for different walking speeds and slopes. For regular walking with a speed of 3 km/h, a comparison is done between trials with and without orthosis. The orthosis will be used as passive brace, with the proposed controller and a simple controller, which changes between the states locking and free only depending on the foot pressure sensors, the so called foot-switch controller. The latter is similar to a situation with badly tuned damping, as the onset is steep after heel-strike and the toe-off leads to abrupt unlocking of the joint.

To evaluate the interaction, we employ electromyography (EMG) to monitor muscle activity and motion capture (MoCAP) to monitor the bodies pose under

influence of the brace and controllers. The changes from free walking to walking with the uncontrolled, free orthosis will tell us about the order of magnitude of changes induced by the brace and the controller, respectively. Furthermore, the experiments with the free orthosis will allow us to define the baseline for controller experiments. Therefore, we will briefly introduce these techniques.

Here, we want to thank Leonardo Gizzi, Daniela Wedeking and Dario Farina for providing the gait lab, the realisation of the setup and the operation of the gait lab.

### 10.1.1. Motion Capture

The motion capture system uses a set of 8 high-speed cameras (Qualisys OQUS 300+) to track reflecting markers which are attached to the patient. We will not go into a detailed description of the method. Instead, we will briefly present the approach taken in our experiments.

After calibration with a defined set of markers, the MoCAP system is able to determine the 3D-Positions of the marker positions based on their placement in the frames of several cameras. Depending on the distance to the marker in the previous frame, the system can collect positions to trajectories. Further manual post-processing can merge and label the trajectories, where the automatic system did not succeed. Some systems allow for a model based identification. Here, we want to thank Leonardo Gizzi again for his efforts to provide us with a completely labelled set of recordings.

From the trajectories of these markers, the joint angles can be derived. To derive the joint angle  $\psi_j$  of a joint at position  $\vec{j}$ , we take positions on the neighbouring

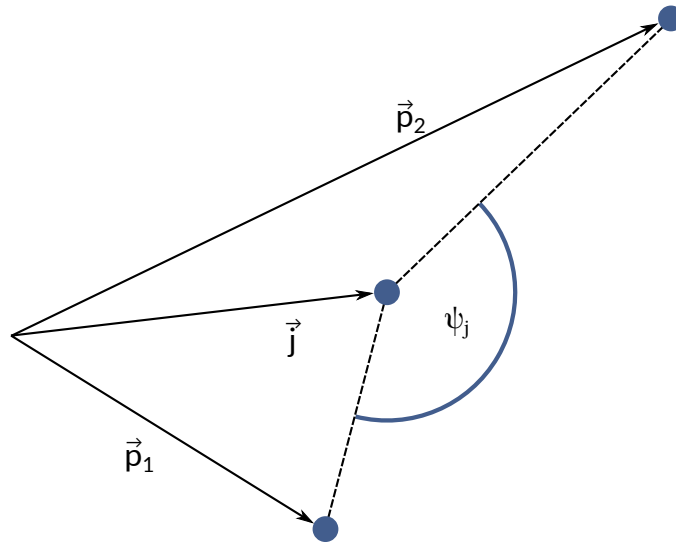


**Figure 10.1.:** Calculation of joint angles form marker trajectories. The vectors from the joint to its neighbouring markers are used to calculate the angle.

joints or limbs  $\vec{p}_2$  and  $\vec{p}_1$  as shown in Figure 10.1 and find

$$\begin{aligned} \cos(\psi_j) &= (\vec{p}_2 - \vec{j}) \cdot (\vec{p}_1 - \vec{j}) \\ \sin(\psi_j) &= (\vec{p}_2 - \vec{j}) \times (\vec{p}_1 - \vec{j}) \\ \psi_j &= \arctan\left(\frac{\sin(\psi_j)}{\cos(\psi_j)}\right), \quad \cos(\psi_j) \neq 0 \end{aligned}$$

The advantage of this formulation is that many libraries for mathematical operations provide a variation of the arctan function, which will take two arguments and handles the distinction of cases to choose the correct quadrant for  $\psi_j$ , simplifying the procedure and being applicable for all values of  $\cos(\psi_j)$ .

### 10.1.2. Electromyography

Electromyography (EMG) denominates the recording of muscular activity via intramuscular or surface electrodes. To gain a better understanding of these recordings, we will revisit the underlying muscle activity, together with a short

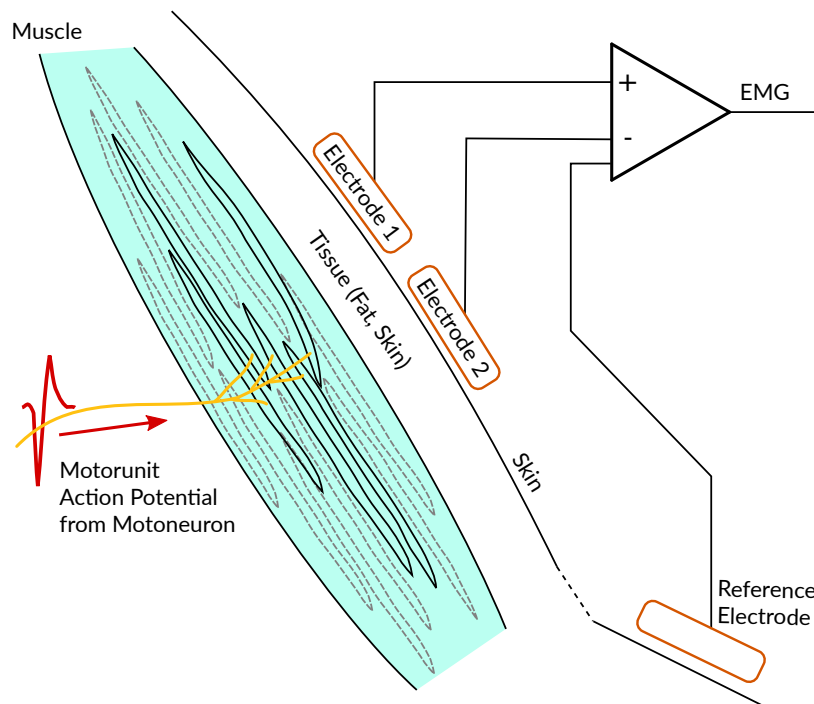


**Figure 10.2.:** For surface EMG, two electrodes per muscles are placed as close as possible to the midline of the muscle belly [13]. The EMG-Signal is the difference between the recordings of these electrodes against a reference electrode on unrelated tissue, see equation (10.1).

glimpse on the recording technique for surface electrodes, which was used for the presented results.

### The Recorded Electromyography (EMG)-Signal

Therefore, we follow up on the general description of the efferent neural pathways for muscle control in section 2.4.1. Figure 10.2 starts where Figure 2.5 ends: at the muscle fibres. The muscle fibres contract after excitation from a spinal motoneuron. The motoneuron together with the excited muscle fibres is called a *motor unit*, the motoneurons action potential which excites the muscle fibres is called motor unit action potential (MUAP).

To create a muscle contraction of with specific force and/or velocity, a set of motor units is recruited. Although the exact processes are not of interest to us, it is important to know that there are different muscle fibre types and motor units of different sizes. Thus, different motor units provide varying forces and by selection of different motor units and changing numbers, the nervous system can exert fine control over muscle forces.

The MUAP is a temporal change of membrane potential, that travels along the motorneurons axon to the muscle fibres of the MUAP, which are spread over the muscle. In the muscle and on its surface, the superposition of all active MUAPs (which are distributed over the muscle), filtered through the muscle tissue itself can be recorded via intramuscular electrodes [91]. For surface EMG, further tissue, e.g., fat and skin, are filtering and distorting the signal on its way to the surface electrodes (Figure 10.2).

Consider recordings  $r_1$  and  $r_2$  from electrodes 1 and 2, respectively, against a reference electrode on unrelated tissue as in Figure 10.2. We assume the recordings to be constituted of the EMG signals  $s_1$  and  $s_2$  + some common noise  $n$ , for example from power lines. Using differential amplification, this common noise can be excluded to gain the EMG signal  $s$  [14]:

$$\begin{aligned}r_1 &= s_1 + n \\r_2 &= s_2 + n \\s &= r_1 - r_2 = s_1 - s_2\end{aligned}\tag{10.1}$$

The resulting EMG-signal  $s$  describes the difference of potential at the locations of the electrode. This potential difference reflects the superposition of all MUAPs, from all excited muscle fibres as filtered through the tissue, e.g., fat and skin, along the paths of different lengths from the muscle fibre to the electrodes.



## Analysis and Use of EMG-Recordings

Two common ways to analyse EMG signals are the investigation of signal amplitude and the identification of actual activity by identification of the MUAPs which contribute to the signal  $s$ , see for example [91] for intramuscular electrodes and [20] for how to decode the muscle driving signals from surface EMGs with a direct comparison to signal amplitude analysis.

When analysing the signal amplitude, [42] found a linear correlation between signal amplitude and the generated torque for vastus lateralis, rectus femoris and vastus medialis during a brief contraction. A positive correlation between the mean frequency of the power spectrum and muscle torque were only found for a majority of 17 – 18 out of 21 subjects. [20] lists other studies and estimators for signal amplitude, enumerating

1. size differences of surface action potentials between motor units and across conditions, preventing the inference of motor neuron discharges;
2. amplitude cancellation, which describes the fact, that the sum of surface action potentials is less than the sum of individual potentials.

In this study, we want to investigate the impact of the orthosis on the human gait in terms of muscle activity. While the identification of actual MUAP activity provides much more detail, a simpler estimation of the muscular activity is sufficient, which allows us to determine the existence and timing of the muscle activity. To this means, an investigation based on signal amplitude is sufficient.

## 10.2. Experimental Setup

The experiments took place in the gait lab of the Farina Labs in Göttingen. We were using MoCAP and EMG recording equipment. For MoCAP, the lab provides high speed cameras which sample with 256 Hz. The EMG recordings

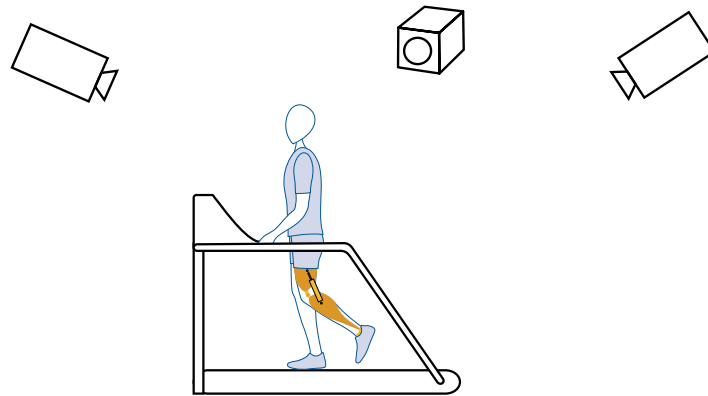


**Figure 10.3.:** Lab setup: The MoCAP camera system was mounted on the walls surrounding the lab. The treadmill was placed in the central area of the camera system to provide good marker coverage except for direct treadmill frame occlusion.

were done with 16-channels at 2048 Hz, and the orthosis' data acquisition (DAQ) hardware samples its sensors with 100 Hz (compare chapter 7).

Walking took place on a treadmill to allow precise control over slope and average velocity. The treadmill was positioned in centre of the MoCAP system so that as many cameras as possible could resolve the markers, except when hidden by the treadmill frame.

To synchronise the different recording systems, the MoCAP system provides external analogue inputs. The left tibialis anterior (TA)-channel and the heel-strike-FSR for the orthosis were thus sampled a second time with 256 Hz.

### **10.2.1. Experimental Procedure**

The conducted trials are listed in Table 10.1. They combine slopes of  $0^\circ$ ,  $10^\circ$ , and  $-10^\circ$  at speeds of 1 km/h, 3 km/h, and 4 km/h. To determine the impact of the brace, we made trials without orthosis and with inactive orthosis, i.e., without any controller passively attached to the leg. Then, to determine the impact of the controller in comparison to the brace, we conducted experiments with the

presented controller and the simple foot-switch controller, which is described below in more detail.

For each trial, after the setup of the treadmill to the desired angle, the speed was configured and the subject walked for two minutes to get used to the controller, speed and slope. After two minutes, the EMG and MoCAP recording equipment was enabled. Small breaks were done in between and the EMG recordings were observed to make sure, that they showed no signs of fatigue.

The orthosis was worn on the right leg, when referred to it the designations “right” and “ipsilateral” will be used. The other leg will be identified by the designations “left” and “contralateral”.

### **The Presented Controller**

As the walking conditions on the treadmill provide no variation, but only a simple walking experience with a fixed velocity, only one feed-forward controller was activated. It has been training with gait samples for simple walking, i.e., flat ground and small slopes.

According to the counsel of an orthopaedic technician, the applied knee damping was tuned in way to provide prolonged knee support at the end of the stance phase to mimic safety considerations.

### **Foot-Switch Controller**

The foot switch controller works solely on the FSRs below the foot at heel and toe position. The calibration normalises the the FSR readings to the interval  $[-1, 1]$  representing maximum pressure for a value of  $-1$  and no pressure for a value of  $1$ . When one of these two FSRs readings goes below  $0.75$ , the knee joint provides full damping. If both sensors provide readings above  $0.9$ , the knee joint is unlocked. The hysteresis is introduced to to prevent fast switching near the threshold.

#	velocity [km/h]	Slope [°]	Device Status
1	3	0	without orthosis
2	1	0	without orthosis
3	4	0	without orthosis
4	1	10	without orthosis
5	3	10	without orthosis
6	4	10	without orthosis
7	3	0	inactive orthosis
8	3	0	active controller
9	1	0	inactive orthosis
10	1	0	active controller
11	4	0	inactive orthosis
12	4	0	active controller
13	3	10	inactive orthosis
14	3	10	active controller
15	1	10	active controller
16	4	10	active controller
17	3	0	foot-switch controller
18	3	-10	inactive orthosis
19	3	-10	active controller

**Table 10.1.:** Recording trials and conditions, i.e., treadmill velocity, slope, and orthosis status as detailed in section 10.2.1.

Marker Label		Position
Contralateral	Ipsilateral	
LM <sub>5</sub>	RM <sub>5</sub>	Outer metatarsal bone on the foot
LANK	RANK	Ankle
LKNEE	RKNEE	Knee joint
LWRIST	RWRIST	Wrist
LELB	RELB	Elbow
LSHO	RSHO	Shoulder
LHIP	RHIP	Hip joint
LASI	RASI	Anterior superior iliac spine
LPSI	RPSI	Posterior superior iliac spine
STE		Sternum
L4_		lumbar vertebrae L4

**Table 10.2.:** Marker-positions for MoCAP recording. Donning of the orthosis required the replacement of the markers on the right leg.

### 10.2.2. Motion Capture

For motion capture, reflective markers were placed on the joints of the lower limb and upper limbs, the iliac spine, the sternum and the lumbar vertebrae L4, as listed in Table 10.2 and shown in Figure 10.4, compare to Figure 10.7. The markers on the right leg from the hip marker downwards had to be replaced after donning the orthosis.

### 10.2.3. EMG

To prevent AC noise from the power circuits to disturb the frequency content of the recordings, the DAQ for EMG-sampling was driven by a DC truck battery.

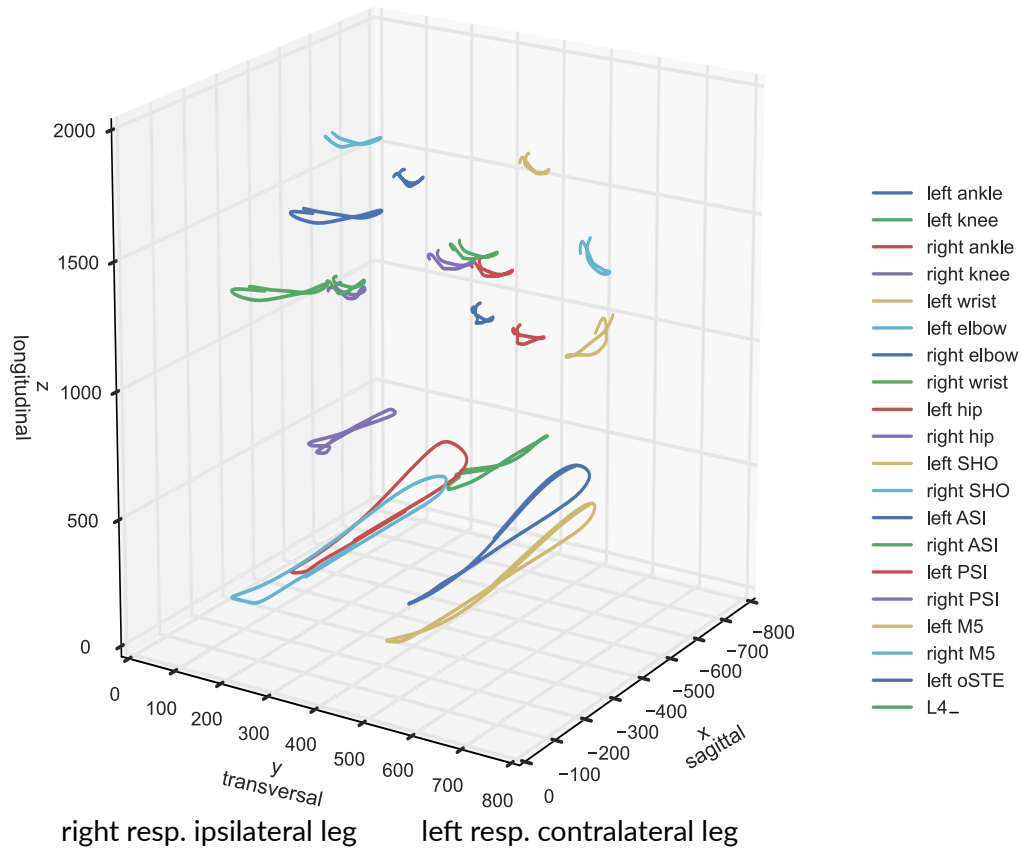
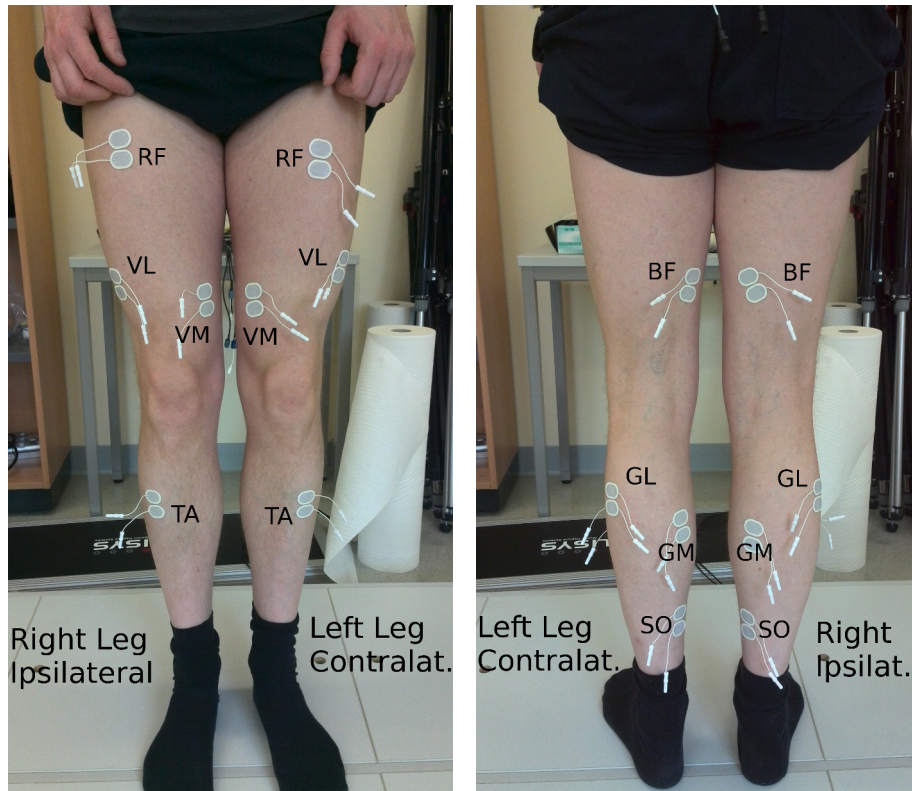


**Figure 10.4.:** Approximately one step of a MoCAP recording at 3 km/h and a slope of 0°, showing the marker positions and slight variations from step to step, which seem to be higher for the upper body.

After shaving of the concerned skin areas, the recording electrodes were placed on both legs over soleus (SO) and tibialis anterior (TA) for the ankle joint, gastrocnemicus medialis (GM) and gastrocnemicus lateralis (GL) for ankle and knee joints, vastus medialis (VM) and vastus lateralis (VL) for the knee only, and biceps femoris (BF) and rectus femoris (RF) for the hip and knee joint, the detailed roles are listed in Table 10.3 and the used electrode positions can be seen in Figure 10.5. It is important to note, that for the ankle joint, the role of flexion and extension seems inverted, as the flexor muscle (SO) is actually pushing the foot down. This perceived inversion is due to anatomical differences in animals' legs (e.g., a horse) in comparison to the human foot, where the ankle's joint range is changed.

The electrodes had a gel film attached to optimise surface contact and eliminate air-filled gaps of varying size. To secure the electrodes against shearing forces and to provide strain-relief for the connectors, the electrodes and cables were fixated with bandages.

As the same muscles are instrumented on both legs, we have two channels per muscle, one for each leg.



(a) Front Side

(b) Back Side

**Figure 10.5.:** Placement of electrodes for the recordings. For muscle abbreviations and functions, please consult Table 10.3.



Muscle	Abbrev.	Joint	Function
Rectus Femoris	RF	Hip	Flexion
		Knee	Extension
Biceps Femoris	BF	Hip	Extension
		Knee	Flexion
Vastus Lateralis	VL	Knee	Extension
Vastus Medialis	VM	Knee	Extension
Gastrocnemicus Lateralis	GL	Knee	Flexion
		Ankle	Plantarflexion
Gastrocnemicus Medialis	GM	Knee	Flexion
		Ankle	Plantarflexion
Tibialis Anterior	TA	Ankle	Dorsal Extension
Soleus	SO	Ankle	Plantarflexion

**Table 10.3.:** Recorded muscles for the EMG experiments. Electrodes for these 8 muscles were placed on both legs (cmp. Figure 10.5).

## 10.3. Methods

After the description of the experimental procedure, in this section, we will describe the steps used for the processing and analysis of the recorded data.

### 10.3.1. Analysis Pre-Processing

The pre-processing covers preparation for later analysis. We will cover the synchronisation of the data from the different sources, i.e., MoCAP, EMG, and the orthosis, as well as the segmentation of the time series to steps.

## **Synchronisation of Different Data Sources**

Synchronisation of the MoCAP, EMG, and the orthosis recordings is based on the common channels in the auxiliary analogue MoCAP-recording channels, as listed in section 10.2. The detailed procedure was handled as follows:

1. As these common channels were recorded by the MoCAP equipment with 256 Hz, the corresponding channels in the EMG and orthosis recordings were resampled to this frequency.
2. As the three recording systems were started independently, the offset for the different recordings had to be determined. The best fit was determined with the standard correlation function of the `scipy` module [40]. To be independent of the changing sequence of recordings,
  - the middle half of the EMG recordings was matched against the whole MoCAP synchronisation channel;
  - for the orthosis channel this was not necessary, as the orthosis recording was running longer than all other sources.
3. As the sources used internal and thus independent clock sources, the resampling had to be corrected to include the frequency errors relative to the MoCAP DAQ. Using the results of the previous steps, the mismatch in the common channels was measured in samples (absolute error in Table 10.4) and used to correct the resampling frequencies relative to the MoCAP frequency (relative error in the same Table) and the previous steps were repeated until the common channels were matching.
4. The thus determined synchronisation points were used to cut the recordings to a common time scale. For analysis, the recordings were used with their original sampling.

## Heel-Strike Approximation and Recording Segmentation

When comparing an ensemble of steps, the analysis used throughout the thesis is based on signals segmented in steps and normalised to a common step length (256 samples for MoCAP data and 2048 samples for EMG data based on step times  $\gtrsim 1$  s). This procedure allows a comparison independent of stride length and duration. When working with orthosis recordings, the FSR below the heel allows accurate heel strike detection and therefore good segmentation of the recording into individual steps. Because of the high sensitivity of the FSRs, only the onset of the heel strike can be determined (section 8.3.3).

As some trials in this chapter were recorded without orthosis, we could not rely on this method. For consistency and comparability with earlier chapters, we have to find a comparable measure which will provide a good fit to the heel-strike evens provided by the FSR, but is based on features of the MoCAP or EMG recordings. Due to the complexity of the EMG-signals, the MoCAP signals were preferred.

Given the employed methods, consistent heel-strike detection is especially important for the EMG recordings, for which we want to determine the onset and ending over the gait phase (see below). As we do not investigate the timing of features in the presented MoCAP analysis, the presented results for MoCAP recordings do not depend that strongly on the heel-strike detection.

### 10.3.2. Motion Capture Data Analysis

The MoCAP recordings provide marker trajectories from which we derive joint angles and body axis orientations for further analysis. The brace with its attached damper, as well as the additional weight, will influence the joint dynamics. We will start with simple measures as joint ranges and go on to more complex measures, which we will apply after segmentation and time-normalisation to stride cycle duration. Thereby, in turn, we check the body dynamics from the lower limbs to the upper body.

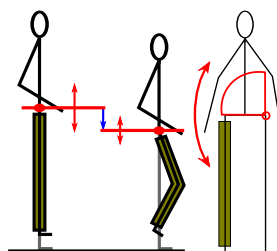


**Figure 10.6.:** Assuming, that suboptimal orthosis control forces the patient to employ avoidance movements, an angle sensor on hip level can show us to which degree the device forces the patient to an asymmetric gait in terms of a tilting in the hip plane. This gives no insight into the general gait quality, but shows to if the patients may bend their knees equally.

## **Joint Motion Ranges**

For the joint motion ranges, we will look at the joint dynamics of the hip and knee joints. In chapter 3 we saw an example for asymmetry in joint ranges for an orthosis patient. Here, we will check for the influence of the presented brace and controllers on the brace's user. The joint ranges will give a direct impression of changes at the level of the lower limbs. We investigated the mean of the segmented joint angle trajectories, as the mean corresponds to the centre of the periodic motion to find changes in the pose of the limb. Furthermore, we investigated the standard deviation of the segmented joint angle trajectories, as the standard deviation provides a measure for the amplitude.

## **Influence on Body-Axes**

We will consider different body axes to try to find distinctive features indicating changes in the patients posture. The body axes will allow us to infer changes above the directly affected lower limbs, which we want to relate to problems mentioned in section 3.3.2.

**Hip tilt:** We will consider the tilt of the horizontal hip axis (see Figure 10.6), to find indications of posture asymmetry directly above the limb. We use the x-y components along the vector from the LASI-marker to the RASI-marker and derive the angle against the vertical axis.

**Vertical leaning:** The second body axis we want to investigate, is the leaning of the upper body against the vertical. The vertical leaning should give a general impression, if the posture drifts in reaction to the orthosis, due to an evasive positioning of the upper body. To investigate the vertical leaning, we determine the angle of the vector from markers L4\_ to STE against the vertical as in Figure 10.7, i.e., the unit vector in z-direction  $(0, 0, 1)^T$ .

**Trunk rotation:** Hoorn et al [97] investigated changes in variability of movement between the pelvis and thorax (trunk) in the transverse plane as consequence of low back pain (LBP). Their Finding was, that for patients with LBP, the variability in thorax and pelvis were unchanged, but a higher coupling between these two reduced the variability in the difference between them (the trunk angle).

Although the experimental condition is different, the trunk rotation might reveal more about changes in upper body posture, than the two previous, simpler axes. Therefore, we will determine the pelvis orientation  $\vec{o}_{pelvis}$  in the x-y-plane by use of the LPSI, LASI, RPSI, and RASI markers, i.e., the rectangle inscribed in the iliac spine. We use the vectors indicating the markers' position, gaining

$$\begin{aligned}\vec{p}_1 &= \text{LPSI} + \frac{1}{2} (\text{RPSI} - \text{LPSI}) \\ \vec{p}_2 &= \text{LASI} + \frac{1}{2} * (\text{RASI} - \text{LASI}) \\ \vec{o}_{pelvis} &= \vec{p}_2 - \vec{p}_1\end{aligned}$$

For the thorax orientation  $\vec{o}_{thorax}$ , we evaluate the orientation in the x-y-plane by use of STE, LSHO, and RSHO, i.e., the triangle formed by the shoulders and

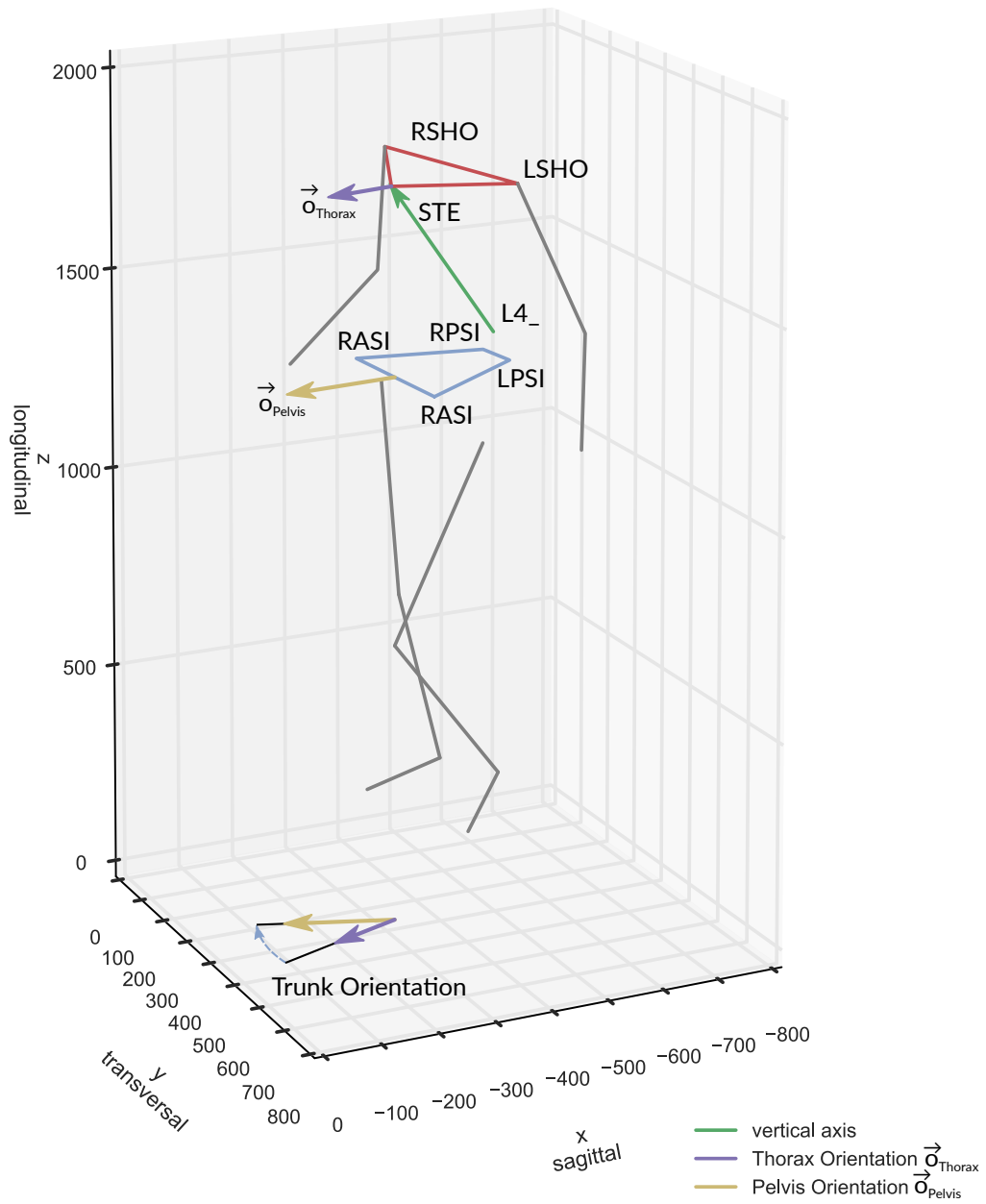


Figure 10.7.: Body axes

the sternum.

$$\vec{o}_{thorax} = STE - \left[ LSHO + \frac{1}{2} * (RSHO - LSHO) \right]$$

Both orientations are plotted in Figure 10.7. The trunk rotation is defined as the angle between the two vectors after setting the z-components zero.

According to [97], we calculate the average orientation angle over all steps (the average rotational component). Then we determine the stride to stride variability by subtracting the average rotational component from every normalised step to gain the residual rotations for each step. The average of these residual rotations is what is called the mean absolute residual rotation in [97]. This mean absolute residual rotation was calculated for pelvis, thorax, and trunk. We then find the median of each mean absolute residual rotation vector to represent the variability in degrees for each speed.

Furthermore, we looked at the mean of the transversal body plane orientation for all steps.

### 10.3.3. EMG Data Analysis

The brief collection of studies on EMG analysis in section 10.1.2 already makes clear that there are different approaches to analyse EMG data. For the scope of this thesis, we will not go into the details to analyse activity on MUAP-level, but we want to gain an initial understanding, how the interaction between the brace and its user will change the general muscle activation. Therefore, we will go for simpler measures. Instead of the reconstruction of active units, we will investigate the envelope of the signal.

#### The Envelope of Muscle Activity

The envelope of the EMG signal simplifies the distorted recordings of single MUAPs to a signal which represents the general amplitude of the muscle activity.

The filter we applied uses three steps:

1. a 2<sup>nd</sup> order Butterworth band-pass filter for the the frequency range of 10 to 350 Hz,
2. followed by the rectification of the signal, and
3. a final 2<sup>nd</sup> order Butterworth low-pass filter for the frequency range below 10 Hz.

The exact frequencies used vary from study to study. Another example would be to use a combination of a high-pass for above 450 Hz followed by rectification and a low-pass for below 6 Hz. This filter uses similar steps and frequencies to [26]. The final result can be seen in Figure 10.8.

### **Changes in Muscle Activation**

To assess general changes in muscle activation, we will look at the distribution for two measures for the segmented recordings: the area below the EMG signal and the amplitude of the signal estimated by the standard deviation. This will provide us with an overview of which muscles might show activity changes of interest.

After this general investigation of muscle activation, we investigate the average times of activation onset and ending for the individual muscles over the stride. This will show periods of extended, shortened, omitted, or additional muscle activity. To this end, we will normalise the EMG-recordings for each step to the range of  $[0, 1]$  to gain amplitude independent measure of activity onset. After this normalisation, we will derive the average normalised activity, which we will compare against a channel-specific threshold to determine the phases of muscle activity.

For both investigations, we will need to derive a threshold for comparison. To define this threshold, we will compare four methods according to their ability to capture the features of the recordings at hand.



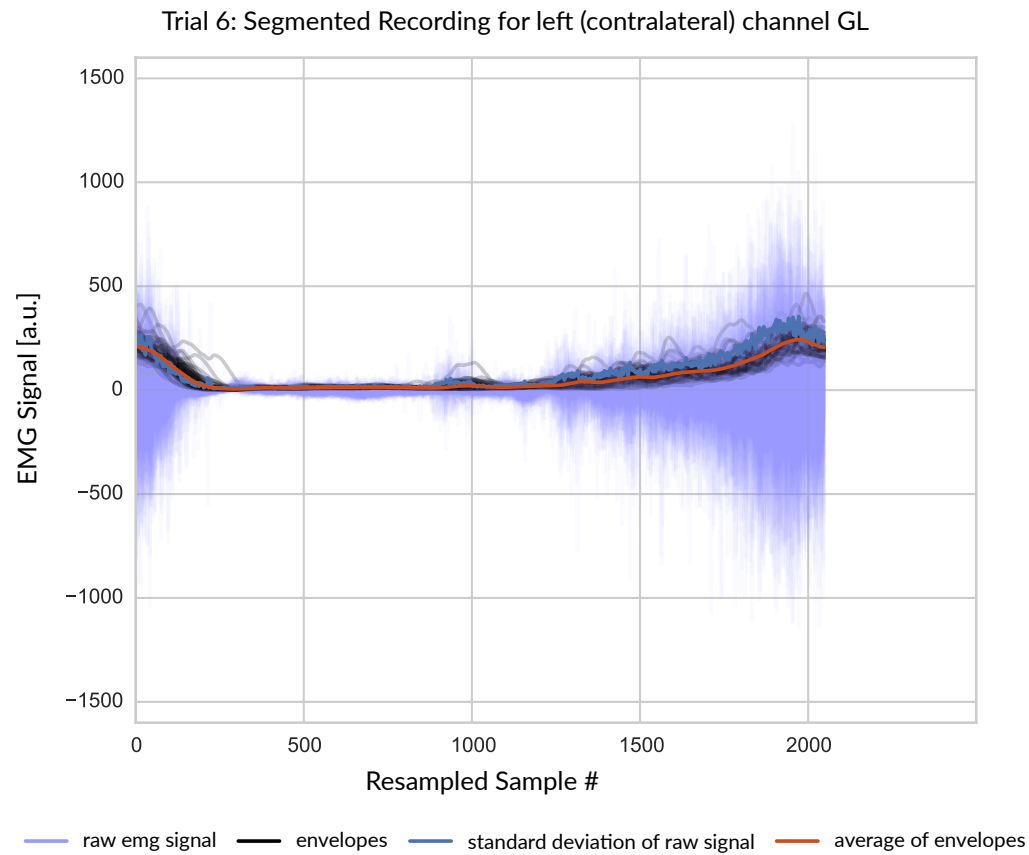


**Figure 10.8.:** The segmented recording of contralateral channel GL for trial 6. Each step was resampled to 2048 time steps. The raw signal is in light blue in the background. On top, in black, the envelopes of the signal. The standard deviation of the raw signal over all steps and the average of the envelopes are plotted in dark blue and orange.

1. We chose minimal amplitude as threshold. To estimate the minimal amplitude, each step is divided into 10 bins. For each of these bins, the area under the signal is determined. For the bin with the smallest area, the standard deviation is calculated as a measure for the minimal amplitude. To get one threshold per channel, the maximum of the standard deviations is determined.
2. For the same set of minimal amplitudes for each step as in the preceding method, we choose the median of the distribution of minimal amplitudes over all steps to reduce the impact of outliers,
3. After segmentation, we calculate the average signal over all steps. We divide the average step into ten bins. Then we chose the mean of the bin with the smallest area as threshold. The mean is used due to the low fluctuations after averaging.
4. For the average step, the global minimum and maximum are determined. The threshold is set to the minimum plus  $\frac{1}{5}$  of the range between minimum and maximum.

## 10.4. General Results

Before we will go on the the analysis of the subject's gait, we will start with the necessary analysis of the recordings, their synchronisation and segmentation. Due to the amount of the presented data, the presentation of results and the discussion will be done separately for MoCAP and EMG data.

From the subjects perspective, walking with orthosis was more exhausting than free walking. Especially for higher velocities. In walking with the proposed controller the safety tuning was noticeable in higher velocities. The foot-switch controller provided abrupt locking and unlocking which felt highly uncomfortable and more disturbing for higher velocities.

source	absolute error [samples]	relative error	absolute error [s]
EMG	$18 \pm 1$	$1.0006 \pm 0.0001$	4
Orthosis	$46 \pm 1$	$0.9985 \pm 0.0001$	11

**Table 10.4.:** Sampling frequency errors as determined by samplewise comparison of the correlated synchronisation channels for 31122 samples.

The pre-processing done on the data allows to compare the data of different sources and to produce analysis which can be compared to the earlier chapters of this thesis. We will start with the synchronisation of the time-series of different sources.

### 10.4.1. Recording Synchronisation

The sampling frequencies showed a systematic discrepancy between the recording devices over all trials (see Table 10.4). The relative frequency error was determined on the synchronisation channels of the MoCAP recorder on a recording of 31122 samples  $\approx 121.6$  s and manually checked against all other recordings. The absolute deviation of recording frequencies on the same time axis accumulates to  $\approx 4$  s for the EMG recordings, the frequency error for the orthosis recordings accumulated to  $\approx 11$  s over the recorded  $\approx 120$  s. Assuming a step duration of  $\approx 1$  s, we see that the delays cover a shift of several steps over the whole recording when not corrected.

### 10.4.2. Heel-Strike Approximation

As already mentioned in section 10.3.1, we want to find an approach for recording segmentation, which is comparable to the approach used in the earlier chapters, to get a common gait phase coordinate. As the first experimental runs were trials without orthosis, a method to approximate the heel strike from the motion

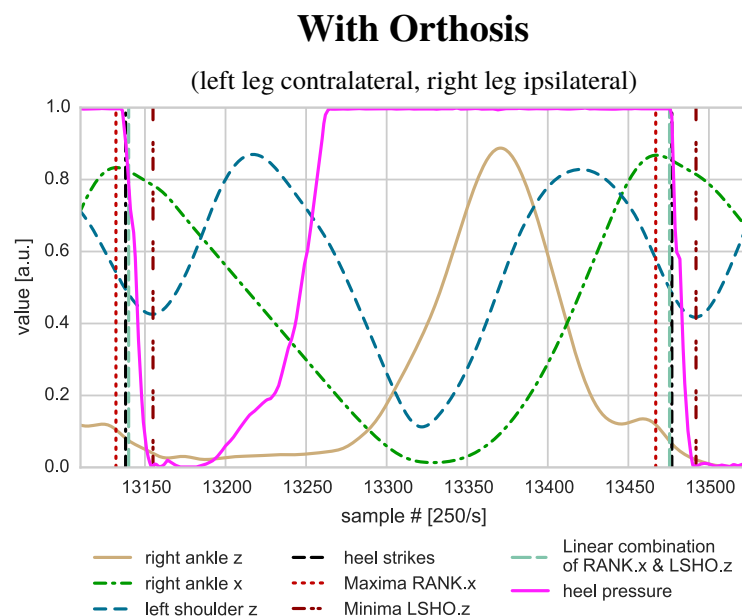


**Figure 10.9.:** Comparison of different heel strike approximations on flat ground. When taking the heel FSR flank onset as reference (heel pressure), the linear combination of ipsilateral ankle x and contralateral shoulder z provides the best fit. For errors see Figure 10.11, for a comparison to the ankle z component, see Figure 10.10.

capture recording is needed. For reasons of consistency and comparability, we will then use only this heel strike approximation in this chapter.

Depending on the exact marker positions, in the literature often the z-component of the ankle or heel-markers are used [97]. As we can see in Figures 10.9 and 10.10, which show selected marker-trajectories on the treadmill for  $0^\circ$  slope with orthosis, the neighbouring events do not match the onset of heel-pressure as recorded with the heel-FSR of the orthosis. We see that in general there is no single channel, which easily reproduces the heel strike with the same timing as the heel-FSR.

Figure 10.10 shows in more detail that the Ankle z-component is not mimicking the force sensing resistor, but shows several local minimums with the heel-

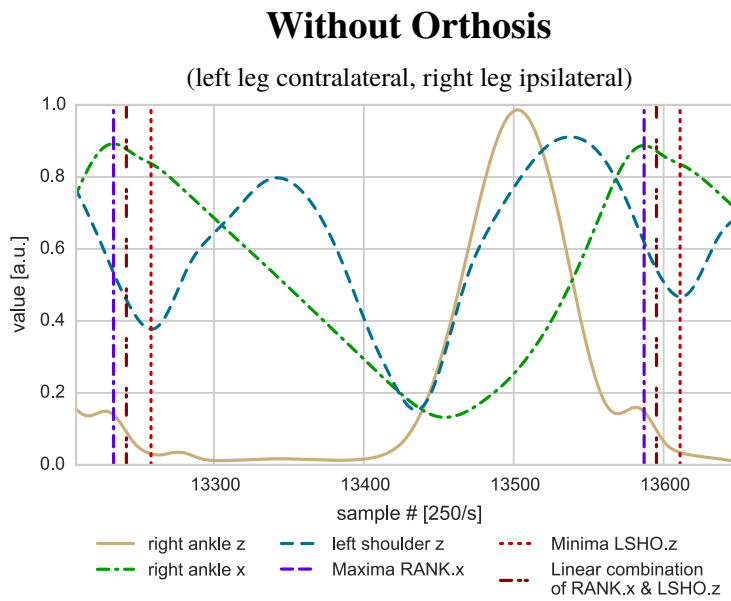


**Figure 10.10.:** Heel strike approximation without force sensing resistor at the heel: The linear combination of ipsilateral ankle x and contralateral shoulder z coincides with the second flank of the ankle z. When comparing the both plotted heel-strikes, the first heel strike has one local maximum more for the ankle z component.

pressure onset lying on a slope of the RANK marker's z-trajectory, shortly after onset of the swing-leg retraction (compare section 2.3). This makes an exact and consistent pinning of the heel-strike difficult: The relative location is not fixed and the existence of features for the ankle z-component depend on individual steps and on the slope: the exact number of local minimums per step varies, when comparing the left and right heel-strikes in Figure 10.10. Here, depending on the slope, things will change completely, for example on  $-10^\circ$ , the z-coordinate will generally be decreasing throughout the step (data not shown).

**Flat Ground** For flat ground, we use data from trials 7, 8, 9, 10, 11, and 12, i.e., all trials with orthosis on a slope of  $0^\circ$  except the foot-switch controller trial. In Figure 10.9 we see that the maximum of the ipsilateral ankle's x-component and a minimum of the contralateral shoulder's z-component are in the vicinity of the heel-strike. These features are show simpler features than the RANK marker's z-coordinate. The ankle's x-component's minimum at sample  $t_{RANK}$  is systematically too early, due to swing leg retraction, and the shoulder-maximum at sample  $t_{LSHO}$  is systematically too late. Experimental evaluation of the event sample numbers  $t_{LSHO}$  and  $t_{RANK}$  together with their respective deviations from the FSR onset in samples ( $\Delta_{LSHO}$  and  $\Delta_{RANK}$ ) for all experiments on flat ground were used to approximate the sample number of the heel-strike  $\hat{t}$  with a linear combination of these two events as

$$\begin{aligned}\beta &= 1 - \frac{\Delta_{LSHO}}{\Delta_{LSHO} + \Delta_{RANK}} \\ &= \frac{\Delta_{RANK}}{\Delta_{LSHO} + \Delta_{RANK}} \\ \hat{t} &= \beta t_{LSHO} + (1 - \beta) t_{RANK}\end{aligned}$$

For a comparison to runs without the orthosis, please compare to the ankle marker's z-component in Figure 10.10. The location of the heel-strike approximations keep their locations relative to the ankle marker's z-component.

Trial #	Left Shoulder z		Right Ankle x	
	$\Delta_{LSHO}$ [samples]	$1 - \beta$	$\Delta_{RANK}$ [samples]	$\beta$
<b>Flat Ground</b>				
7	1619	0.673	786	0.327
8	1357	0.667	678	0.333
9	1053	0.533	923	0.467
10	1093	0.675	526	0.325
11	1497	0.689	676	0.311
12	1448	0.706	603	0.294
average		$0.657 \pm 0.057$		$0.343 \pm 0.57$
<b>Slope Down</b>				
18	2923	0.817	653	0.183
19	2364	0.728	883	0.272
average		$0.773 \pm 0.045$		$0.227 \pm 0.045$

**Table 10.5.:** Coefficients for heel-strike approximation from MoCAP marker trajectories. The errors for the average coefficients were derived from the standard deviation over the trials and does not reflect the errors per step. For the distribution of these with the weights  $\beta$  and  $1 - \beta$  from this table, please consider Figure 10.11. Due to the high overlap and the width of the distributions of the per-heel-strike errors, the averaged weights were used for the presented approach.

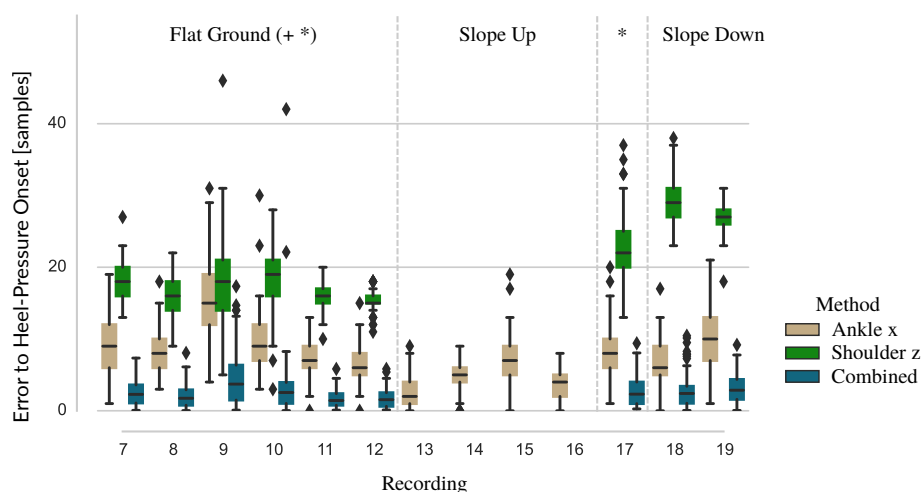


**Figure 10.11.:** Distributions of absolute errors in samples for different methods to derive the onset of the heel strike from motion capture channels against the heel-FSR reference. For recording 15, spurious events were removed ( $1 \times$  ankle x and  $2 \times$  FSR).

**Slopes** For high slopes (trials 18 and 19 with orthosis) the maximum ankle's x-component was used, as the swing leg retraction did not lead to a earlier direction reversal in this case. For slope descent, the flat ground method for heel-strike approximation could be used.

In this way, for all three slopes an approximation with errors below 20 samples were achieved, except for two outliers in trial 10 (plotted in Figure 10.11). The outliers in trial 10 are of no concern in this study, as it was a run with 1 km/h, which was not evaluated. To compare the runs with and without the orthosis, we will only use this motion capture approximation of heel strike for the further evaluation.

### 10.4.3. Step Filters and Recording Quality

In general, the quality of EMG and MoCAP recordings was good. Each trial typically provided 50 – 56 steps for 1 km/h, 80 – 89 steps for 3 km/h with the exception of trial 18 with 98 steps, and 87 – 98 steps for 4 km/h.



Channel	Number of steps without saturation per trial												
<b>Contralateral Side</b>													
trial	7	8	9	10	11	12	13	14	15	16	17	18	19
SO	0	0	0	0	0	3	6	0	0	2	0	0	0
<b>Ipsilateral Side</b>													
trial	1	5	6	15	16	17	18	19					
GL	5	62	18										
VM				27	3	57	88	0					

**Table 10.6.:** For recordings with saturation, this table contains the remaining steps after removal of steps with saturation. Where no number is given the whole recording of 120 s could be used, which typically amounted to 50 – 56 steps for 1 km/h, 80 – 89 steps for 3 km/h with the exception of trial 18 with 98 steps, and 87 – 98 steps for 4 km/h.

However, a set of EMG channels showed saturation. These included contralateral SO for all trials with orthosis and some trials of ipsilateral GL and VM as listed in Table 10.6. As the further analysis is based on steps, we removed steps which included saturated samples.

## 10.5. Motion Capture Data

Here, we will present and discuss the results for the MoCAP data. In the next section, we present the EMG data.

### 10.5.1. Results

Based on the step segmentation, we now move on to investigation of changes in joint motion and body axes. We start with the joint motion.

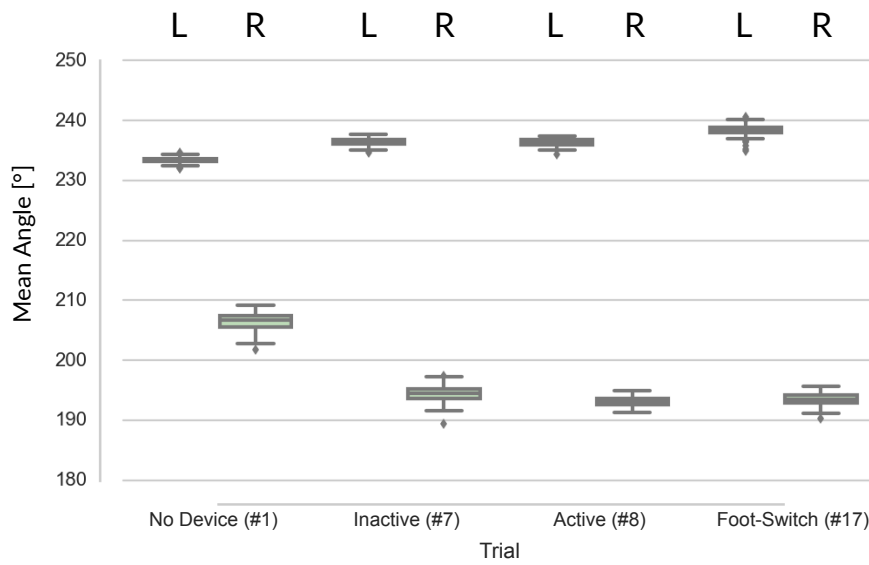
## **Joint Motion**

When looking at the distribution of the average joint position per step, and the variation over all steps of a trial in Figure 10.12, we note that the initial condition is asymmetric in the trial without orthosis. As the hip angle is calculated against ASI and KNEE markers, a difference of 1 cm can already provide a difference of  $7^\circ$ . While part of this could be due to marker placement, the knee shows a similar asymmetry for trial 1. The same effect may be responsible for the drop in ipsilateral hip angles due marker-position changes after donning the orthosis. This makes the interpretation quite difficult.

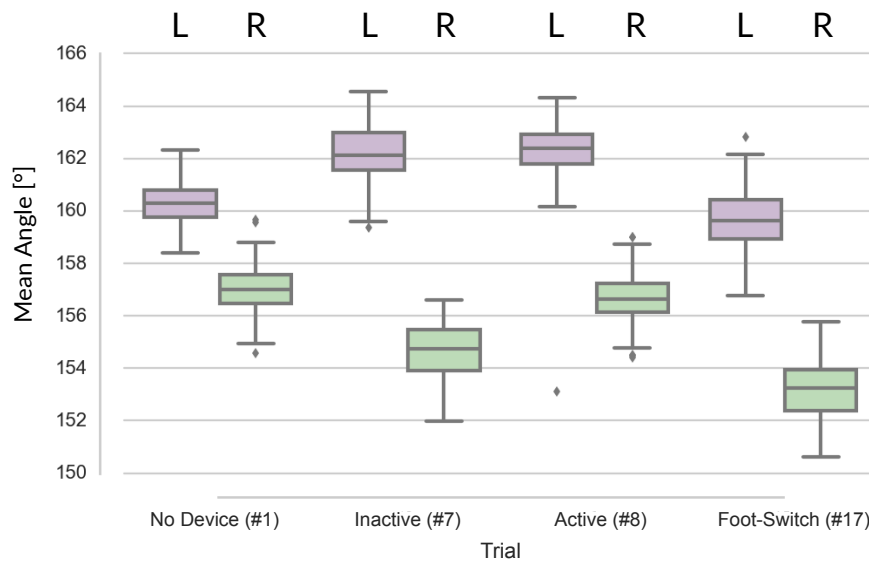
That said, we observe that the contralateral hip mean position in Figure 10.12(a) slightly increases when donning the orthosis, showing an almost complete overlap with and without controller. For the foot-switch controller (trial 17) the distribution of mean positions spreads and further increases. On the ipsilateral side, the hip angle cannot be compared to the trial without orthosis, but all distributions with orthosis overlap.

The distribution of mean knee angles in Figure 10.12(b) shows an increase in the average joint position when donning the orthosis with our controller and without controller, meaning a more pronounced knee extension. In contrast, the trial with foot-switch controller only provides an overlap of the outer percentile with the other orthosis trials, but a high overlap with the first trial. Still, the overall difference for the medians is about  $3^\circ$  and leads to a height difference of the contralateral hip of around 1.7 cm, for the hip at 1 m above the ground. On the ipsilateral side the first trial again cannot be considered for comparison. The other trials show an overlap with the presented controller leading to a slightly higher knee extension when compared to the uncontrolled orthosis and the foot-switch-controller, which shows even higher flexion than the uncontrolled orthosis. Here too, the overall difference of the medians is about  $3^\circ$  which makes the ipsilateral hip height difference around 2.2 cm, in the same order of magnitude: the knee is stronger flexed with the foot-switch-controller.

In the following we will also analyse angles which were not influenced by orthosis donning, as the used markers stayed in position over all trials.



(a) Mean Hip Angle



(b) Mean Knee Angle

**Figure 10.12.:** Changes of the mean hip and knee angle for different conditions. As the marker positions changed, the right leg values are not comparable to the condition without orthosis.

## **Hip Tilt**

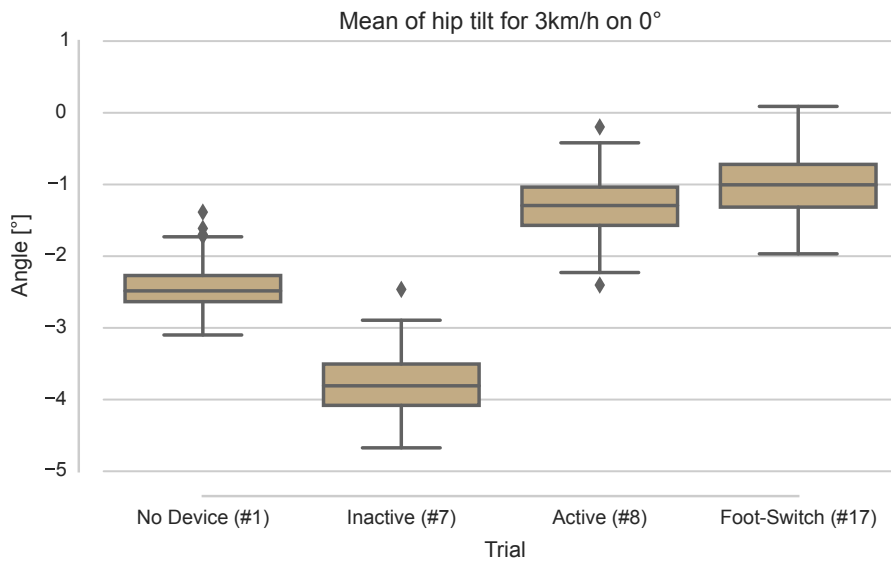
The investigation of hip tilting in Figure 10.13 shows a general lift of the hip axis with a controlled orthosis, indicating a leaning on the contralateral leg. Interestingly, with the uncontrolled orthosis the mean hip elevation of the ipsilateral side is reduced. The range of hip motion (indicated by the standard deviation) increases with inactive orthosis and even further with controlled orthosis.

## **Vertical Body Axis Tilt**

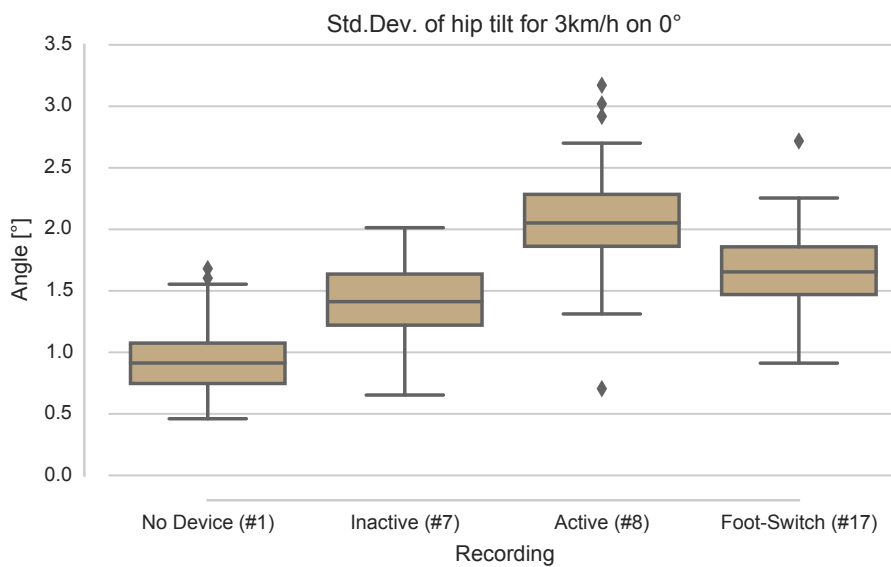
For the orientation of the vertical body axis (L4 to upper sternum) in Figure 10.14, we see a clear effect on the mean orientation. The body leaning is increased with orthosis. The proposed controller does not further increase the mean leaning, it lead to an increase in the fluctuation of the vertical axis. The foot-switch controller in general has the highest increases, showing a higher lean, a slightly higher standard deviation per step and a broader distribution in the range. Still, the overlap between the two controlled runs is high for the standard deviation and the range.

## **Trunk Rotation**

Before the detailed investigation of step-to-step variability of the trunk according to [97], as described in section 10.3.2, we will investigate simpler metrics in Figure 10.15, e.g., the distribution of mean trunk orientation per step and the distribution of standard deviations per step for the trunk angle in the transversal plane.

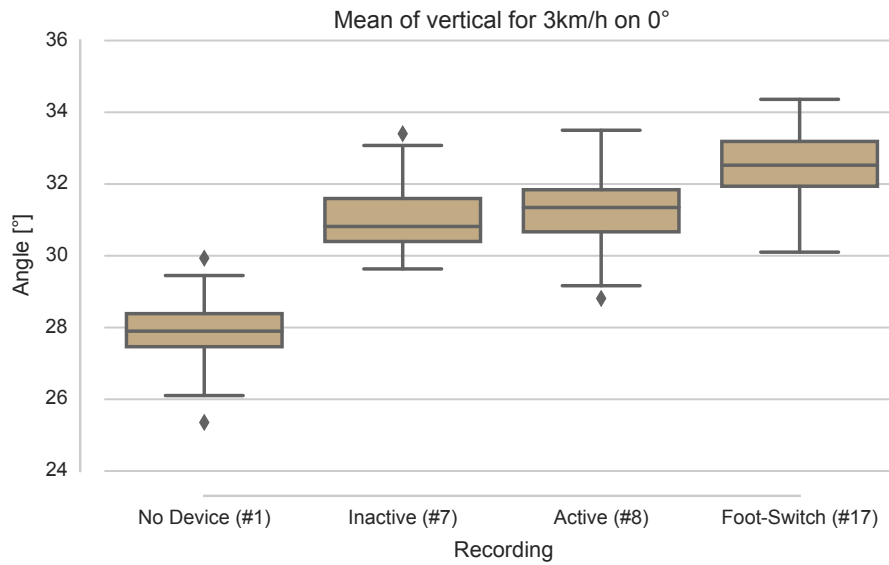


(a) Hip Tilt Mean

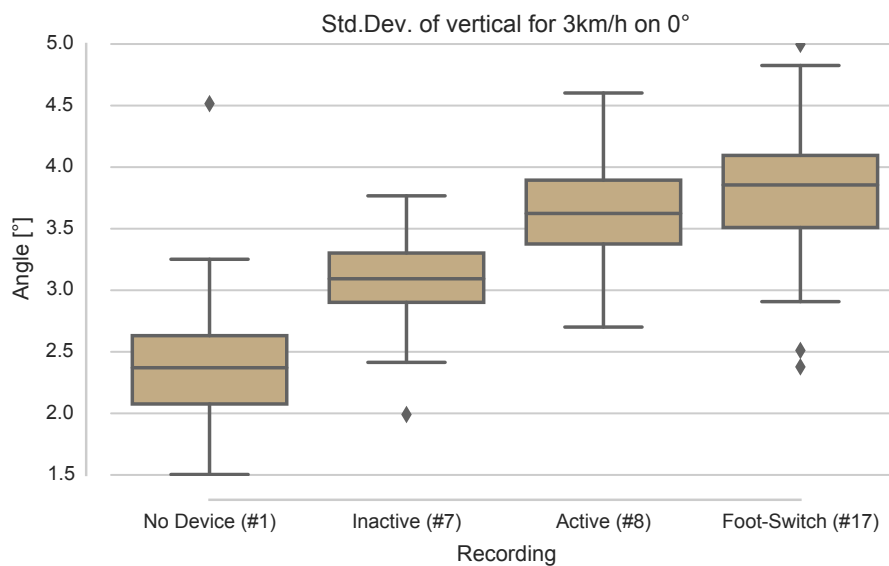


(b) Hip Tilt Std. Dev.

**Figure 10.13.:** Tilting of Hip in the Frontal Plane: Distribution of mean hip tilt angles and distribution of hip tilting ranges per step. Top: the hip height increases with the controlled orthosis, but drops with the inactive orthosis. Bottom: the orthosis with and without controllers lead to an increase in range.

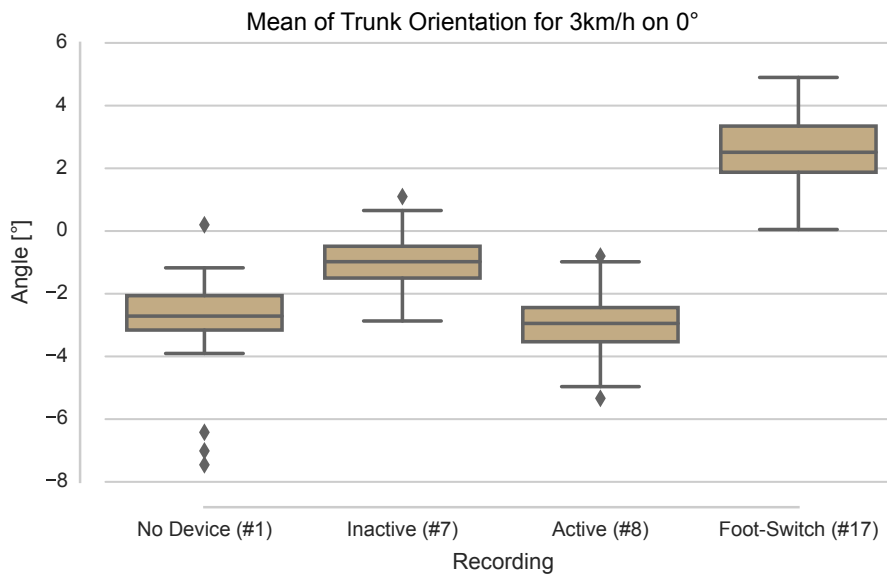


(a) Vertical Body Axis Mean

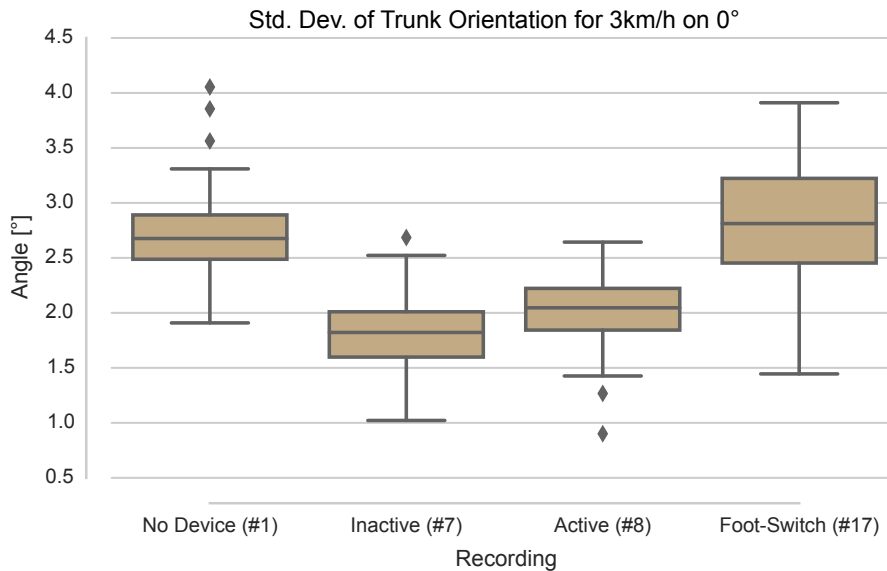


(b) Vertical Body Axis Std. Dev.

**Figure 10.14.:** Leaning of the vertical axis: the orthosis leads to an increase in the angle of the vertical axis. The presented controller shows no further increase of the average lean, but all trials with active orthosis show an further increase in the range of the motion.



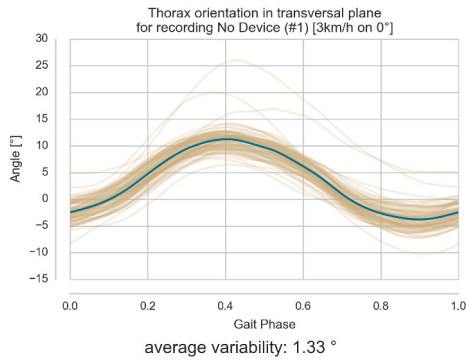
(a) Trunk Mean



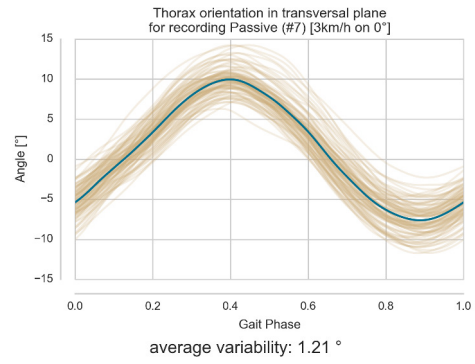
(b) Trunk Std. Dev.

**Figure 10.15.:** Orientation and amplitude of trunk orientation. The mean orientation increases slightly with inactive orthosis and shows a large deviation for the foot-switch controller. The proposed controller shows a similar mean orientation as the trial without orthosis but with higher variation. The standard deviation as a measure for rotational amplitude is increased with inactive orthosis and the presented controller. Here, the foot-switch controller shows a similar level but a huge increase in range.

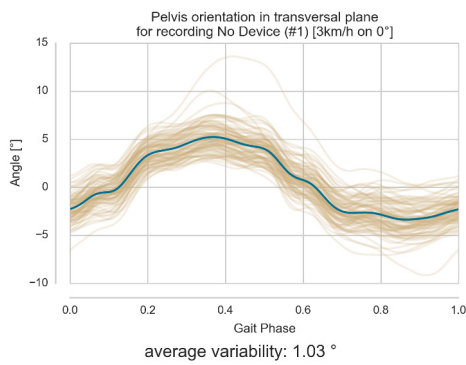
*User-Device-Interaction*



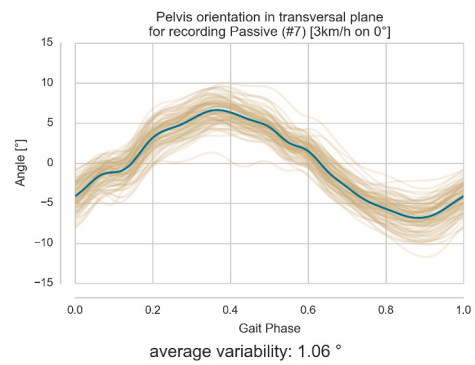
(a) Thorax orientation for free walking condition



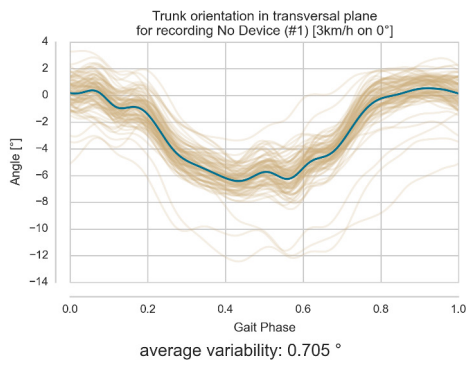
(b) Thorax orientation with inactive orthosis



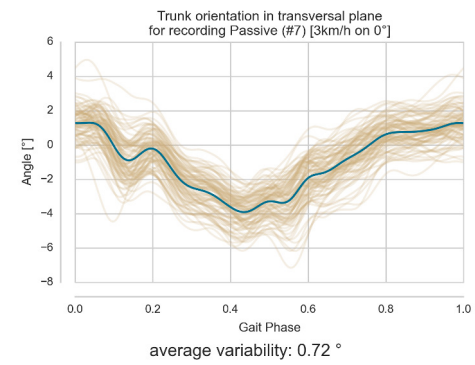
(e) Pelvis orientation for free walking condition



(f) Pelvis orientation with inactive orthosis



(i) Trunk orientation for free walking condition

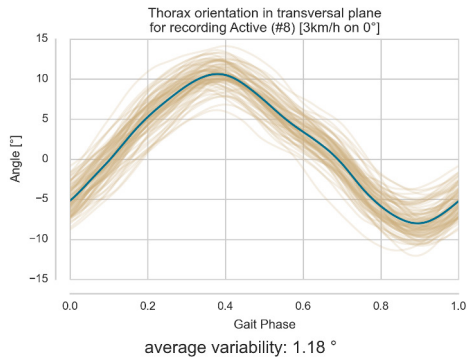


(j) Trunk orientation with inactive orthosis

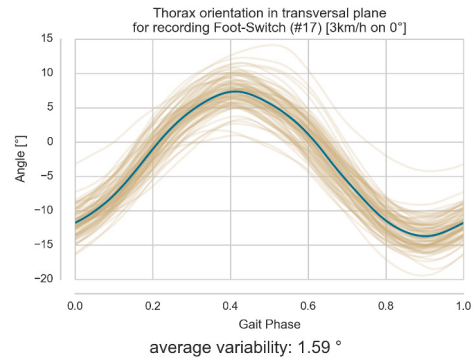
**Figure 10.16.:** Variability in trunk rotation, as derived from thorax and pelvis rotation. The curves show the segmented angle trajectories. (Continues on next page.)



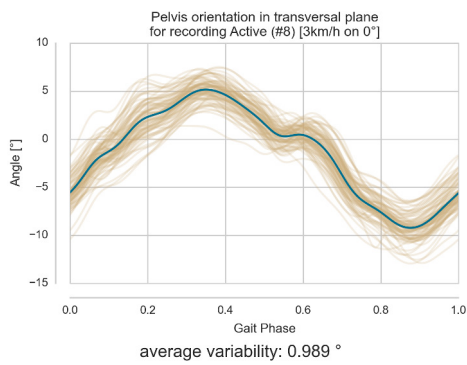
## 10.5. Motion Capture Data



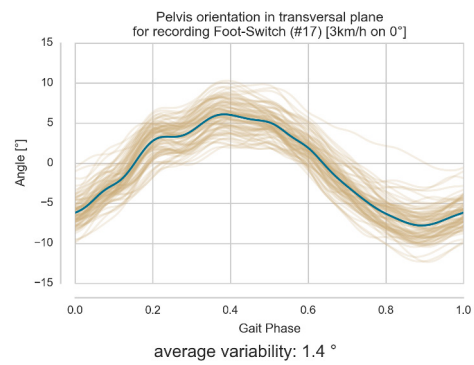
(c) Thorax orientation for the presented controller



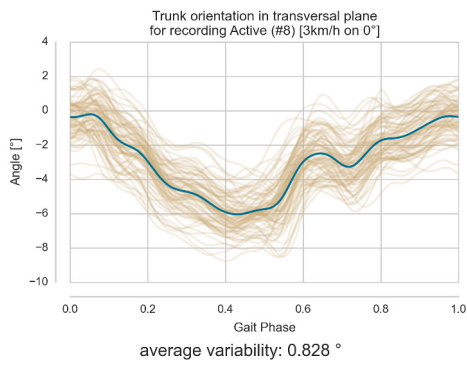
(d) Thorax orientation for the foot-switch-controller



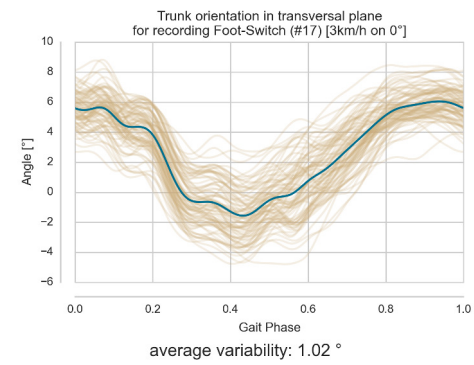
(g) Pelvis orientation for the presented controller



(h) Pelvis orientation for the foot-switch-controller



(k) Trunk orientation for the presented controller



(l) Trunk orientation for the foot-switch-controller

**Figure 10.16.:** (Continuation) The average variability is printed below the curves. The amplitude for thorax orientation is increased for the foot-switching controller.

The mean trunk orientation rises with the donning of the orthosis and makes a huge rise for the foot-switching controller. With the presented controller, the orientation shows a large overlap with the free walking condition. The standard deviation, as a measure for trunk rotation amplitude sinks with the orthosis and increases slightly with the presented orthosis controller. With the foot-switch controller, the standard deviation is on a similar level as without device, but the distribution has broadened massive. The foot-switching controller leads to a large change in trunk orientation and shows highly varying amplitude.

In Figure 10.16, we compare free walking against orthosis and different controllers using the same metric as presented in section 10.3.2 [97].

We find that the pelvis angle is reduced only slightly with the orthosis or the presented controller. In contrast, for the foot-switch controller it leads to a huge increase to the average variability (from  $1.03^\circ$  to  $1.4^\circ$  with the switching controller.)

Larger changes can be found for the thorax angle. From  $1.33^\circ$  for free walking, it decreases to  $1.21^\circ$  with orthosis and  $1.18^\circ$  with the proposed controller. For the switching controller, we again see the opposite effect with an increase to  $1.59^\circ$ . Furthermore, the foot-switch controller also produces a higher amplitude in the thorax orientation.

For the trunk angle, we always see an increase in average variability in comparison to the trial without orthosis. From  $0.705^\circ$  for free walking, over  $0.72^\circ$  with orthosis to  $0.828^\circ$  with the proposed controller. The foot-switch controller again produces a larger increase to  $1.02^\circ$ .

We see a higher slope and a pronounced local minimum in the curves for Pelvis and Trunk orientation for the presented controller around foot-off. For the foot-switch controller, the slope at contralateral foot-off is higher. Both controllers show higher asymmetry in the trunk orientation.

## 10.5.2. Discussion

Here, we discuss the findings from analysis of MoCAP data, before we go on to the results of the EMG data in the next section. We keep the order and start with the joint angle motion.

Due to the volume of data, and the scope of this document (which lies on the controller architecture), we limit the evaluation to trials at 3 km/h with a slope of 0°. The data provided in this chapter demonstrates that already the brace strongly influences the gait only by a fixation of the plane of motion for the knee and ankle joint (e.g., the mean orientation of the vertical body axis Figure 10.14(a)). Mostly, the controllers would increase this deviation (e.g., the standard deviation of the vertical body axis in Figure 10.14(b)), except for the mean of the hip tilting, which was corrected to the opposite side as compared to the free walking condition without orthosis (Figure 10.13(a)). Another exception was the mean of the trunk orientation, which was restored for the presented controller. The median of the per-step standard deviation of the trunk orientation, as a measure for the amplitude of trunk rotation, was restored by the foot-switching controller, but at the same time, the range was highly increased (Figure 10.15).

This means, that the introduction of the orthosis is the dominating disturbance for many metrics when it comes to changes in the orientation. The controllers, which further disturb the walker, introduce a higher variability into these metrics.

**Average Joint Positions** The change of marker positions on the ipsilateral leg after donning the orthosis makes the interpretation of the lower-limb joint ranges quite difficult. Interestingly, the average knee joint position is more extended for the presented controller. In Figure 10.12(a), we see an increase of mean hip angle bending on the contralateral side in trials with the orthosis, while the ipsilateral hip joint seems less influenced in comparison to the trials with inactive orthosis and the presented controller. This could be interpreted as an indication

of a limping motion, where the contralateral leg has a mean orientation in front of the ipsilateral leg.

For the knee angle in the same figure, we can observe a drop of ipsilateral knee use with orthosis and switching controller. For the proposed controller, we see an increase of the original knee motion with orthosis. On the contralateral leg, we see a higher average knee bending with orthosis and the proposed controller, whereas the switching controller leads to a relaxation of the average knee bending towards the condition without orthosis. The additional extension could indicate additional hip height for foot clearance of the ipsilateral leg, but the hip tilting investigations (Figure 10.13) do not support this notion for the case of the inactive orthosis.

### **Hip-Tilt**

The mean hip tilt decreases with inactive orthosis, whereas it increases largely for the trials with controlled orthosis. The foot-switch-controller shows a tendency to a higher tilt. The drop in the uncontrolled orthosis tilt makes it difficult to define the baseline for the controlled orthosis trials.

The hip tilt amplitude, approximated by the standard deviation of the per-step hip tilt increases with the inactive brace, further for the foot-switch controller and most for the presented controller. This effect could be due to safety provisions for the tuned knee damping, which provide long stance support till after the foot off. This effect has been similarly observed in the evaluation of the trunk angle trajectories.

This increase of the per-step amplitude could be indicative of stronger orthosis-user-interaction.

### Vertical Body Axis

The vertical body axes defines the lean of trunk. Generally, the lean increases with the orthosis, but stronger with foot switch controller, e.g., the presented orthosis is neutral in terms of lean when compared to the inactive orthosis. When the amplitude of the per-step fluctuations in the vertical lean are investigated, we see that additional locking at the knee joint due to a controller seems to lead to an increase in upper body motion fluctuations irrespective of the controller type.

### Trunk Orientation

The investigation of the mean trunk orientation yielded a stronger distinction of the foot-switch controller. The latter lead to a strong average rotation of about  $5^\circ$  when compared to the case without brace. In comparison, the inactive orthosis provided only a slight increase, and the presented controller shows the least deviation from the trial without brace. For the amplitudes (standard deviation) of trunk orientation, the brace leads to a reduction of upper-body dynamics, with a tendency towards restoration for the presented controller. While the median of trunk orientation amplitude is similar for the foot-switching controller, the variation in amplitude is much larger (the distance from the 25 % percentile to the 75 % percentile is almost twice as large as for the case without brace).

Both observations indicate a strong influence of the lower limb disturbance on the upper body, which we investigated with the more complex measure of step-to-step variability in the upper-body rotations [97].

Hoorn et al investigated changes in variability of movement between the pelvis and thorax (the trunk orientation) in the transverse plane under the influence of low back pain (LBP) in [97]. They found that for patients with LBP, the variability in thorax and pelvis were unchanged, but a higher coupling between these two body planes reduced the variability in the difference between them, i.e., the trunk orientation showed reduced step-to-step variability.

A possible interpretation is that while their LBP subjects try to avoid probably painful motions and therefore reduce the variability respectively stiffen their motion.

Like Hoorn and colleagues, we observed a huge increase in the pelvis variability for the foot-switch controller, which might indicate a direct disturbance of the pelvis through the blocked knee joint.

For the thorax orientation we see a decrease with inactive controller and orthosis, whereas the foot-switch controller provides a boost to the thorax orientation variability. The huge disturbance in the pelvis seems to propagate directly to the thorax. For the inactive brace or the presented controller, the subject seems to reduce upper body variability.

For the trunk orientation, the effect was in general opposite in comparison to LBP patients: we always see an increase in average variability. From  $0.705^\circ$  without orthosis, over  $0.72^\circ$  with inactive orthosis to  $0.828^\circ$  with the proposed controller. The foot-switch controller again produces a larger increase to  $1.02^\circ$ .

While the hip motions increases in amplitude only slightly with a similar variability, the thorax is greatly extending the amplitude of motion, which could correct disturbances through leg stiffening. Additionally, the mean thorax orientation changes, which could indicate a higher asymmetry in the subject's motion. This can be seen in the trunk orientation trajectories of the controlled brace in Figure 10.16 (i-e).

Given the different background of the studies, the differences in the amplitude of trunk rotations are no surprise. A possible interpretation in relation to [97] is that the disturbance induced by the orthosis/controller-pair leads to a higher variation of trunk rotations because of compensating movements in the upper body, whereas the LBP-patients try to avoid a high variability. For the foot-switch controller, the disturbance es even stronger, possibly to a direct transfer of impact forces to the upper body.

LBP is a typical secondary condition for people with amputation [21]. Although prosthesis and orthosis use are not directly comparable, future research should investigate, if increased variability of trunk rotation could be a cause for LBP.

## Summary

While the evaluation of average joint positions and hip tilt gave no strong indication of controller differences, the presented controller produces less noticeable deviations than the foot-switching controller for the vertical body axis and the thorax and trunk orientation. An exception are effects which might be caused by a prolonged knee damping at the end of the stance phase due to conservative tuning of the presented controller.

The presented evaluation indicates that the upper body provides the strongest deviations in response to disturbance in the lower limbs. The pelvis orientation as well as the hip tilt do not seem to change as much as the thorax and trunk orientation and variability. For this metric, the presented controller produces smaller effects than the foot-switch controller with a reduction of variability by a factor of 4 % (from 1.03 to 0.989). The foot-switch controller increased the variability by 36 %. The comparison of the trial without and with inactive orthosis showed an increase of 3 %.

Concerning measures of orthosis controller tuning quality, the presented study is not conclusive, but it indicates that additional sensors on the upper body might be of advantage to allow the controller to assess the consequences of its tuning. While extensive sensors on the upper body will decrease the patient's acceptance, an approach similar to [37] would be the use of end user devices like smartphones, smartwatches and fitness trackers as non-invasive IMUs. In our framework, this could be easily combined with the graphical user interface to the orthosis controller.

## 10.6. EMG Data

After the presentation and discussion of the MoCAP results, here we investigate the EMG data to find further indication of user-device-interaction.

### 10.6.1. Results

For the analysis of the EMG data, we used the same synchronisation and segmentation techniques for pre-processing as in the analysis of the MoCAP data. Here, we will first present results on the methods for threshold determination from section 10.3.3, before we select a method for further analysis of muscle activity.

#### Thresholds for EMG activity

In Figure 10.17, we plotted three muscles from the same recording (trial #12) in the rows. The columns show the results for four methods to determine the threshold as described in section 10.3.3. The three EMG-channels were selected to represent the available range of activity and variation. Still, for other trials things are looking different and a previously good threshold seems to miss many features. For further examples, please compare to Figures 10.18, 10.19

For the first column of Figure 10.17, we determined for each step the bin (out of 10) with the smallest area. Then, for this bin, we determined the standard deviation in this bin. To get the baseline for all steps, we used the maximum of the standard deviations determined for the individual steps, which results in comparatively huge thresholds. This is working quite fine, in general, but in subplot (e), even for recordings which seem to have small deviations in the bins of small area, this can result in high thresholds. For subplot (i) this misses the small activity around the heel strike (gait phase  $\approx 0.95$ ). However, for individual steps this raise in activity is probably not that refined as for the average.

To reduce the impact of outliers, in the second column we chose the median of the bin with smallest area as threshold in the second column: The resulting



threshold is generally lower, even when using 7 times the median, especially for the contralateral GM recording, where the threshold lies very low.

In column three, we first average all steps, before the binning is done. As this procedure provides smooth results, we used the mean signal level in the bin with the smallest area as threshold. After rescaling the minimum to zero and following averaging, this reflects the standard deviation.

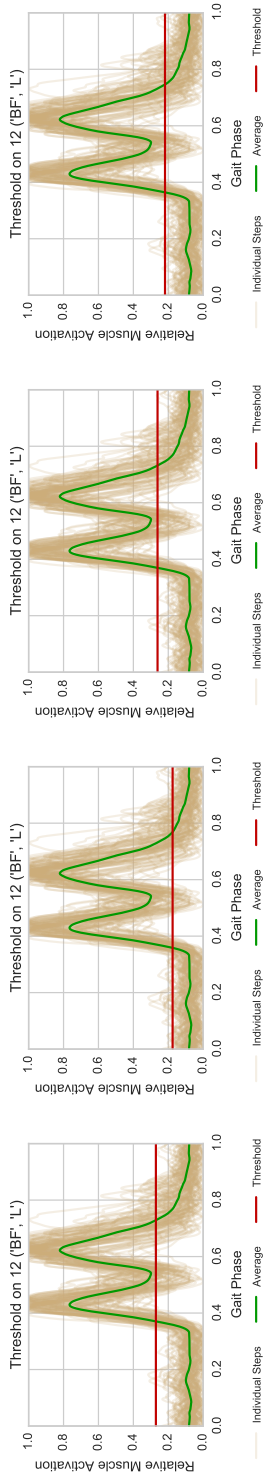
In the fourth and last column the threshold was calculated using the minimum and maximum of the average step. We set the threshold to the global minimum of the average step plus  $\frac{1}{5}^{th}$  of the range between minimum and maximum. This method provides an easy way to define the relative activation above minimum signal level, which we count as muscle activity for further analysis. We will refer to this method as *ranged based method* in the following.

No method resolves the double-peak feature of the contralateral BF-recording. However, most of the presented methods can resolve the more pronounced double peak of the ipsilateral GM-recording. Using a higher threshold would resolve the first double peak, but would eliminate smaller peaks. This problem cannot be overcome with a singular threshold and will be discussed later.

Anyway, each method performs good on some signals but shows problems with other signals. An example for a recording that leads to problems with the range based method can be seen in Figure 10.18. The high standard deviation of the individual signals and the low amplitude of the average signal lead to a better threshold with the first method. In Figure 10.19 an example for a recording for which the range based threshold is working better.

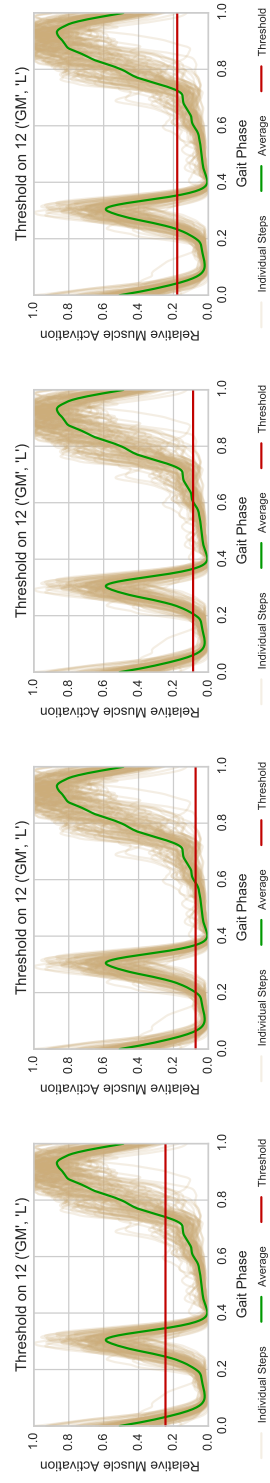
We decided to perform the timing analysis on the average step, leaving the investigation of the step-to-step variation of muscle activity for future studies. Aside from very high noise, which proves difficult for any threshold, the range based method allows to easily determine the relative activation which is counted as an

### RECORDING 12, BICEPS FEMORIS (BF), LEFT SIDE (CONTRALATERAL LEG)



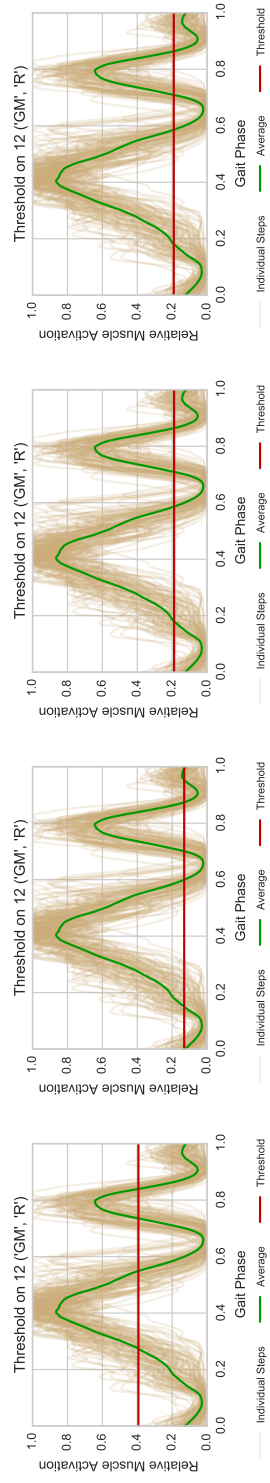
(a) (b) (c) (d)

### RECORDING 12, GASTROCNEMICUS MEDIALIS (GM), LEFT SIDE (CONTRALATERAL LEG)



(e) (f) (g) (h)

### RECORDING 12, GASTROCNEMICUS MEDIALIS (GM), RIGHT SIDE (IPSILATERAL LEG)

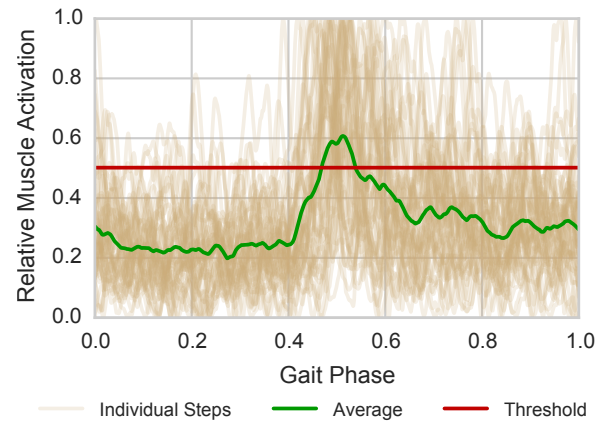


(i)  $3.5 \times$  Std. dev. of bin with min area (j)  $7 \times$  Median of bin with min area (max. (k)  $3.5 \times$  Mean of bin with min area in av- (l)  $1/5$  th between min and max of average (max. for all steps) for all steps) erage step step

**Figure 10.17.:** Determining thresholds for normalised steps, i.e., every step rescaled to the interval  $[0, 1]$

## THRESHOLD METHOD 1 ON BICEPS FEMORIS (BF)

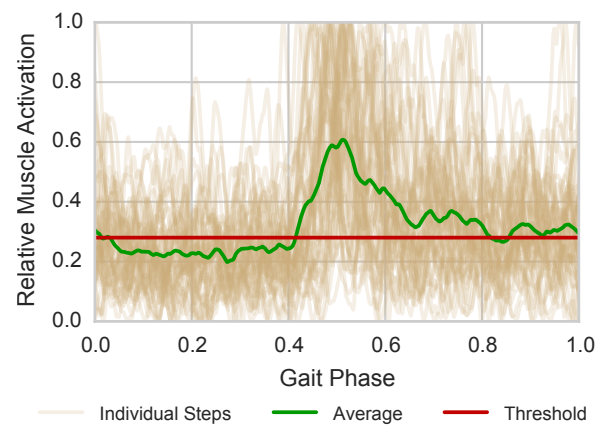
## LEFT SIDE (CONTRALATERAL LEG)



(a)  $3.5 \times$  Std. dev. of bin with min area (max. for all steps)

## RANGE BASED METHOD ON BICEPS FEMORIS (BF),

## LEFT SIDE (CONTRALATERAL LEG)

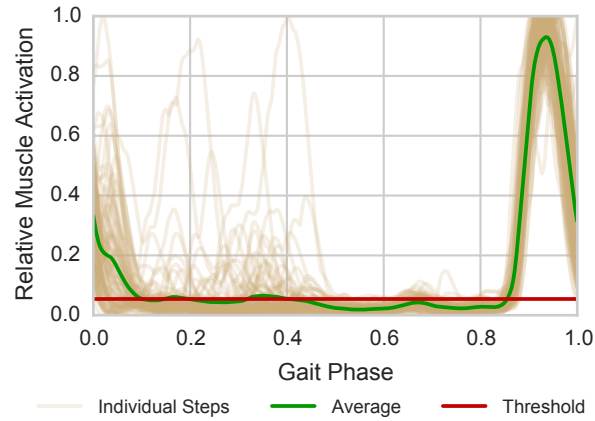


(b)  $1/5$  th between min and max of average step

**Figure 10.18.:** Normalised activity and average step activation for contralateral BF in trial #2: A recording with very much noise for the first and last threshold determination method from Figure 10.17. The standard deviation is high in comparison to the average signal content in (a), whereas the range based threshold in (b) is too low.

THRESHOLD METHOD 1 ON BICEPS FEMORIS (BF)

RIGHT SIDE (IPSI LATERAL LEG)

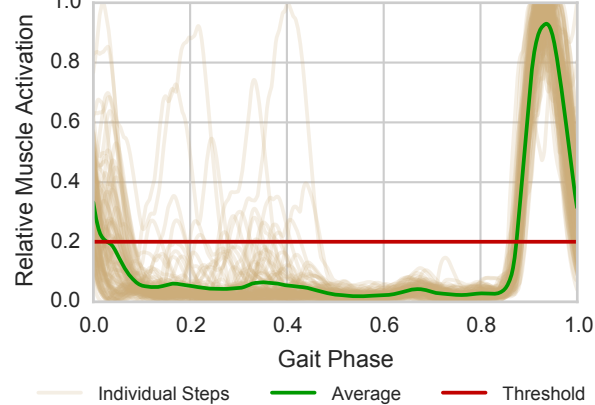


(a)  $3.5 \times$  Std. dev. of bin with min area (max. for all steps)

RANGE BASED METHOD ON BICEPS FEMORIS (BF),

RIGHT SIDE (IPSI LATERAL LEG)

Trial 1, Without Orthosis



(b)  $1/5$  th between min and max of average step

**Figure 10.19.:** Normalised activity and average step activation for ipsilateral BF in trial #1: A recording with few noise for the first and last threshold determination method from Figure 10.17. The standard deviation is low in comparison to the average signal content in (a), whereas the range based threshold in (b) is working well.

period of muscle activity. Thus, the range based method was used for further analyses (Figures 10.22 and 10.27).

### Overview over activity changes

To gain an overview over the changes in EMG activity, we investigate the standard deviation of the non-normalised steps in Figure 10.20. As the standard deviation is used as measure for the amplitude, the differences are evened for normalised steps. Due to saturated recordings, the contralateral SO and ipsilateral GL allow no analysis.

For all other channels, the standard deviation is large and with high overlap. There is a tendency towards higher standard deviations for the presented controller on both sides for GM and GL, i.e., for knee bending and ankle flexion. And for the ipsilateral SO (ankle flexion) and RF (hip flexion). A tendency to lower amplitudes can be seen for the contralateral VM (knee extension), whereas contralateral VL (knee extension) is increased for all trials with orthosis.

When investigating the area below the non-normalised envelopes in Figure 10.21, the results are similar: the standard deviations are large and with high overlap. The foot-switch controller provides a peak for ipsilateral TA (ankle extension). In general there is a huge increase for contralateral VL and ipsilateral BF, and VM on trials with orthosis.

But due to the high overlap, we will not discuss these graphs in detail and go on to the analysis of EMG activity onsets and endings.

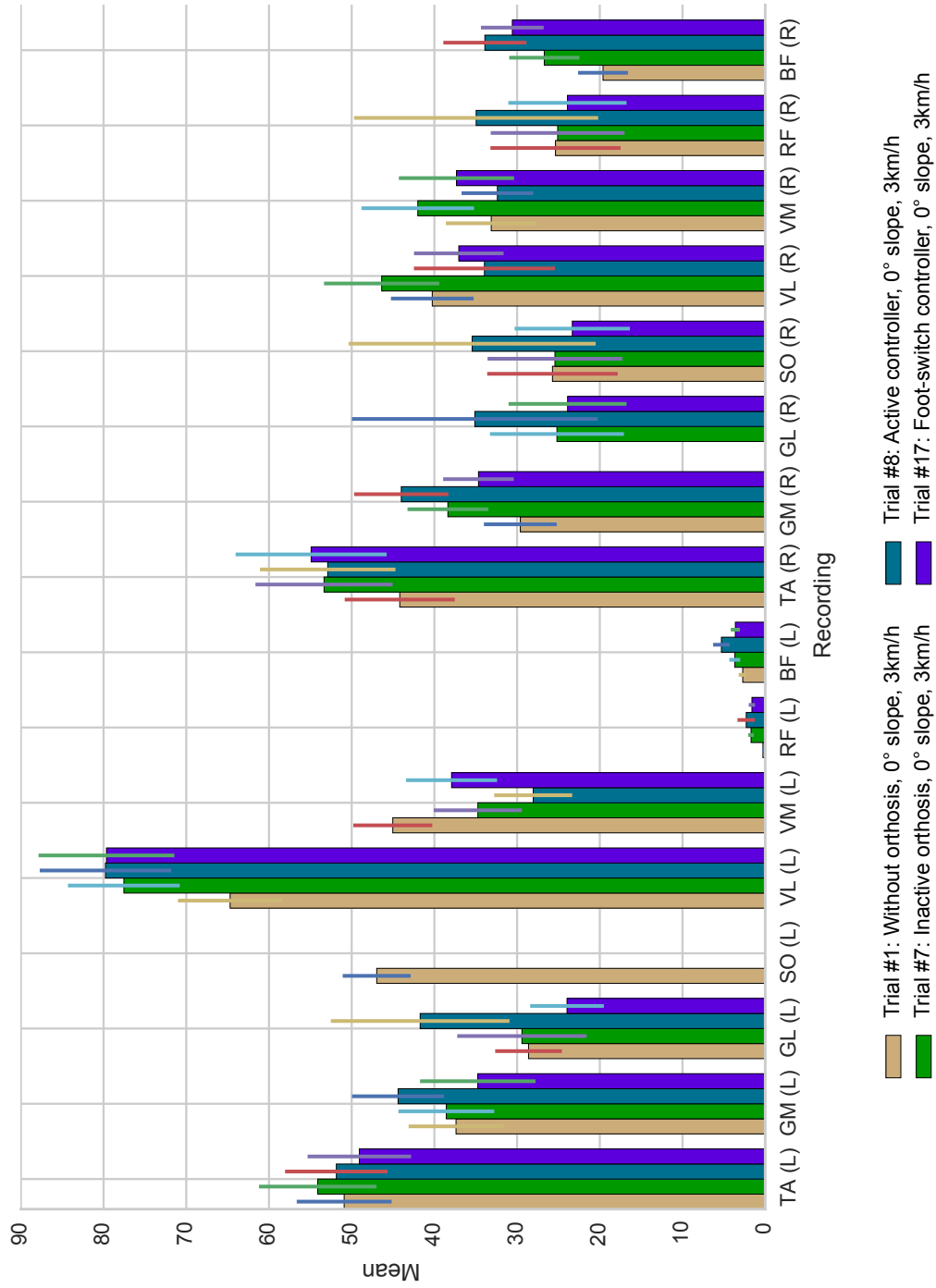


**Figure 10.20.:** Distribution of standard deviations per step for EMG-recordings with 3 km/h on 0° slope. Almost all distributions show a high overlap, indicating no significant differences. Channels are missing for contralateral SO and ipsilateral GL.

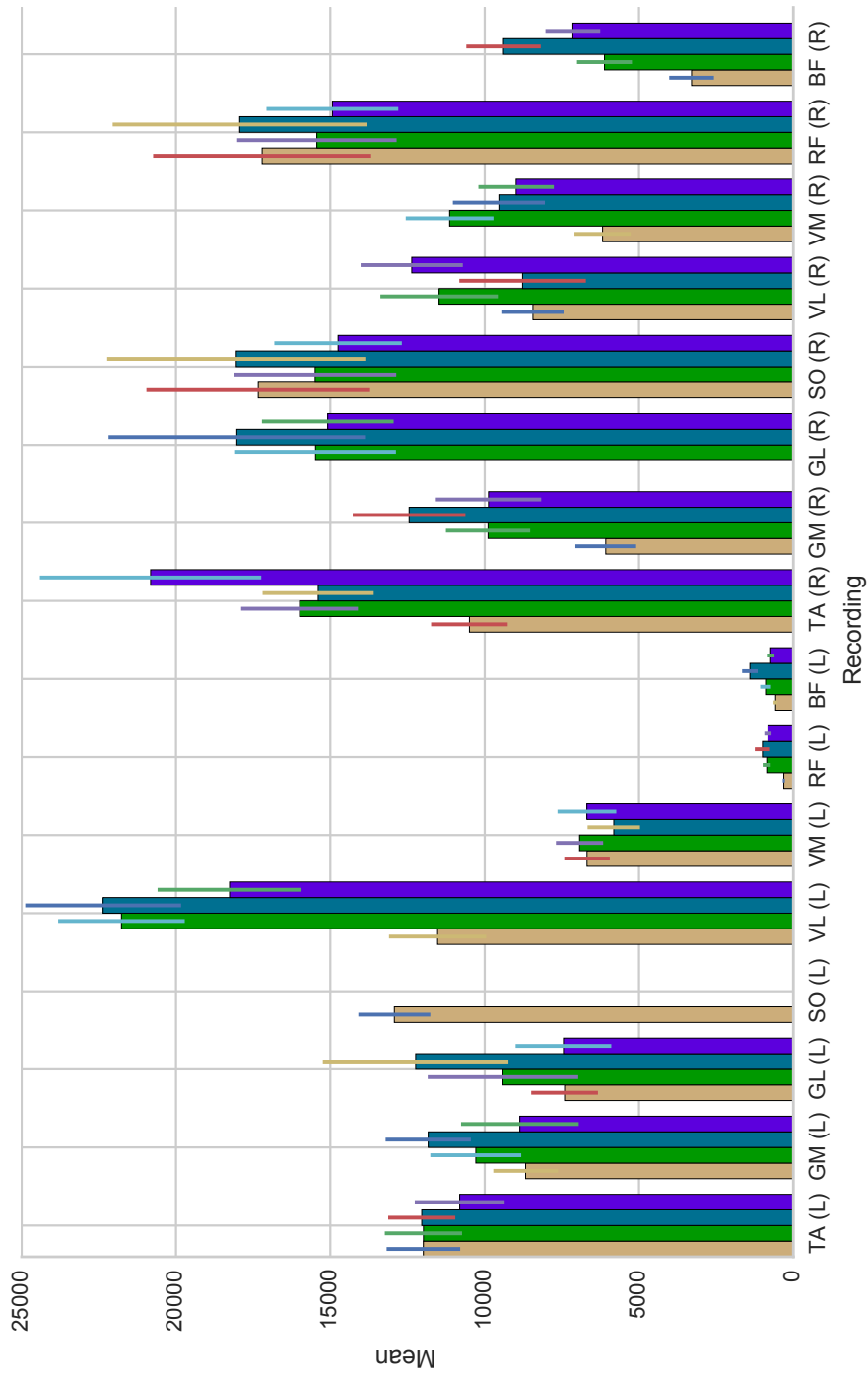


**Figure 10.21.:** Distribution of area below the envelope for EMG-recordings with 3 km/h on 0° slope. Channels are missing for contralateral SO and ipsilateral GL.

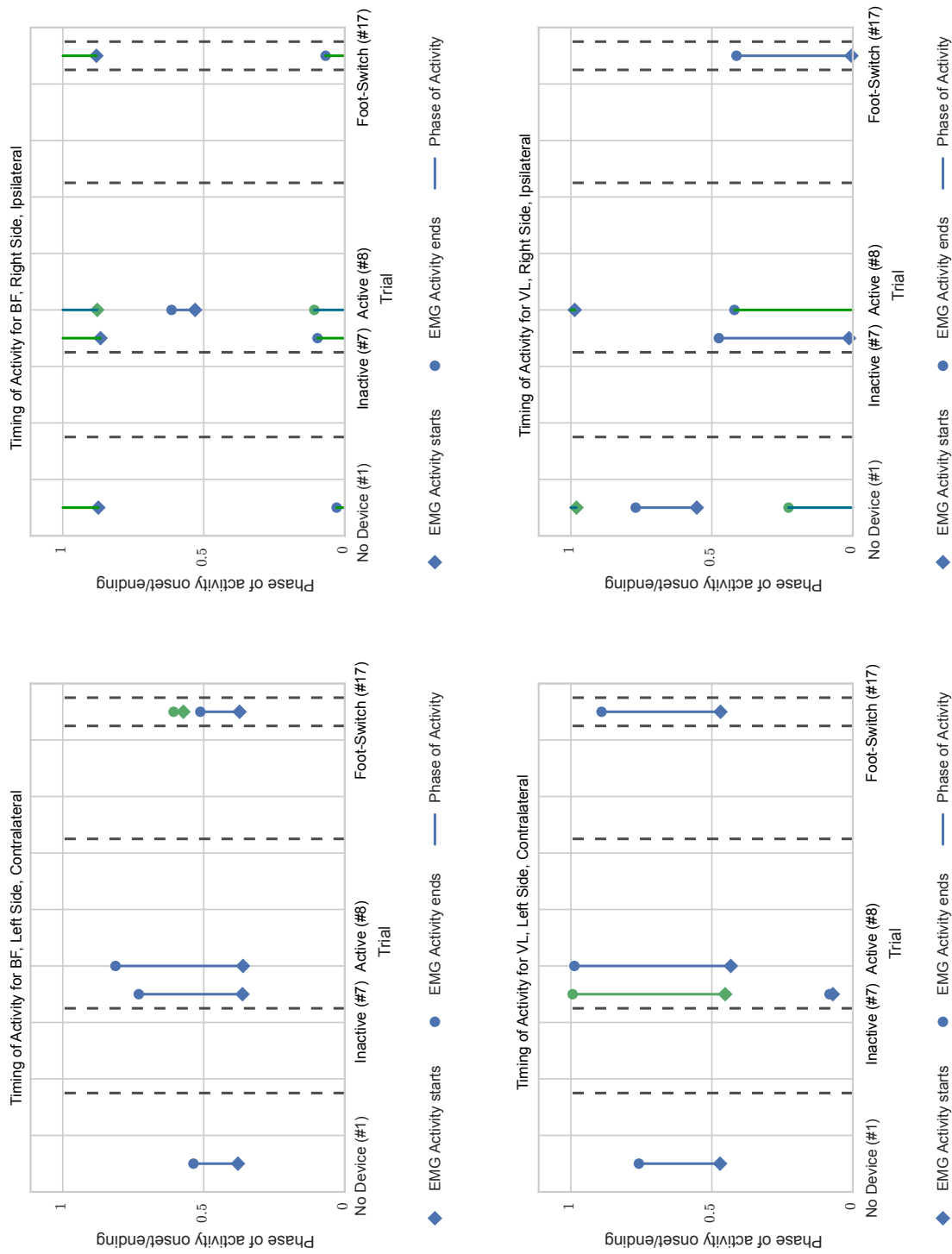


**Figure 10.22.:** Activities of BF and VL show changes for the four investigated trials.



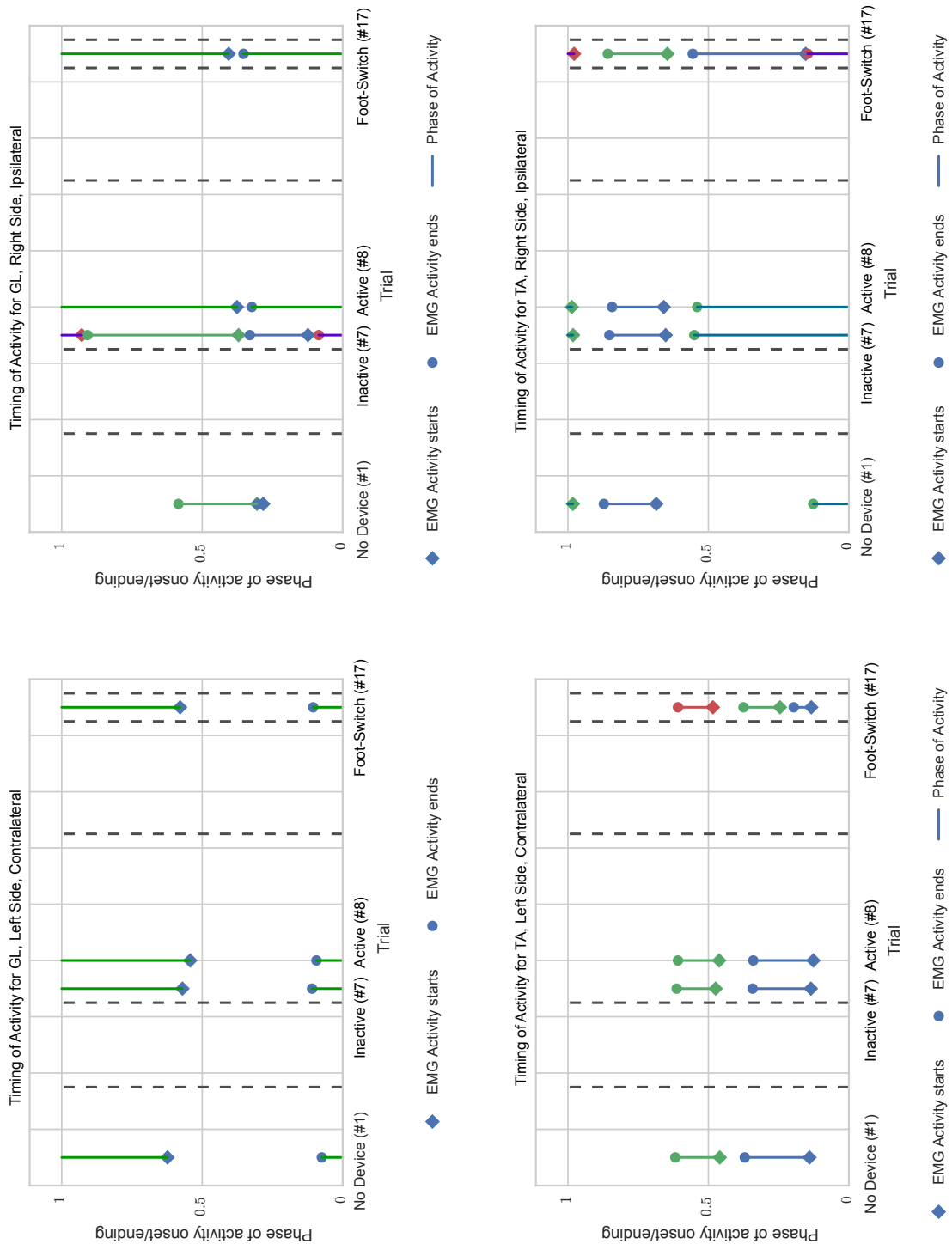


**Figure 10.22.:** Activities of GL and TA show changes for the four investigated trials.

## **EMG Activity Onsets and Endings**

Using the threshold described in section 10.6.1, we determined the onset and ending of EMG activity in Figures 10.22 and 10.27. On the x-axis we show the trial number and on the y-axis the gait phase in  $[0, 1)$ . Continuous activity above the threshold is connect by a line. The diamonds mark activity onset and the circles the ending. (Figure 10.27 collects channels in which controller, slope and speed changes do not alter the activation patterns.)

Figure 10.22 shows channels with variations for trials at 3 km/h on  $0^\circ$  slope, i.e., recordings no 1, 7, 8, 17, corresponding to regular walking, uncontrolled orthosis, the presented controller and the foot-switch controller, respectively.

In Figure 10.22(a), we see a prolonged activity for contralateral BF when used with orthosis with a double event for the foot-switch controller. For the ipsilateral side, in Figure 10.22(b), we see an additional peak for the presented controller around foot-off, which can be seen in more detail in Figure 10.23.

For the VL-channel we see prolonged activity on the contralateral side for all trials with orthosis (Figure 10.22(c)). For the ipsilateral side, we see a prolonged activity after heel-strike and a drop of activity at foot-off (Figure 10.22(d)). The prolonged activity stems from a slowly decaying muscle activity, which provides additional features for the two controlled trials (Figure 10.24).

While the contralateral GL activity stays unchanged (Figure 10.22(a)), the ipsilateral activity is extended over the whole stride, showing high fluctuations leading to average levels between 0.4 and 0.6 (Figures 10.22(b), 10.25). Note, that only five steps were evaluated for ipsilateral GL in Trial 1.

For ipsilateral TA, we see a significant increase of spurious activity in the single support phase, showing as a prolonged activity in stance phase in Figure 10.22(d). This is slightly reduced for the foot-switch controller (Figure 10.24).

DETAILS FOR BICEPS FEMORIS (BF), RIGHT SIDE (IPSI LATERAL)

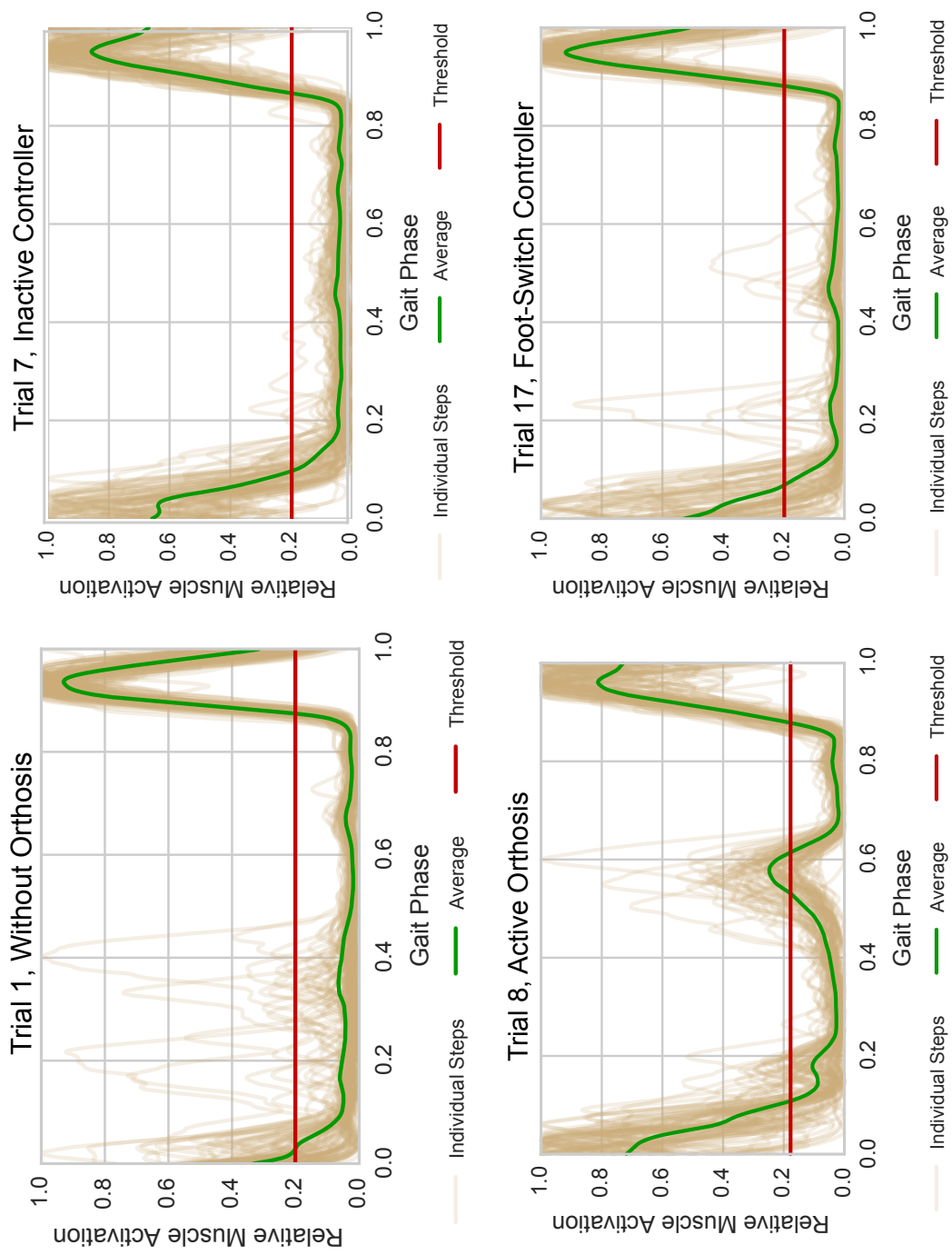
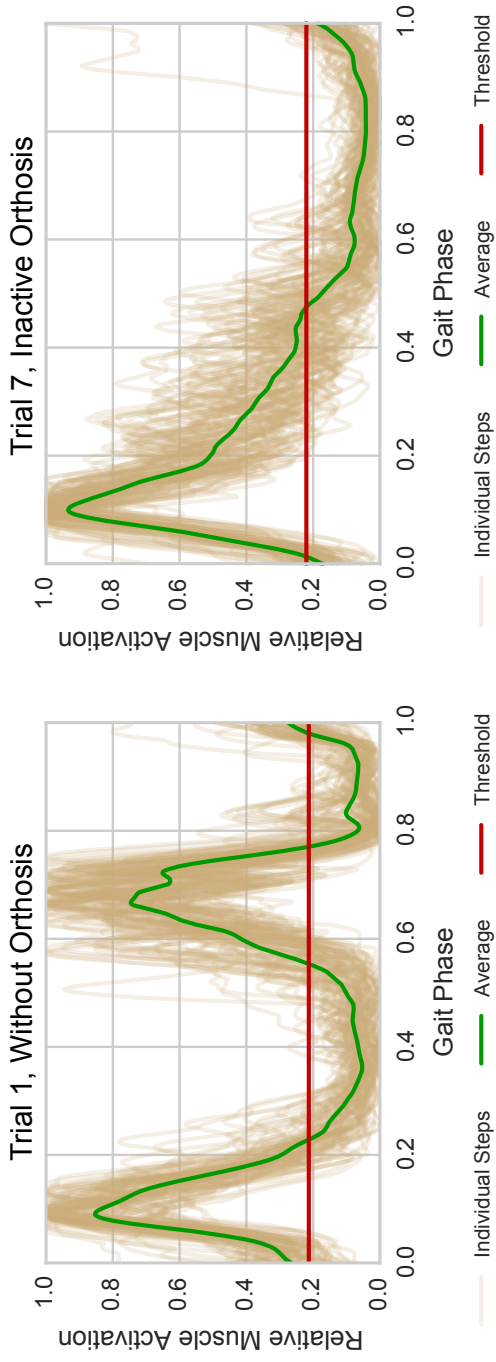


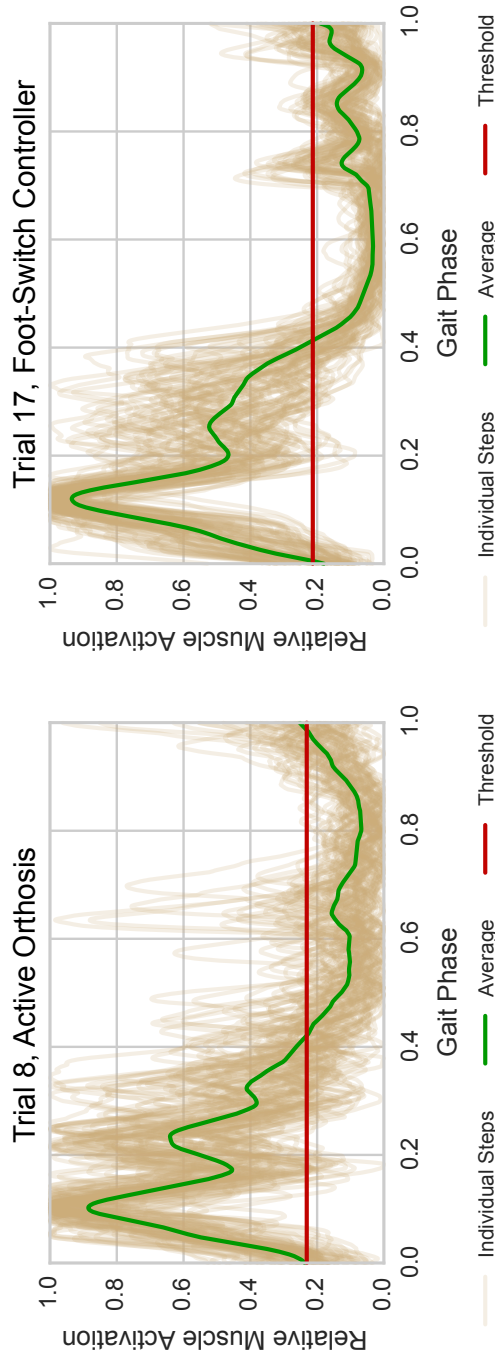
Figure 10.23.: Details for channel BF, R for recordings with 3 km/h on 0° slope and range based threshold.

DETAILS FOR VASTUS LATERALIS (VL), RIGHT SIDE (IPSI LATERAL)



(a) Recording #1

(b) Recording #7

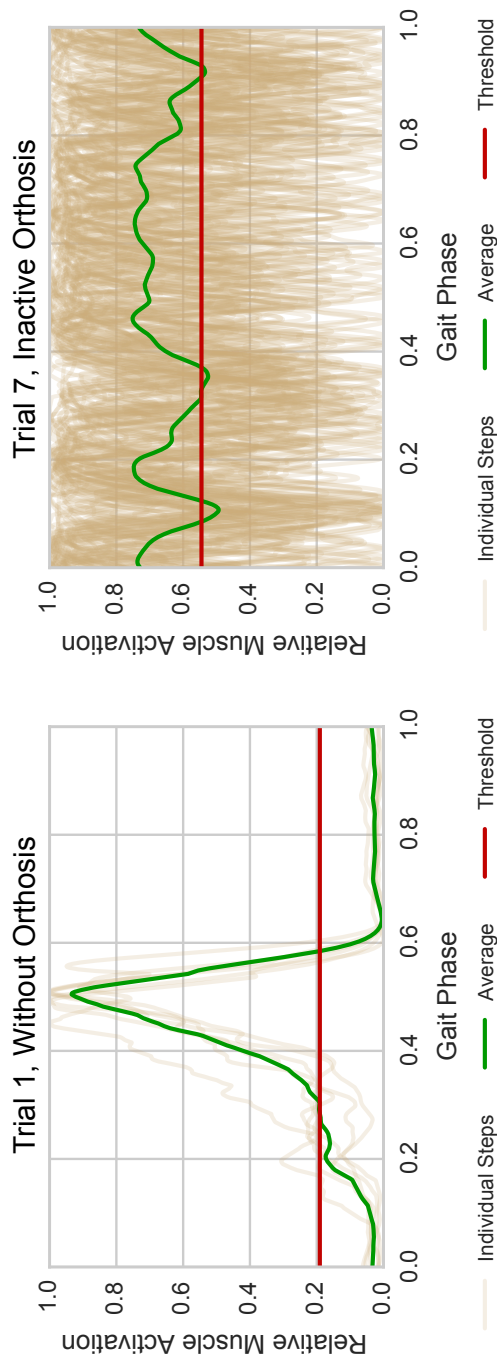


(c) Recording #8

(d) Recording #17

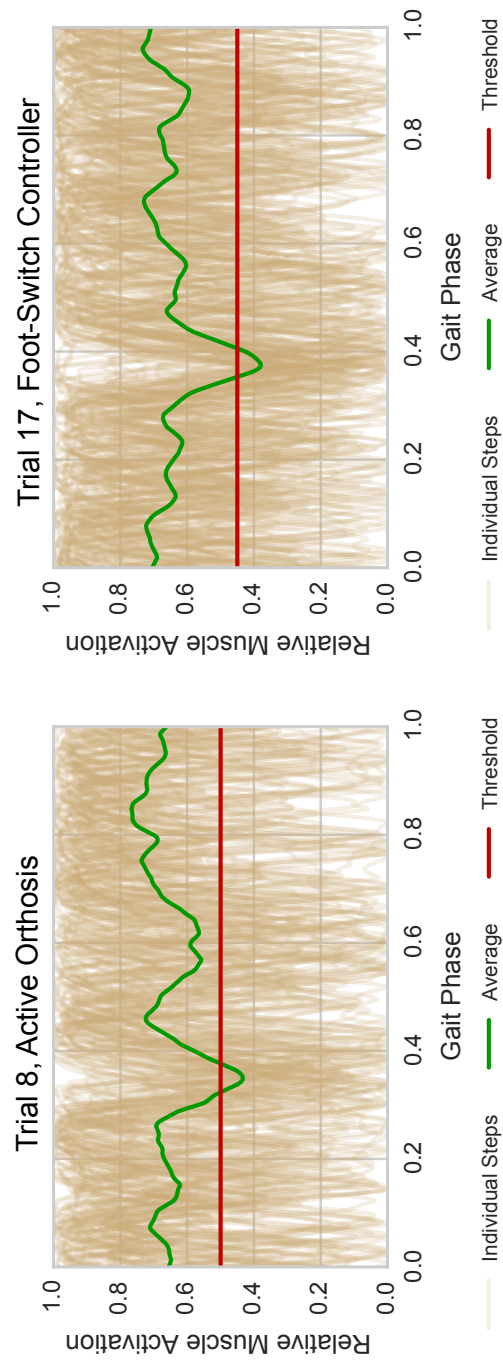
**Figure 10.24.:** Details for channel ipsilateral VL for recordings with 3 km/h on 0° slope and range based threshold.

DETAILS FOR GASTROCNEMICUS LATERALIS (GL), RIGHT SIDE (IPSI LATERAL)



(a) Recording #1

(b) Recording #7



(c) Recording #8

(d) Recording #17

**Figure 10.25.:** Details for channel ipsilateral GL for recordings with 3 km/h on 0° slope and range based threshold. Only five steps remained for trial 1.

DETAILS FOR TIBIALIS ANTERIOR (TA), RIGHT SIDE (IPSI LATERAL)

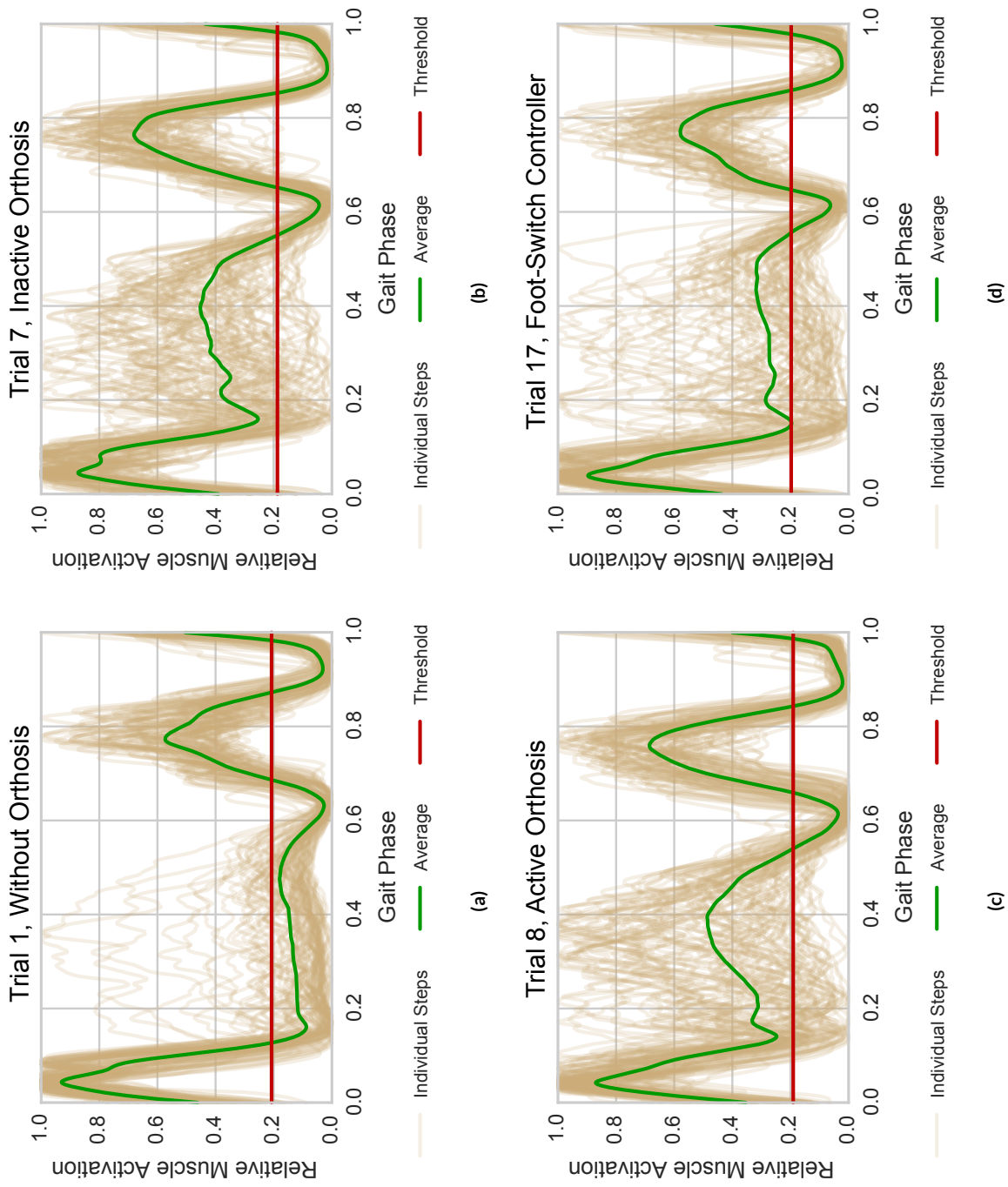


**Figure 10.26.:** Details for channel ipsilateral TA for recordings with 3 km/h on 0° slope and range based threshold.

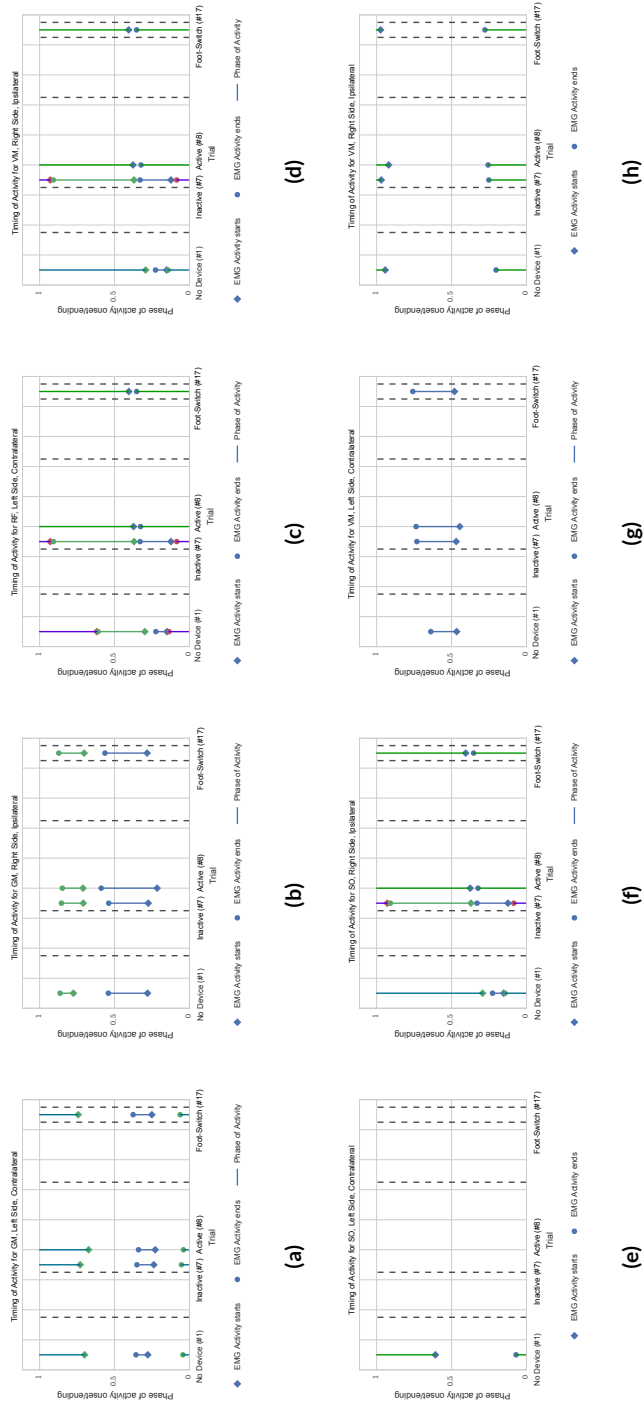


**Figure 10.27.:** Phases of activity for EMG channels which show no huge changes.

## **10.6.2. Summary EMG**

Although they are harder to analyse and interpret than the MoCAP recordings, the EMG data yield supporting results. The step to step variations produce large standard deviations (Figures 10.20 and 10.21) which make an interpretation difficult and hinder the definition of thresholds to determine activity for the different channels. Therefore, we focused on the determination of the onset-times of muscular activity on segmented recordings with normalised amplitudes. We used a simple method to determine a threshold, but for more complex analyses the investigation of rises and drops in the signal should be preferred over a simple threshold, especially as the application of filters invoke low-pass characteristics which will lead to a merging of neighbouring sharp peaks.

A comparison of contralateral SO (ankle flexion) and ipsilateral GL (knee flexion and ankle flexion) was impossible due to frequent saturation in the recordings. Especially the SO channel might have been interesting, as the ankle flexion might play a role due to higher load and limited foot clearance due to the brace on the ipsilateral side.

When investigating the onset and ending of muscle activity, we found few remarkable changes. For BF on both sides (hip extension and knee flexion) and ipsilateral VL (knee extension) around the end of the stance phase. Ipsilateral TA (ankle extension) shows an extended period of activity during singles support phase, which is also present for some steps without orthosis, but for far fewer steps. Ipsilateral GL (knee flexion and ankle flexion) shows almost constant average activity, due a generally high signal level and high step to step variation.

The most interesting feature is an additional peak for the ipsilateral BF for the presented controller, which might very well be connected to the already mentioned prolonged knee-support at foot-off, which was actively tuned by the subject.

The prolonged contralateral VL activity in all trials with orthosis might be an



indication of additional knee-extension. Due to the marker changes after donning the brace, we cannot relate this to the MoCAP data, but given the changes in trunk orientation, it might be indicative for a favoured contralateral leg.

Although these results do not show clear changes like in the upper body motion found in MoCAP data, they indicate that the EMG-activity can be used to identify when the user is working against the orthosis, like for the additional ipsilateral BF peak. A more detailed timing analysis on single step basis and the evaluation of the step to step variability in the EMG signals might reveal additional control impulses to compensate disturbances through the controller.

## 10.7. Conclusions

In this chapter we investigated how the orthosis and the controller will interact with one healthy walker's gait. We were testing a simple foot-switch controller, which provides a hard onset and end of the knee-damping, to compare the amount of change induced by such a simple control mechanism as compared to the controller developed in this. Further experiments without and with an undamped orthosis enable a two-way comparison against the baseline of the inactive orthosis on one side, and against a quite uncomfortable controller on the other side, to see if the subjective measure of comfort translates into the investigated measures. To this end, we were testing trajectories of joints and markers with MoCAP recordings and muscle activation with EMG recordings.

After discussion of the respective findings in section 10.5.2 and 10.6.2, we find that changes in MoCAP and EMG data are most strongly influenced by the presence of the brace than by the selected controller. Still, the presented controller provokes fewer disturbances in the upper body dynamics than the foot-switch controller, except for artefacts at the initiation of swing-phase. These artefacts can be explained by conservative tuning of the controller which provided prolonged knee damping. Similar artefacts can be seen in the ipsilateral BF-channel.

### *User-Device-Interaction*

BF activity results in hip extension and knee flexion, therefore supporting that the user is working against the prolonged knee damping.

These findings have an impact on the design of self-learning orthoses: to investigate the disturbance of the user's gait, the upper body dynamics should be observed.

Furthermore, EMG analysis might be able provide times of extra activity, which relate to the resistance of the device against its user's motions. This extra muscle activity could be used for controller optimisation. Nonetheless, these effects might be less prominent for patients, which get an orthosis prescription due to reduced muscle forces. Patient tests have to show if the findings of this investigation can be carried over to real world use.

Thus, the analysis presented in this chapter provides features that could possibly be used for optimisation of orthosis control, but still have to be tested for suitability on each individual patient.

## **Part V.**

# **Conclusions & Outlook**



*We can forgive a man for making a useful thing as long as he does not admire it. The only excuse for making a useless thing is that one admires it intensely.*

Oscar Wilde

# 11

## Conclusions

The thesis at hand presents the implementation of a control architecture for orthoses which is able to provide individual tuning and fitting of individual patient support independent of the brace or patient in question. We planned towards a flexible controller, whose design does not limit the gaits and environments it suits and allows to be adjusted by non-experts. The architecture is modular to support easy extension with further gaits or the exchange of components and the methods have been chosen to allow adaptation at run-time.

The thesis presents a modular, adaptive controller architecture. Consistently, every component has been designed to provide a good solution to the individual problem, implemented with methods which provide means for adaptation. As a whole, we contribute a complete framework which sets the groundwork to explore self-adapting controllers for orthoses, which is a difficult task as patients rely on the assistive device to support them in every day tasks. The methods have been designed for semi-active (or quasi-passive) devices, but the central components, like the timing unit and gait recognition are of use for active devices and exoskeletons, too. The individual presented methods have been discussed in their appropriate chapters (see sections 6.5, 8.5, 9.6, and 10.7). Therefore, we

## Conclusions

only briefly present the findings and limitations and discuss how they are placed in the bigger picture, before we go on to the outlook in the next chapter.

# 11.1. Summary of Contributions and Limitations

## 11.1.1. Feed-Forward Controller

In chapters 5 to 8, we developed the modular feed-forward controller. It consists of the *timing unit*, which abstracts individual gait to a linear, cyclic description of step progress, the gait phase  $\varphi$ . A simple multi-layer perceptron provides the means to learn individual gait from gait samples. This network tracks the gait and thus overcomes the necessity to bind the controller's function to the accomplishment of specific thresholds. It is complemented by the shaping unit, which defines the control output as a function of the gait phase  $\varphi$ .

### Timing Unit

The affinity of the gait-tracking to the user through learning based on gait samples removes controller requirements onto the patient's remaining abilities which are present in other approaches whose controller depends on the patient to reach specific thresholds in joint range or ground reaction force. As long as the patient is able to provide cyclic motion which the timing unit can track with appropriate sensors, our approach can be applied. Thus, the generality and the abstraction of individual gait enlarge the possible targeted patient group. The continuous tracking of the user's dynamics together with the time-independent feed-forward properties provide inherent safety through instantaneous representation of the current gait status and the immediate application of the control output. The presented approach is equivalent to a generalised FSM based controller which provides a fixed control-output sequence (in time) which can easily be tuned or be created with musculoskeletal models or for example by a timed replay of muscle activity [80].

### 11.1. Summary of Contributions and Limitations

Through use of joint variables, only, which are not dependent on the terrain, e.g., slope, or patient-brace-interactions, this approach overcomes problems of techniques that have to estimate these aspects in the surroundings, for example to correct the estimated ground reaction force. The use of the angular component  $\varphi$  makes the timing units output independent of the output's absolute values, only using the phase between the outputs. This provides independence to changed scaling in the input.

Furthermore, the use of positional sensors as inputs makes the presented approach independent of the hardware and allows it to run without any explicit dynamic model of the brace. The differences in the control output can be hidden in the shaping unit. The controller was used already on prototypes with compliant and free ankle joint without any modifications.

#### Shaping Unit

The *shaping unit* is used to apply arbitrary functions of the gait phase  $\varphi$  which define the desired knee joint damping. It is implemented as a RBF-Network, whose training data is provided by a *graphical user interface*. This user interface lets the user or orthopaedic staff define the device's control output. It places the user in a feedback loop with the controller. This enables the tuning of the provided support to level required. And at the same time, the feedback includes the patient's opinion directly into the process of orthosis fitting, which was described as an one of the top reasons for device abandonment in [76].

#### Limitations

We were able to show that the approach provides smooth and linear tracking of gait progress. But the approach of learning on gait samples specialises the timing unit to the presented gait. Thus, the specialisation leads to optimal coverage of the learned gait, but leads to erratic tracking, for example piece-wise constant,

## *Conclusions*

or not covering the whole range of the cyclic gait phase  $\varphi$ , when confronted with an unknown gait.

### **11.1.2. Multi-Gait Support**

Therefore, in chapter 9, we extended the presented approach with the ability to recognise the current gait and switch between a set of feed-forward controllers.

#### **Gait Switching**

The gait switching is based on internal models, which predict the next sensory input based on the recent history. The decision is made on the prediction error, which decreases for the correct gait and increases for all other gaits. The history length therefore defines the switching frequency, the allowed error margins define the switching delay, which can be considered shorter than the history length. As a safety measure, the switching mechanism is conservative, providing the opportunity to not match the gait. A fall-back controller of arbitrary complexity can be used to ensure safe operations.

The gait recognition and switching extends the smooth tracking the single-gait feed-forward controller provides to a set of defined gaits. In contrast to many approaches in the literature, the procedure to extend the number of known gaits is always the same: Based on a set of gait samples, the controller is extended with a module for this gait consisting of the timing unit, shaping unit and the predicting model of gait-dynamics. This procedure works, as long as the dynamics of the sensory input for all supported gaits are sufficiently different. The addition of suitable sensors is possible to improve the discrimination between gaits. This procedure does not limit number of supported motions, enabling further enhancement of the patient's mobility to fit their everyday needs. Furthermore, the gait recognition module forms an important component for learning and adaptation applications, as it allows the controller to associate sensory input with specific movements.



## **Gait Switching Performance**

Benchmarking of the gait switching showed a good recognition of the underlying gaits with average success rate for all gaits above 94 %. But the benchmark used has difficulties with ambiguities in transition steps. They show the necessity to control gait on time-scales much shorter than the step: due to the nature of walking, the transitions can happen at almost any time. While a specific gait which provides statistical variability which is captured by the predicting models, gait transitions have an often singular nature. The transition depends on many factors, like distance to and speed of an obstacle, walking speed, evenness of the ground and others, which are not available from the brace. In consequence, on inspection a gait's dynamics in the history of the sensory reading, we will find transitions where the dynamics in the history overlap and others will lie outside of any gaits dynamics, directly going from one gait to another as shown in Figure 9.9 on page 176. The number of gaits as well as the number of sensors and the length of the history space define the amount of overlap between different gaits. More volumes of overlap provide more possibilities of gait transition without use of the fall-back controller. As the gait dynamics is similar for the stance phase, the transitions without overlap will happen in swing phase, before the heel-strike. Manual inspection showed that the false-positives were associated with transition steps in the swing phase which showed a mismatch in joint angle range and dynamics with the gait the subject used. The presented approach has the benefit, that if the allowed error margins are well-chosen, the selected gait will match the dynamic of the sensory input, even if it does not match the name of the gait.

## **Benchmarking of Switching Performance**

Concerning the quality of the benchmark, these ambiguities in joint angle ranges and sensor dynamics at the transition make it difficult to define a measure for performance comparison. A probable solution for this problem would be a way to assess the amount of work the user is performing against the controller, to show

## *Conclusions*

that the chosen gait reduces the confinement. This would need additional instrumentation of the brace and will be discussed in the outlook. Still, with the general inability to regain normal gait with a passive device (see section 4.3.2), the definition of a useful benchmark criterion is difficult and is probably best done for a healthy walker or an additionally supported patient against the uncontrolled brace, as described in chapter 10, evaluating the work the patient is performing against the controller.

## **Comparability to Other Approaches**

For similar reasons, the comparison to the literature has proven unsatisfactory as explained in section 9.6.2. The presented controllers provide support for selected gaits, which either are very similar, like the transitions between slopes, or are very different, like standing and walking, or stair climbing and descending. They probably provide less ambiguities in different gaits, as for example the swing end for flat walking and descending stair motions. By construction, most controllers presented in sections 9.6.2 and 5.2 support a fixed number of gaits and miss the flexibility and extensibility of the presented controller. In consequence, the fixed set of supported gaits of these controllers differs too much from the gaits chosen in chapter 9 to provide the grounds for a significant comparison of the methods. Other controller developments, for example the recognition of standing or slopes, are implicitly handled by the timing unit, which transparently handles slight shifts or stopped motion.

### **11.1.3. Interaction Between the User and the Device**

We concluded the design of the controller architecture with an investigation of the interaction between the orthosis-controller-pair on one side with a healthy walker on the other in chapter 10. For this aim, we compared treadmill walking at 3 km/h on 0° slope without orthosis and with orthosis in free and controlled

### *11.1. Summary of Contributions and Limitations*

conditions. As controllers, we chose the presented controller and a simple foot-pressure activated controller.

In these experiments, the device-controller combinations served as disturbances to the healthy walker's gait. We were employing MoCAP and EMG to determine the impact of this disturbance.

#### **Motion Capture**

For the motion capture data, this experiment revealed no significant changes of joint motion for the healthy walker, but it revealed clear changes in upper body orientation, i.e., rotation and leaning against the vertical axes. These results show that changes induced by the device and controller, cannot be easily observed on the level of the leg, but produce the biggest deviations at the upper body. The presented controller showed a tendency to fewer changes in the upper body than the simple foot-pressure based controller.

#### **Consequences for Online Adaptation**

This has consequences for online-adaptation and surveillance approaches, as the sensory equipment is restricted to the brace. We need to use additional, non-invasive IMUs, for example in smartphones, smartwatches, or fitness trackers, to get access to the upper body dynamics without comfort loss (like difficulties at donning the device with additional sensors).

#### **Electromyographic Recordings**

Results for EMG were not that substantial. We found additional activity for ipsilateral BF around the end of the stance phase for the presented controller compared to all other conditions. This indicates additional work for hip extension or knee flexion, but this might be due to explicit tuning to hold the knee

## Conclusions

support according to orthopaedic advice from our cooperation partner. For ipsilateral VL, activity around foot-off was gone for all orthosis trials. This loss of knee extension activity demonstrates the brace's ability to support patients for knee-extension as well as the subjects habituation to the orthosis. For ipsilateral activity on TA and GL, all orthosis modes showed a massive increase in activity, for the latter an almost constant activation was shown.

### Impact on the User's Gait

The experiments with a healthy walker show, that the subject's impairment due to the brace are stronger than the improvements by the controller. This is in accordance to the discussion in section 4.3, where we argued that a passive orthosis which dissipates energy and any corresponding controller can 1. not restore the gait that of a healthy walker without orthosis and 2. the dissipation of energy leads to inefficiencies. Thus, patient experiments have to be conducted to reveal the advantages of the presented controller.

## 11.2. Contributions in the Broader Context

The controller architecture addresses important problems of orthotic devices for the lower limbs. It allows to *individualise* the controller-behaviour to the patient's remaining abilities, optimising control to the typical movements of the subject. It allows the easy *extension* with additional movements, enabling more flexibility and mobility. During device-fitting, user-feedback is incorporated in the final setup of the controller. We believe, that these advances will help improve the acceptance of assistive devices by the patient and enhance their *independence*.

At the same time, the abstractions used in the feed-forward controller and the choice of sensors provides an architecture that is hardware independent.

### *11.2. Contributions in the Broader Context*

For the future, this framework enables the study of self-learning assistive devices, which can provide a new level of support. This would allow to develop a controller that the patients can setup alone. The device then learns to support the patient optimally on its own. Such a device should be able to incorporate changes in the patient's gait due to 1. improvements in the patient's gait caused by the device, or 2. general changes in the patient's conditions. The presented controller architecture provides the groundwork with a modular and adaptive design. Future work needs to developed learning tasks, which employ the flexibility inherent to the presented approach. This was out of the scope of this thesis.

An important contribution for the development of such learning tasks is, that we gained a better expectation of the dynamic variables that can provide a feedback about the controller's impact on the patient. For a healthy walker, we found 1. the trunk to show the clearest deviations in response to the disturbance by the orthosis, and 2. that additional, localised EMG activity hints at extra work the user has to perform against the orthosis. Both findings allow a goal-oriented adaptation of the controller.

These findings have to be confirmed and extended in patient experiments to derive measures which can serve to drive adaptation and at the same time monitor the patient's condition, to be able to provide professional assistance when/if needed.



*The Road goes ever on and on  
Down from the door where it began.  
Now far ahead the Road has gone,  
And I must follow, if I can,  
Pursuing it with weary feet,  
Until it joins some larger way,  
Where many paths and errands meet.  
And whither then? I cannot say.*

J.R.R. Tolkien, *The Fellowship of the Ring*

# 12

## Outlook

The controller architecture developed in this thesis was designed with the idea of online adaptation of its own behaviour. Important components are implemented with artificial neural networks, which provide easy access to adaptation algorithms. The brief study of user-device-interaction in the gait-lab demonstrated how the device alters the gait of a healthy walker.

Here, we will discuss possible future work concerning the controller architecture. Aspects specific to certain components have already been discussed in the specific chapters (see sections 8.5.6 and 9.6.4) if they had a direct impact.

Based on this groundwork, there are several aspects for further research. We want to focus on two:

1. the adaptation of the device on to a self-learning device and
2. the thorough study of the interaction between the user and the orthosis.

These two topics are strongly connected, as both aspects cover changes in gait over time. Here, we will focus on controller development for the first part, and the patient's perspective in the second. We discuss the inherently connected

questions of how to derive the need for adaption and which actions must be taken.

## **12.1. Adaptation**

Section 5.1 showed adaptive facets, ranging from changes in the patient's behaviour or new gaits to the tuning of the applied damping, especially changes which to the sensory input and changes applied to the control output.

Furthermore, we have to distinguish between different kinds of learning: unsupervised and supervised. Unsupervised learning with trial-and-error phases is not suitable for the application on orthoses if patients are involved. Falling patients are not an option! In consequence, someone, either the patient or an orthopaedist, has to supervise changes. Or the controller must know how to guide the adaptation.

### **12.1.1. Adaptation to Changes in Gait**

As described in chapters 8 and 9: The decision unit derives a measure of unfitness which describes the probability that specific sensory input does not belong to a specific gait. The prediction error could be used to save gait samples into a training database for the timing unit and the predicting model associated with a specific gait. In this way, the controller can adapt to slight changes in gaits, by replacing outdated gait samples with newer ones.

When selecting samples for relearning, the allowed range of errors has to be small enough to only cover a specific gait, but large enough to allow a gradual change of gait. For example when users adapt their gait to the device. Only steps without gait transition should be selected. Studies like [35, 36] suggest timescales of months for the process of the user adapting to the device, which is important when considering the interaction of different adaption mechanisms.

Further details can be found in sections 8.5.6 and section 9.6.4.



### **12.1.2. Adaptation to New Gaits**

A more complex process is the recognition of new gaits. The adaptation to changes in gait works on recognised gaits. The creation of a module for a new gait, including timing unit, shaping unit, and predicting model, works on steps which are handled by the fall-back controller. Whereas the procedure described in section 9.6.4 would allow the creation of these components, the output tuning would have to be handled differently. For example by notification of the user, or by application of suitable optimisation based on the fall-back controller's behaviour.

### **12.1.3. Adaptation of Control Output**

The previous two sections described adaptations to changes on the input side of the controller, which should be handled by the learning algorithms for the perceptrons used in the implementation. To adapt the control output, other strategies have to be applied. As already mentioned, unsupervised methods should not be used for patients. Therefore only methods which include direct supervision by human operators or expert knowledge will be considered. We will differentiate between directed optimisation of the output, based on error signals, and undirected trial-and-error experiments, whose safety is ensured by further knowledge or interaction. Detailed suggestions or experiments concerning such error signals is presented in section 12.1.5.

In general, an adaptation of control output can happen to support rehabilitation by reducing the support when not needed, or increasing the level of support in reaction to muscle fatigue or changed patient's conditions.

## **Directed Optimisation**

Directed optimisation can be used, when the system has a clear measure which indicates the need of change (e.g.an error signal) and additionally can automatically determine the direction of the change. Two possible hypotheses for future work are:

- To attach a set of IMUs before and after the knee joint. They could be used to derive the effect of damping on the impact force. If the joint is blocked, the brace will transfer the ground reaction forces directly to the pelvis, which could indicate a later onset of the damping to prevent shocks to reach the spine.
- EMG-activity could be monitored and compared to the control output of the device. Possible actions could be preventing user and orthosis from working against each other or altering the support according to the patient's needs. In this context, Massimo Sartori suggested to use a musculoskeletal model [86] to provide the controller with an estimation of the torque the EMG-activity should provide. That could be compared to the actually generated torque, the torque the device's damping provides and the current need based on the gait phase.

## **Parametrisation**

Crucial for directed optimisation is an appropriate parametrisation of the control output, which allows to perform the intended change. This parametrisation, as well as the measure to optimise have to be derived experimentally in future studies.

## **Undirected Adaptation**

Undirected adaptation can be understood as a random walk through the parameter space of the controller. The parameters defining the control output are

changed randomly. And a later evaluation provides the system with feedback whether a specific measure improved or worsened.

In machine learning, these approaches are known as **Reinforcement Learning**. In our case a supervisor, which could be the patient or an objective error function, attributes a reward to each change of parameters which define controller behaviour. The task of the reinforcement learning algorithm is to maximise the expected reward. This reward tells the controller if a change induced a desired or undesired behaviour.

Such an approach requires additional safety measures. An example would be to provide ranges in the gait phase, where the damping only should be changed very slowly, e.g., to prevent an unblocked knee in the stance phase. Another possibility would be to always force the application of a minimal damping level in the stance phase, which only allows a very slow bending of the knee, to give the user time to react.

#### **12.1.4. Self-Learning Controller**

A self-learning controller needs to support two phases. First the initial bootstrapping, which allows the patient to start walking, as covered in section 8.5.1. Followed by a continual process of adaptation to individual gait (section 12.1.1) and the setup of gait modules for all gaits encountered (section 12.1.2).

#### **12.1.5. Online Gait Analysis**

In this context, online gait analysis means the transfer of a measure, which monitors the patient's condition or indicates the need for controller adaptation, to the sensory equipment of the orthosis, possibly the extension of the sensory equipment, at best to sensors firmly attached to the orthosis. Thus, providing the controller with desired error-signals to facilitate learning. While sensors attached to other parts of the body are possible, like the contralateral leg or foot, the trunk,

## *Outlook*

or camera systems in glasses, the comfort is reduced if the procedure of donning the device is becoming more complex.

A possible approach, which promises easier setup and needs less reference data, leverages the knowledge about unwanted side-effects and long-term defects of prosthesis use (compare section 3.3.2). This can include the analysis of gait laboratory data, as discussed in chapter 10.

Additionally to the examples mentioned above, candidates which indicate gait asymmetry and can be determined with sensors attached to the device are

- Average hip tilt angle
- Stance phase proportion
- Angular range at the ipsilateral knee [35, 36]

These are promising candidates for error functions for undirected optimisation.

It is important to note, that such measures allow no inferences about subjective gait comfort or clinical gait quality assessments, but allow to estimate a reduction in possibly damaging gait asymmetry and therefore a possibility to improve gait support. Patient experiments have to verify these hypothesis.

### **Hip Tilt Angle**

The hip tilt angle has been introduced as part of the motion capture (MoCAP) experiments in chapter 10. It can be measured with an IMU based angle sensor. For example attached to the patient's belt. The results with a healthy walker did not indicate significant changes when changing the operational mode of the orthosis, nonetheless, the outcome can be different for patients.

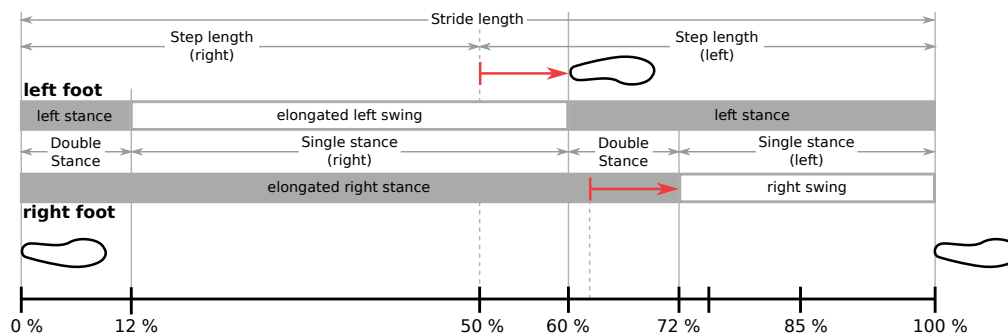


**Figure 12.1.:** When one leg is favoured to avoid load on the other leg, the resulting limping motion can be derived by the proportion of the stance phase in comparison to the stride.

### Stance Phase Proportion

For regular walking, the relation from stance-phase to swing-phase is around 60 : 40 (compare chapter 2), with the double stance-phases covering about 24 %. These relations cover symmetric gait. From the ratio of ipsilateral stance-phase to swing-phase-length we can estimate gait asymmetry. This immediately gives a measure for the amount of hobbling (compare Figure 12.1).

#### 12.1.6. Conflicting Adaptation by User and Device—Timescales of Adaptation

The reasons for adaptation given as examples in this section cover a wide range of timescales. Studies indicate, that the process of the user adapting to the supportive device will happen on the timescale of months [35, 36]. Other patient centred effects, for example the patient's conditions, change on timescales of days to months, depending on the medical indication. Some can change in hours, like muscle fatigue for patients with muscle disease.

All these effects, together with their timescales, have to be considered when different mechanisms of adaptation are active at the same time. The outcome can be unpredictable if a mechanism intended to capture changes in the patient's

## *Outlook*

gait over months is interfering with a daily pattern of increasing muscle fatigue. Therefore, further research has to cover how the mechanisms interact with each other and the patient.

### **12.1.7. Summary—Adaptation**

The questions when to learn, when to stop learning, what not to learn (e.g., what to optimise) and on which timescales provide an interesting field for future studies. Especially the different timescales of learning and their interaction will need thorough investigation to prevent the user and the device from progressing into a negative feedback loop.

As devices on the market do not provide means to change their behaviour at runtime, online adaptation is mostly relevant for academic research. Nonetheless, the patient could benefit from such mechanisms: If the device is able to optimise gait support, consequential damages can be reduced. The introduction of patient surveillance can help the patient by indicating the need to visit an orthopaedist to check the device or the patient's condition. These measures can increase the independence of the patient as well as help to improve the patient's condition. Given online optimisation which is guided by measures for gait quality, the device could be used for training purposes, slowly changing the device's support in a way that allows the patient to gradually improve their gait.

## **12.2. Next Steps**

Patient and further gait lab experiments play a crucial role in future development. Patient tests are needed to evaluate all controller components to get an impression of **(i)** how the controller performs to support the patient in general and in comparison to other controllers and **(ii)** in which way adaptation can be employed to actually improve the patient's situation.

Therefore, we propose a set of patient studies which investigate the device-user-interaction, providing measures to quantify the impact on the patient's gait. These measures have to be compared against orthopaedic measures of improved gait and the patient's subjective sense of comfort. Only if we can bring these two aspects together, the patient can enjoy the device and improved living quality.

Based on these measures, we can investigate the usefulness of the proposed approach with regard to

1. Damping adjustment: does the approach provide a reliable and intuitive way for the individual patient to optimise walking? How can we optimise this process to provide measurably better gait?
2. Gait switching: Does it provide a seamless and reliable working experience when walking in different environments?
3. Does the device and its tuning (including individual gait patterns, damping output, and gait switching) provide a significant change of the patients' gaits towards healthy or more symmetric gait?

With these aspects of the device-user-interaction understood, we can proceed to implement an adaptive and self-learning controller. The important questions are then

- If the system is able to learn the gait cycle of a patient. For example, whether or not a generic timing unit can be used so the device can gradually adapt to the patient's individual gait (section 12.1.1).
- Do the patient's adaptation to the device and vice versa interfere?
- Are there gait measures which align with the patient's subjective sense of comfort?
- Given a measure which indicates need for controller optimisation, can we derive a parametrisation which allows directed adaptation?

### *Outlook*

In summary, can we achieve comfortable gait support which will reduce consequential damages.

These questions could not be answered, as healthy walkers do not depend on the device's assistance.



# Bibliography

- [1] Richard Baker. The history of gait analysis before the advent of modern computers. *Gait & Posture*, 26(3):331–342, 2007. ISSN 0966-6362. doi: 10.1016/j.gaitpost.2006.10.014. URL <http://www.sciencedirect.com/science/article/pii/S0966636206003225>.
- [2] J.V. Basmajian and C.J. De Luca. *Muscles Alive*. Williams and Wilkins, 1985.
- [3] Kathie A Bernhardt, Steven E Irby, and Kenton R Kaufman. Consumer opinions of a stance control knee orthosis. *Prosthetics and orthotics international*, 30(3):246–256, 2006.
- [4] Bernstein-Focus-Neurotechnology. Zwischenbericht 2011 des bernstein fokus neurotechnologie (bfnt) göttingen. Technical report, Bernstein-Focus-Neurotechnology, 2011.
- [5] M.S.H. Bhuiyan, I.A. Choudhury, and M. Dahari. Development of a control system for artificially rehabilitated limbs: a review. *Biological Cybernetics*, 109(2):141–162, 2015. ISSN 0340-1200. doi: 10.1007/s00422-014-0635-1. URL <http://dx.doi.org/10.1007/s00422-014-0635-1>.
- [6] Joaquin Blaya and Hugh Herr. Adaptive control of a variable-impedance ankle-foot orthosis to assist drop-foot gait. *Neural Systems and Rehabilitation Engineering, IEEE Transactions on*, 12(1):24–31, 2004.
- [7] Jan-Matthias Braun, Florentin Wörgötter, and Poramate Manoonpong. Internal models support specific gaits in orthotic devices. In *Mobile Service Robotics*, number 17 in Proceedings of the International Conference on Climbing and Walking Robots, pages 539–546, 2014.

## Bibliography

- [8] Jan-Matthias Braun, Florentin Wörgötter, and Poramate Manoonpong. Orthosis controller with internal models supports individual gaits. In *Proceedings of the 9th Annual Dynamic Walking Conference*, number 9 in Proceedings of the 9th Annual Dynamic Walking Conference, 2014.
- [9] Jan-Matthias Braun, Poramate Manoonpong, and Florentin Wörgötter. Individual patient support on lower leg orthoses by continuous control over the whole gait cycle. Unpublished, accepted for SWARM 2015, 2015.
- [10] Martin D Buhmann. *Radial basis functions: theory and implementations*, volume 12. Cambridge university press, 2003.
- [11] Creative Commons. URL <https://creativecommons.org/licenses/by/3.0/deed.en>.
- [12] Sakyasingha Dasgupta, Dennis Goldschmidt, Florentin Wörgötter, and Poramate Manoonpong. Distributed recurrent neural forward models with synaptic adaptation and cpg-based control for complex behaviors of walking robots. *Frontiers in Neurorobotics*, 9(10), 2015. ISSN 1662-5218. doi: 10.3389/fnbot.2015.00010. URL <http://www.frontiersin.org/neurorobotics/10.3389/fnbot.2015.00010/abstract>.
- [13] Carlo J De Luca. The use of surface electromyography in biomechanics. *Journal of applied biomechanics*, 13:135–163, 1997.
- [14] Carlo J. De Luca. *DEELSYS SURFACE ELECTROMYOGRAPHY: DETECTION AND RECORDING*. DelSys, 2002.
- [15] Frederick J Diedrich and William H Warren Jr. Why change gaits? dynamics of the walk-run transition. *Journal of Experimental Psychology: Human Perception and Performance*, 21(1):183, 1995.
- [16] T. Ding. A robust identification approach to gait recognition. In *Computer Vision and Pattern Recognition, 2008. CVPR 2008. IEEE Conference on*, pages 1–8, 2008. doi: 10.1109/CVPR.2008.4587634.

- [17] Aaron M Dollar and Hugh Herr. Lower extremity exoskeletons and active orthoses: challenges and state-of-the-art. *Robotics, IEEE Transactions on*, 24(1):144–158, 2008.
- [18] R Ekkelenkamp, J Veneman, and H Van der Kooij. Lopes: Selective control of gait functions during the gait rehabilitation of cva patients. pages 361–364, 2005.
- [19] Interlink Electronics. *FSR<sup>®</sup> Force Sensing Resistors<sup>®</sup> FSR<sup>®</sup> Integration Guide*. Interlink Electronics, document part number eig-10000 rev. a edition, Juli 2013. URL <http://www.interlinkelectronics.com/FSR400.php>.
- [20] Dario Farina, Aleš Holobar, Roberto Merletti, and Roger M. Enoka. Decoding the neural drive to muscles from the surface electromyogram. *Clinical Neurophysiology*, 121(10):1616 – 1623, 2010. ISSN 1388-2457. doi: <http://dx.doi.org/10.1016/j.clinph.2009.10.040>. URL <http://www.sciencedirect.com/science/article/pii/S1388245710003457>.
- [21] Robert Gailey, Kerry Allen, Julie Castles, Jennifer Kucharik, and Mariah Roeder. Review of secondary physical conditions associated with lower-limb amputation and long-term prosthesis use. *Journal of rehabilitation research and development*, 45(1):15, 2008.
- [22] J.G. Gamble and J. Rose. *Human walking*, chapter 14, pages 223–228. Williams & Wilkins, 1994.
- [23] T. Geng, B. Porr, and F. Wörgötter. Fast biped walking with a reflexive neuronal controller and real-time online learning. *Int. Journal of Robotics Res*, 3:243–261, 2006. Speed adaptation with reinforcement learning.
- [24] Tao Geng, Bernd Porr, and Florentin Wörgötter. Fast biped walking with a reflexive controller and real-time policy searching. pages 427–434, 2005.

## Bibliography

- [25] Tao Geng, Bernd Porr, and Bernd Florentinwörgötter. A reflexive neural network for dynamic biped walking control. *Neural computation*, 18(5): 1156–1196, 2006.
- [26] Leonardo Gizzi, Jørgen Feldbæk Nielsen, Francesco Felici, Yuri P Ivanenko, and Dario Farina. Impulses of activation but not motor modules are preserved in the locomotion of subacute stroke patients. *Journal of neurophysiology*, 106(1):202–210, 2011.
- [27] Jeffrey M Hausdorff. Gait dynamics, fractals and falls: finding meaning in the stride-to-stride fluctuations of human walking. *Human movement science*, 26(4):555–589, 2007.
- [28] Jeffrey M Hausdorff. Gait dynamics in parkinson’s disease: common and distinct behavior among stride length, gait variability, and fractal-like scaling. *Chaos: An Interdisciplinary Journal of Nonlinear Science*, 19(2): 026113, 2009.
- [29] Hugh Herr, Ari Wilkenfeld, and Joaquin Blaya. Patient-adaptive prosthetic and orthotic leg systems. pages 123–128, 2002.
- [30] Frank Mori Hess, Ian Abbott, et al. Linux control and measurement device interface, 1998–. URL <http://www.comedi.org/>. [Online; accessed 2015-07-02].
- [31] AV Hill. The heat of shortening and the dynamic constants of muscle. *Proceedings of the Royal Society of London B: Biological Sciences*, 126 (843):136–195, 1938.
- [32] C Hong, EB San Luis, and S Chung. Follow-up study on the use of leg braces issued to spinal cord injury patients. *Spinal Cord*, 28(3):172–177, 1990.
- [33] John D Hsu, John Michael, and John Fisk. *AAOS atlas of orthoses and assistive devices*. Elsevier Health Sciences, 2008.

- [34] J.D. Hunter. Matplotlib: A 2d graphics environment. *Computing in Science Engineering*, 9(3):90–95, May 2007. ISSN 1521-9615. doi: 10.1109/MCSE.2007.55.
- [35] Steven E Irby, Kathie A Bernhardt, and Kenton R Kaufman. Gait of stance control orthosis users: the dynamic knee brace system. *Prosthetics and orthotics international*, 29(3):269–282, 2005.
- [36] Steven E Irby, Kathie A Bernhardt, and Kenton R Kaufman. Gait changes over time in stance control orthosis users. *Prosthetics and orthotics international*, 31(4):353–361, 2007.
- [37] Toshiki Iso and Kenichi Yamazaki. Gait analyzer based on a cell phone with a single three-axis accelerometer. In *Proceedings of the 8th conference on Human-computer interaction with mobile devices and services, MobileHCI '06*, page 141–144, New York, NY, USA, 2006. ACM. ISBN 1-59593-390-5. doi: 10.1145/1152215.1152244. URL <http://doi.acm.org/10.1145/1152215.1152244>.
- [38] Vladimír Janda. *Manuelle Muskelfunktionsdiagnostik*. Elsevier, Urban&FischerVerlag, 2009.
- [39] René Jimenez-Fabian and Olivier Verlinden. Review of control algorithms for robotic ankle systems in lower-limb orthoses, prostheses, and exoskeletons. *Medical engineering & physics*, 34(4):397–408, 2012.
- [40] Eric Jones, Travis Oliphant, Pearu Peterson, et al. SciPy: Open source scientific tools for Python, 2001–. URL <http://www.scipy.org/>. [Online; accessed 2015-07-02].
- [41] Vojislav D Kalanovic, Dejan Popovic, and Nils T Skaug. Feedback error learning neural network for trans-femoral prosthesis. *Rehabilitation Engineering, IEEE Transactions on*, 8(1):71–80, 2000.
- [42] Stefan Karlsson and Björn Gerdle. Mean frequency and signal amplitude of the surface {EMG} of the quadriceps muscles increase with increasing torque — a study using the continuous wavelet transform.

## Bibliography

- Journal of Electromyography and Kinesiology*, 11(2):131 – 140, 2001. ISSN 1050-6411. doi: [http://dx.doi.org/10.1016/S1050-6411\(00\)00046-8](http://dx.doi.org/10.1016/S1050-6411(00)00046-8). URL <http://www.sciencedirect.com/science/article/pii/S1050641100000468>. Quadriceps – torque relates to EMG Amplitude and mean frequency (spectrum analysis). Paper on this finding and method for power spectrum analysis with fewer restraints than fourier transform.s.
- [43] K. R. Kaufman and D.H. Sutherland. *Human walking*, chapter 3, pages 33–51. Williams & Wilkins, 1994.
- [44] Kenton R Kaufman, SE Irby, JW Mathewson, RW Wirta, and DH Sutherland. Energy-efficient knee-ankle-foot orthosis: A case study. *JPO: Journal of Prosthetics and Orthotics*, 8(3):79–85, 1996.
- [45] Ilyas Kuhlemann, Jan-Matthias Braun, Florentin Wörgötter, and Poramate Manoonpong. Comparing arc-shaped feet and rigid ankles with flat feet and compliant ankles for a dynamic walker. In *Mobile Service Robotics*, number 17 in Proceedings of the International Conference on Climbing and Walking Robots, pages 353–360, 2014.
- [46] T. Kulvicius, T. Geng, B. Porr, and F. Wörgötter. Speed optimization of a 2d walking robot through stdp. In *Dynamical principles for neuroscience and intelligent biomimetic devices: EPFL LATSIS Symposium 2006*, pages 99–100, 2006. Speed optimisation with STDP -> Learn to target a specific delay between left and right leg. (Speed).
- [47] Lutz Kunze. Elektromechanische modellierung und leistungsvergleich am zweibeinigen robot runbot mit elastischem fußgelenk. Dipl.-ing., University of Applied Sciences Jena, 2010.
- [48] Arthur D. Kuo. Energetics of actively powered locomotion using the simplest walking model. *Journal of Biomechanical Engineering*, 124: 113–120, September 2001. doi: [doi:10.1115/1.1427703](https://doi.org/10.1115/1.1427703). URL <http://dx.doi.org/10.1115/1.1427703>.

- [49] Arthur D Kuo. The six determinants of gait and the inverted pendulum analogy: A dynamic walking perspective. *Human movement science*, 26(4):617–656, 2007.
- [50] B. Lawson, H.A. Varol, A. Huff, E. Erdemir, and M. Goldfarb. Control of stair ascent and descent with a powered transfemoral prosthesis. *Neural Systems and Rehabilitation Engineering, IEEE Transactions on*, 21(3):466–473, 2013. ISSN 1534-4320. doi: 10.1109/TNSRE.2012.2225640.
- [51] Brian E Lawson, Huseyin Atakan Varol, and Michael Goldfarb. Ground adaptive standing controller for a powered transfemoral prosthesis. In *Rehabilitation Robotics (ICORR), 2011 IEEE International Conference on*, pages 1–6. IEEE, 2011.
- [52] E.D. Lemaire, L. Goudreau, T. Yakimovich, and J. Kofman. Angular-Velocity Control Approach for Stance-Control Orthoses. *Neural Systems and Rehabilitation Engineering, IEEE Transactions on*, 17(5):497–503, oct. 2009. ISSN 1534-4320. doi: 10.1109/TNSRE.2009.2023308.
- [53] Juan Li, Weida Li, Chunguang Li, Haiyan Hu, Hao Guo, Shumei Yu, Rongchuan Sun, and Lining Sun. Joint parameter mapping method for the control of knee prosthesis. In *Mobile Service Robotics*, number 17 in Proceedings of the International Conference on Climbing and Walking Robots, pages 45–52, 2014.
- [54] Susanne W Lipfert, Michael Günther, Daniel Renjewski, and Andre Seyfarth. Impulsive ankle push-off powers leg swing in human walking. *The Journal of experimental biology*, 217(8):1218–1228, 2014.
- [55] Benchmarking Bipedal Locomotion. URL <http://www.benchmarkinglocomotion.org/>.
- [56] Philippe Malcolm, Wim Derave, Samuel Galle, and Dirk De Clercq. A simple exoskeleton that assists plantarflexion can reduce the metabolic cost of human walking. *PLoS ONE*, 8(2):e56137, 02 2013. doi: 10.

## Bibliography

1371/journal.pone.0056137. URL <http://dx.doi.org/10.1371/journal.pone.0056137>.

- [57] P. Manoonpong, T. Geng, and F. Wörgötter. Exploring the dynamic walking range of the biped robot runbot with an active upper-body component. In *IEEE-RAS International Conference on Humanoid Robots Humanoids 2006*, pages 418–424, 2006. Upper body component, slopes, parameters for different joints.
- [58] P. Manoonpong, T. Geng, B. Porr, and F. Wörgötter. The runbot architecture for adaptive, fast, dynamic walking. In *IEEE International Symposium on Circuits and Systems ISCAS, New Orleans, USA*, pages 1181–1184, 2007. UBC + IR + ICO -> Slope adaptation.
- [59] Poramate Manoonpong, Tao Geng, Tomas Kulvicius, Bernd Porr, and Florentin Wörgötter. Adaptive, fast walking in a biped robot under neuronal control and learning. *PLoS Comput Biol*, 3(7):e134, 07 2007. doi: 10.1371/journal.pcbi.0030134. URL <http://dx.plos.org/10.1371/journal.pcbi.0030134>. Speed, UBC, IR-Slopes + ACC.
- [60] M.C. Mazzaro, M. Sznaier, and O. Camps. A model (in)validation approach to gait classification. *Pattern Analysis and Machine Intelligence, IEEE Transactions on*, 27(11):1820–1825, 2005. ISSN 0162-8828. doi: 10.1109/TPAMI.2005.210.
- [61] Pat R. McKee and Annette Rivard. Biopsychosocial approach to orthotic intervention. *Journal of Hand Therapy*, 24(2):155–163, 2011.
- [62] S. Mefoued, M.E. Daachi, B. Daachi, S. Mohammed, and Y. Amirat. A robust adaptive neural controller to drive a knee joint actuated orthosis. In *Robotics and Biomimetics (ROBIO), 2012 IEEE International Conference on*, page 1656–1661, 2012. doi: 10.1109/ROBIO.2012.6491205.
- [63] Dorthe Meyer. Human gait classification based on hidden markov models. In *3D Image Analysis and Synthesis*, pages 139–146, 1997.



- [64] Rose Mikelberg and Sheila Reid. Spinal cord lesions and lower extremity bracing: an overview and follow-up study. *Spinal Cord*, 19(6):379–385, 1981.
- [65] Kathryn Mills, Peter Blanch, Andrew R Chapman, Thomas G McPoil, and Bill Vicenzino. Foot orthoses and gait: a systematic review and meta-analysis of literature pertaining to potential mechanisms. *British journal of sports medicine*, 44(14):1035–1046, 2010.
- [66] John Milton, Juan Luis Cabrera, Toru Ohira, Shigeru Tajima, Yukinori Tonosaki, Christian W Eurich, and Sue Ann Campbell. The time-delayed inverted pendulum: implications for human balance control. *Chaos: An Interdisciplinary Journal of Nonlinear Science*, 19(2):026110, 2009.
- [67] Luke Mooney, Elliott Rouse, and Hugh Herr. Autonomous exoskeleton reduces metabolic cost of human walking during load carriage. *Journal of NeuroEngineering and Rehabilitation*, 11(1):80, 2014. ISSN 1743-0003. doi: 10.1186/1743-0003-11-80. URL <http://www.jneuroengrehab.com/content/11/1/80>.
- [68] Andreas G Nerlich, Albert Zink, Ulrike Szeimies, and Hjalmar G Hagedorn. Ancient egyptian prosthesis of the big toe. *The Lancet*, 356(9248): 2176–2179, 2000.
- [69] S. Nissen. Implementation of a fast artificial neural network library (fann). Technical report, Department of Computer Science University of Copenhagen (DIKU), 2003. <http://fann.sf.net>.
- [70] John F Nunn. *Ancient egyptian medicine*. University of Oklahoma Press, 2002.
- [71] openstax. URL <http://cnx.org/content/col11496/1.6/>.
- [72] Otto Bock. *Product Information: E-MAG Active FachInformation*. Otto Bock HealthCare GmbH, July 2010. URL [http://www.ottobock.com/cps/rde/xchg/ob\\_at\\_de/hs.xsl/19150.html?id=19152#t19152](http://www.ottobock.com/cps/rde/xchg/ob_at_de/hs.xsl/19150.html?id=19152#t19152).

## Bibliography

- [73] J. Park and I. W. Sandberg. Universal approximation using radial-basis-function networks. *Neural Computation*, 3(2):246–257, June 1991. ISSN 0899-7667. doi: 10.1162/neco.1991.3.2.246. URL <http://dx.doi.org/10.1162/neco.1991.3.2.246>.
- [74] Jacquelin Perry. *Gait analysis*, volume 1. Urban & Fischer Verlag/Elsevier GmbH, 2003.
- [75] F. Pérez and B.E. Granger. Ipython: A system for interactive scientific computing. *Computing in Science Engineering*, 9(3):21–29, May 2007. ISSN 1521-9615. doi: 10.1109/MCSE.2007.53.
- [76] Betsy Phillips and Hongxin Zhao. Predictors of assistive technology abandonment. *Assistive Technology*, 5(1):36–45, 1993.
- [77] K.L. Poggensee, M.A. Sharbafi, and A. Seyfarth. Characterizing swing-leg retraction in human locomotion. In *Mobile Service Robotics*, number 17 in Proceedings of the International Conference on Climbing and Walking Robots, pages 539–546, 2014.
- [78] Bernd Porr et al. Linux usb data acquisition unit. URL <http://www.linux-usb-daq.co.uk/>. [Online; accessed 2015-07-02].
- [79] Jerry E Pratt and Russ Tedrake. Velocity-based stability margins for fast bipedal walking. In *Fast Motions in Biomechanics and Robotics*, pages 299–324. Springer, 2006.
- [80] S. D. Prentice, A. E. Patla, and D. A. Stacey. Simple artificial neural network models can generate basic muscle activity patterns for human locomotion at different speeds. *Experimental Brain Research*, 123:474–480, 1998. ISSN 0014-4819. URL <http://dx.doi.org/10.1007/s002210050591>. 10.1007/s002210050591.
- [81] Daniel Renjewski and André Seyfarth. Robots in human biomechanics—a study on ankle push-off in walking. *Bioinspiration & Biomimetics*, 7(3):036005, 2012. doi: doi:10.1088/1748-3182/7/3/036005. URL <http://stacks.iop.org/1748-3190/7/i=3/a=036005>.

- [82] Robert Riener. Robot-aided rehabilitation of neural function in the upper extremities. In Damianos E. Sakas, Brian A. Simpson, and Elliott S. Krames, editors, *Operative Neuromodulation*, volume 97/1 of *Acta Neurochirurgica Supplements*, pages 465–471. Springer Vienna, 2007. ISBN 978-3-211-33078-4. doi: 10.1007/978-3-211-33079-1\_61. URL [http://dx.doi.org/10.1007/978-3-211-33079-1\\_61](http://dx.doi.org/10.1007/978-3-211-33079-1_61).
- [83] Vicky Robinson, Kate Sansam, Lynn Hirst, and Vera Neumann. Major lower limb amputation—what, why and how to achieve the best results. *Orthopaedics and Trauma*, 24(4):276–285, 2010.
- [84] J. Rose and J.G. Gamble. *Human walking*. Williams & Wilkins, 1994. ISBN 9780683073607. URL <http://books.google.de/books?id=HdNqAAAAMAAJ>.
- [85] U. Römer, F. Baier, and A. Fidlin. Transition from walking to running of a bipedal robot to optimize energy efficiency. In *Mobile Service Robotics*, number 17 in Proceedings of the International Conference on Climbing and Walking Robots, pages 539–546, 2014.
- [86] Massimo Sartori, Leonardo Gizzi, David G Lloyd, and Dario Farina. A musculoskeletal model of human locomotion driven by a low dimensional set of impulsive excitation primitives. *Frontiers in computational neuroscience*, 7, 2013. Isolation of 5 timings which can drive the previously EMG-Driven musculoskeletal model.
- [87] L.M. Schutte, U. Narayanan, J.L. Stout, P. Selber, J.R. Gage, and M.H. Schwartz. An index for quantifying deviations from normal gait. *Gait & Posture*, 11(1):25–31, 2000. ISSN 0966-6362. doi: 10.1016/S0966-6362(99)00047-8. URL <http://www.sciencedirect.com/science/article/pii/S0966636299000478>.
- [88] Michael H. Schwartz and Adam Rozumalski. The gait deviation index: A new comprehensive index of gait pathology. *Gait & Posture*, 28(3): 351–357, 2008. ISSN 0966-6362. doi: 10.1016/j.gaitpost.2008.05.001.

## Bibliography

URL <http://www.sciencedirect.com/science/article/pii/S0966636208001136>.

- [89] W.I. Schöllhorn. Applications of artificial neural nets in clinical biomechanics. *Clinical Biomechanics*, 19(9):876–898, 2004. doi: 10.1016/j.clinbiomech.2004.04.005. URL <http://dx.doi.org/10.1016/j.clinbiomech.2004.04.005>.
- [90] Kamran Shamaei, Massimo Cenciarini, Albert Adams, Karen N Gregorczyk, Jeffrey M Schiffman, Aaron M Dollar, et al. Design and evaluation of a quasi-passive knee exoskeleton for investigation of motor adaptation in lower extremity joints. *Biomedical Engineering, IEEE Transactions on*, 61(6):1809–1821, 2014.
- [91] Dan Stashuk. EMG signal decomposition: how can it be accomplished and used? *Journal of Electromyography and Kinesiology*, 11(3):151 – 173, 2001. ISSN 1050-6411. doi: [http://dx.doi.org/10.1016/S1050-6411\(00\)00050-X](http://dx.doi.org/10.1016/S1050-6411(00)00050-X). URL <http://www.sciencedirect.com/science/article/pii/S105064110000050X>. For intramuscular electrodes: what is recorded and how it is composed from MUAPs.
- [92] H. Stinus. Biomechanik und beurteilung des mikroprozessorgesteuerten exoprothesenkniegelenkes c-leg. *Zeitschrift für Orthopädie und ihre Grenzgebiete*, 138(03):278–282, 2000.
- [93] F. Sup, H.A. Varol, J. Mitchell, T.J. Withrow, and M. Goldfarb. Self-contained powered knee and ankle prosthesis: Initial evaluation on a transfemoral amputee. In *Rehabilitation Robotics, 2009. ICORR 2009. IEEE International Conference on*, pages 638–644, June 2009. doi: 10.1109/ICORR.2009.5209625.
- [94] Frank Sup, Amit Bohara, and Michael Goldfarb. Design and control of a powered transfemoral prosthesis. *The International journal of robotics research*, 27(2):263–273, 2008.

- [95] Frank Sup, H.A. Varol, and M. Goldfarb. Upslope walking with a powered knee and ankle prosthesis: Initial results with an amputee subject. *Neural Systems and Rehabilitation Engineering, IEEE Transactions on*, 19(1):71–78, 2011. ISSN 1534-4320. doi: 10.1109/TNSRE.2010.2087360.
- [96] David H. Sutherland, Richard Olshen, L. Cooper, and S. Ly Woo. The development of mature gait. *J Bone Joint Surg Am*, 62(3):336–53, 1980.
- [97] W. van den Hoorn, S.M. Bruijn, O.G. Meijer, P.W. Hodges, and J.H. van Dieën. Mechanical coupling between transverse plane pelvis and thorax rotations during gait is higher in people with low back pain. *Journal of Biomechanics*, 45(2):342 – 347, 2012. ISSN 0021-9290. doi: <http://dx.doi.org/10.1016/j.jbiomech.2011.10.024>. URL <http://www.sciencedirect.com/science/article/pii/S002192901100666X>.
- [98] S. van der Walt, S.C. Colbert, and G. Varoquaux. The numpy array: A structure for efficient numerical computation. *Computing in Science Engineering*, 13(2):22–30, March 2011. ISSN 1521-9615. doi: 10.1109/MCSE.2011.37.
- [99] H.A. Varol, Frank Sup, and M. Goldfarb. Real-time gait mode intent recognition of a powered knee and ankle prosthesis for standing and walking. In *Biomedical Robotics and Biomechatronics, 2008. BioRob 2008. 2nd IEEE RAS EMBS International Conference on*, pages 66–72, 2008. doi: 10.1109/BIOROB.2008.4762860.
- [100] H.A. Varol, Frank Sup, and M. Goldfarb. Multiclass real-time intent recognition of a powered lower limb prosthesis. *Biomedical Engineering, IEEE Transactions on*, 57(3):542–551, 2010. ISSN 0018-9294. doi: 10.1109/TBME.2009.2034734.
- [101] Michael W. Whittle. Clinical gait analysis: A review. *Human Movement Science*, 15(3):369–387, 1996. ISSN 0167-9457. doi: [http://dx.doi.org/10.1016/0167-9457\(96\)00006-1](http://dx.doi.org/10.1016/0167-9457(96)00006-1). URL <http://www.sciencedirect.com/science/article/pii/0167945796000061>.

- [102] Travis Wiens. Radial basis function network, 2010. URL <http://www.mathworks.com/matlabcentral/fileexchange/22173-radial-basis-function-network>.
- [103] David A Winter. Kinematic and kinetic patterns in human gait: variability and compensating effects. *Human Movement Science*, 3(1):51–76, 1984.
- [104] David A Winter. Human balance and posture control during standing and walking. *Gait & posture*, 3(4):193–214, 1995.
- [105] Jack M. Winters. *Multiple Muscle Systems Biomechanics and Movement Organization*, chapter Hill-Based Muscle Models: A Systems Engineering Perspective, pages 69–93. Springer, 1990.
- [106] T. Yakimovich, J. Kofman, and E.D. Lemaire. Design and Evaluation of a Stance-Control Knee-Ankle-Foot Orthosis Knee Joint. *Neural Systems and Rehabilitation Engineering, IEEE Transactions on*, 14(3):361–369, sept. 2006. ISSN 1534-4320. doi: 10.1109/TNSRE.2006.881578.
- [107] Terris Yakimovich, Edward D. Lemaire, and Jonathan Kofman. Engineering design review of stance-control knee-ankle-foot orthoses. *Journal of Rehabilitation Research & Development*, 46(2):257–268, 2009.
- [108] George I. Zahalak. *Multiple Muscle Systems Biomechanics and Movement Organization*, chapter Modelling Muscle Mechanics (and Energetics), pages 1–23. Springer, 1990.
- [109] Daniel Zlatnik, Beatrice Steiner, and Gerhard Schweitzer. Finite-state control of a trans-femoral (tf) prosthesis. *Control Systems Technology, IEEE Transactions on*, 10(3):408–420, 2002.

*Only kings, presidents, editors, and people with tapeworms have the right to use the editorial “we”.*

Mark Twain

## Acknowledgements

This work would not have been possible without the cooperation and support of many individuals and institutions. This thesis is big enough as it is so I cannot name every individual who contributed in one way or another. Please forgive me if I forgot you.

I want to start with thanking my thesis advisory committee members, namely Prof. Dr. Florentin Wörgötter, Prof. Dr. Dario Farina and Prof. Dr. Alexander Gail for their ongoing support, supervision, and insightful discussion. My extended thanks go to Prof. Dr. Florentin Wörgötter for welcoming me into his group, his backing, and especially for teaching me how to ski.

Next is the whole working group for their warm reception, interest and will to explore the work of their colleagues. Explicit thanks go to Poramate Manoonpong for guidance and advise. Kejun Ning and Harm-Friedrich Steinmetz for their support in matters of electronics. Christoph Kolodziejewski for mentoring and counsel. Christian Tetzlaff for his sharp mind and helpful criticism. Michael Fauth for helpful discussions and the good spirits we enjoyed together. Simon Reich for the early morning break. And of course Alexey Abramov, Eren Erdal Aksoy, and Tomas Kulvicius. The coffee circle should not be forgotten as well. It provided an endless resource for the necessary amount of everyday insanity. This includes especially Anja Huss.

The ability to pursue this work was heavily dependent on our secretaries Ursula Hahn-Wörgötter and Sabine Huhnold, all the people from the GGNB offices, es-

pecially Yvonne Reimann and Rike Göbel, Thomas Geiling, Dieter Hille and his mechanics workshop, who were always able to provide assistance with stubborn hardware, and the electronics workshop.

Further thanks go to Massimo Sartori for information and discussion on everything musculoskeletal model related and Leonardo Gizzi for his support and advise, without whom the whole gait lab chapter would never have been written.

For their cooperation in the BFNT Project, I want to extend my thanks to the cooperation partners at Otto Bock HealthCare, especially Vishal Patel, Timo von Marcard, Markus Tüttemann, Alexander Pappe, and the friendly people from Otto Bock Vienna.

For reading meter after meter of this thesis, my heartfelt thanks again to Christian Tetzlaff, Michael Fauth, Simon Reich, and Jan Schrewe, who provided their feedback to help me get things straight.

Last but not least I want to thank my friends and my family for holding my mood up. Especially, things would have been difficult without my mother and my mother-in-law who spent too much time taking care of my daughter while I was working late. But nothing would have worked out without my beloved daughter Lene and my beloved wife Simone! An extensive work like this is a family effort: Without your love, affection and assistance, this work would not exist.

Thank you all!



No work is fair without suitable tools. This work would not have been possible—or at least several magnitudes more difficult without the following excellent tools:

1. Digital data acquisition with USB-Dux [78] and the comedi-library [30] made it easy to interact with robots and orthosis-prototypes.
2. For many artificial neural networks I could rely on the FANN library [69] for fast and painless inclusion in my projects.
3. Evaluations, algorithmic experiments and analyses would have been cumbersome without python—especially numpy [98], scipy [40], ipython [75], and matplotlib [34], as well as uncounted other packages, which accompanied me for years.
4. And of course Linux in all its facets, which powered every laptop and pc that was part of this work.

The research leading to these results has received funding from the BMBF-funded BFNT & BCCN Göttingen with grant numbers 01GQ0810 (project 3A) and 01GQ1005A (project D1), respectively, and the Emmy Noether Program (DFG, MA4464/3-1).



# Affidavit

I hereby declare that my doctoral thesis entitled “Modular Architecture for an Adaptive, Personalisable Knee-Ankle-Foot-Orthosis Controlled by Artificial Neural Networks” has been written independently and with no other sources and aids than quoted.

Göttingen, October 2015,

---

(Jan-Matthias Braun)



# Academic Curriculum Vitae

## Personal Details

---

Family name	Braun
First name	Jan-Matthias
Nationality	German
Date of birth	1979-10-05
Place of birth	Göttingen, Germany

## Education

---

since 2012	PhD-student at the Göttingen Graduate School for Neurosciences, Biophysics, and Molecular Biosciences (GGNB), Georg-August University, Göttingen, Germany
2006 - 2007	Diploma Thesis on <i>Partial Barriers and Eigenfunctions in Systems with Mixed Phase-Space</i>
2000 - 2007	Studies of Physics, Faculty of Physics, TU-Dresden, Dresden, Germany
1999	Abitur (university-entrance diploma), Hainberg-Gymnasium, Göttingen, Germany

## Patent Applications

---

2014	The application “Orthesensteuerung” (“Orthosis control”) has been published with publication numbers DE201210107117 (Germany), and WO2014019872 A1 (WIPO) with PCT number PCT/EP2013/065285.
2015	The application has been published under the application numbers CN104661620 A (China), EP2879622 A1 (European Patent Office), and US20150190250 A1 (US).

## Peer-Reviewed Conference Publications

---

- 2014 **Braun, J.-M.**, Wörgötter, F., and Manoonpong, P. (2014), “Internal Models Support Specific Gaits in Orthotic Devices”, Mobile Service Robotics, number 17 in Proceedings of the International Conference on Climbing and Walking Robots, pages 539–546.
- Kuhlemann, I., **Braun, J.-M.**, Wörgötter, F., and Manoonpong, P. (2014), “Comparing arc-shaped feet and rigid ankles with flat feet and compliant ankles for a dynamic walker”, Mobile Service Robotics, number 17 in Proceedings of the International Conference on Climbing and Walking Robots, pages 353–360.
- Braun, J.-M.**, Wörgötter, F. and Manoonpong, P. (2014), “Orthosis Controller with Internal Models Supports Individual Gaits”, The 9th Annual Dynamic Walking Conference.
- 2015 **Braun, J.-M.**, Manoonpong, P., and Wörgötter, F. (2015), “Individual Patient Support on Lower Leg Orthoses by Continuous Control over the Whole Gait Cycle”, accepted for SWARM 2015.
- Widenka, J., Xiong, X., **Braun, J.-M.**, Manoonpong, P., and Wörgötter, F. (2015), “Neuromechanical Control for dynamic bipedal walking with reduced impact forces”, accepted for SWARM 2015.